SAND78-8015

Unlimited Release

UC-62

Semiannual Review of Solar Thermal Central Power Systems

Prepared by Sandia Laboratories, Albuquerque, New Mexico 87115 and Livermore, California 94550 for the United States Department of Energy under Contract AT (29-1)-789.

Printed April 1978

Sandia Laboratories
energy report

SF 2900-QQB(3-74)

Issued by Sandia Laboratories, operated for the United States Department of Energy by Sandia Corporation.

NOTICE

Printed in the United States of America
Available From
National Technical Information Service
U. S. Department of Commerce
5285 Port Royal Road
Springfield, VA 22161
Price: Printed Copy $8.00; Microfiche $3.00

SAND78-8015
Unlimited Release
Printed April 1978

UC-62

SEMIANNUAL REVIEW OF SOLAR THERMAL CENTRAL POWER SYSTEMS

Sponsored by

Department of Energy
Division of Solar Technology
Washington, D. C.

ABSTRACT

This report presents the highlights of the Department of Energy (DOE) Solar Thermal Central Power Systems Semiannual Review held in San Diego, California, on March 2-3, 1978.

CONTENTS

SEMIANNUAL REVIEW OF SOLAR THERMAL CENTRAL POWER SYSTEMS

Introduction

This report summarizes information presented at the Department of Energy's Solar Thermal Projects Semiannual Review held at San Diego, California, on March 2-3, 1978. The purpose of this meeting was to review the status of the research and development activities associated with the solar central power systems that are being developed as part of the Thermal Power Systems Program.

The overall objective of the central power system development effort is to establish central solar thermal power systems as an economically viable power generation resource for electric utilities by the mid-1980s. To meet this objective, the development of central receiver technology has been divided into four phases.

The initial phase consists of verifying the designs of major subsystems for water/steam central power systems in support of the 10-MWe central receiver pilot plant to be operational at Barstow, California, in 1981.

Next, existing oil and natural gas fueled power plants in the southwestern U.S. will be repowered with 10-50 MW water/steam central power systems. The primary goal is to displace natural gas and imported oil as well as to provide a sound basis for evaluating the system operations for the storage coupled intermediate capacity factor plants. These plants will provide for competition within the heliostat industry and provide the production and system experience necessary to reduce heliostat and system costs.

Following the 10-50 MW plants will be 50 to 200-MW water/steam systems that include storage and are based on advanced rankine and/or brayton cycles (500-800°C). These plants will complement coal and nuclear power plants and will displace not only fossil fuel use but also plant capacity. These systems will further stimulate competition in the production of hardware and equipment and extend the technology in the use of brayton cycle and the coupling of solar thermodynamic cycles with low-cost thermal storage systems.

In the final phase, 100 to 500-MW central receiver and distributed receiver systems based on advanced rankine and/or brayton cycles and operating in the range of 1000 to 2500°F will be applied to the production of electricity and transportable fuels and chemicals. These plants will provide an alternative to coal and nuclear plants and will displace depletable fuel sources in all sectors of national energy market. These systems will require further development of high-temperature technology and long-term storage systems.

DOE OVERVIEW

Department of Energy
San Francisco Operations Office

R. W. Hughey

Since the last semiannual review, several events have occurred that will have a definite effect on the solar energy program. For one, ERDA passed away and DOE was created. As shown in Figure 1, solar energy development is now under two Assistant Secretaries. Solar electric and biomass are under the Assistant Secretary for Energy and Technology; heating and cooling are under the Assistant Secretary for Conservation and Solar Applications.

Under ERDA, solar electric energy was looked upon as a contributor to long-term goals. Under DOE, solar electric is also asked to contribute to near and mid-term needs, particularly as an oil and gas "fuel saver."

A number of other factors tell us that we must accelerate our solar electric program, e.g.:

1. More and more we are realizing that oil and gas are going down in availability and up in cost; that nuclear and coal are in serious trouble; and that fusion is still far off. So, sources like solar and geothermal must be pushed harder and sooner.

2. DOE would like its alternative technologies (nuclear, fossil, solar, geothermal, fusion, conservation) to contribute one Q by 1985. Solar must do its share. Ten Q is an enormous quantity--like 30-40 power plants of 1,000 MWe capacity.

3. Congress is pushing DOE to increase its solar program. The House Science and Technology Committee has recently marked up the President's FY 79 Solar Electric Budget from $287 M to $358 M, and it may go still higher.

Figures 2, 3, 4, and 5 show the Thermal Power Systems (TPS) program, its objectives, organization, projected achievements for FY 79, and applications. Three of these applications are of key significance:

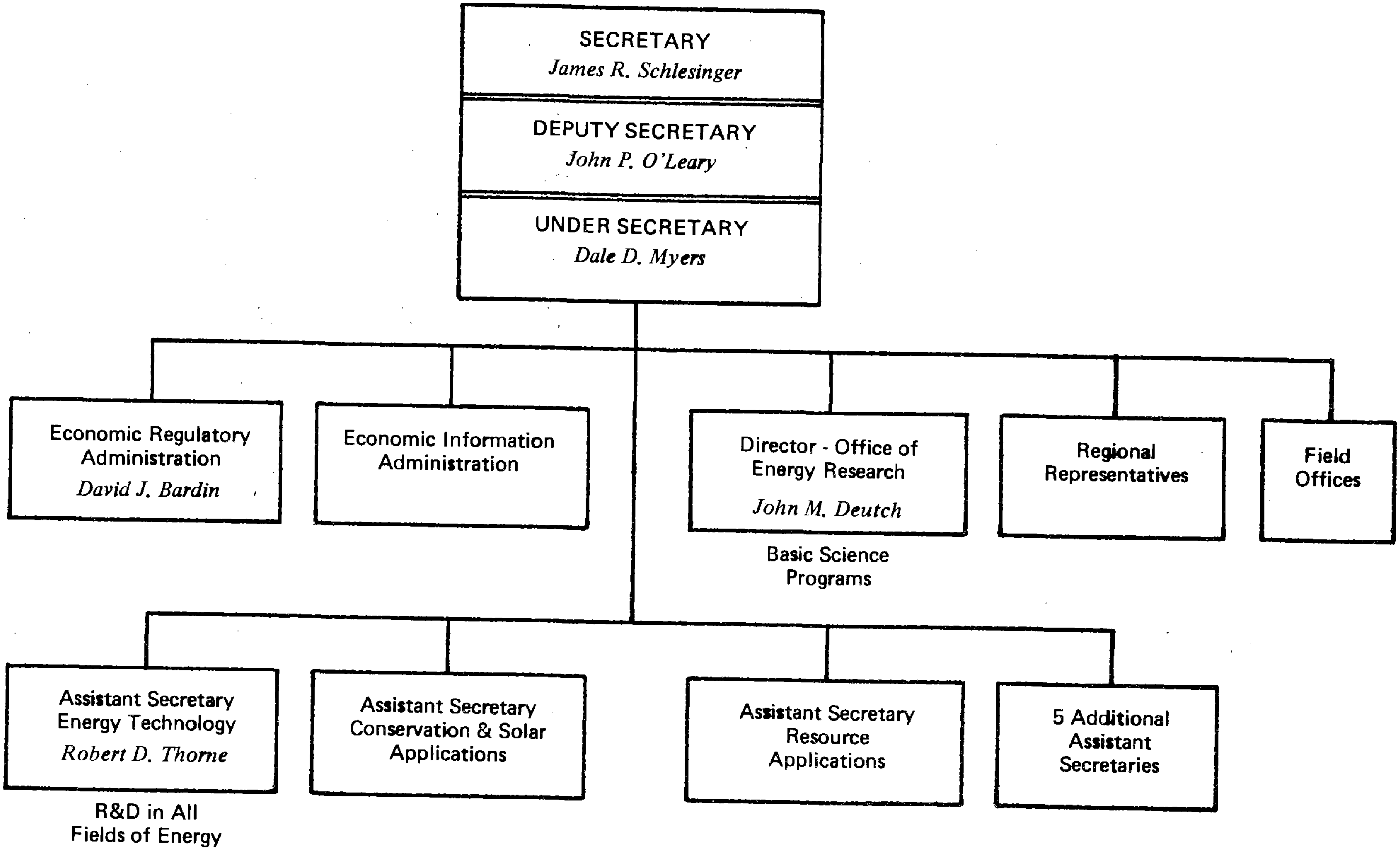

*Excluding Those Primarily Concerned With Weapons and Naval Reactor Programs

Figure 1. Department of Energy

- Initial Commercial Implementation of Dispersed Solar Thermal Power Systems by Early-1980s

- Establish Central Solar Thermal Power Systems As Economically Viable Generation Resource for Electric Utilities by Mid-1980s

Figure 2. Program Objectives

Central Power Applications	Advanced Technology	Dispersed Power Applications
• Storage Coupled Systems	• Supporting Technology	• Total Energy Solar Systems
• Repowering of Fossil Fuel Plants	• New Components and Processes	• Irrigation Pumping Systems
• New Solar Fossil Hybrid Systems	• Advanced System and Subsystem Development	• Small Power Systems
• Central Receiver Subsystems and Components	• Far Term Applications	
	• Facility Usage	

Figure 3. Program Organization

Dispersed Power Applications

- Complete Design and Initiate Construction of 3 Large-Scale Total Energy Experiments
  - Fort Hood, Texas
  - Shenandoah, Georgia
  - Mississippi County Community College, Blytheville, Arkansas
- Initial Operation of Second Solar Thermal Irrigation Pumping Experiment - Willard, New Mexico
- Site Selection for First Small Community Experiment

Central Power Applications

- Repowering Existing Power Plants
  - Complete Market and Concept Definition Studies
  - Establish Program for Feasibility Demonstration Experiments
- Initiate Support of EPRI Brayton Cycle Central Receiver Experiment
- Complete Concept and Definition Evaluation of
  - Alternative Central Receiver Concepts
  - Hybrid Systems
  - Low Cost Receiver and Heliostat Designs
- Break Ground for Barstow 10 MWe Central Receiver System Experiment

Figure 4. 1979 Projected Achievements

- Central Receiver
  - 10 MWe Pilot Plant
  - Alternative Concepts
  - Hybrid Concepts (Solar/Fossil)

    Repowering
    New Plants
- Linear Receiver
- Component Development
  - Low Cost Heliostats
  - Low Cost Receivers
- Solar Thermal Test Facility (STTF)

Figure 5. Central Power Applications

1. 10 MWe Pilot Plant at Barstow

   This plant is of crucial importance because it will provide the necessary "gate" of large-scale hard data and experience between the relatively small subsystem research experiments carried out during the preliminary design phase and STTF testing on the one hand, and the large advanced systems and hybrids of the future on the other hand.

2. Repowering

   With the new emphasis on near-term payoff, repowering represents an early market entry point. Repowering is an approach that can be readily integrated into existing utility systems.

3. Low Cost Heliostats

   The whole central power program can succeed only if low cost heliostats can be developed because over half the cost of of a central power plant is the collector subsystem.

Figure 6 shows a possible schedule which calls for six central receiver plants being on-line by 1986. Nothing on this chart is firm except the Barstow plant schedule. However, this chart does show one possible way of achieving the goal of establishing central power systems as an economically viable generation resource by the mid-1980s. Six plants on-line by 1986 represent a very large acceleration of the program. It might cost in the range of $3-4 billion of government and private funding. It would impose heavy problems of funding, manpower, materials availability, site availability, environmental assessments, and permits. And that's the good news. The bad news is that even if we somehow accomplished all those projects, they would be contributing only a small fraction of one Q! The point of such a program, however, is to furnish a solid base of experience and confidence from which a significant solar electric industry can grow.

	Capacity (MW)	Start Conceptual Design	Select Conceptual Design	Detailed Design	Operational
Barstow, Calif. Pilot Plant	10	6/75	8/77	9/78	9/81
Repowering I	25	2/78	11/78	4/80	11/82
Hybrid Fossil (with EPRI)	3	12/74	3/79	3/79	3/83
Repowering II	50	2/78	2/80	6/80	11/83
Hybrid Critical Module	50-300	8/78	3/81	3/82	3/85
Solar Storage Critical Module	50-300	6/75	9/82	9/83	9/86

Figure 6. Central Power Applications Projects

TECHNICAL OVERVIEW
SOLAR THERMAL CENTRAL POWER SYSTEMS PROGRAM

Sandia Laboratories
Livermore, California

Alan Skinrood

The elements of the central power programs are listed in Figure 1. The dates shown in Figure 2 for the projects are quite indefinite with the exception of the pilot plant at Barstow, California. The systems development part of the program consists of some advanced central receiver contracts, a repowering study that has been started, hybrid systems studies that will be started soon with the issuance of an RFP, and studies on linear focus systems for central power applications. The objective of the linear focus studies, which represent a broadening of the program, is to examine the possibility of dispersed collectors being used for centralized power on a large scale. The last part of the program is component development where individual receivers, receiver studies, heliostats, and energy storage work will be done.

Figure 3 shows the accomplishments since the last semiannual in Seattle. The Barstow activities are well under way at this point. All the reports from the original four major contracts for the pilot plant design--Boeing, Honeywell, Martin Marietta, and Stearns-Roger--are now available from TIC. The test facility in Albuquerque is nearing completion, and four advanced systems and four prototype heliostat contracts have been awarded. There was a workshop held in November, 1977, in Dublin, California, on systems analysis, and a follow-up workshop will be held in March, 1978.

The major advanced central receiver systems studies under way are shown in Figure 4. Both Atomics International and General Electric are exploring the possibility of using sodium as a coolant for the central receiver. Molten salt as a heat transfer fluid is being investigated by Martin Marietta. SAN has let a contract for the continuation of the EPRI work with Boeing, in which Boeing is performing more systems analyses and trade-offs on the concept that they started under EPRI funding. We expect to complete the last of the Phase I of the advanced systems contracts January, 1979. This date represents a slip in the program schedule. This slip resulted because some

PROJECTS

- BARSTOW, CALIFORNIA PILOT PLANT
- REPOWERING
- HYBRID/SOLAR/NON-SOLAR LARGE SCALE EXPERIMENT
- STORAGE COUPLED
- LINEAR FOCUS LARGE SCALE EXPERIMENT

SYSTEMS DEVELOPMENT

- ADVANCED CENTRAL RECEIVER CONTRACTS
- REPOWERING STUDY
- HYBRID SYSTEMS STUDIES
- LINEAR FOCUS SYSTEMS STUDIES

COMPONENT DEVELOPMENT

- RECEIVER
- HELIOSTATS
- ENERGY STORAGE

Figure 1. Solar Thermal Central Power Program

	CAPACITY (MW)	SELECT CONCEPTUAL DESIGN	START DETAILED DESIGN	OPERATIONAL
APPROVED				
BARSTOW, CALIF PILOT PLANT	10	8/77	9/78	9/81
TENTATIVELY PROPOSED				
REPOWERING I	25	11/79	4/80	11/82
HYBRID FOSSIL (WITH EPRI)	3	3/79	3/79	3/83
REPOWERING II	50	2/80	6/80	11/83
HYBRID CRITICAL MODULE	50 - 300	3/81	3/82	3/85
SOLAR STORAGE CRITICAL MODULE	50 - 300	9/82	9/83	9/86

Figure 2. Central Power Applications Projects

- BARSTOW PILOT PLANT ACTIVITIES UNDERWAY
- CONTRACTOR REPORTS ON FIRST GENERATION TECHNOLOGY PUBLISHED
- TEST FACILITY IN ALBUQUERQUE NEARING COMPLETION
- 4 ADVANCED SYSTEMS AND 4 PROTOTYPE HELIOSTAT CONTRACTS AWARDED
- REPOWERING STUDY STARTED
- SYSTEMS ANALYSIS WORKSHOP HELD
- HELIOSTAT CODES DOCUMENTED

Figure 3. Accomplishments Since Last Semiannual in August, 1977

OBJECTIVE:	DEVELOP ADVANCED SYSTEM CONCEPTS
STATUS:	CONTRACTS AWARDED FOR SODIUM COOLANT SYSTEMS (ATOMICS INTERNATIONAL AND GENERAL ELECTRIC);
	MOLTEN SALT (MARTIN MARIETTA) AND BRAYTON CYCLE (BOEING)
	SPECIAL BRAYTON CYCLE STUDIES CONTINUING (DYNATHERM AND SANDERS ASSOCIATES)
MILESTONES:	OCTOBER, 1977 .....PHASE 1 CONTRACTS AWARDED
	- JANUARY, 1978
	JANUARY, 1979 ...... PHASE 1 COMPLETE
	FEBRUARY, 1980..... PHASE 2 COMPLETE

Figure 4. Advanced Central Receiver Systems Studies

contracts were late in being initiated. The Phase II shown is an experimental phase, which will be completed in 1980.

The repowering study that has been started at the Public Service of New Mexico is summarized in Figure 5. They have completed their market survey of the nine states and will have the initial phase of the study done in November of this year. We plan to extend the market survey to the rest of the U.S. to determine the total market for repowering.

Figure 6 summarizes the hybrid systems development. As shown, an RFP has been prepared; our goal is to issue it in March, 1978, and have contracts before the end of the fiscal year. A one-year initial paper study will be conducted, followed by a one-year study that combines experiments with analysis.

An RFP prepared on linear focus systems is nearing completion (see Figure 7). The RFP is in draft form, and the target date for issuance is April, 1978. The same general format will be followed--initially a one-year study program, followed by some experimentation.

As shown in Figure 8, we plan to issue an RFP on advanced water/steam development to to determine whether there are improvements that can be made to the first-generation technology of water/steam. Again, the target date for issuance is April, 1978.

Now, in addition to the major component development, individual studies are being conducted with universities and private industrial organizations. They are listed in Figure 9 and are discussed in detail later in this report. We do want to conduct a series of topical studies and are entertaining suggestions on what individual studies need to be done. In particular, we'd like to encourage more university participation. Some universities are represented, but we would like to encourage more university participation in studies of some of the aspect of receiver design. One major study we feel to be important is the development of a scheme for estimating tower costs for receivers. Such a scheme would be a parametric series of curves where you could find the tower cost versus height versus weight versus earthquake design load. The contractor for that study has not been selected yet.

Several other studies are either planned or on-going. The sodium test program will be coordinated with GE and AI, who are the major developers of sodium receivers. We will also conduct a molten salt study because the molten salt stability measurements and compatibility testing are applicable to both receivers and storage. The direct absorption study is being done in-house and will be covered in a separate semiannual report.

Figure 10 shows that the goal of the heliostat development program is to achieve a cost of \$72/m^2 of reflectivity. This figure was obtained by dividing the original program goal of \$65/m^2 by the reflectivity to put both

OBJECTIVE:	DEVELOP METHODS FOR ADDING SOLAR CENTRAL RECEIVER SYSTEMS TO EXISTING FOSSIL FUEL POWER PLANTS
STATUS:	STUDY BEING CONDUCTED BY THE PUBLIC SERVICE COMPANY OF NEW MEXICO, INCLUDING MARKET SURVEY OF 9 STATES
MILESTONES:	FEBRUARY, 1978 . . . CONTRACT AWARDED
	APRIL, 1978. . . INITIATE MARKET SURVEY FOR BALANCE OF U.S.
	NOVEMBER, 1978. . . . . . STUDY COMPLETE

Figure 5. Repowering Study

OBJECTIVE:	DEVELOP CONCEPTUAL DESIGNS FOR POWER PLANTS COMBINING A SOLAR CENTRAL RECEIVER ENERGY SOURCE WITH A NON-NUCLEAR ENERGY SOURCE
STATUS:	RFP HAS BEEN PREPARED
MILESTONES:	MARCH, 1978 . . . . ISSUE RFP
	AUGUST, 1978. . . . . . . AWARD CONTRACTS
	AUGUST, 1979. . . . . COMPLETE PHASE 1
	SEPTEMBER, 1980 . . . . COMPLETE PHASE 2

Figure 6. Hybrid Systems Development

OBJECTIVE:	DEVELOP SOLAR THERMAL POWER PLANTS WHICH UTILIZE LINEAR RECEIVERS TO COLLECT SOLAR ENERGY REDIRECTED BY MIRRORS TRACKING IN A SINGLE AXIS
STATUS:	RFP PREPARED
MILESTONES:	APRIL, 1978.................. ISSUE RFP
	SEPTEMBER, 1978 ... AWARD CONTRACTS
	SEPTEMBER, 1979 .... COMPLETE PHASE 1
	OCTOBER, 1980 ...... COMPLETE PHASE 2

Figure 7. Linear Focus Systems Development

OBJECTIVE:	DEVELOP IMPROVED RECEIVERS UTILIZING STATE-OF-THE-ART WATER STEAM TECHNOLOGY AND EXPLORE HIGHER PRESSURE, HIGHER TEMPERATURE RECEIVERS
SCOPE:	RFP PREPARED
MILESTONES:	APRIL, 1978............... RELEASE RFP
	AUGUST, 1978....... AWARD CONTRACTS
	AUGUST, 1979........ COMPLETE PHASE 1
	SEPTEMBER, 1980 .... COMPLETE PHASE 2

Figure 8. Receiver Development - Advanced Water/Steam

- CONVECTIVE LOSSES - UNIVERSITY OF ILLINOIS
- TWO PHASE FLOW - UNIVERSITY OF MINNESOTA
- CODE REQUIREMENTS - FOSTER WHEELER
- MATERIALS TESTING - ARGONNE LABORATORIES
- TOWERS - CONTRACTOR TO BE SELECTED
- SALT STABILITY/COMPATABILITY TESTING - SANDIA LABORATORIES, MARTIN MARIETTA
- SODIUM TESTING - CONTRACTORS TO BE SELECTED
- DIRECT ABSORPTION - SANDIA LABORATORIES

Figure 9. Receiver Development - Special Studies

OBJECTIVE:	DEVELOP LOW COST HELIOSTATS WHICH APPROACH THE DOE GOAL OF $72/M^2 REFLECTIVITY
STATUS:	PROTOTYPE HELIOSTAT CONTRACTS AWARDED TO BOEING, GENERAL ELECTRIC, MCDONNELL DOUGLAS, SOLARAMICS "IDEA" HELIOSTAT RFP BEING PREPARED
MILESTONES:	PROTOTYPE HELIOSTAT CONTRACTS
	SEPTEMBER, 1977 . . .PHASE 1 CONTRACTS AWARDED
	- JANUARY, 1978
	SEPTEMBER, 1978 . . . . PHASE 1 COMPLETE
	OCTOBER, 1979 . . . . . . PHASE 2 COMPLETE
	"NEW IDEA" RFP
	MAY, 1978 . . . . RELEASE RFP
	SEPTEMBER, 1978 . . . AWARD CONTRACTS
	JUNE, 1979 . . . . COMPLETE PHASE 1

Figure 10. Heliostat Development

the plastic and glass mirror designs on a par so that heliostats with different reflectivities can be compared. One activity in the heliostat area of particular interest is the "idea" heliostat RFP which is being prepared. Tentatively, the goal is to make it easier for small businesses to participate in the heliostat program by making both small and large awards under the idea heliostat RFP. The RFP is planned for release in May, 1978.

We would like to do generic development on heliostats, including mirror modules and production processes, and would welcome unsolicited ideas and proposals for the areas where more work is needed. In previous contracts for development of a complete heliostat, it has been impossible to explore in detail all of the subsystem alternatives. Thus we propose to do some generic studies and make the results available to everybody who is working on heliostats.

The remaining studies listed on Figure 11 are discussed specifically later in this report. There is not a specific presentation on the wind studies, but each of the contractors--Boeing, Honeywell, Martin Marietta, and McDonnell Douglas--have conducted or are planning to conduct wind tunnel testing and the results will be factored into what the actual wind design requirements should be, and the wind's effects on the field.

The energy storage activities are listed in Figure 12, and as many of you know, the DOE's Division of Energy Storage is doing most of the energy storage subsystem development. There are some storage activities in the Solar Program; also, some of the funding from Solar has gone over to the Division of Energy Storage for storage studies. One thing needed is a definition of the storage requirements for the Central Power program. We are preparing a draft of these requirements that will be issued in March, 1978.

Figure 13 summarizes the overall schedule for all of the central power projects. The goal of the program is to develop technology alternatives by 1980 for use in the proposed projects.

- GLASS SOURCE SURVEY - BATTELLE
- FOAM CHARACTERIZATION - BATTELLE
- FIELD COMMUNICATIONS - HONEYWELL
- GENERIC DEVELOPMENT TO BE STARTED
  - DRIVE SYSTEMS
  - MIRROR MODULES
  - PRODUCTION PROCESSES
- INVERTED STOW REQUIREMENTS - MCDONNELL DOUGLAS
- ONE PIECE PLASTIC DOME - BOEING
- GLASS AGING - SANDIA LABORATORIES
- DUST BUILD-UP & CLEANING - SANDIA LABORATORIES
- WIND STUDY - SANDIA LABORATOIES
- OPTIMIZATION STUDIES - SANDIA LABORATORIES
- INSTRUMENTATION DEVELOPMENT - SANDIA LABORATORIES

Figure 11. Heliostat Development - Special Studies

- OIL SIDESTREAM PROCESSOR DEVELOPMENT - MARTIN MARIETTA
- FLOW LOOP TESTING - MCDONNELL DOUGLAS
- REQUIREMENTS DOCUMENT - SANDIA LABORATORIES
- SALT/ROCK TESTING - SANDIA LABORATORIES
- STORAGE OIL STABILITY TESTING - SANDIA LABORATORIES

Figure 12. Energy Storage

CENTRAL POWER SYSTEMS R&D SCHEDULE

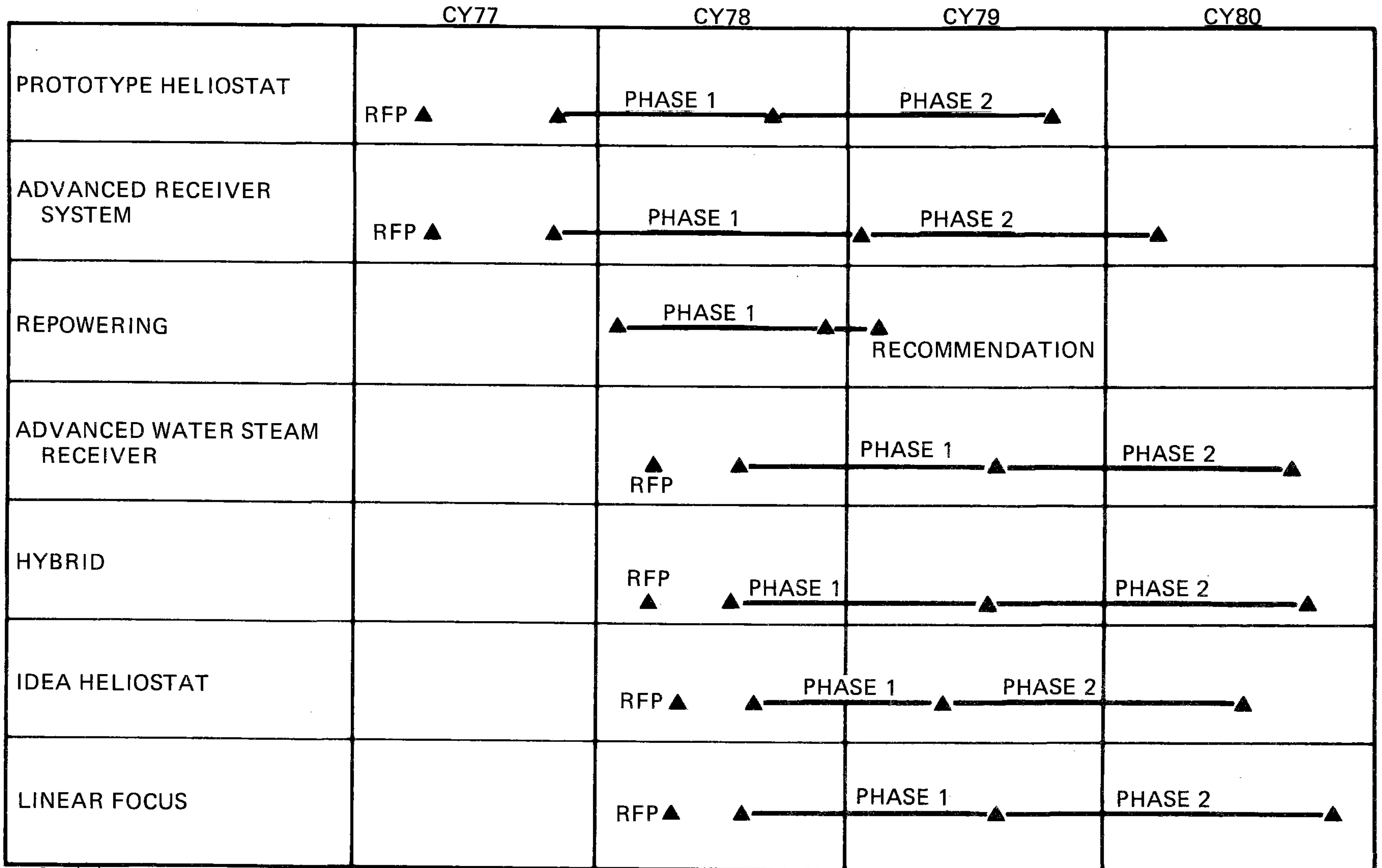

ACS:2/9/78

Figure 13. Central Power Systems R&D Schedule

SOLAR-THERMAL CONVERSION PROGRAM

Electric Power Research Institute
J. E. Bigger

Introduction

The Electric Power Research Institute is a nonprofit R&D organization that is supported by the electric utility industry. Over 500 member utilities support the Institute; investor-owned companies, publically-owned utilities, and rural cooperatives are all members. The Institute receives no federal funds, but does participate in many joint projects in various technical areas.

The Institute's 1978 total R&D budget is about $195 million. There is very little in-house research done at EPRI; the R&D is contracted out to industry, the academic community, and others.

EPRI Solar Program

The EPRI Solar Program is divided into three major areas of effort:

- Solar Heating and Cooling of Buildings (SHAC)
- Solar Electric Conversion
- Technology Assessment

The five-year Solar Program budget estimate is a little over $24 million; the 1978 budget is about $4 million. There are two major thrusts in the Solar Program: (1) SHAC, and (2) solar-thermal; the first has just over 40 percent of the budget, and the second has slightly under 40 percent.

The EPRI Solar Program is supporting studies, hardware, and systems development. The studies stress the impact and interface questions and problems as they relate to the electric utility industry. The electric utilities, after all, will be the major market for solar-thermal conversion systems, not only central receiver concepts but also the distributed and disbursed systems.

Solar-Thermal Conversion Program

One of the major objectives of the EPRI Solar-Thermal Program is to develop systems that have potential benefit for electric power generation application. To achieve that, the development of two brayton-cycle central receiver concepts is being supported: a closed-cycle design is now under development at Boeing Engineering and Construction and an open-cycle design with Black & Veatch Consulting Engineers. The Boeing bench model receiver uses air as the heat transfer gas; has Inconel 617 superalloy heat exchanger panels; and is designed to heat gas to 815°C (1500°F). The Black & Veatch bench model receiver design uses air as the heat transfer gas; uses ceramic heat exchanger tubes (SiC); and will be designed to heat air to 1065°C (1950°F). At this time, ceramic-to-ceramic and ceramic-to-metal joint development is continuing. If the joint designs are successfully qualified, this second receiver will be fabricated later this year.

Figure 1 outlines the schedule and phases for the two EPRI central receiver projects. The major progress to date is the fabrication of a 1-MWt, bench model receiver by Boeing and their subcontractors (Figure 2). This unit will be tested initially in Seattle, Washington, and then on June 1, 1978, it will arrive at the 5-MWt Solar-Thermal Test Facility at Albuquerque, New Mexico. The solar testing of the receiver, a joint EPRI-DOE test program, will begin in July and is expected to last throughout the summer.

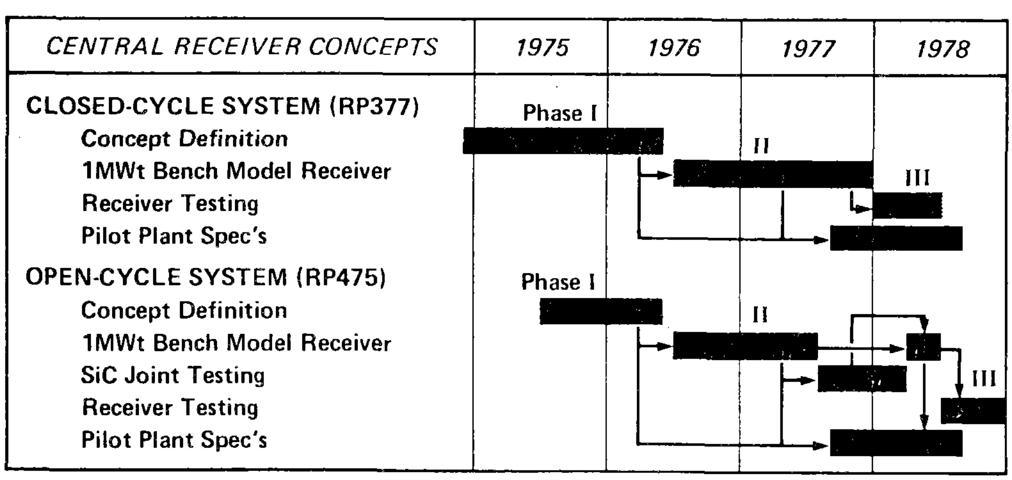

Figure 1. Solar Thermal Conversion Subprogram

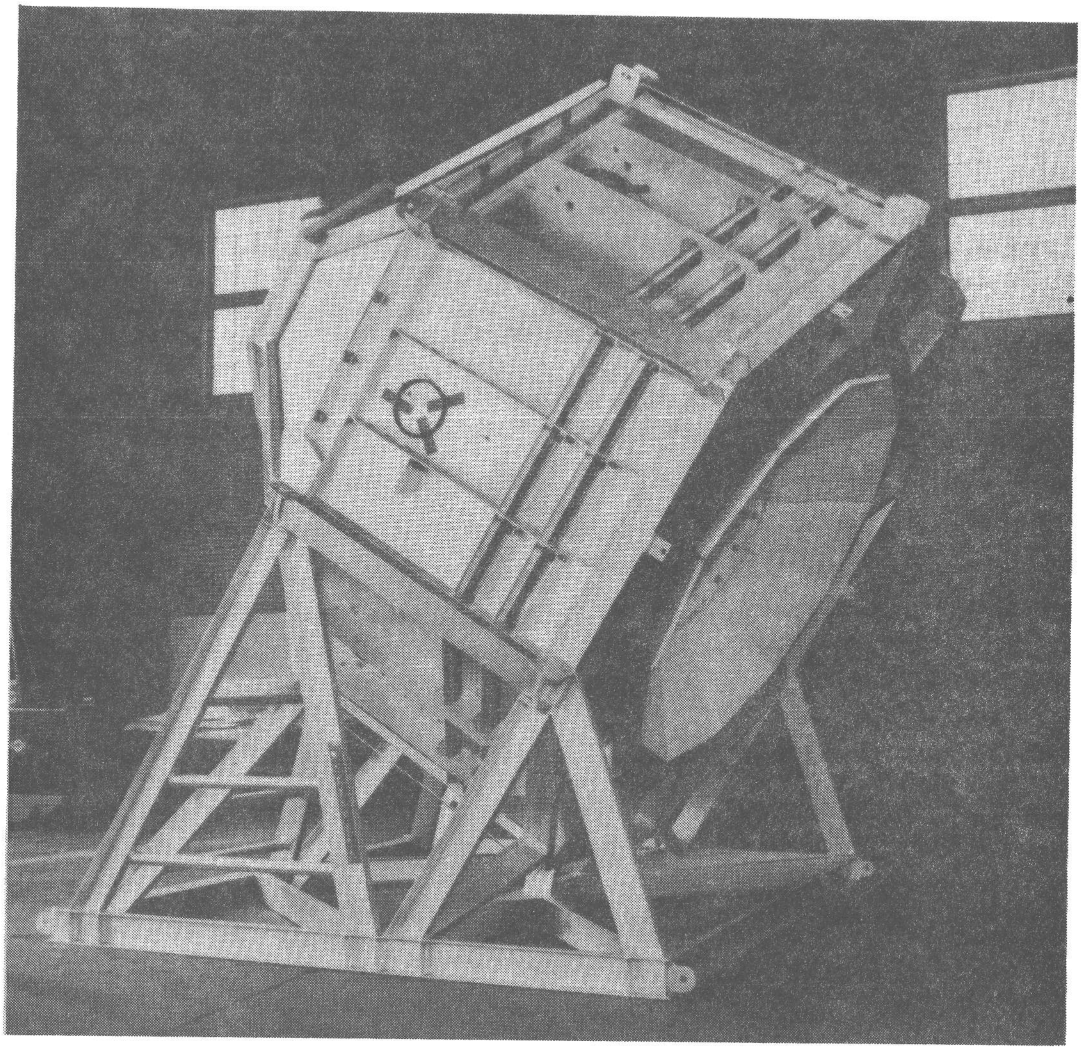

Figure 2. Boeing Designed 1-MWt Solar Bench Model Receiver

In addition to the central receiver projects, a smaller effort is answering specific questions about one distributed receiver concept; this is the General Atomics fixed mirror solar concentrator. A laboratory testing project is just being completed to examine the various heat loss characteristics of the receiver with various materials and design configurations.

A second major objective of the EPRI Solar-Thermal Program is to assess the value and impact of solar-thermal power plants on electric utility systems. A number of projects are under way or being completed that support this effort:

- Requirements Definition and Impact Analysis - A study to evaluate the technical and economic value of solar thermal power plants on actual electric utility systems using utility system tools [Westinghouse Electric Corporation (RP648)] .

- Environmental Impact Assessments -

  (1) Develop and modify a highly innovative methodology to address problems of environmental impact of solar-thermal power plants [Woodward Clyde Consultants (RP551)].

  (2) Develop a methodology and assess the environmental effects of several types of solar energy plants [Black & Veatch Consulting Engineers (RP955)].

- Solar-Fossil Hybrid Retrofit - Assess the technical and economic feasibility of repowering existing oil- and gas-fueled power plants with solar-thermal rankine and brayton-cycle systems. EPRI, DOE, West Associates, and specific electric utilities are funding this effort [Public Service Company of New Mexico (TPS 77-730)].

- Heliostat Cost Study - An independent assessment of the cost reduction potential for the four ERDA/DOE developed heliostat designs [A. D. Little, Inc. (RP1091)].

- Gas Turbine Modification and Test - A test program to address the technical aspects of operating a commercial gas turbine in a solar-fossil hybrid mode [Solar Turbines International (RP1270)].

Figure 3 outlines the schedule and phases for the technical assessment projects in the EPRI Solar-Thermal Program.

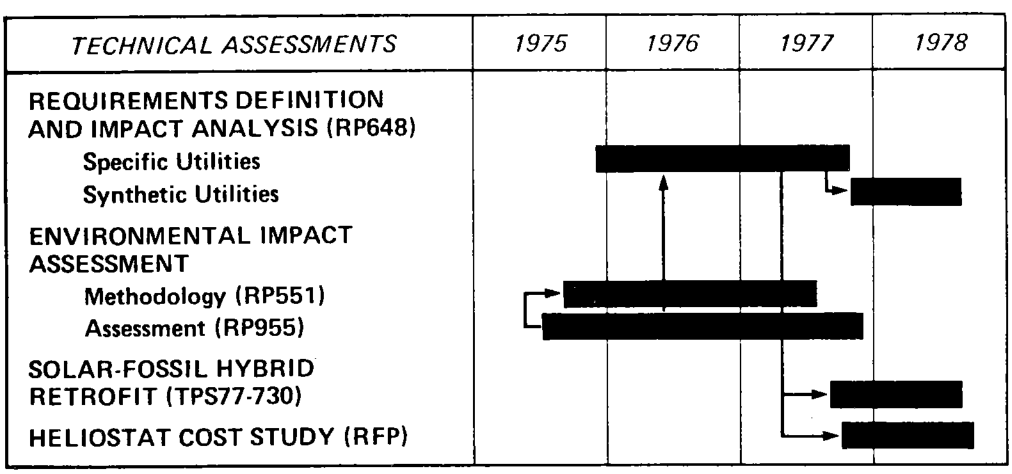

Figure 3. Solar Thermal Conversion Subprogram

10-MWe Scale Pilot Plant

Included in the EPRI Solar-Thermal Program are plans for a 10-MWe scale brayton-cycle pilot plant. This plant would have only one quadrant of the heliostat field, would use fossil fuel as a back-up energy source instead of thermal storage, and would use a commercially available gas turbine with an electrical output in the 2.7-MWe range.

The two EPRI contractors (Boeing and Black & Veatch) now working on central receiver concepts are also working on pilot plant definition studies. The presently scheduled operating date for the 10-MWe scale pilot plant is the first quarter of 1983.

Summary

The EPRI Solar-Thermal Program is a complement to the much larger federal program, and is addressing those questions specifically related to the electric utility industry's use of solar-thermal systems. The commitment of resources, both technical and financial, in support of both the EPRI and the federal solar thermal programs is an indication of interest in seeing these systems develop into viable electric power generation resources in the not-too-distant future.

FIELD PROGRAM MANAGEMENT

Solar Energy Division, DOE-SAN

Robert W. Hughey

Current DOE management policy is toward decentralization from Headquarters to the Field. The overall Solar Thermal Power Systems Management Plan, which has been approved and issued, provides a framework and guide for decentralization. It describes the roles, responsibilities, authorities, and relationships of the principal participating organizations in the Thermal Power Systems Program.

The Central Power Systems Program is in the process of being decentralized, consistent with the overall Thermal Power Systems Management Plan. A functional chart of the principal participants of the Central Power Systems Program is shown in Figure 1. Under the DOE decentralization philosophy, the Field Program Manager does not have to be a DOE Field Office such as SAN or ALO. In some cases, depending on the optimum matching of field resources to program management requirements, it may prove most effective to designate a JPL, Sandia, or SERI to be the Field Program Manager.

In the case of the Central Power Systems Program, a management plan has been developed which splits the field program management responsibility between SAN and SLL as shown in Figures 2 and 3. The element of the Central Power Systems Program that has been most clearly decentralized is the 10-MW pilot plant. Dick Schweinberg addresses that project and its management on page 43 of this report.

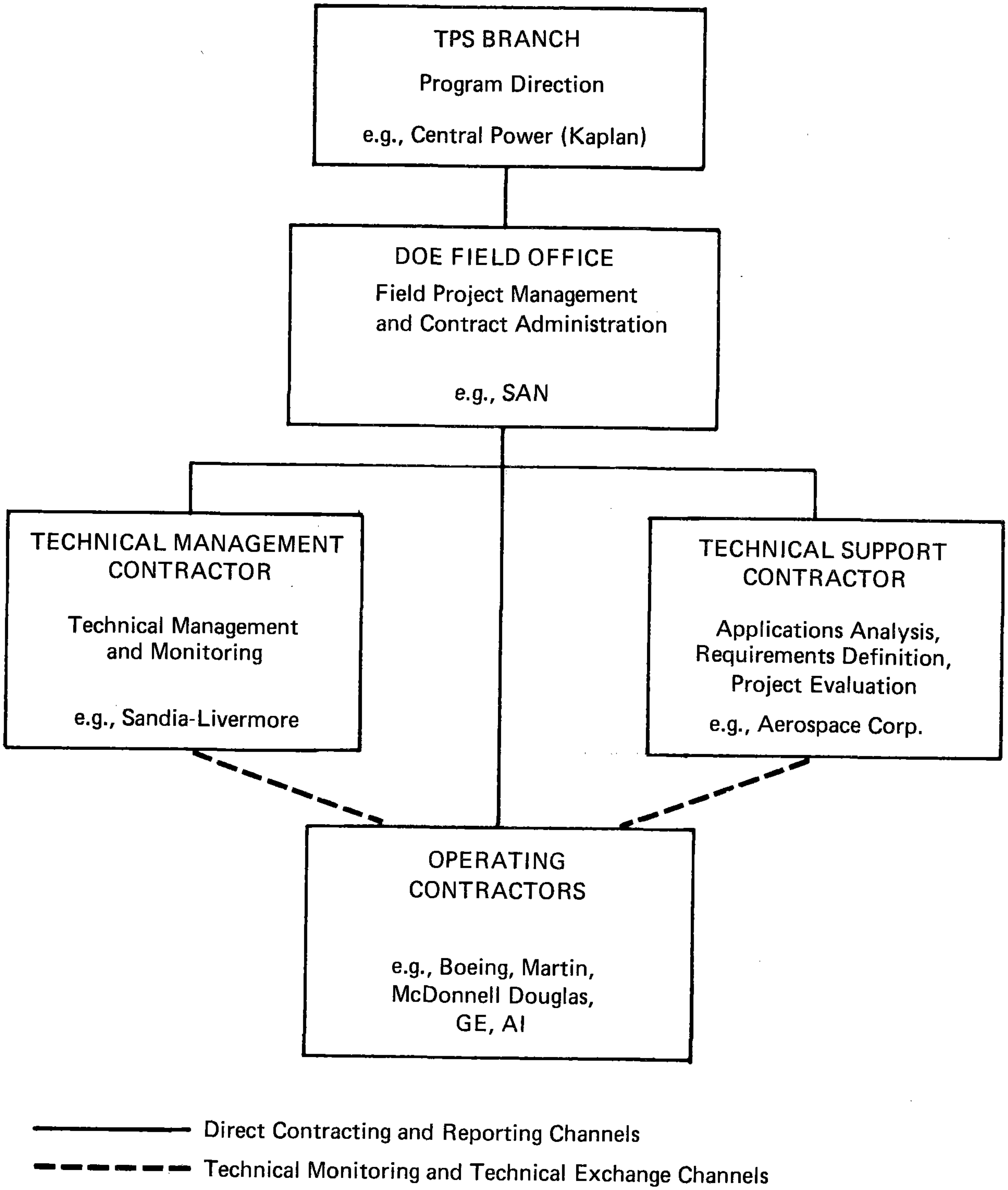

Figure 1. Principal Participants - Central Power Systems Program

SYSTEMS DEVELOPMENT PROJECTS

Program Coordination and Contract Administration by SAN;
Technical Management, Supporting Systems Analysis by SLL.

Advanced Central Receiver Systems Project

Solar Hybrid Repowering Project

Solar Central Receiver Hybrid Power Systems Project

Line-Focus Central Receiver Systems Project

Figure 2

COMPONENT DEVELOPMENT PROJECTS

Contract Administration and Technical Management by SLL;
SAN Maintains Programmatic Awareness, Provides Support As Required.

Heliostat Development

Receiver Development

Energy Storage Development

Electric Power Generation Systems Requirements Definition

Control Systems Requirements Definition and Modelling

Figure 3

THE SOLAR ENERGY RESEARCH INSTITUTE

Charles J. Bishop

The Solar Energy Research Institute's overall mission is to provide significant support to the national program of research, development, demonstration, and deployment of solar energy. A central responsibility in this effort is to contribute to the establishment of a solar energy industrial base capable of supporting the widespread commercial use of the technology.

SERI is working toward the creation of a national center of excellence-- a resouce dedicated to serving the solar energy needs of the public and industry. SERI is initiating continuing programs in:

- research,
- analysis and assessment,
- information and education,
- technology commercialization, and
- international solar energy efforts.

In addition, we expect to assume responsibility for the technical monitoring of a number of existing and planned federal solar R&D programs

We interpret our charter as rather broad. Our programmatic efforts can be grouped into five general areas:

1. Conducting applied research directed toward the timely development of solar energy technologies which have long-term promise.

2. Participating in an important way in the conception, evaluation, and development of innovative methods for solar energy conversion.

3. Undertaking further analysis of issues which affect the near-term utilization of solar energy.

4. Carrying out efforts designed to reduce remaining uncertainties associated with solar energy--technical uncertainties, institutional uncertainties, economic uncertainties, and social uncertainties.

5. Developing and implementing methods of providing direct assistance to the public and industry--assistance in the form of information dissemination and technology transfer designed to facilitate consumer and business decisions regarding solar energy.

SERI is organized into five operating divisions as shown in Figure 1. The staff currently numbers 185. Our plans call for a total staff of 300 by October 1, 1978; and 480 by October 1, 1979 (Figure 2).

SERI is now housed in interim facilities in Golden, Colorado. We presently have 33,000 square feet of space. An additional 66,000 square feet will be added in summer 1978, when the second building is completed. The first experimental laboratories will be designed into the building scheduled for 1978 completion. The Department of Energy (DOE) now holds an option on 300 acres atop South Table Mountain in Golden for the possible site of the permanent facilities.

Our programmatic and operational objectives are becoming more clearly defined as we continually assess perceptions of SERI's mission (Figure 3). Clearly, we will be conducting solar energy R&D for all the major functional solar technologies. Support of disciplines such as materials, corrosion, and surface physics will be undertaken. Analysis and assessment efforts will include evaluation of national solar energy programs.

We expect to play an important role in the administration of university solar energy research programs--including the evaluation of proposals and the management of contracts. SERI wants to encourage the universities to get back into the creative mode with respect to solar energy.

The technology commercialization effort includes a technology transfer program, a program of assistance to business and industry, and a liaison function--all designed to promote early utilization of solar energy.

SERI has already begun to assume a central responsibility for U.S. involvment in international solar energy programs--including research, information exchange, and technology transfer. A recent agreement has been reached with the Saudi Arabian government to expend $100 million ($50 million by each country) over the next five years for joint solar energy research and development. SERI will manage that effort the first year.

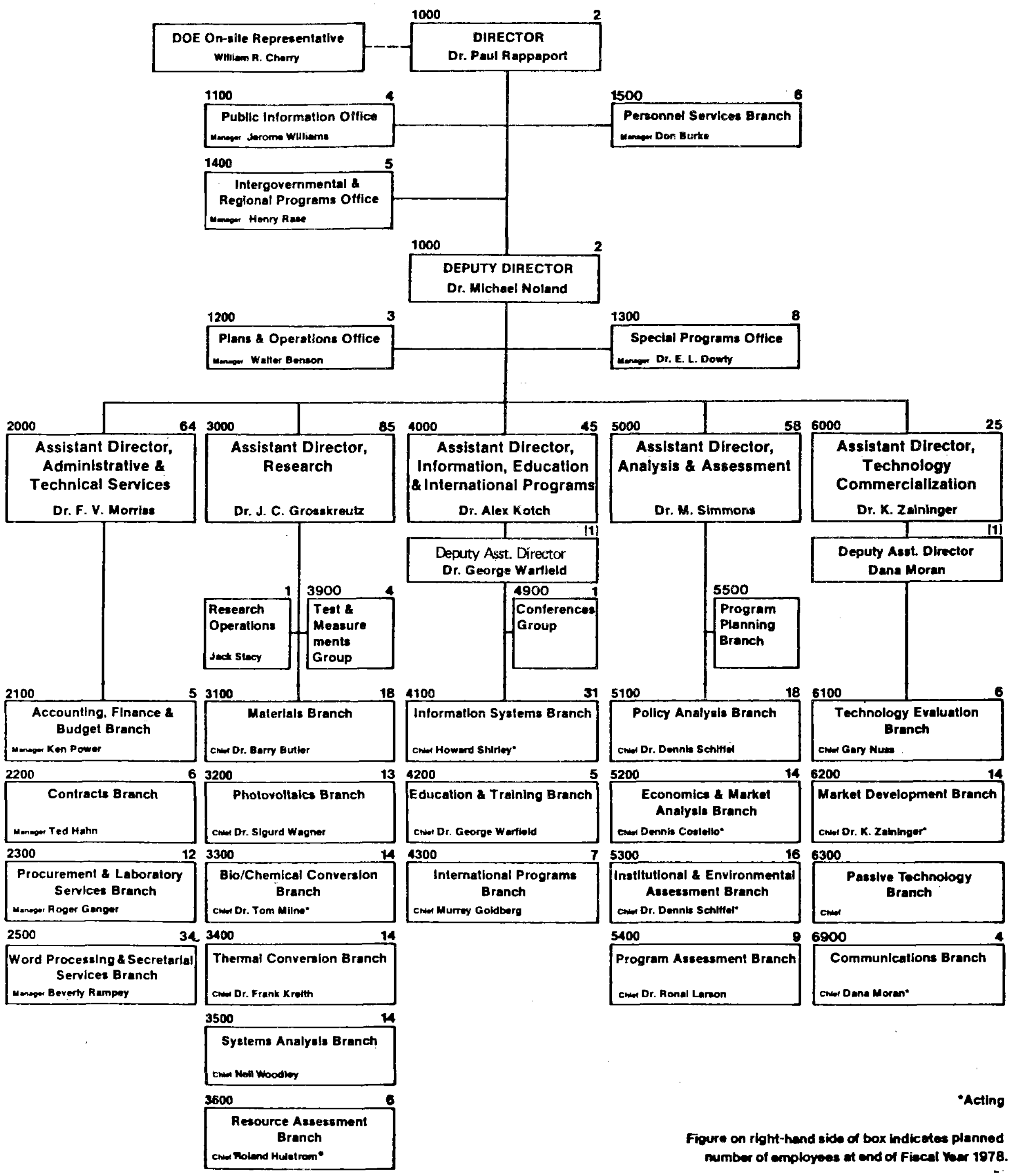

Figure 1. Solar Energy Research Institute Organization Chart

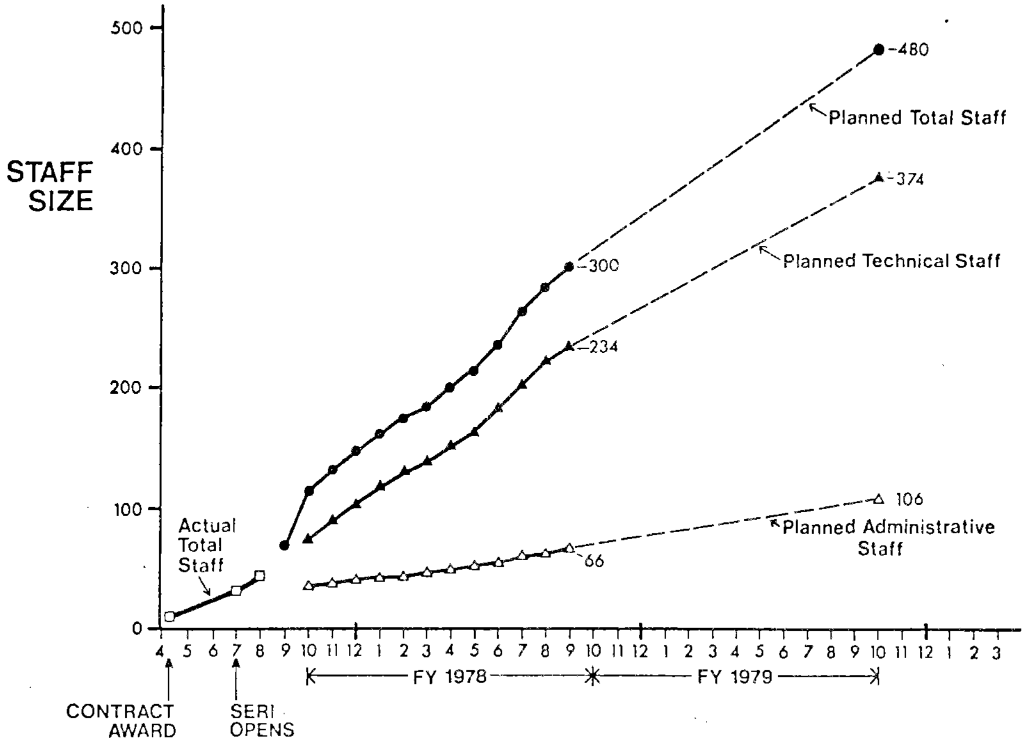

Figure 2. Solar Energy Research Institute Staffing Plan

- **Conduct Solar Energy R & D**
- **Evaluate Solar Energy Programs**
- **Administer Contract and University Research**
- **Promote Early Utilization of Solar Energy**
- **Coordinate U.S. Involvement in International Solar Energy Programs**
- **Establish Solar Energy Information Data Bank**
- **Conduct Solar Energy Conferences**
- **Develop Plans for Permanent SERI Facilities**

Figure 3. Solar Energy Research Institute Objectives

We are establishing an information data bank and library which we expect to become the most extensive solar energy information resource in the nation--indeed, in the world. Utilizing this resource, we should be able to contribute significantly to the Department of Energy's program of providing information on solar energy to the public.

We host and conduct solar energy conferences, seminars, and workshops--those conceived and organized by SERI or DOE and, by request, those which are part of other efforts.

Finally, we have developed a plan for the permanent SERI facilities including research laboratories, a conference center, a library, and administrative facilities.

Several key projects are currently under way although the staff is by no means complete. The staffing plan, initial task definitions, and FY78 financial plan are all complete. The Mission Definition Report, which details the mission, philosophy, and goals of SERI; why it exists; and what it is expected to contribute to the national solar energy program, has been completed and submitted in preliminary draft form to DOE. The Annual Operating Plan, which describes in greater detail the tasks SERI will undertake in FY78, and the Facilitites Plan, which will include plans for both the interim facilities and a preliminary version of what the permanent facilities might look like, have been submitted for DOE approval.

In summary, SERI is now an operating organization with a team of highly qualified professionals totally dedicated to the concept of SERI and actively carrying out its intended mission to contribute significantly to the commercial development of solar energy.

SOLAR CENTRAL RECEIVER 10-MWe PILOT PLANT

Department of Energy

Richard N. Schweinberg

Southern California Edison Company

J. Lynn Rasband

Background

At the Seattle meeting in August, 1977, DOE announced the concepts selected for the pilot plant subsystems and reviewed the project objectives. In keeping with DOE's increased emphasis on near term reduction of oil and gas usage, the pilot plant objectives, shown in Table I, now place particular emphasis on satisfying the technical feasibility and economic data needs for retrofit applications of solar boilers to existing power plants fueled by oil or natural gas.

TABLE I

PROJECT OBJECTIVES

Principal Objectives

- Establish technical feasibility of solar thermal power plants of the central receiver type, particularly for retrofit applications of solar boilers to existing power plants fueled by oil or natural gas.
- Obtain sufficient development, production, operating and maintenance cost data to identify potential economics of commercial solar plants of similar design, especially retrofit applications of a comparable scale.
- Determine environmental impact.

Other Objectives

- Establish system dynamics, stability, and safety.
- Develop industry acceptance of solar thermal systems.
- Stimulate industrial manufacture and further development.
- Enhance public acceptance.

The pilot plant is a cooperative effort between DOE and the Associates (Southern California Edison, Los Angeles Dept. of Water and Power, and the California Energy Commission). The day-to-day management responsibility has been assigned to a dedicated project office now located in Los Angeles.

Southern California Edison's participation stems from their search for alternate generating concepts such as geothermal, fuel cells, wind, photovoltaic, and solar thermal. Solar thermal is attractive because of the high insolation available in large, unpopulated desert areas. Solar energy would be available during peak electric usage periods to help electric utilities meet maximum power demands, and solar plants would provide the energy without emitting air contaminants and without using exhaustible energy sources.

Answers to many questions must be known in detail before utilities will be willing to commit large expenditures to build commercial solar generating plants. These questions include:

Heliostats

- Glass versus support interface
- Track accurately versus time
- Washing frequency
- Potential for cost reduction
- Reliability of equipment

Receiver/Boiler

- Temperature cycling
- Tube pluggage/blockage
- Black surface lifetime
- Control system reliability

Thermal Storage

- Fluid life expectancy
- Verification of thermal performance

Turbine-Generator

- Temperature cycling

System Requirements

- Overall reliability
- Overall maintenance cost
- Subsystems function as team
- Start up/shut down rates
- Control and mode switching

Extrapolate Economics

- Cost to build plant
- Less associated R&D
- Economy of scale credits
- Production break-through credits

The pilot plant will provide invaluable experience and data to permit utilities to understand technical feasibility and to extrapolate capital and operating costs to project economic feasibility.

The total project costs, shown in Figure 1, are divided between DOE and the Associates. DOE will fund the solar facilities, and the Associates will fund the turbine-generator facilities. The 90-day DOE deferral of a portion of the project's FY78 funding has been lifted and the full $41M has been restored. Congress has been requested to provide $28M in FY79 obligational authority.

• TOTAL PROJECT	$120M
• DEPARTMENT OF ENERGY	$100M
• UTILITY	$ 20M

Figure 1. Project Costs

The change in the project completion date to September, 1981 (see Figure 2), is a result of DOE's revised schedule for selecting the solar facilities designers and the fiscal year funding projected for government obligations.

- PRELIMINARY ENGINEERING, DESIGN AND CONSTRUCTION

  DOE SELECTS SITE . . . . JANUARY 6, 1977

  DOE SELECTS SOLAR CONTRACTOR . . . . . AUG-SEPT, 1978

  START PLANT CONSTRUCTION . . . . JANUARY, 1979

  COMPLETE CONSTRUCTION . . . . APRIL, 1981

  INITIATE PLANT OPERATION . . . . SEPTEMBER 1981

- TESTING PERIOD

  5 YEARS

Figure 2. Program Schedule

Plant Requirements

A major effort of the Project Office has been to finalize the overall plant requirements. One approach to sizing the plant is to assess the hours of 10-MWe operation possible during various days of the year (see Figure 3). The benefit from adding additional heliostats to obtain additional hours of 10-MWe operation appears to be of diminishing return above about 1900 heliostats. Thermal storage sizing can be tied to accommodating all excess energy above that to operate at 10-MWe on the best day of the year. Actual Barstow, California, environmental data (Figure 4) has been assimilated and is available from Aerospace Corporation.

A dynamic computer simulation of the Pilot Plant is being developed and will be available for distribution in April, 1978.

The project office has been cognizant of the ASME code-related activities being performed by Foster Wheeler and the ASME Solar Task Group. It is anticipated that the pilot plant receiver will be code-stamped to ASME Section I with supplemental rules applied from Section VIII and Code Case N-47.

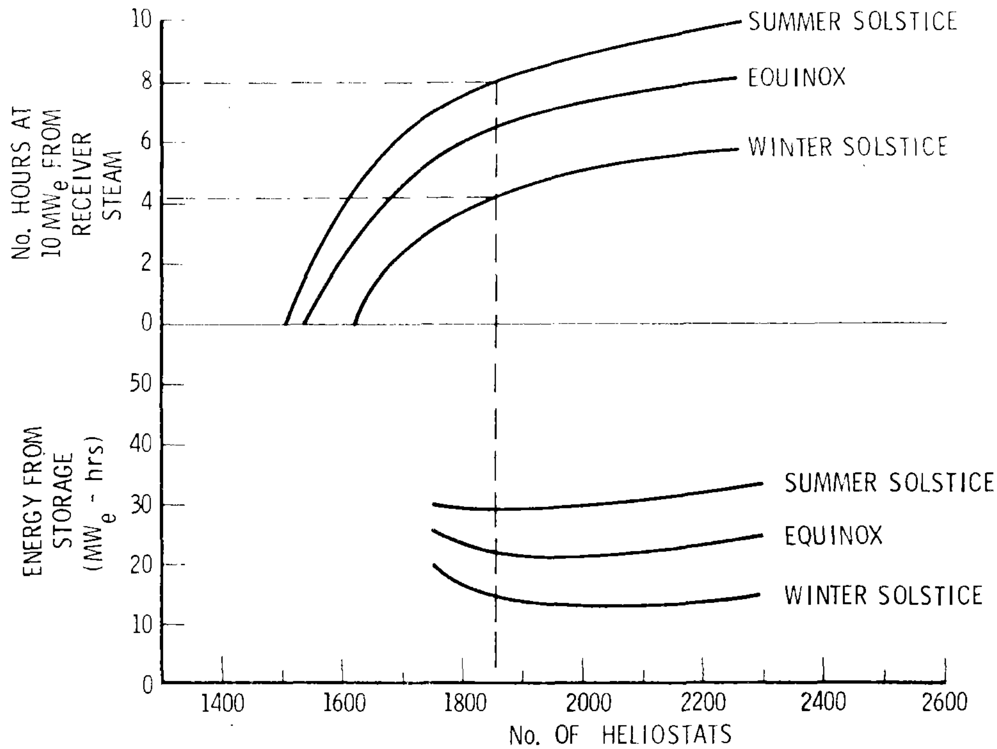

Figure 3. Plant Sizing

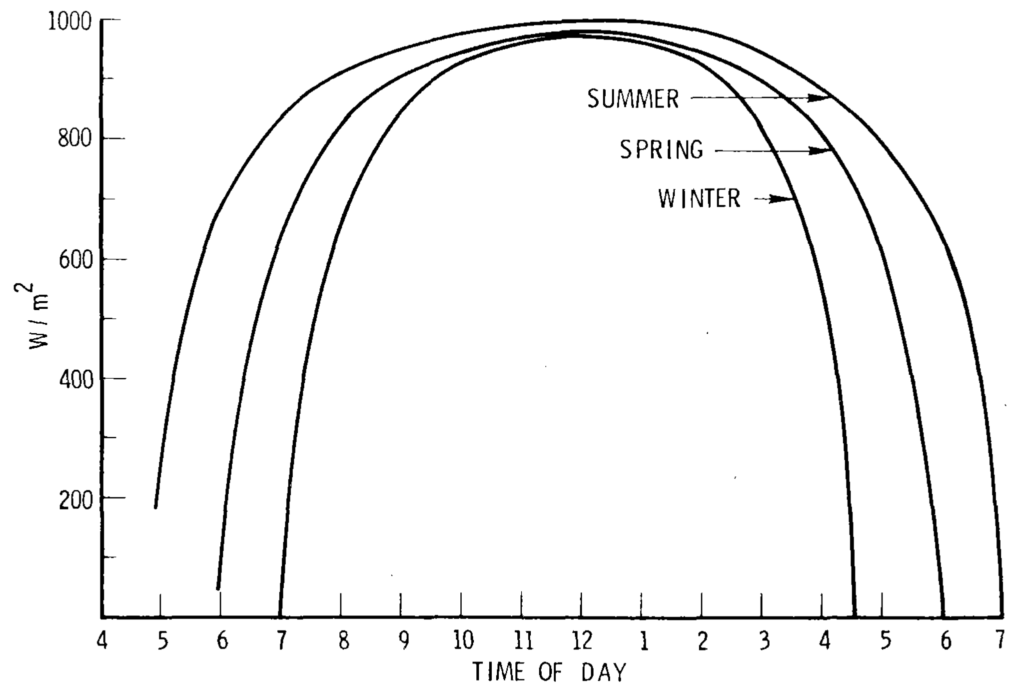

Figure 4. Barstow Insolation (1976)

Contractor Selections

The DOE solar facilities design/hardware selections have been initiated. The process involves evaluation by a DOE board and a selection by the Asst. Secretary for Energy Technology.

Capital and Operating Cost Comparisons

Figure 5 plots delivered energy versus plant capacity factor for several alternative generation sources. Capacity factor is the ratio of kilowatt-hours produced to the kilowatt hours that a plant could produce if operated at maximum capacity for the entire year. The cost of all alternatives was estimated using a common 1980 inservice date and levelized annual costs for the plant's economic life.

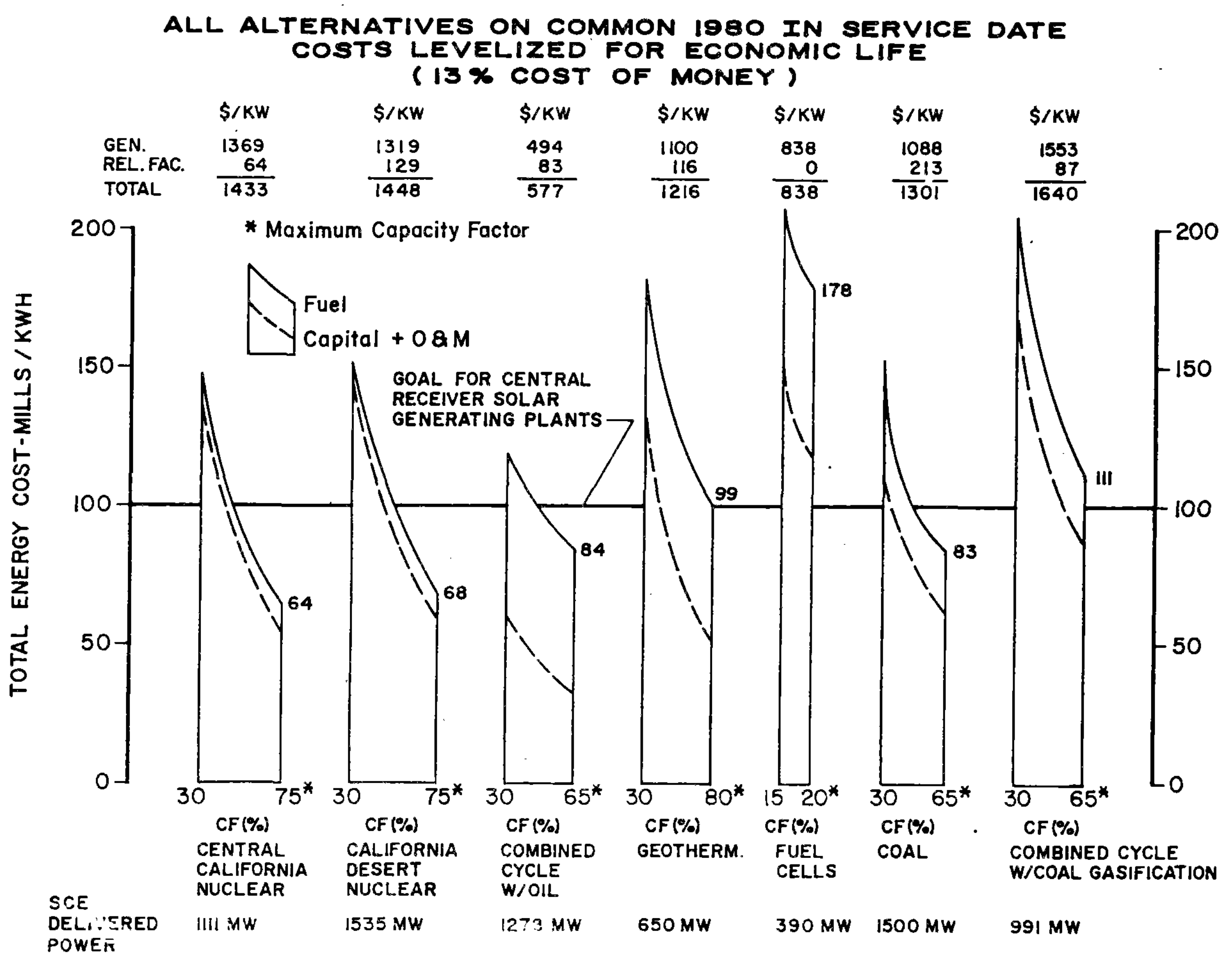

Figure 5. Capital and Operating Cost Comparisons

Daily Load Shape With and Without Solar

Figure 6 shows that with significant penetration (10%) of solar generation capacity in conjunction with 6 hours of thermal energy storage, approximately 10 percent peak demand reductions can be achieved. However, each utility will have to determine for each particular condition whether it prefers to maximize energy output by generating as much as possible by not "filling" thermal storage; or whether it prefers to reserve generating capability until non-solar hours and accepting less kilowatt-hour production because of the inefficiencies associated with thermal storage systems.

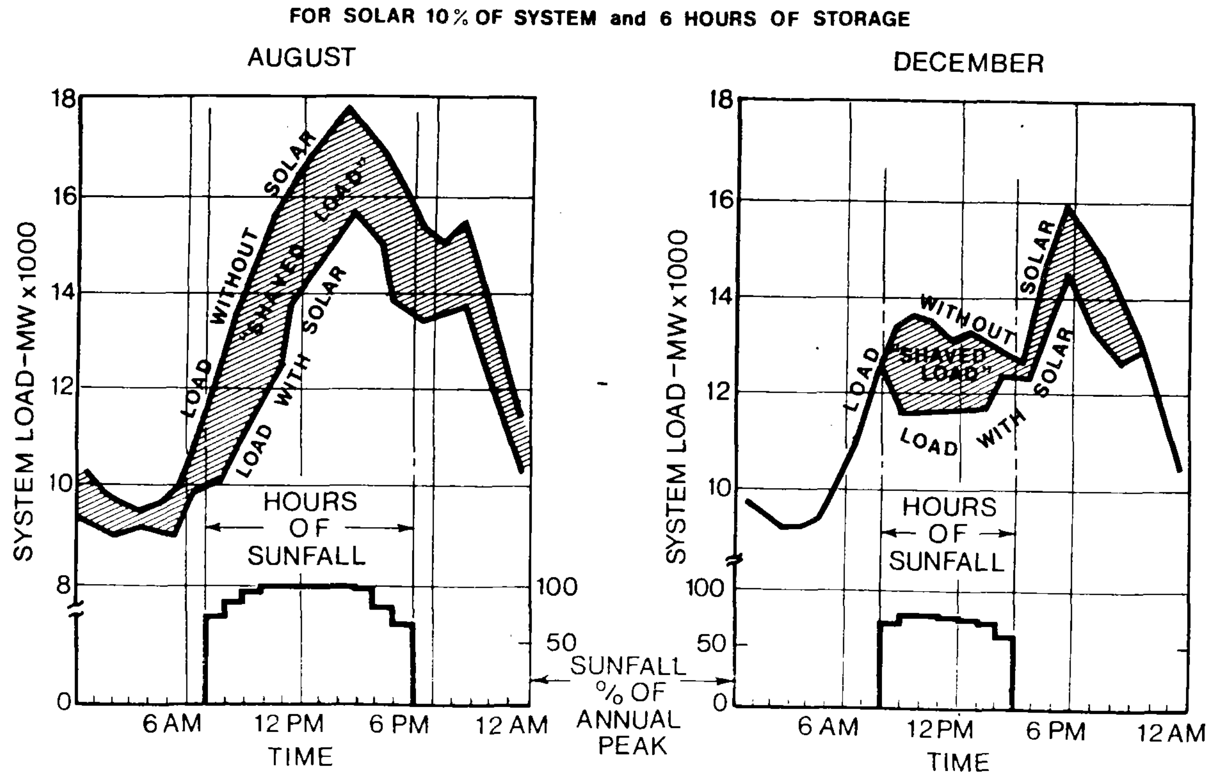

Figure 6. Daily Load Shape With and Without Solar

Environmental Review Process

San Bernardino County has been designated as the lead agency for state and local environmental review and permitting requirements associated with the pilot plant. In that role, San Bernardino County representatives have coordinated preparation of environmental impact documentation for use in satisfying both federal and state requirements. On December 13, 1977, the Environmental Review Board (ERB) of San Bernardino County determined that the Draft Environmental Impact Report for the pilot plant was an adequate environmental document relative to County guidelines implementing the California Environmental Quality Act. The ERB further determined that implementation of the zone change, location, and development plan will not have a significant adverse affect on the environment.

Following successful rulings by the San Bernardino Planning Commission and the Board of Supervisors, building and construction permits will be obtained for the pilot plant.

Local Impacts

Water will be pumped from existing wells located near the pilot plant. These wells presently serve the existing generating plants and farming operations on Edison-owned land. It is expected that the pilot plant will use approximately 220 acre-feet of water per year. This will be supplied by water diverted from agricultural use and will not require additional pumping from the ground water basin.

It is anticipated that 50,000 visitors per year could be attracted to a Visitor's Information Center with little more publicity than notification signs on the two nearby freeways. We expect that additional publicity could easily increase this by another 50 to 100,000 visitors per year.

Plant Operating Modes

To date, our engineers have completed heat balance diagrams and flow and control schematics. The seven following modes of operation are being planned:

Mode 1 - Collector and receiver systems powering the turbine-generator system.

Mode 2 - Collector and receiver systems powering the turbine-generator system and simultaneously sharing thermal storage system.

Mode 3 - Collector and receiver and thermal storage systems all powering turbine-generator system.

Mode 4 - Collector and receiver charging thermal storage system, while thermal storage powers turbine-generator system.

Mode 5 - Collector and receiver systems charge thermal storage system only.

Mode 6 - Thermal storage system powers turbine-generator system.

Mode 7 - Collector and receiver systems power turbine-generator system, while charging thermal storage system; thermal storage system also powers turbine-generator system (transitional mode for other modes).

THE TECHNICAL AND ECONOMIC ASSESSMENT OF SOLAR HYBRID REPOWERING

Public Service Company of New Mexico

J. D. Maddox

Contract No. EG-77-C-03-1608
Contract Value - $812,000

The Public Service Company of New Mexico (PNM) is performing an investigation of the solar hybrid repowering concept for the Department of Energy. This concept (Figure 1) consists of placing solar hardware adjacent and connected to existing gas and oil-fueled electric generation units to displace a portion or all of the fossil fuel normally used during daylight hours. The 12-month study will assess the technical and economic viability of the concept as applied to a PNM system located in the Southwest. Results of the study will enable DOE to assess the desirability of constructing a demonstration plant within the PNM service territory.

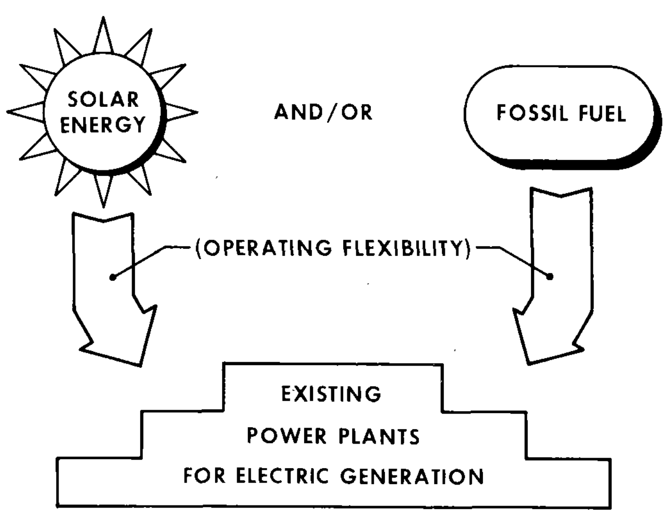

Figure 1. Hybrid Repowering Concept

As shown in Figure 2, the project is approximately on schedule with a slight delay in Tasks 1100, 1200, and 1600, as technical efforts are being slowed by contractual issues. Task 1100, the Market Survey and Cost Benefit Analysis, has obtained a 75 percent survey response to date; out of 80 utilities addressed, 60 have responded. The results, presented in Table I, indicate a solar repowering market exists in the nine-state area in excess of 10,000 MWe. With respect to utility interest in solar hybrid repowering, out of 53 utilities electing to respond, only 26 had considered solar power generation as a future alternative. After an explanation and consideration of the solar hybrid repowering concept, 48 out of 51 utilities which elected to respond on this issue indicated their interest. Specifically, they answered positively that they would be interested in participating in a solar hybrid repowering plant program if financial incentives made it equivalent to existing generation alternatives. A cost benefit analysis to identify the benefits of the total market has been initiated.

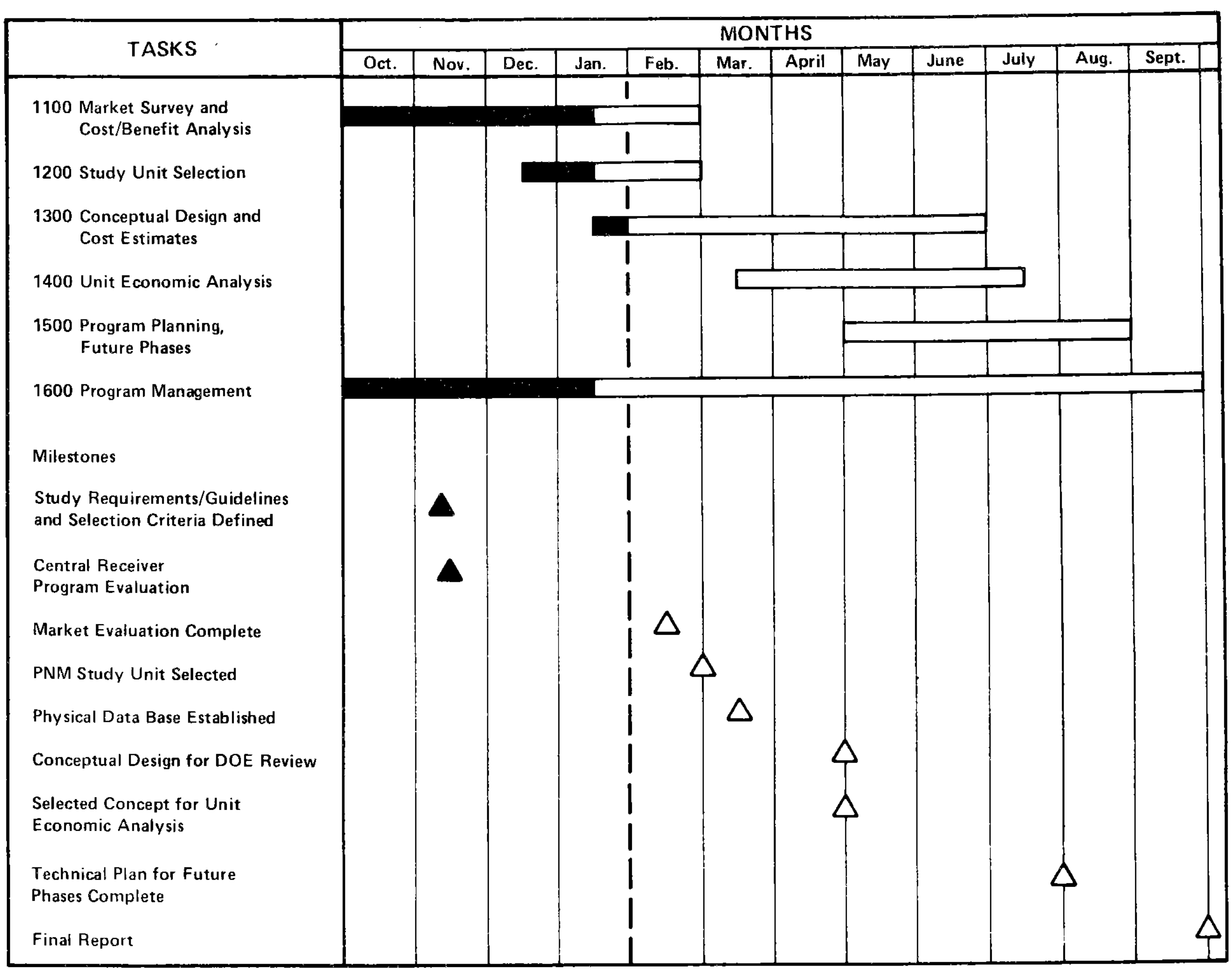

Figure 2. Schedule and Milestone Status For Solar Hybrid Repowering Study

TABLE I

MARKET EVALUATION SUMMARY

CATEGORY	NUMBER OF UNITS	TOTAL MWe
POTENTIAL MARKET SIZE (RATED MWe)		
LITERATURE SURVEY	755	40,954
UTILITY SURVEY	251	18,414
SOLAR REPOWERING POTENTIAL (EFFECTIVE MWe)		
BASED ON LAND AVAILABILITY	251	10,494
AND <2500 FT. FROM PLANT	192	7031
AND >50% REPOWERING	70	4577
AND UTILITY INTEREST	70	4577

Task 1200, the Study Unit Selection, is under way. Requirements and guidelines for the selection are listed in Table II. The PNM system has been surveyed and these 13 items have been applied to various units within the system. Candidate plants most likely for a large-scale steam rankine cycle repowering demonstration appear to be the Reeves and Person Units, which have ratings varying from 22 to 66 MWe and consist of seven units. The generation planning department of PNM will address the init and system impacts and the optimum fit of solar repowering into the utility grid.

The market survey identified a typical candidate plant for solar hybrid repowering based upon the large number of utility responses received. The plant characteristics and historic plant data are given in Table III.

Task 1300, Conceptual Design and Cost Estimates, is approximately five percent under way. A general arrangement of the plant has been established. The solar system design has been initiated, as has the assessment of modifications to existing equipment. Table IV presents the repowering conceptual design approach. The plant operating modes, the EPGS arrangement, computer modeling, piping interfaces, control system, and water treatment criteria are being addressed.

TABLE II

SOLAR HYBRID REPOWERING PROJECT
CANDIDATE UNIT SELECTION CRITERIA

- UNIT TYPE, LOCATION, AND RATING
- ADJACENT LAND AVAILABILITY/ SURROUNDING STRUCTURES
- DATE CONSTRUCTED
- UNIT CONDITION / REMAINING USEFUL LIFE
- INSOLATION AND CLIMATEOLOGICAL CHARACTERISTICS
- FUELS USED / FUEL OPTIONS
- TURBINE TYPE / OPERATING CONDITIONS
- PLANT OPERATION / AVAILABILITY REQUIREMENT
- SOLAR / FOSSIL INTERFACES
- CURRENT USE / PLANNED FUTURE USE
- ENVIRONMENTAL IMPACTS
- SITE CHARACTERISTICS / TERRAIN
- SAFETY

TABLE III

TYPICAL CANDIDATE PLANT FOR SOLAR HYBRID REPOWERING

• PLANT CHARACTERISTICS	
TYPE	NON-REHEAT STEAM TURBINE UNIT
RATING	10 TO 50 MWe
TURBINE INLET	850 PSI/900°F
• HISTORIC PLANT DATA	
YEAR BUILT	1950 - 1960
UNIT CONDITION	GOOD
CURRENT USE	INTERMEDIATE/PEAK
LOCATION	RURAL
ESTIMATED RETIREMENT	BEFORE 2000

TABLE IV

REPOWERING CONCEPTUAL DESIGN APPROACH

• Solar System Based on 10MW Solar Central Receiver
• Reeves Station Unit-2
• Approximately 50% Repowering
• Preliminary Collector Field Layout
• Definition of Possible Plant Operating Modes
• Preliminary EPGS General Arrangements
• Computer Modeling of Basic Fossil/Solar Cycle to Provide Heat Balance Data
• Cycle Piping Interface Location
• Minimum Change to Existing Plant Control System
• Water Treatment System Design Based on Once Through Boiler Requirements

Figure 3 is a schematic of the Reeves Unit 2. The repowering system will require the addition of the No. 6 and No. 7 feedwater heaters, an additional feedwater pump, various interconnecting piping from the first- and second-stage turbine extraction ports, and feedwater and steam lines to and from the solar receiver. A steam attemperator and moisture separator will be included to minimize solar thermal transients and assure steam quality.

Under Task 1600, Program Planning for Future Phases, additional utilities have been requested to join PNM in a supporting or advisory capacity to the study. It now appears that approximately 60 utilities will be enrolled in either the supporting or advising utility program.

A preliminary schedule (Figure 4) has been developed for the solar hybrid repowering demonstration. The detailed design work is based on a 50 percent repowered 50-MWe oil-fired unit. Construction may be completed in three years, and demonstration of the facility could occur three and one-half years after initiation of the detailed design. The potential for more rapid heliostat production is being investigated and may accelerate this schedule.

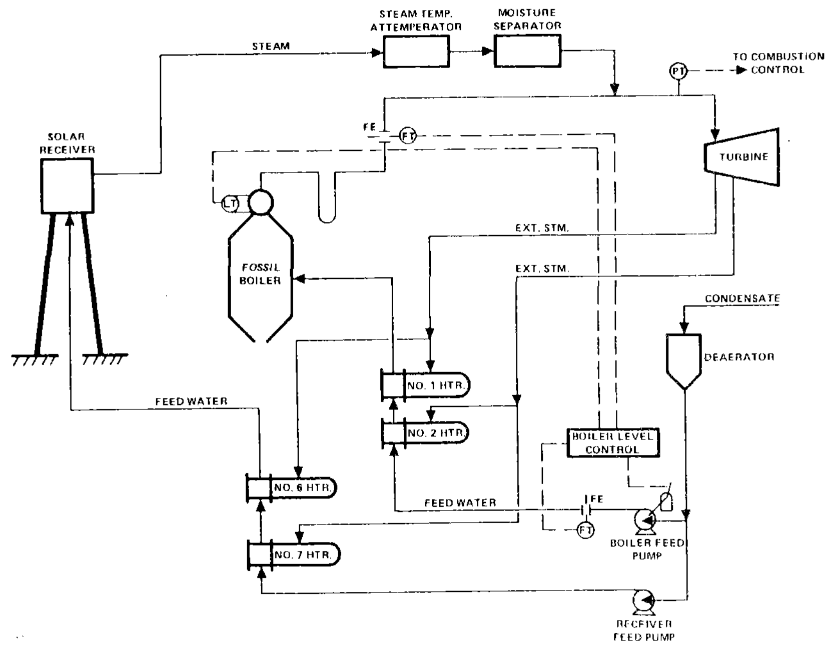

Figure 3. Reeves Unit-2 Solar Repowering System Schematic

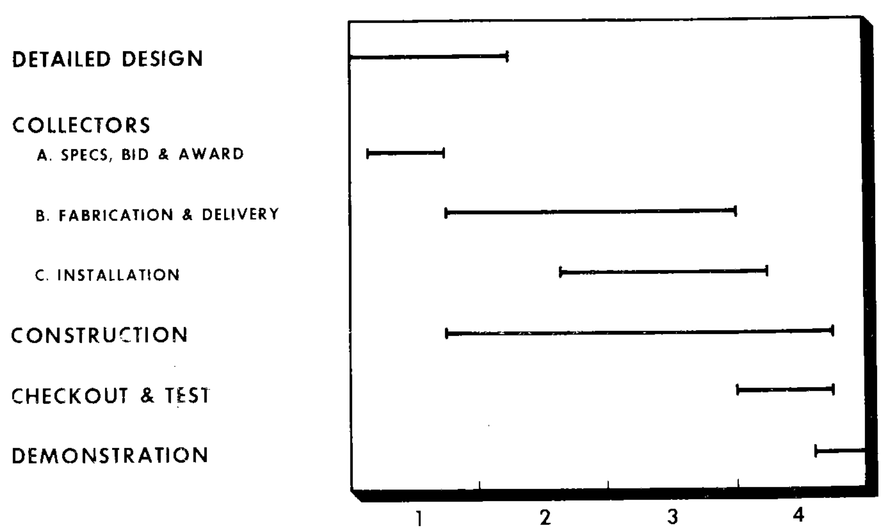

Figure 4. Preliminary Schedule - Hybrid Repowering Demonstration

CONCEPTUAL DESIGN OF SODIUM-COOLED ADVANCED CENTRAL RECEIVER POWER SYSTEM

Atomics International
McDonnell Douglas
Stearns-Roger
The University of Houston
Salt River Project

T. Springer

Introduction

The use of liquid sodium as a heat transport medium in an advanced central receiver concept is being studied by a team consisting of Atomics International (prime contractor), McDonnell-Douglas, Stearns-Roger, The University of Houston, and Salt River Project. The purpose of this study is to determine the technical and economic advantages of this concept for commercial-scale power plants.

The basic configuration is depicted in Figure 1. In this particular arrangement, sodium is pumped up to the receiver where it is heated. The sodium then flows down the tower, through a pressure reducing device, and into a large storage tank located at ground level. From this tank, the sodium is pumped through a system of sodium-to-water steam generators. The steam generator system consists of a separate superheater and reheater operating in parallel and an evaporator unit operating in series with the other two units. The sodium flowing from the evaporator tank is piped to a cold storage tank and then pumped up to the top of the tower to complete the cycle. The steam generated in the steam generators is fed to a conventional "off-the-shelf," high-efficiency turbine. The steam loop operates in a conventional rankine cycle with the steam generators serving the same purpose as a conventional boiler, and water being fed to the evaporator with conventional feedwater pumps. The pressure reducing device (a standard drag valve, for example) serves to mitigate the pressure caused by the static head of sodium, and thus allows the large tanks to operate at ambient pressure conditions.

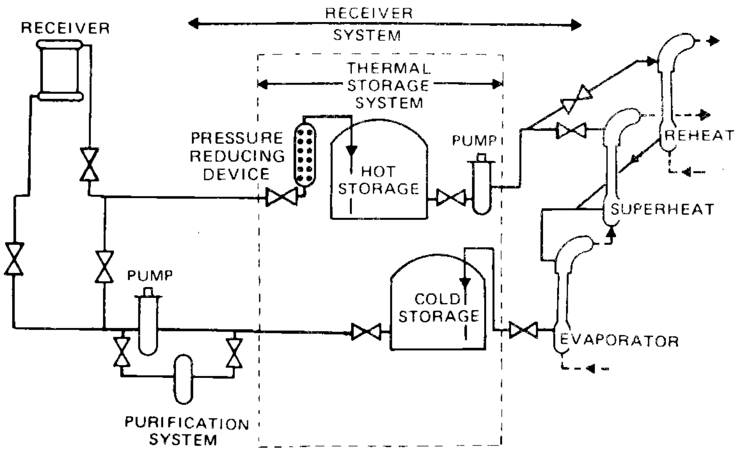

Figure 1. Sodium-Cooled Advanced Central Receiver Power System

There are several advantages to the sodium-cooled system. First, the heat transport fluid remains in the liquid state at all times; therefore, control of the system is simpler, and there is not a large density change between inlet and outlet. Second, liquid sodium is a very good heat transfer material; consequently, the receiver can be made smaller, and the heat flux can be substantially higher. Third, the heat transport fluid can also serve as the heat storage material in some cases, and operation from storage can be accomplished under the same thermodynamic conditions as would exist when operating directly from the receiver. In addition, the receiver, which is subject to varying heat input, can be totally decoupled from the power cycle. Finally, the sodium system is capable of providing steam to a turbine at temperatures and pressures commensurate with or exceeding modern steam plant requirements and can conveniently incorporate a reheat cycle. These advantages are offset, to some extend, by the need for some additional pieces of equipment not necessarily required by a water/steam system. However, the cost of these additional items is more than compensated by the substantial increase in system efficiency.

The technical approach adopted on this program was to establish a reference baseline configuration and then perform various subsystem and system-level trade studies and parametric analysis in order to evaluate various potential improvements. As superior subsystems are identified on the basis of cost, performance, and operating characteristics, the reference baseline configuration is updated. In this way, a preferred commercial system configuration can be developed, designed, and evaluated on the basis of economic merit.

Some of the performance data for the reference baseline configuration that was used to initiate this program are given in the column labeled "baseline configuration - 6 hours" in Table I. This reference baseline was adopted on the basis of a study conducted by The University of Houston, McDonnel-Douglas, and Atomics International under a grant made in 1976 to The University of Houston (see Semiannual Review Reports SAND 77-8011 and SAND 77-8513).

Two major changes in this reference configuration required in the light of the specifications provided by DOE were made during the first few weeks of the program. The changes consisted of reducing the solar multiple from 1.66 to 1.5 and using a storage time of 3 hours instead of 6. The new conditions are delineated in the column in Table I labeled "advanced baseline - 3 hours." This is the reference configuration against which parametric analyses were initially compared on the program.

TABLE I

ADVANCED CENTRAL RECEIVER
BASELINE DATA
SUMMARY
(1976 DOLLARS)

SYSTEM	PARAMETER	UNITS	CONFIGURATION: INITIAL BASELINE (6HR)	CONFIGURATION: INITIAL BASELINE (3 HR)
ELECTRIC	NET POWER	MWe	100	100
	GROSS POWER	MWe	113	113
	CYCLE EFFICIENCY	%	39.5	39.5
RECEIVER	SOLAR MULTIPLE	–	1.66	1.50
	NOM. THERMAL POWER	MWt	286	286
	MAX. THERMAL POWER	MWt	474.9	429
STORAGE (100% POWER)	OPERATING TIME	hr	6	3
	ENERGY	MWt-hr	1,610*	805*
	QUANTITY OF SODIUM	10^6 kg (10^6 lb)	15.3 (33.6)	7.6 (16.8)
	HOT TANK – VOLUME	10^3 m^3 (10^3 ft^3)	19 (68)	9.6 (340)
EPG	TURBINE IN PRESS.	MN/m^2 (psig)	13.8 (2,000)	13.8 (2,000)
	SUPERHEATER TEMP.	°C (°F)	538 (1,000)	538 (1,000)
	REHEATER TEMP.	°C (°F)	538 (1,000)	538 (1,000)

*INCLUDES REDUCTION IN NIGHT PARASITIC POWER TO 6 MWe

Parametric Analysis

Single Tower/Multitower

Solar central receiver power plants with a single receiver and tower were compared to those having multiple tower arrangements. In all cases, there was a single turbine and generator. The multiple tower configurations were joined by horizontal piping runs that contained the sodium heat transport fluid. Both external and cavity receivers were considered, and thermal loss models for these receivers were calculated. It was found that a single tower with an external receiver had a relative cost of 107.2 \$/MWt-hr while that of a cavity receiver plant was 128.8 \$/MWt-hr, or 20.1% greater. The cavity receiver has much lower thermal losses (5.2% versus about 11.0%). However, the external receiver plant has a shorter tower, a much smaller receiver, and a reduced collector size. Design studies of various sodium-cooled cavity receivers showed them to be large and complex with a significantly higher cost. Thus the external receiver was chosen for future studies.

Thermal Energy Storage

The baseline thermal storage system consists of an all-sodium concept with a single hot tank and a single cold tank. This concept was selected over concepts that use multiple tanks and single tank thermocline systems using sodium and some heat sink material such as iron. These alternative concepts did not show an economic advantage, and in addition, the sodium thermocline systems did not provide complete decoupling between the receiver and the steam generator units such as is provided by the all-sodium storage system. Alternative storage fluids in the thermal storage system, such as draw salts, also have been considered. While the cost of draw salt is attractive, the added heat exchanger to interface with the sodium system and the added cost of the steam generator unit more than offset the low cost of the material itself. A draw salt-to-water steam generator requires increased heat transfer area over that of a sodium-to-water unit due to the poor heat transfer properties of draw salt.

Other thermal storage concept studies are continuing.

Electric Power Generating Subsystem

The initial baseline turbine generating system includes a standard 100-MWe net reheat design operating at 15.2 MN/m^2 2200 psig with a throttle temperature of 538°C (1000°F), a reheat temperature of 538°C (1000°F), and a gross cycle efficiency of 39.5%. Many alternative turbine cycles were studied to determine the cost and performance contribution due to reheat, throttle pressure, throttle temperature, reheat temperature, and number of feedwater heaters and last-stage turbine blade length. The study included the effect of turbine cycle efficiency on collector, receiver, and thermal storage subsystem size. The comparison of costs and benefits showed that performance improvements associated with reheat more than offset the added cost in the turbine unit and the added cost of the sodium reheat unit. The steam generator arrangements considered included (1) a once through unit without reheat; (2) separate evaporator and superheat units without reheat; and (3) separate evaporator, superheat, and reheat units. The latter two arrangements require a steam separator drum to ensure that water does not enter the superheater unit. Figure 2 shows a summary curve giving plant capital cost increments as a function of sodium loop temperature difference for various turbine inlet pressures. All curves in this figure are for 538°C (1000°F)-superheat and 538°C (1000°F)-reheat temperatures. The figure shows the minimum cost to occur for a 12.4 MN/m^2 (1800-psig) turbine system with a sodium loop temperature difference of 305°C (550°F). The turbine cycle arrangement selected consists of an 12.4 MN/m^2 (1800-psig) reheat system with 538°C (1000°F) reheat, which gives a cycle efficiency of 43.1%. The revised baseline characteristics described in the next section reflect this improvement in cycle efficiency.

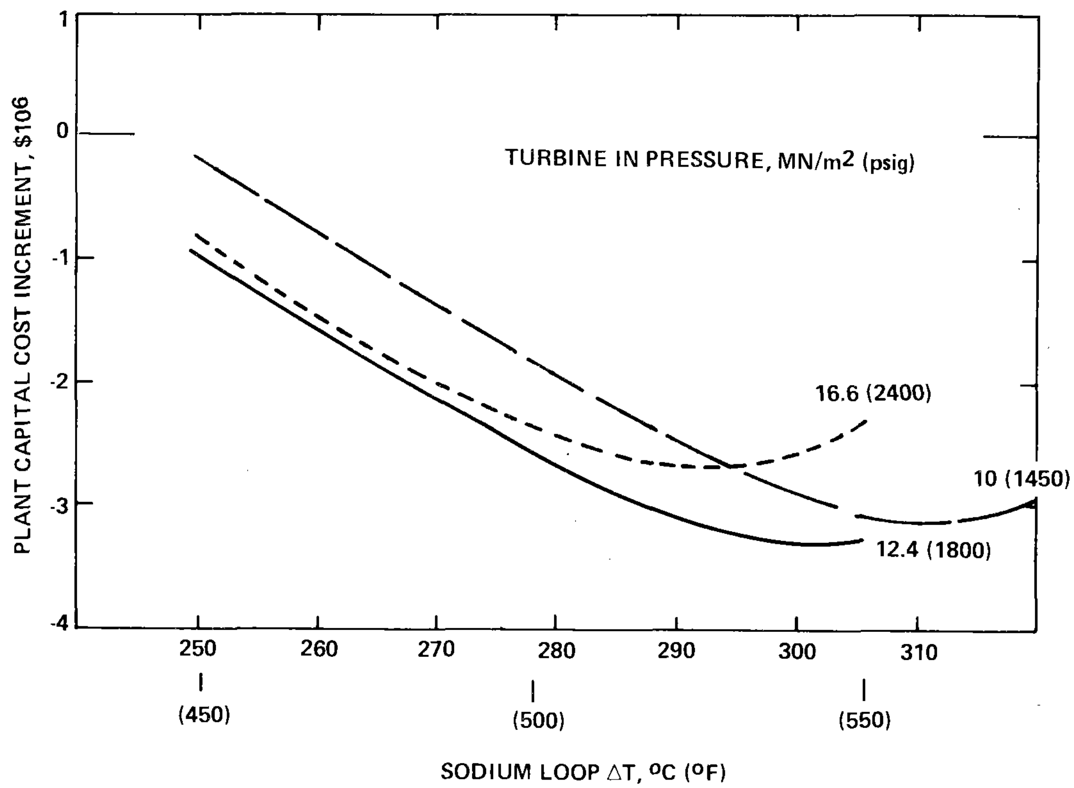

Figure 2. Summation of Plant Capital Cost Increments

Master Control Subsystem

The master control subsystem for the advanced central receiver using liquid sodium is similar in many respects to the one required for the water/steam system. The major differences relate to the impact of the series thermal storage concept. The large thermal mass in series effectively decouples the receiver and its coolant loop from the steam generator loop. Insolation conditions are, therefore, not reflected in steam quality; there is a single source and single quality of steam, Also, from the reverse viewpoint, the receiver loop is isolated from turbine/generator transients so that receiver operation is not affected by the steam load.

A major task of master control in the water/steam system is sequencing the system through mode changes in response to insolation changes. The system decoupling described above simplifies this sequencing function. The mode change activities for master control in the advanced concept are primarily startup and shutdown sequencing and decision-making regarding the amount of energy remaining in storage.

Figure 3 indicates the preliminary conceptual master control system configuration. Subsystem process control is accomplished with a process controller system based on distributed digital technology, interconnecting on a redundant data base. Controller microprocessors implement standard process controller functions, integrate well into a computer-directed system, and easily allow such features as self-checking, alarm on failure, and automatic redundant takeover.

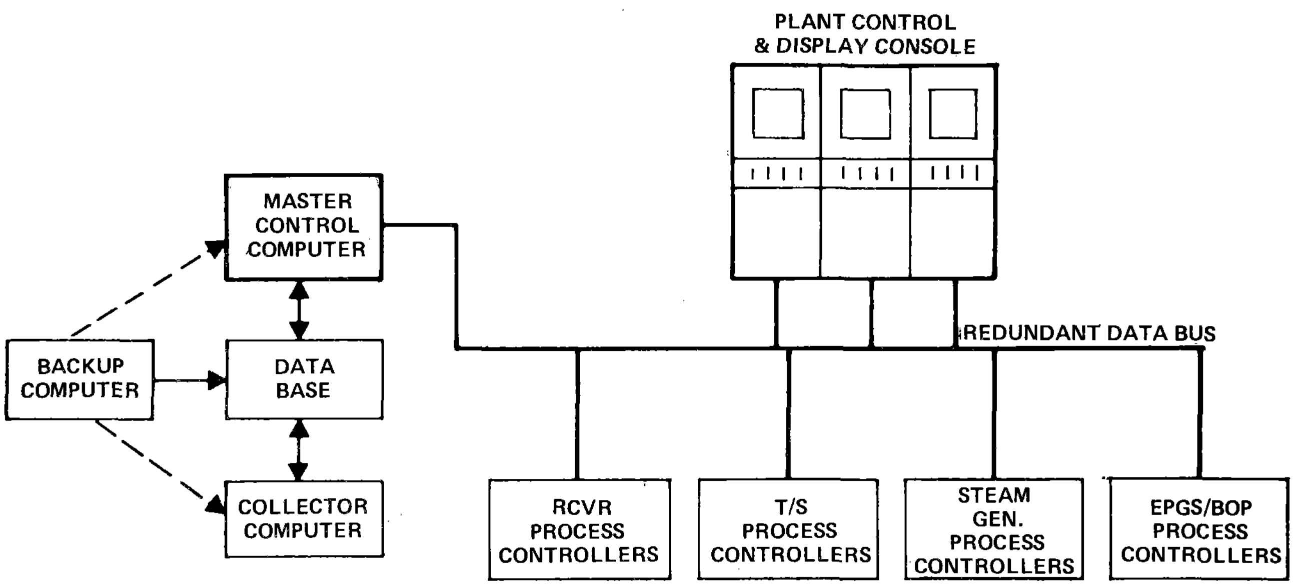

Figure 3. Conceptual MCS Configuration

The master control computer operates the system in a supervisory manner through the process controllers. Its functions, in addition to directing operations, include monitoring, logging, alarming, and computation for control decisions and reporting.

The master control computer, the collector subsystem computer, and the backup computer all tie to a common data level. This arrangement facilitates transfer of information among the three machines and allows the backup computer to take over, as needed, from either the master control or the collection computers.

Collector Subsystem

The collector field for the sodium-cooled central receiver plant is a single, 360-degree array that is north-biased. There are 18,596 square heliostats that measure 6.5 x 6.5 m on the sides. The total field area is $2.97 \times 10^6 m^2$ of which the mirror area is $7.05 \times 10^5 m^2$, such that the glass area density is 23.7%. The annual collectable energy is 1.20×10^6 MWHt, which is about 4.80×10^5 MWHe. The heliostats have a radial stagger arrangement. The aim strategy with respect to the receiver is single-point aim at the receiver equator.

The mirror surface is second surface silvered float glass with a reflectivity of 91.0%. The combined standard deviation of the mirror aiming accuracy is 3.0 milli-radians.

Sodium Loop

The sodium loop consists of two basic parts: (1) the energy absorbing part, which supplies sodium to the receiver from the cold sodium storage tank, absorbs the insolation energy gained by the receiver and transports it to the hot sodium storage tank; and (2) the energy utilization part, which transports the energy from the hot sodium tank to the steam generator complex and returns the thermal energy remaining in the sodium to the cold storage tank. This arrangement permits the sodium system temperatures to remain constant during power operation, thus avoiding excessive thermal stress cycling, which is one of the basic factors that usually determines the design life of sodium components.

The relatively high elevation of the receiver generates a significant static pressure in the sodium piping at the base of the tower. This pressure must be contained, dissipated, or used to economic advantage or minimum economic disadvantage. The various alternatives considered were as follows:

1. A closed system that accepts the hydraulic pressure in the storage tanks. Because of the large size of these tanks, pressure-containing tanks become very expensive.

2. A system utilizing an isolating heat exchanger was rejected because the heat exchanger cost exceeds the savings from recovering the head.

3. A system utilizing the turbine in the downcomer connected to a pump in the riser is attractive, but operating cost economics are small and tend to be overshadowed by the development cost.

4. Elevating the storage tank to allow the elimination of the steam generator pump proved to be uneconomic.

Commercial Plant Configuration

Based on the above subsystem studies, the revised baseline commercial plant configuration continues to be represented by a single tower field with the reflected radiant energy absorbed by a cylindrical external receiver. The storage system is the hot and cold tank all-sodium concept, though additional tradeoff studies on other storage concepts are continuing. In addition to other storage concepts, longer duration storage periods are being considered. The studies confirmed that the reheat cycle was cost effective and that the optimum sodium temperature between the hot tank and the cold tank is 305°C (580°F). The turbine inlet pressure was lowered to 12.4 MN/m^2 (1800 psig) with a superheat and reheat temperature of 538°C (1000°F) and 538°C (1000°F), respectively. The improved gross cycle efficiency of 43.1% is incorporated in the revised baseline characteristics given in Table II.

Process and Instrumentation Diagram

A summary process and instrumentation diagram is shown in Figure 4. The basic control strategy for the sodium system is to match the heat removal rate to the insolation rate and maintain the sodium loop temperature differences approximately constant. Except for unusual operational options, it is planned to operate the plant at near full power during the day. Sodium from the cold storage tank at 288°C (550°F) is lifted to the tower by the receiver pump, P-1, which operates at constant speed. Reverse flow on loss of pump power is prevented by means of the stop-check valve. Flow modulation is by means of the receiver trim valves shown at R-1. The valve setting is determined by the panel outlet temperature signal. This same signal sets the drag valve to maintain the sodium level in the elevated surge tank constant. A trim signal from the level gauge provides final level control. The

TABLE II

ADVANCED CENTRAL RECEIVER
CURRENT BASELINE DATA
SUMMARY
(1976 DOLLARS)

SYSTEM	PARAMETER	UNITS	CONFIGURATION REVISED ADVANCED BASELINE (3 HR)
ELECTRIC	NET POWER	MWe	100
	GROSS POWER	MWe	112
	CYCLE EFFICIENCY	%	43.1
RECEIVER	SOLAR MULTIPLE		1.50
	NOM. THERMAL POWER	MWt	260
	MAX. THERMAL POWER	MWt	390
STORAGE (100% POWER)	OPERATING TIME	hr	3
	ENERGY	MWt·hr	740*
	QUANTITY OF SODIUM	10^6 kg (10^6 lb)	6.99 (15.4)
	HOT TANK – VOLUME	10^3 m^3 (10^3 ft^3)	8.82 (316)
EPG	TURBINE IN PRESS.	MN/m^2 (psig)	12.4 (1,800)
	SUPERHEATER TEMP.	°C (°F)	538 (1,000)
	REHEATER TEMP.	°C (°F)	538 (1,000)

*INCLUDES REDUCTION IN NIGHT PARASITIC POWER TO 6 MWe.

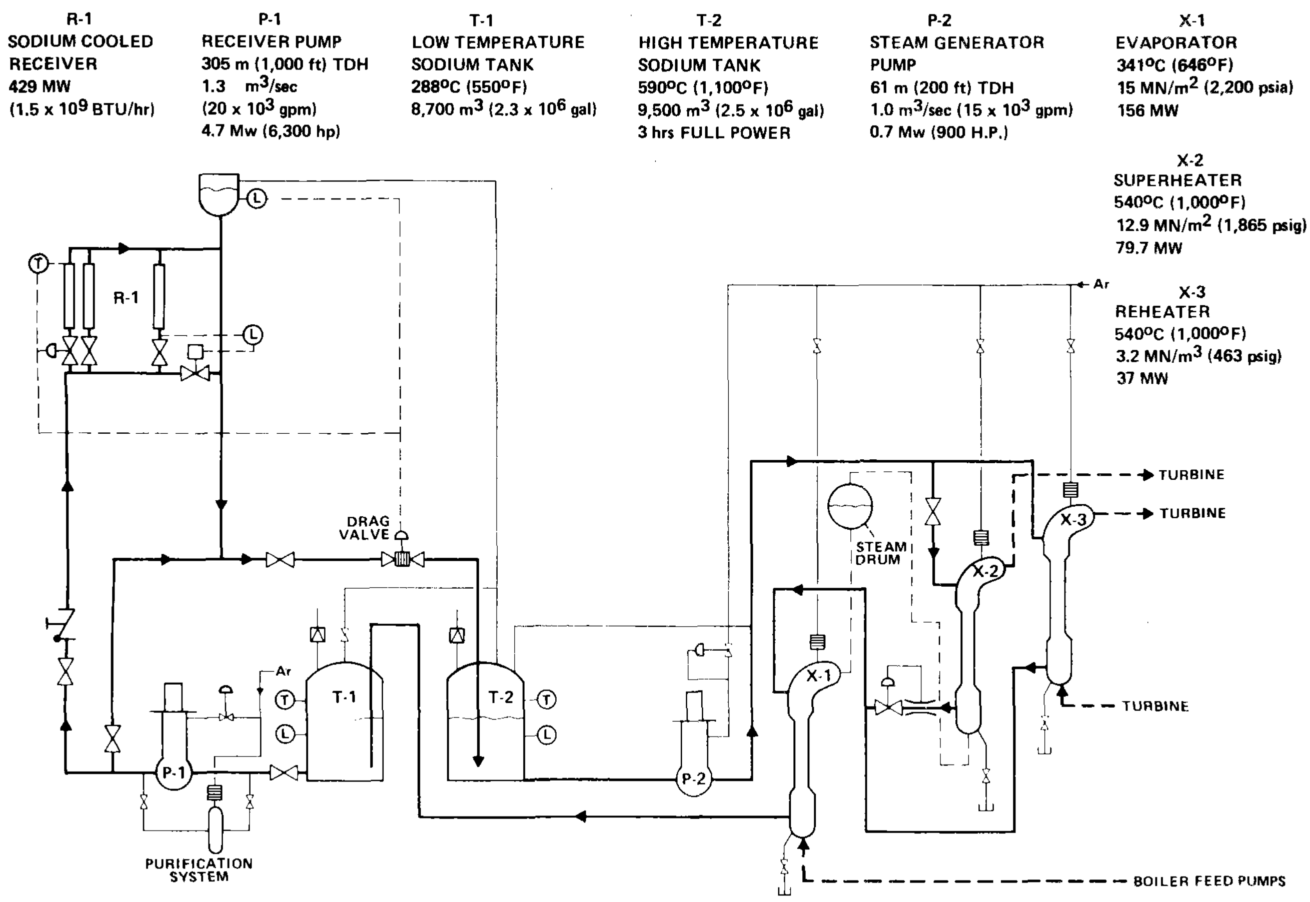

Figure 4. Sodium Advanced Central Receiver

sodium leaves the receiver at a constant 593°C (1100°F) temperature and flows through the pressure reducing (drag) valve and fills the hot storage tank, T-2. (Forty-five percent of this pressure drop is recovered at heat.) Sodium at 593°C (1100°F) is pumped from the hot storage tank to the steam generator complex by means of the steam generator pump, P-2. This pump is driven by a modified Kramer drive and runs at synchronous speed except during startup and periods of off-normal operation. The sodium flows through the superheater, reheater, and evaporator, and then returns to the cold tank, T-2. The flow into the hot tank, T-1, normally exceeds the outflow, and thus energy is accumulated. Up to three full-power hours of energy may be accumulated in this way. If, during the power day, the insolation power falls below turbine input requirements, the level in the tank will fall while the power to the turbine remains approximately fixed. If necessary, it is possible to operate at reduced conditions. On night standby, the receiver is drained to the tops on the panel trim valves. The remaining components remain filled with sodium and are maintained at temperature.

ADVANCED CENTRAL RECEIVER CONCEPT FOR SOLAR THERMAL CENTRAL POWER SYSTEMS

Boeing Engineering and Construction
(A Division of The Boeing Company)

J. B. Schroeder

The baseline system for the Boeing study is shown in Figure 1. The unique features of this concept are:

1. The use of a closed brayton-cycle electric power generation system.

2. The use of sensible heat for energy storage.

The goal of the program is to develop the minimum cost (both capital and energy) plant design for a 100 MWe capacity located at Barstow, California. This goal is to be achieved by:

1. Making parametric trade studies at the subsystem level.

2. Selecting a preferred set of subsystems for the plant.

3. Optimizing the plant design.

4. Determining the operational performance of the plant.

5. Preparing a development plan for a 10 MWe demonstration plant.

Currently, the subsystem parametrics are being completed.

The major subsystems shown in Figure 1 are discussed briefly to indicate the scope of the tradeoff studies and present sample data.

Both glass and plastic heliostats are being considered. The major differences between these two heliostat concepts are the improved reflectance of the glass mirrors and the reduced cost of the plastic heliostats. The field

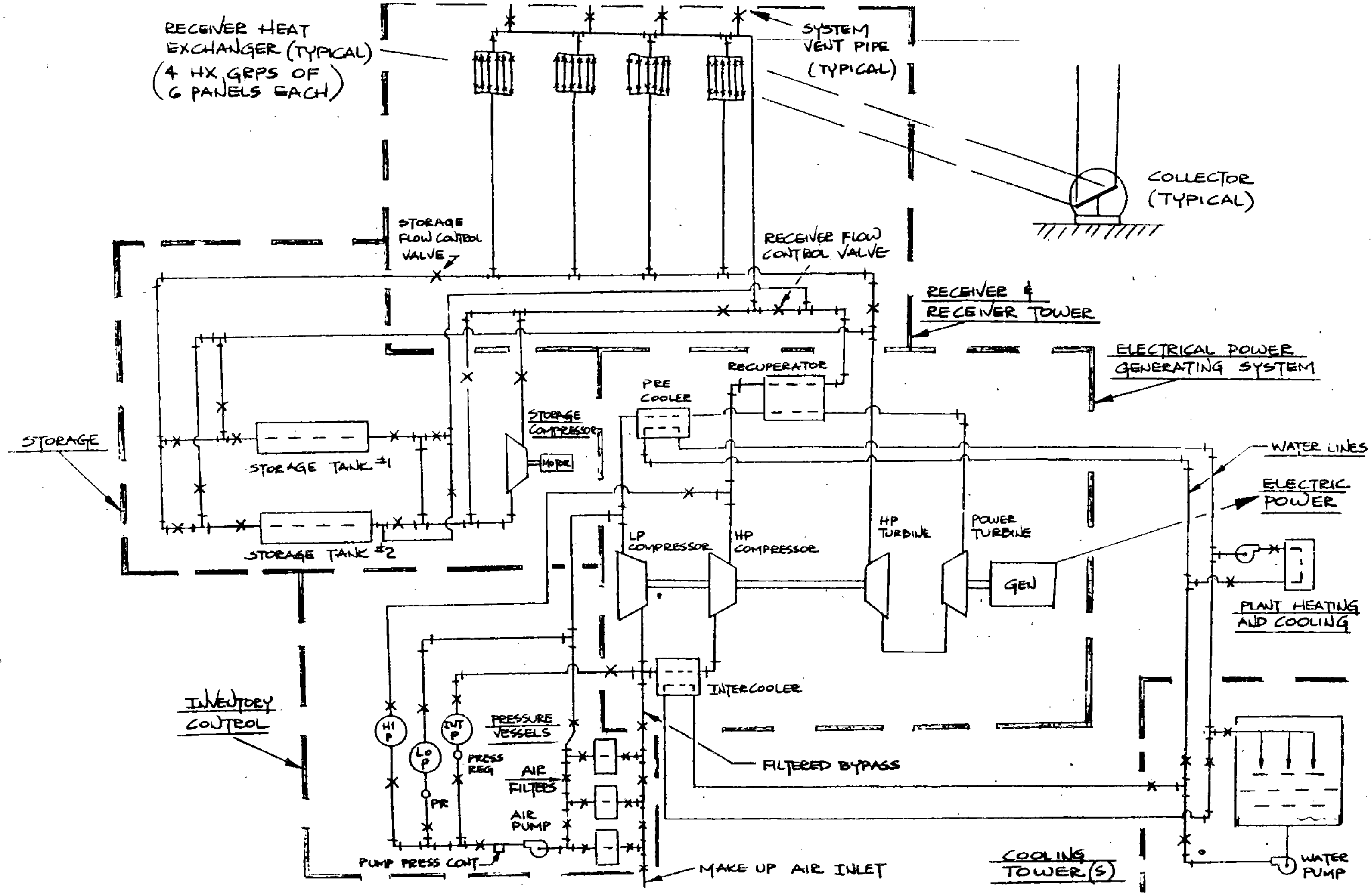

Figure 1. Schematic of Closed Air Brayton-Cycle, Solar Power Plant

efficiency for the required field size is being treated parametrically for a specified plant size, field layout, pointing accuracy, and unit cost for the Barstow insolation.

To take advantage of the capabilities offered by the brayton cycle, it is necessary to employ the maximum possible turbine inlet temperature. A baseline temperature of 820°C and the heat transfer fluxes possible for gaseous working fluids necessitate a cavity-type receiver. Figure 2 compares the efficiencies of internal (cavity) and external receivers for several heat exchanger flux levels. Reasonable heat exchanger designs can handle fluxes up to a few hundred kW/m^2. As shown in Figure 2, these low fluxes are incompatible with high efficiencies for the external receiver but not for the internal or cavity receiver.

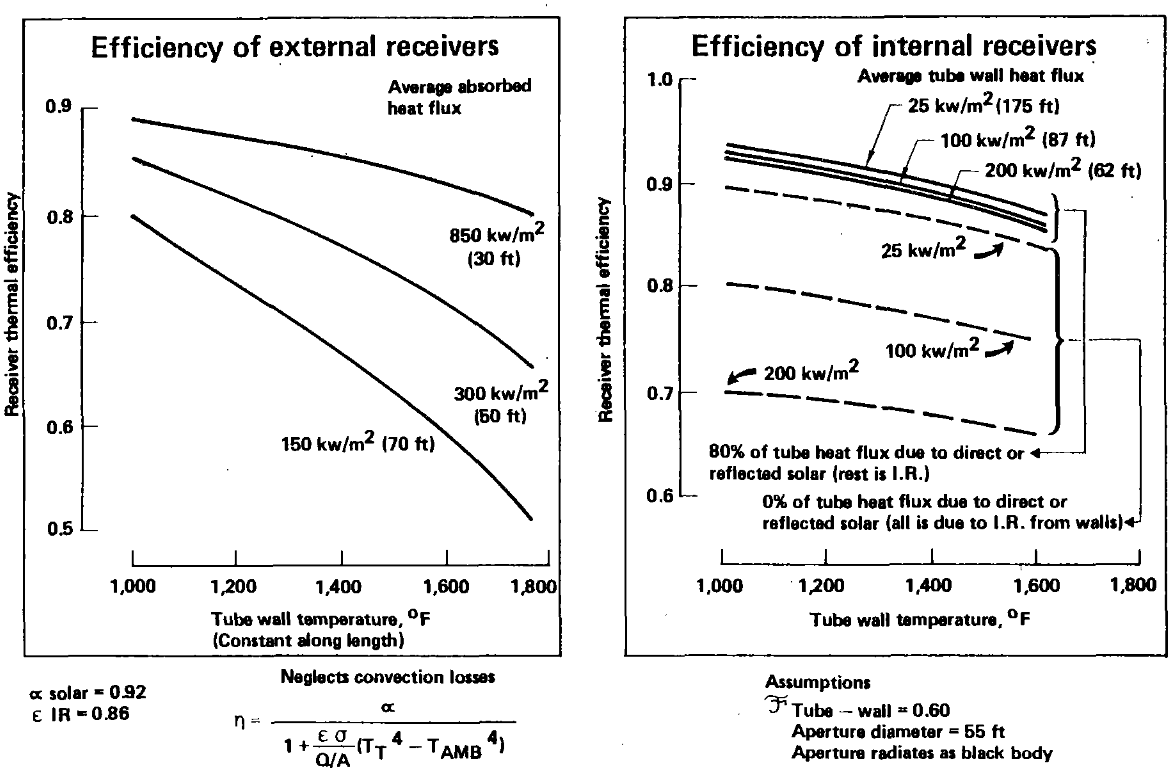

Figure 2. Comparison of Internal and External Receivers For the Brayton-Cycle Plant

Figure 3 shows the cost of the receiver tower as a function of height. This cost curve, derived by Stone and Webster for Boeing load specifications, is governed by the earthquake specification and would be reduced if a less hazardous area had been selected for the test site.

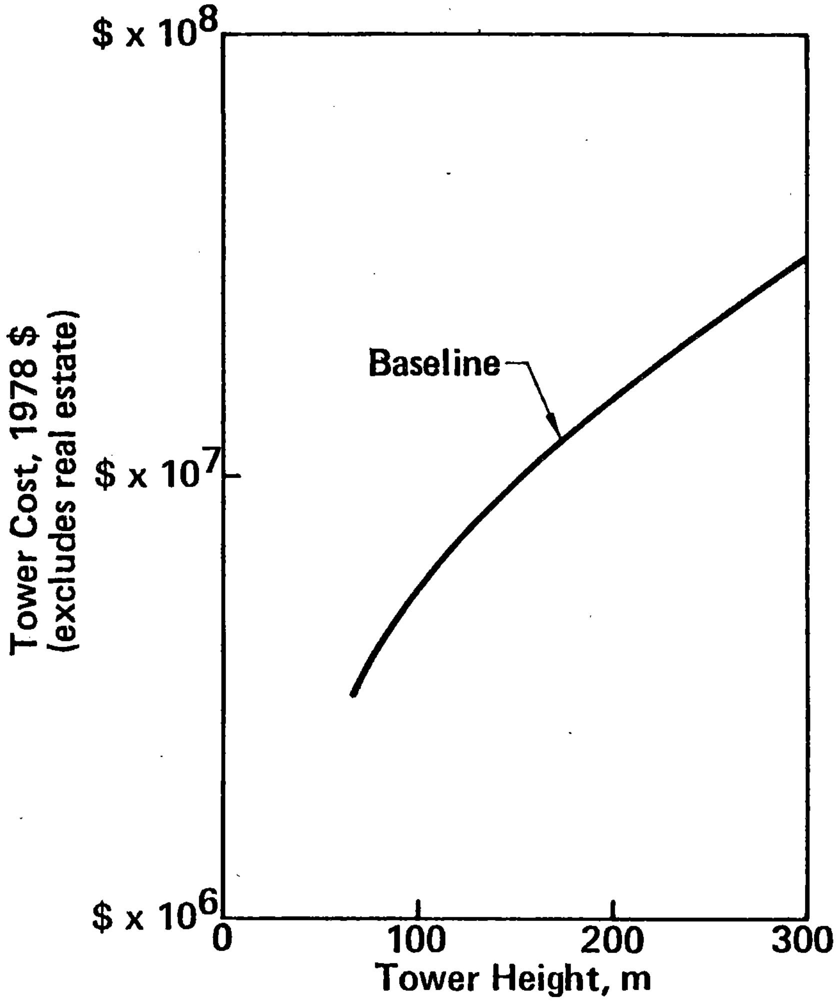

Figure 3. Receiver Tower Cost As a Function of Height (Zone 3 Earthquake Criteria)

A brayton-cycle electric power generating subsystem offers the potential of greater efficiency, and hence lower cost than the conventional steam rankine cycle. Figure 4 shows examples of the operating performance being supplied by United Technology Research Center for our parametric studies.

Figure 5 shows the sensible heat storage subsystem. MgO bricks appear to be the most effective storage media. In order to minimize the parasite pumping losses, the storage tank is segmented so the hot gas only flows through a portion of the total tank at any time. The cost of storage is shown as a function of storage for two different increments of storage.

The above parametric studies are ending and cost data are being generated. However, it is premature to present the cost data at this time, as all of the data are not yet available.

- Subcontract:United Technologies Research Center
- Typical results for close-cycle air turbine, TIT = 820°C (1500°F)

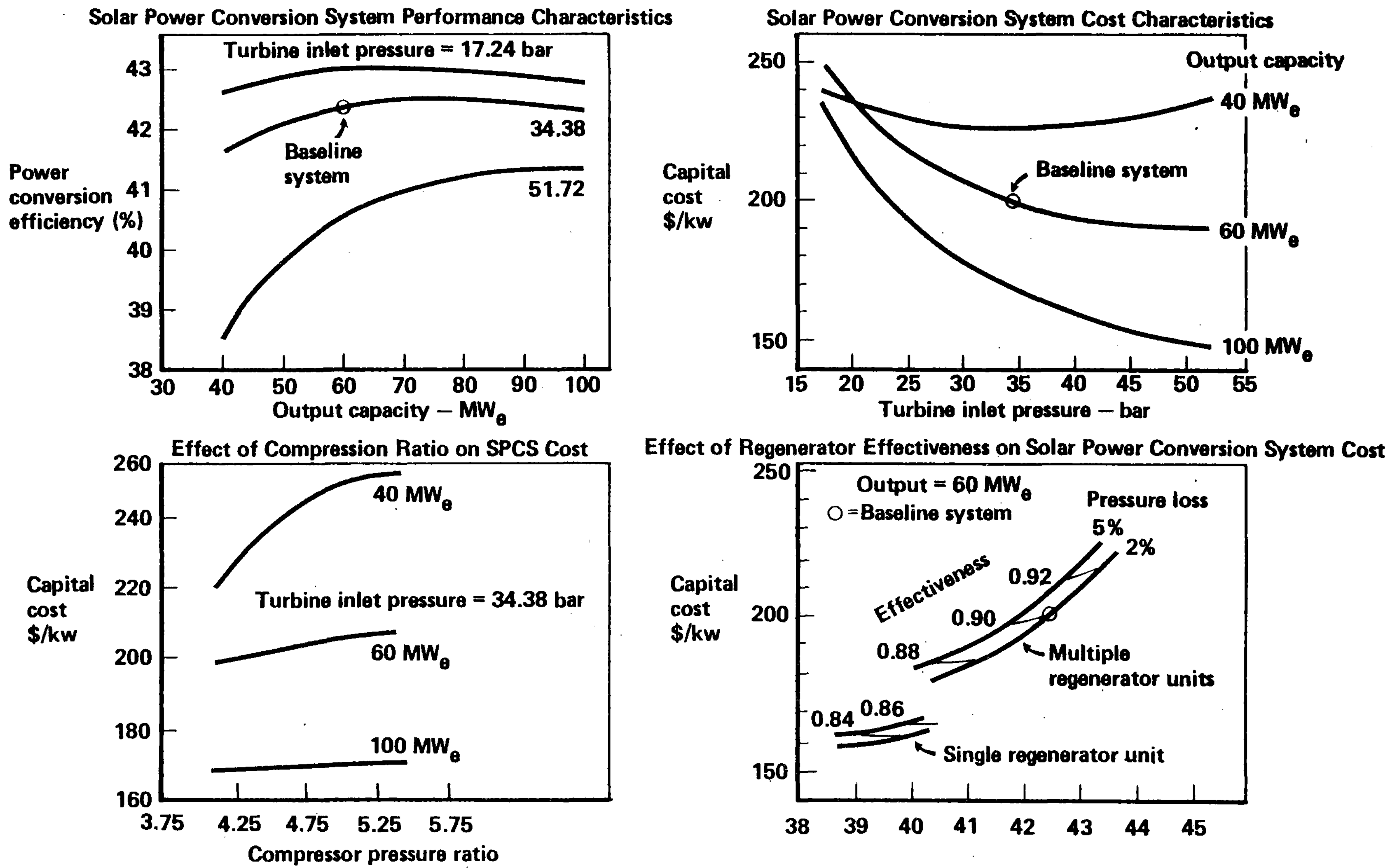

Figure 4. Brayton-Cycle Electric Power Subsystem Performance

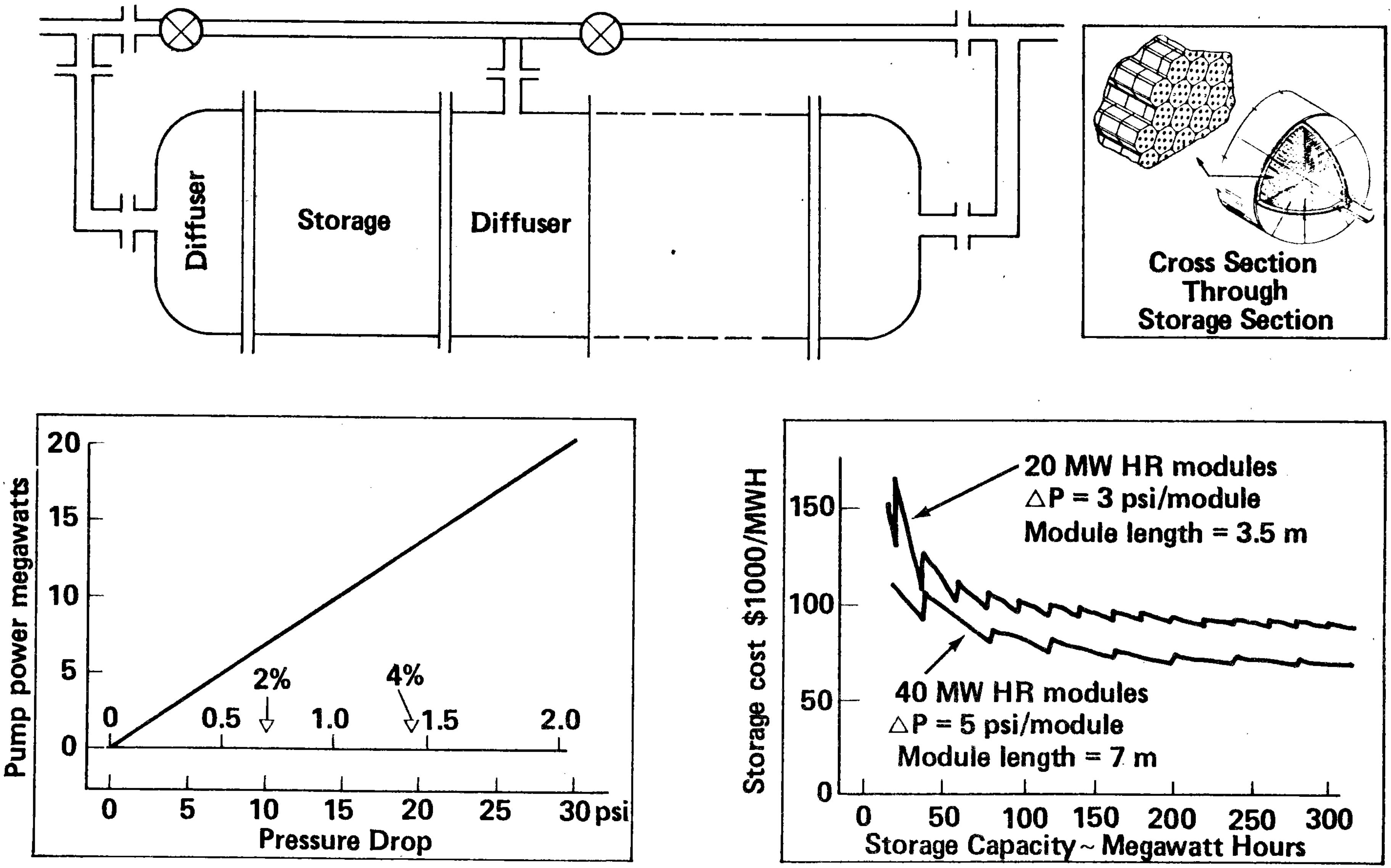

Figure 5. Sensible Heat Storage Subsystem

CONCEPTUAL DESIGN OF ADVANCED CENTRAL RECEIVER POWER SYSTEMS

General Electric Company

R. M. Salemme

The objective of this solar thermal electric study is to develop an advanced central receiver power plant design which offers the potential for significant cost reduction with respect to the water/steam cooled receiver system currently under development by the Department of Energy. A number of subsystem alternatives have been considered, and an approach which combines a sodium cooled receiver with thermal storage and a steam power generation cycle has been selected.

As indicated in Table I, this work is being done under a contract with the Department of Energy which began on February 1, 1978. The contract work schedule is shown in Figure 1. Task 1 has been completed, and the parametric analysis is in progress. Cost and performance data for the advanced central receiver commercial plant design will be available near the end of October, and the final report is scheduled to be issued by the end of January, 1979.

The organization that has been assembled for this program is identified in Table II. General Electric Corporate Research and Development has the prime responsibility for the contract effort, and is directing the program and performing all systems integration required to coordinate the efforts of the other team members. Other General Electric departments are contributing their expertise to the program, and the effort is being supported by the Foster Wheeler Development Corporation, Kaiser Engineers, and the Solar Energy Laboratory of the University of Houston.

Table III summarizes the power plant design concept on a subsystem level. A high efficiency steam turbine cycle has been specified for the electrical power generation subsystem. The selection of steam turbine inlet conditions of 2400 psi and 1000°F with a 1000°F reheat represents a departure from the typical inlet condition of 1800 psi and 950°F with a 950°F reheat for a fossil fired steam plant of 100 MWe capacity. This difference is dictated by economic factors unique to solar thermal power generation

TABLE I

CONCEPTUAL DESIGN OF ADVANCED CENTRAL RECEIVER POWER SYSTEMS

DOE Contract No.:	EG-77-C-03-1725
Objective:	To demonstrate the potential for reducing the cost of electricity produced in a solar central receiver power plant
Contract Value:	$675K
Start Date:	1 February 1978
Period of Performance:	12 Months

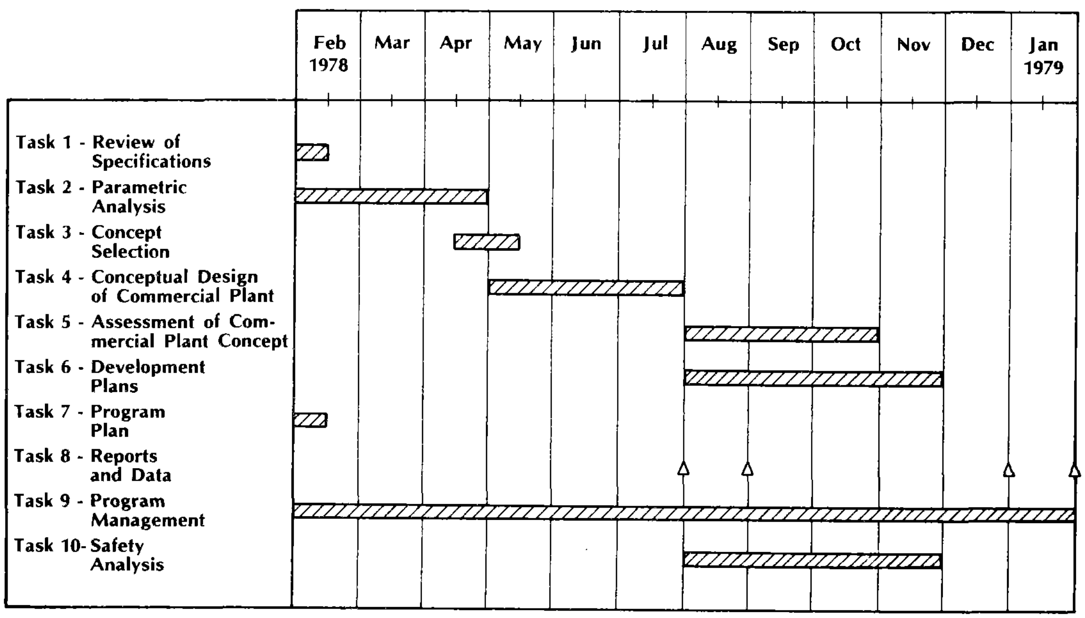

Figure 1. Conceptual Design of Advanced Central Receiver Power Systems Program Schedule

TABLE II

PROGRAM ORGANIZATION

General Electric Company	
Corporate Research & Development	Program Management, Technical Direction and System Integration
Fast Breeder Reactor Department	Receiver, Storage
Energy Systems Programs Department	Heliostats
Medium Steam Turbine Department	Steam Cycle
Electric Utility Systems Engineering Department	Controls, Assessment
Foster Wheeler Development Corporation	Absorber Panels, Storage Vessels
Kaiser Engineers	Storage Vessels, Receiver Tower, Plant Arrangement
University of Houston Solar Energy Laboratory	Heliostat Field Optimization

TABLE III

POWER PLANT DESIGN CONCEPT

Electrical Power Generation Subsystem:	Steam Turbine-Generator
Receiver Subsystem:	Liquid Metal Cooled Tubed Panels
Storage Subsystem:	Sensible Heat
Collector Subsystem:	High Flux Focusing

which require an electrical power generation subsystem that maximizes efficiency, whereas the fossil selection strategy is based on a different set of economic factors.

The receiver and storage subsystems employ liquid sodium as the heat transfer medium. This selection was made as a consequence of the very favorable heat transfer properties of this material which permit accommodation of high thermal fluxes at high temperatures and the storage of thermal energy at high temperature. Consequently, the receiver can be designed as a smaller unit, which reduces its weight, cost, and thermal losses; also, the size of the storage subsystem required to store a unit volume of energy can be reduced. Furthermore, because thermal energy is withdrawn from storage in the form of high temperature liquid sodium, the steam turbine can be operated at the full rated throttle inlet condition during most of the storage discharge cycle. An additional advantage of the concept of using liquid sodium as the heat transfer medium derives from placement of the steam generators at the base of the tower where a reheat cycle becomes practical. The opportunity to improve steam cycle efficiency is not practical when steam is generated directly in the receiver.

This design approach has been integrated into the generalized power plant concept shown schematically in Figure 2. In it, a field of heliostats concentrates solar energy onto a high flux liquid sodium cooled receiver. Thermal energy is transported down the tower to a secondary liquid sodium heat transfer loop. An intermediate heat exchanger (IHX) isolates the high pressure of the primary loop at the bottom of the tower from the secondary loop. Thus the storage vessels, steam generators, and piping need not be designed to handle high-pressure liquid sodium.

Liquid sodium from the hot leg of the secondary loop flows to the steam generators and/or storage and is returned to the IHX at approximately 630°F. During periods when sunlight is not available, hot sodium is withdrawn from the storage subsystem and is used to generate steam. For a substantial fraction of the discharge period, liquid sodium would be available at full design temperature, and steam conditions would remain unchanged.

On the steam side of the system, steam is superheated to the high-pressure turbine inlet condition of 2400 psi and 1000°F. The high-pressure turbine exhaust is reheated to 1000°F, passed through the reheat turbine, and then through the low-presssure turbine. Extraction steam provides feedwater heating as in the case of a fossil fired plant.

The final selection of component and subsystem specifications will result from a parametric analysis being conducted as the initial step in this study. The items being considered in this portion of the study are listed in Table IV. The major collector subsystem decisions will involve the selection of a heliostat and field configuration. The basis of this selection will be the unit cost of thermal energy delivered to the base of the tower.

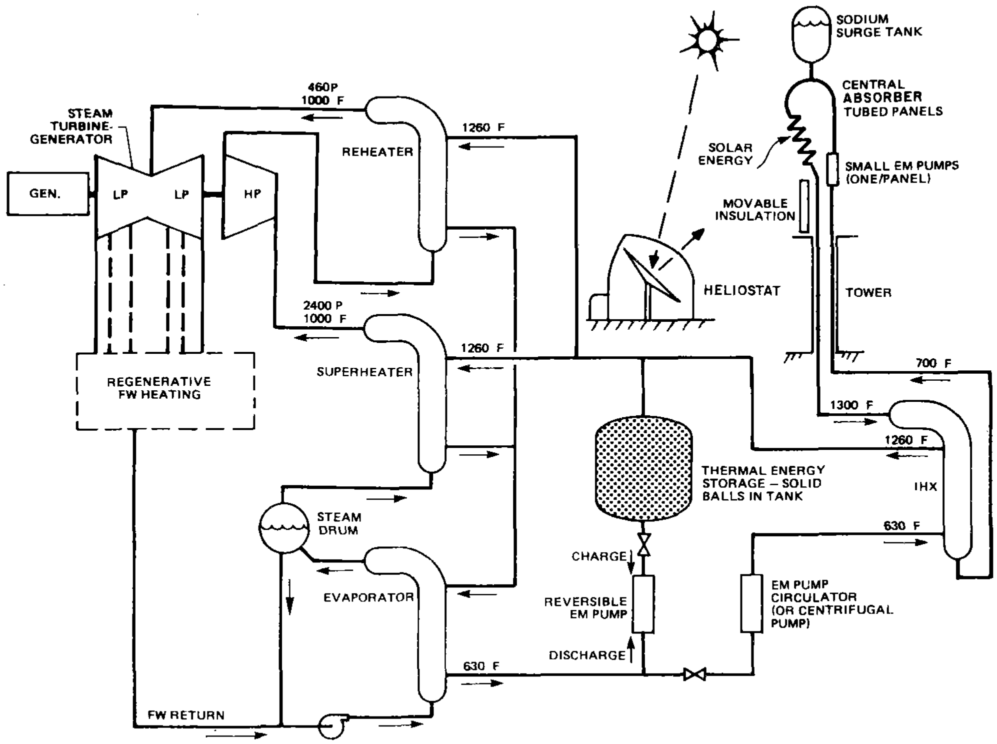

Figure 2. Reference Advanced Central Receiver Power Systems

TABLE IV

SUMMARY OF PARAMETRIC CASES

Subsystem or Component	Options
Heliostat	• GE-Enclosed Heliostat • McDonnell Douglas Heliostat
Heliostat Field	• North Field • 360° Field
Receiver	• 1100 F Peak Sodium Temperature • 1300 F Peak Sodium Temperature
Thermal Storage	• Hot Sodium • Hot Sodium Plus Iron • 1100 F Peak Temperature • 1300 F Peak Temperature • Factory-Assembled Tanks • Field-Assembled Tanks
Steam Cycle	• Steady Steam Conditions (Sodium) • Declining Steam Temperature (Sodium Plus Iron)

The selection of receiver temperature will depend primarily on materials considerations. An upper temperature limit of 1300°F has been identified based on a preliminary selection of Inconel 625 as the hot leg material of construction. The suitability of this material at 1300°F must be confirmed by a detailed engineering analysis and testing.

The objective of the thermal storage parametric analysis is to identify a minimum cost approach that will permit turbine operation at full design inlet conditions over a major fraction of the discharge cycle. Storage at 1300°F would be preferred but must be confirmed as in the case of the receiver, and an analysis of vessel fabrication techniques will identify the lowest cost construction approach. The use of iron filler within the storage vessels to augment the thermal storage capacity shows potential for substantially reducing the storage volume requirement in a cost effective manner provided a design which minimizes dispersion of the thermocline during discharge is identified.

Results of a preliminary analysis of this question are encouraging. Figure 3 presents schematic diagrams of the two storage concepts under consideration: hot sodium in vessels, and hot sodium in vessels containing iron. In the first case at least two vessels would be required. During the charge cycle, cold sodium would be withdrawn from the cold tank, heated, and returned to the hot tank. During the discharge cycle, hot sodium would be withdrawn from the hot tank, used to raise steam, and returned to the cold tank. With this mode of operation, sodium at full rated storage temperature would be available during the entire discharge cycle.

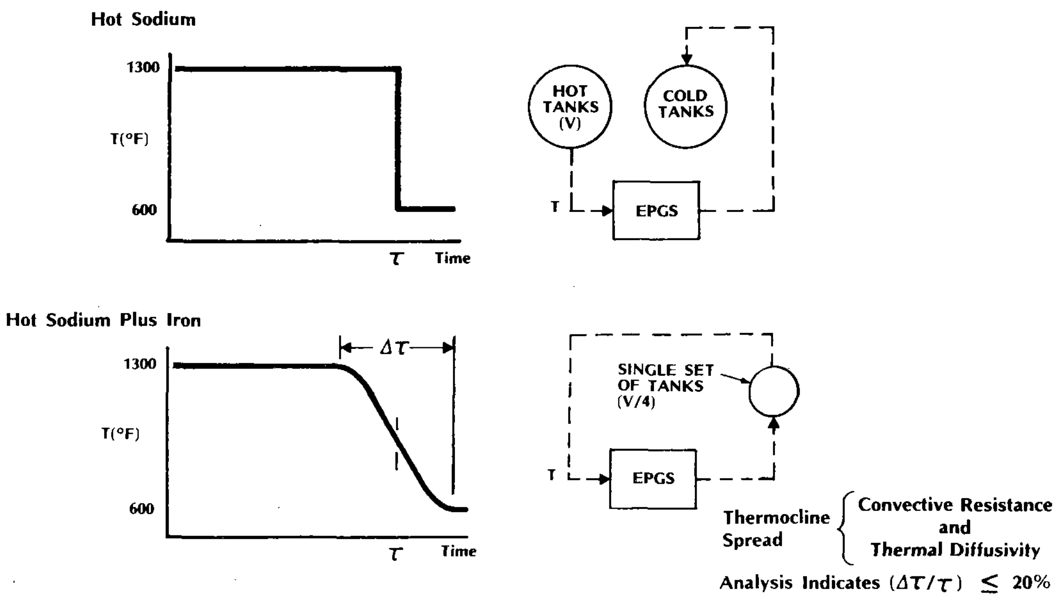

Figure 3. Preliminary Results - Thermal Storage Subsystem

By employing iron filler in the storage vessel to augment the storage capacity of the liquid sodium, a system employing a single vessel with a volume as much as 75 percent less than the two vessels required in the previous case could be designed. A typical discharge cycle would start with the storage vessel full of hot sodium. As hot sodium is withdrawn from the top of the vessel, cold sodium is reintroduced in the bottom. Thus a thermocline will result which will move up the vessel as more hot sodium is withdrawn and which will tend to become diffused with time. Preliminary analysis indicates that this dispersion effect can be minimized so that less than 20 percent of the discharge cycle would require operation of the steam turbine on degraded steam conditions.

In summary, the General Electric Company has considered a number of advanced central receiver power plant concepts and has identified an approach which has high potential for meeting the desired objective of economy. This approach utilizes the very favorable high-temperature thermal properties of liquid sodium to achieve improved plant performance and reduced cost. This contract will provide the conceptual design and analysis needed to quantify the anticipated performance and cost advantages of the proposed approach. It will also develop an implementation plan aimed at further development of this advanced central receiver technology.

CONCEPTUAL DESIGN OF ADVANCED CENTRAL RECEIVER POWER SYSTEMS - PHASE I

Martin Marietta Aerospace
Denver Division

Thomas R. Tracey

Program Plan and Status

The Martin Marietta advanced central receiver system uses a high-temperature salt as the primary heat transfer fluid in both the receiver and thermal storage subsystems. High-temperature salts have been used successfully in commercial heat transfer applications for over 30 years.

As shown in Figure 1, the period of performance is from October 1977 through September 1978. In Task 1 the specification was reviewed and the comments were resolved with the customer. Tasks 2 and 3 are the major study tasks under way at this time. In Task 2 we are performing a wide range of parametric studies and alternative assessments including heliostat field configurations, receiver types, plant size, number of modules, amount of storage, receiver thermal analysis, alternate salt systems, and storage tank designs. The systems analysis effort in Task 3 uses the results of Task 2 to determine minimum cost system configurations. Selection of the baseline system will be made at the end of March. In Task 4 we will perform a conceptual design of this selected system. Task 5 consists of an assessment of the conceptual design including performance, cost, reliability, potential for future improvement, market penetration, and environmental impact. Task 6 will result in the definition of a cost effective development plan leading to construction of the first commercial unit. Alternative development plans will also be defined and compared for technical risk and economics. Specific recommendations for the Phase II hardware development and testing will be made, together with cost and schedule estimates. A conceptual design of a pilot plant for Phase III, including cost and schedule estimates, will also be prepared. The Task 7 program plan was completed early in the program and has been coordinated with DOE. The safety analysis effort in Task 10 will use the results of the first generation studies and the procedures used in industrial salt systems as the starting point for assessing potential safety hazards.

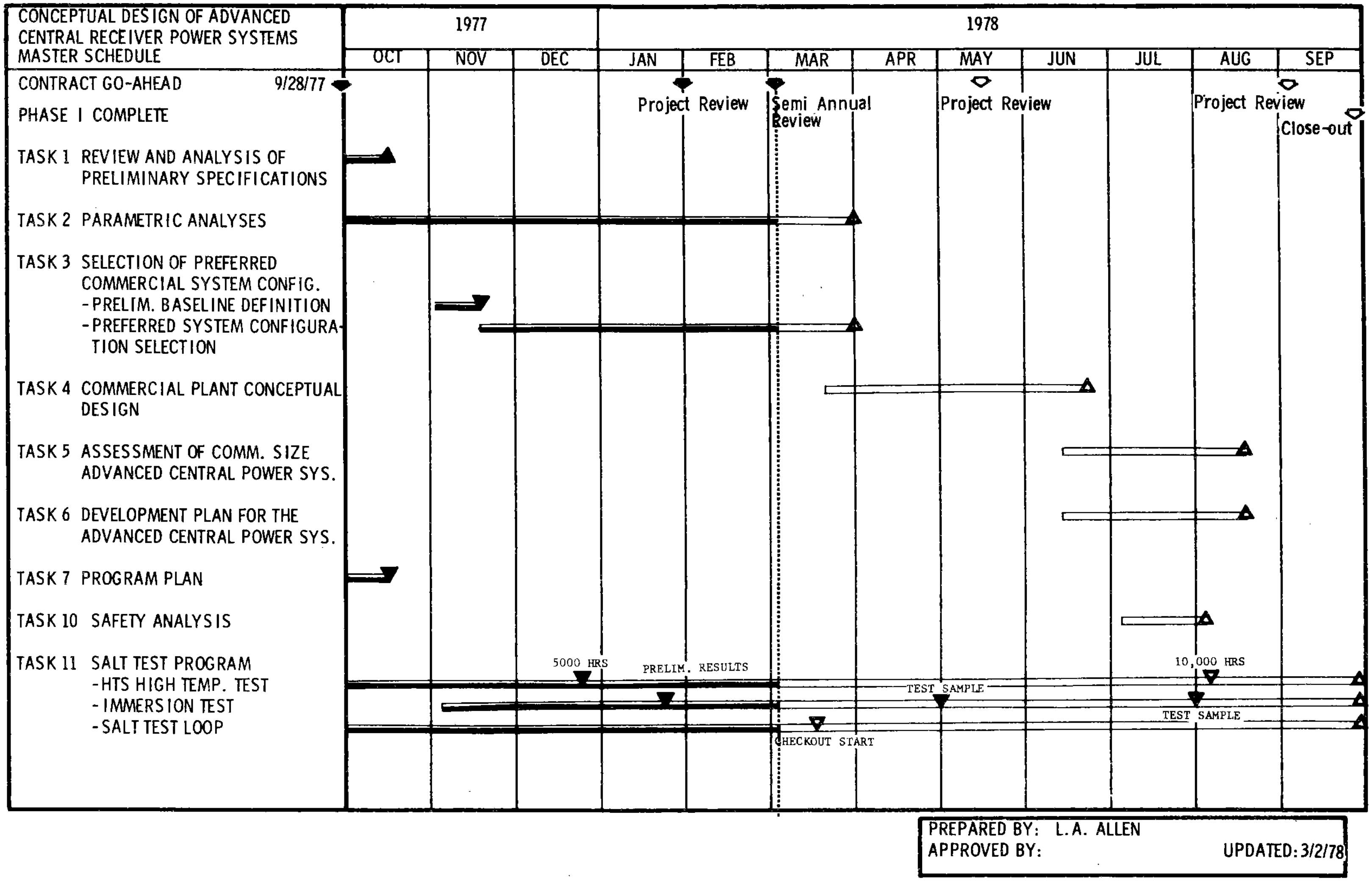

Figure 1. Program Plan

The long-term, high-temperature salt stability tests of Task 11 have run over 5500 hours with negligible decomposition. The immersion tests of potential salt system construction materials show a very small weight increase with time after about 500 hours of test. The rate of the weight increase with time is decreasing as expected. The salt test loop testing will be starting in March 1978.

Team Members and Responsibilities

The team members and their primary responsibilities are given in Table I.

TABLE I

TEAM MEMBERS AND RESPONSIBILITIES

Organization	Responsibility
Martin Marietta Corporation	Program Management System Design and Optimization Interface Definition
Badger Plants Incorporated	Conceptual Design and Optimization of High-Temperature Salt Subsystems
Black & Veatch Consulting Engineers	Conceptual Design, Analysis and Optimization of the Electric Power Generation Subsystem, Tower, and A&E Support
Arizona Public Service	Provide Utility Engineering and Operational Review of the System Design to Maximize Utility Acceptance Support Martin Marietta in Economic Analysis and Optimization

System Description

A functional schematic of the system is shown in Figure 2. The collector subsystem consists of heliostats which reflect the solar energy onto a heat receiver located on top of a tower in the receiver subsystem. A high-temperature salt (typically 50 percent $NaNO_3$; 50 percent KNO_3) is used as the heat transfer fluid in the receiver, the heat transport fluid to transport the heat to the storage subsystem and/or the steam generator, and as the storage fluid. The storage subsystem consists of the tankage to store the salt and the associated piping, valves, and controls. The electric power subsystem contains the steam generator in which the thermal energy in the salt is transferred to the steam/water working fluid used in the turbine, the turbine generator and associated equipment, and the electric power regulation equipment. Each of the subsystems will have their own controls. In addition, a master control subsystem is used to properly sequence the subsystem controls, provide shutdown for unsafe conditions, and provide real time operations information and records of operating data.

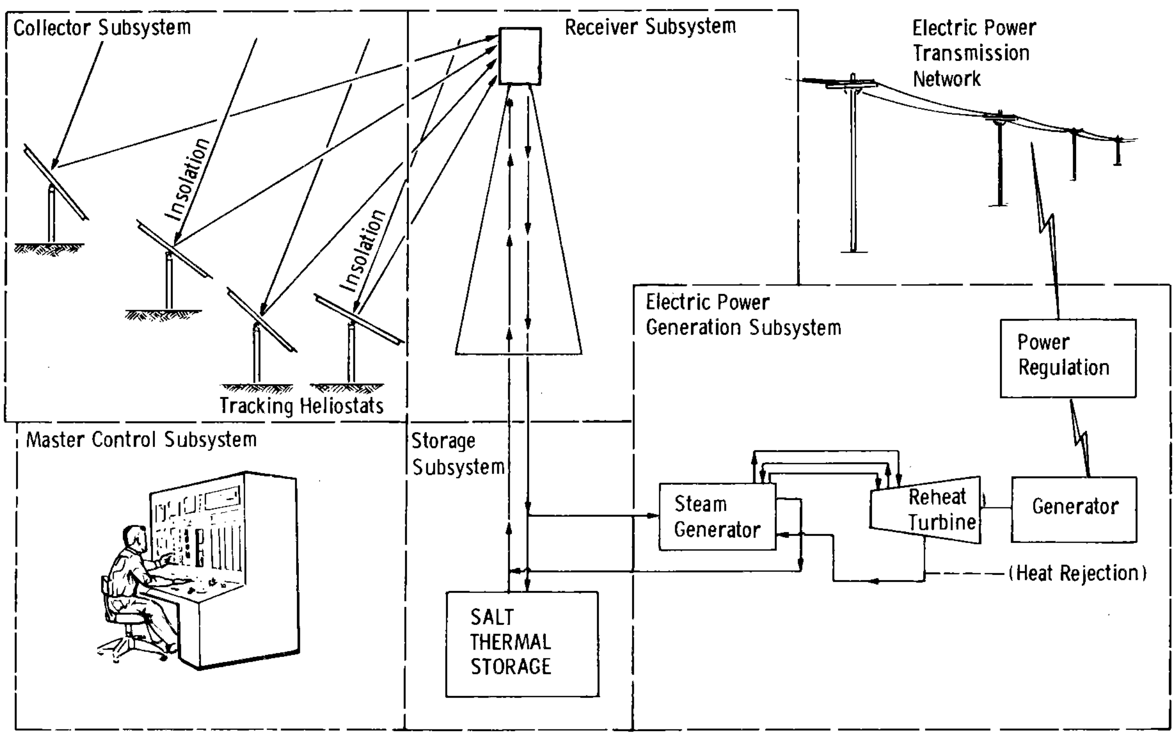

Figure 2. Functional Schematic

A more detailed schematic of the salt subsystems and their interface with the electric power generating subsystem is shown in Figure 3. The salt loop is shown with the heavy lines, and the water/steam loop is shown with the lighter lines. During operation from the receiver, the salt is pumped through the receiver where it increases in temperature from about 550 to 1050°F. The high-temperature salt is pumped to the steam generator and/or storage. During operation from storage, hot salt is pumped from the tank through the steam generator heat exchangers and back to the tank. On the salt side of the heat exchangers, the superheater and reheater are in parallel, and the boiler preheater are in series. The feedwater from the steam cycle is pumped to the steam generator, and steam at about 950°F and 1800 psig is delivered to the turbine. The reheat steam from the turbine is also heated back to approximately 950°F.

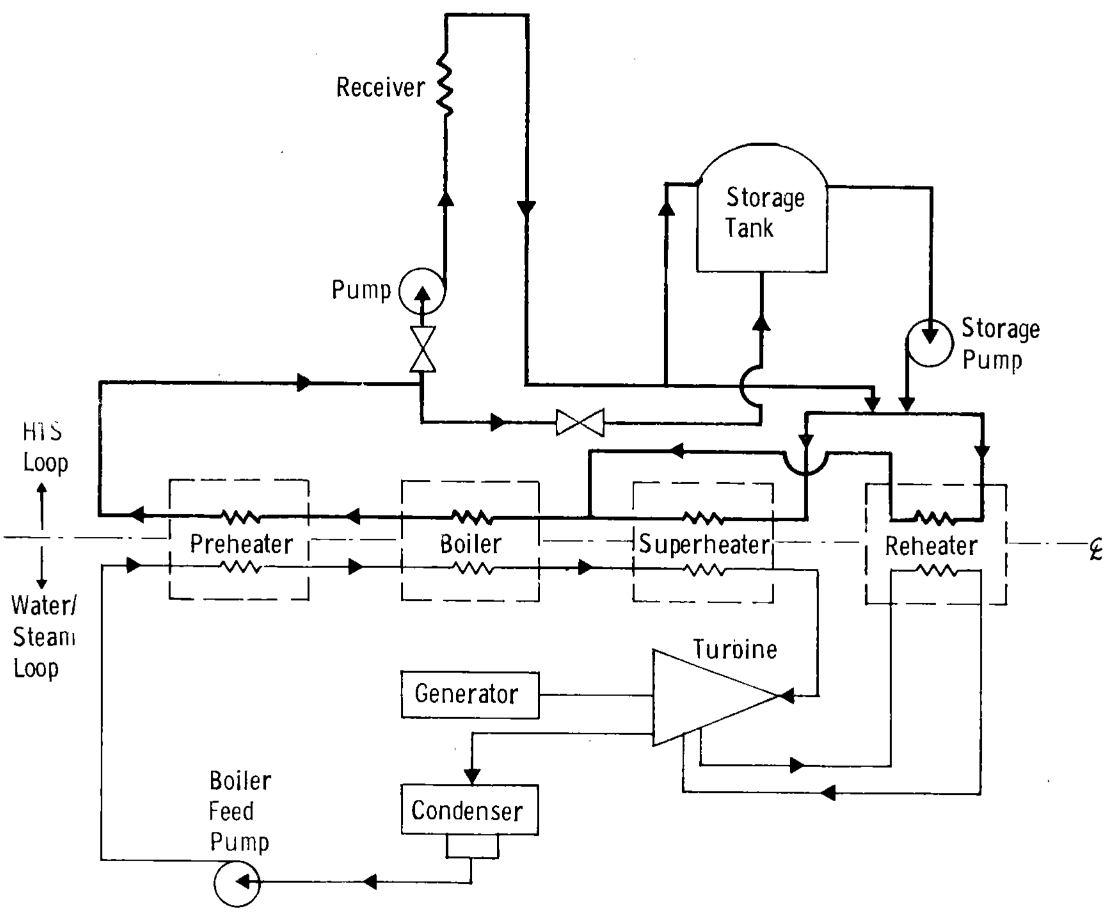

Figure 3. HTS - Rankine-Cycle Flow Schematic

System Performance

The results of preliminary system performance calculations for the preliminary commercial plant configuration are given in Figure 4. The plant output in this example is 100-MWe (net), and the thermal storage capacity is sufficient to run 24 hours at full load at summer solstice. The thermal-to-electrical gross efficiency of 41.5 percent is about 11 percent better than the first-generation system when operating from the receiver and 35 percent better from storage.

Plant Output	100 MW_e (Net)
* Solar Multiple	2.23
Thermal to Electric Conversion Efficiency (gross)	41.5% (from receiver) 41.5% (from storage)
Annual Average Effective Plant Output	.565 x 10^6 MW_e - H
Peak Receiver Energy Collection Rate	605 MW_{th}

*Results in 24 hour operation at 100 MW_e (net) at summer solstice.

Figure 4. Example System Performance Estimate

Potential Advantages of the High-Temperature Salt/Solar System

The potential advantages of the salt/solar system are:

- Improved System Efficiency
  - Reheat is practical
  - Higher pressure turbines are practical
  - Efficiency from storage is the same as from receiver (~35 percent better than first generation)

- Large Improvement in Thermal Storage Economics
  - Fluid Δ T 500°F (typical)
  - Fluid Cost ~9 cents/pound
- Modularity is Practical

  Low piping costs due to:
  - High density specific heat product
  - Low pressure piping
- 30 Years of Industrial Experience With Salt Systems
- Safe Fluid - No Chemical Reactions With Air or Water
- Lower Cost Receiver
- Simpler System

Reheat is practical because the steam generator can be located near the turbine so that the reheat steam piping is short. Turbines with higher inlet pressure can be considered because large amounts of thermal storage are economical, which will result in considerably less thermal cycling than in the first-generation systems. Also, the steam conditions are the same from storage as from the receiver. As a result, the efficiency from storage is much better than in the first-generation systems. (The reason for the reduced steam pressure and temperature from storage in the first-generation systems is that in order to reduce the amount of storage media required it is necessary to reduce the lower operating temperature of the storage media.)

In a sensible heat storage media, the quantity of storage material required is inversely proportional to the temperature difference over which the material is operated. This temperature difference was limited to about 100°F in the first-generation systems to limit the performance reduction when the system was operated from storage. In the salt system, a temperature difference of 500°F is practical, which drastically reduces the amount of storage material required. In addition, the materials for the salt ($NaNO_3$ and KNO_3) are inexpensive; in large quantities it can be procured for about 9 cents per pound.

Modularity in a solar power plant has the potential advantage of minimizing the scaling risks in going from a pilot plant to a commercial plant and results in flexibility to accommodate different plant sizes and storage requirements. The major cost of modularity is piping. The salt system should have relatively low piping costs because it has a high density specific heat product ($37 \frac{Btu}{ft^3/°F}$) and low pressure.

There has been over 30 years of industrial experience with salt systems in the chemical processing industry. The systems have had a very good record of reliability and safety. As an example, Riechold Chemical Co. of Elizabeth, New Jersey, reports 18 years of virtually trouble-free service of the salt system in their Maletic Anhydride plant. As a result of this experience, critical components such as pumps, valves, controls, and instrumentation are readily available with a high reliability and relatively low cost.

The salt has no chemical reaction with air or water and is non-toxic. In fact, similar salts are commonly used in open baths for metal heat treatment.

The heat receiver is a single phase heat exchanger, which is much simpler than a steam generator. Our preliminary studies show that it has the potential to be much lower in cost.

Development Issues

The primary development issues now foreseen for the advanced central receiver salt system are:

1. Long-term, high-temperature stability of the salt, and

2. Long-term, high-temperature material compatibility with the salt.

Test programs are in progress to obtain the required data; the data to date are very encouraging.

Test Program Status

The test program status is as follows:

- Long-Term, High-Temperature Salt Stability
  - The salt is very stable after over 5500 hours at 1100°F
- Material Compatibility With Salt at High Temperature
  - Preliminary data (500 hours) shows small weight gain with significantly decreasing rate of weight gain with time
  - No evidence of stress corrosion at 500 hours

- Fluid Loop
  - Determine fluid dynamic effects on material compatibility
  - Verify heat transfer coefficients over use temperatures
  - Verify thermal and stress analysis of receiver tube
  - Tests to start in March 1978

The long-term, high-temperature salt stability tests were conducted by measuring pressure changes from a sample of salt which was maintained at 1100°F by heaters on a stainless-steel container.

In the immersion tests to investigate material compatibility, standard ASTM test methods are used to measure weight changes of the metal specimens. Standard stress corrosion techniques were used to test the materials for stress effects or corrosion.

The fluid loop has a capacity of about 30 gpm and operates over the full expected temperature range of 550 to 1050°F. Radiant heaters have been designed which simulate the asymmetric radiative heating on the receiver tube test specimens.

SOLAR CENTRAL RECEIVER PROTOTYPE HELIOSTAT

Boeing Engineering and Construction
Seattle, Washington

R. Gillette

DOE Contract EG-77-C-03-1604

In conjunction with the overall national effort to develop solar thermal electrical power as an alternate energy source, Boeing Engineering and Construction is under contract with United States Department of Energy (DOE) to develop a preliminary design (PD) of heliostats for central receiver type plants. Technical monitoring of contract progress is being performed for DOE by Sandia Laboratories. The primary objective of this contract is to establish a heliostat design that, in quantity production, will yield significant reductions in capital and operating costs as compared with existing designs. The scope of the present effort includes:

1. Development of a heliostat preliminary design,
2. Preparation of a conceptual design of required manufacturing, installation, and maintenance processes,
3. Estimation of heliostat cost in several large production quantities,
4. Preparation of plans for Phase II.

The Boeing heliostat preliminary design prepared for the 10-MWe Pilot Plant at Barstow, under DOE Contract EY-76-C-03-1111, is shown in Figure 1. In this concept, circular membrane reflectors formed with aluminized polyester film, direct sunlight to the central receiver. Transparent air-supported plastic enclosures protect the lightweight reflectors from the environment. The reflectors are individually aimed with a 2-axis gimbal that is driven by digital-controlled stepper motors. Minicomputers provide signals to heliostat control electronics, which in turn operate the gimbal stepper motors.

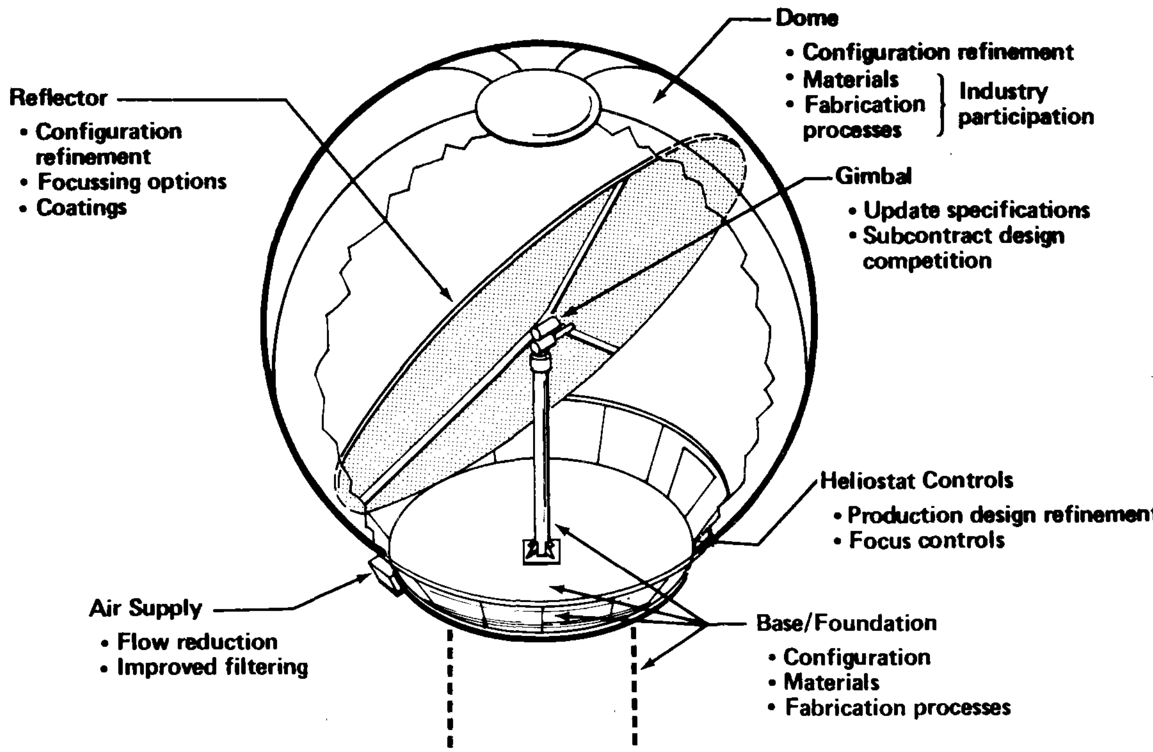

Figure 1. Design Studies

In work performed under contract ERDA EY-76-C-03-1111, prototype heliostats have been fabricated and tested. A total of five heliostats are presently under test at various locations including Boardman, Oregon; Livermore, California; and Tucson, Arizona. Figure 2 shows the heliostat located at Sandia Laboratories in Livermore, California. Heliostats at Boardman have now successfully completed 17 to 19 months of desert exposure.

Presently, studies are under way to select a least-cost design for production rates ranging from 25,000 to 2,500,000 units/year. These studies have thus far included evaluation of a variety of low cost concepts, optical performance optimization analyses, tests to evaluate focusing capability, and tests to determine plastic materials properties and weatherability.

Industry participation has been solicited for various aspects of prototype heliostat design. For example, dome-reflector plastic film requirements were discussed with 25 film manufacturers/processors. Twelve companies were visited by project personnel. Companies presently actively supporting the effort include: Pennwalt, Allied Chemical; Martin Processing; National Metallizing Division (Standard Packaging Corporation); W. T. Grace; Hercules, and

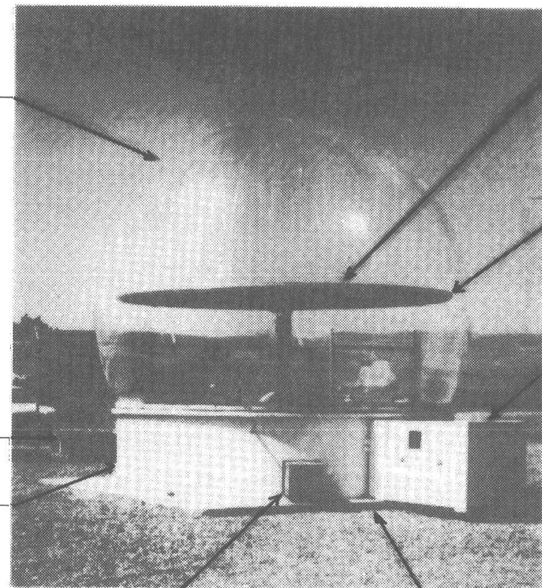

Figure 2. Collector Subsystem - Research Experiment Heliostat

Amoco. Plastic films presently under consideration which could achieve cost objectives include fluorocarbons, polyesters, polycarbonate, and polypropylene. In other industry participation, subcontracts were awarded to Berger-Lahr Corporation and Clifton Precision Corporation for gimbal preliminary design. Cooperative support has also been obtained from numerous other companies for various design details.

One of the concepts being evaluated in detail is shown in Figure 3. It differs from previous heliostat configurations primarily in the base/foundation design. Four concrete pile foundations are utilized; one for reflector support, and three for dome structure support. A tubular steel ring/post support structure transmits wind loads from the dome to the foundation pilings. A semi-spherical rigid shell completes the lower portion of the dome within the support structure. Perforations in the shell include a maintenance hatch, a duct for pressurization air, and electrical cabling pass-throughs.

As part of the prototype heliostat cost optimization studies, focusing of the heliostat was evaluated at Livermore, California. The 15-ft diameter reflector was temporarily modified to permit vacuum focusing of the image on a 600-ft distant target board. Figure 4 shows the reflector directing sunlight onto the target board. Figure 5 shows a visual/photographic comparison of images produced by the reflector with and without vacuum focusing. It should be noted that the image produced without vacuum focusing represents that of a partially gravity-focused reflector. Image power density distribution data for the two respective cases is shown in Figure 6. Exact image size correlation between Figures 5 and 6 is not possible because of the limited range of sensitivity in photographic film.

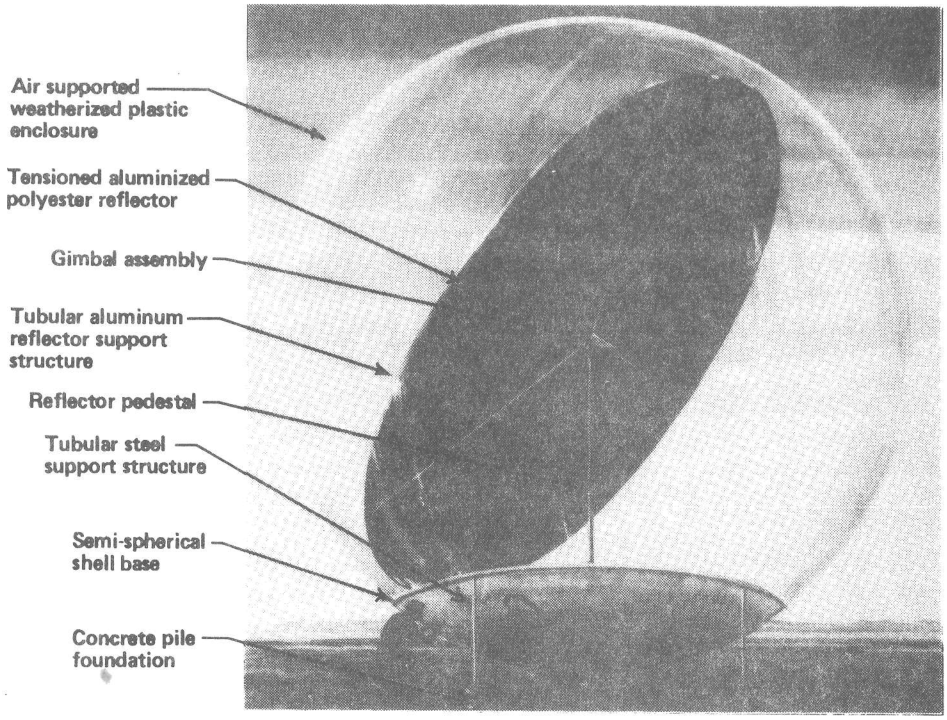

Figure 3. Concept Evaluation

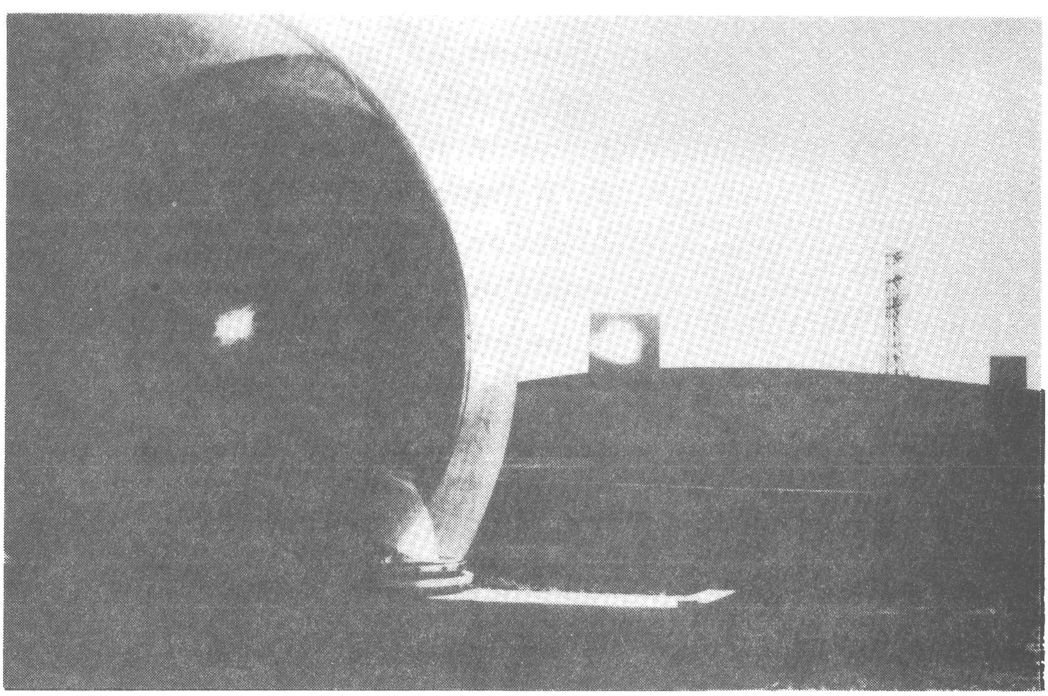

Figure 4. Focusing Test at Livermore

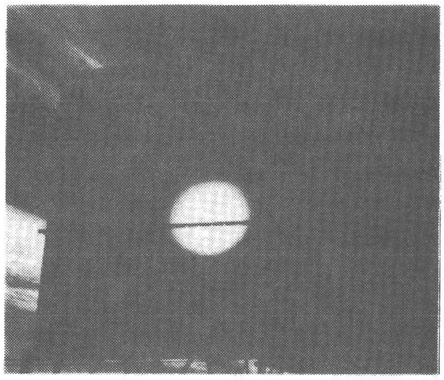

Vacuum Focusing

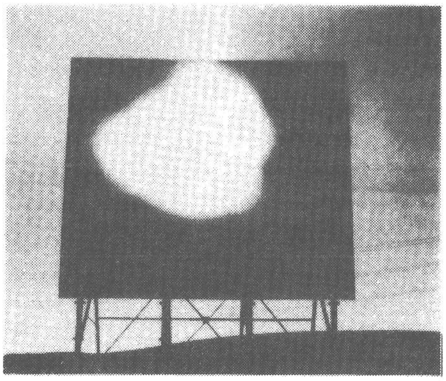

Partial Gravity Focusing

Figure 5. Visual Images at 600-Ft Distance

Partial Gravity-Focused Image

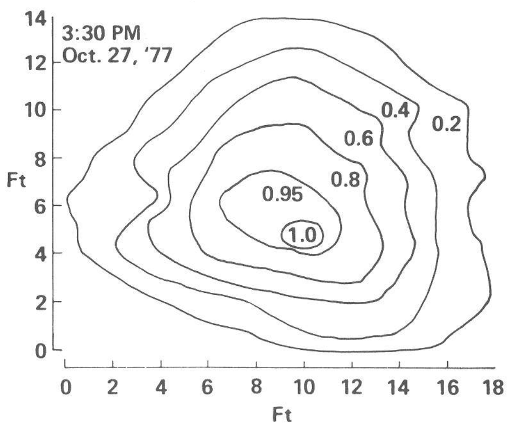

Vacuum-Focused Image

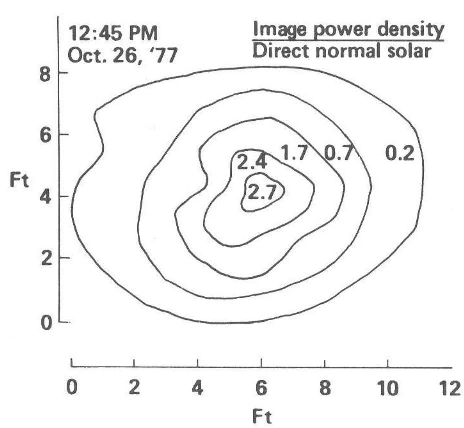

Figure 6. Image Power Density Distribution

Under a companion DOE Contract EY-76-C-03-1111, hailstone tests were conducted on candidate dome materials. The test apparatus used is shown in Figure 7. Specimens were tensioned across the end of a 55-gal drum, air-pressurized to 1.5 in. H_2O, and shaped to an 8-ft radius of curvature to simulate dome conditions. Hailstones ranging from 0.25 to 1.25-in. diameter were propelled at the material with a sling-shot type device as shown in the figure. Velocity of the hailstones was measured with a radar/computer. As shown in Figure 8, hailstones of 0.25 and 0.5-in. diameter produced no visible effect. Hailstones of specification size and velocity (1.0-in. diameter and 75 ft/s) produced small indentations of about 0.38-in. diameter on 4-mil thick Tedlar. Off-normal incidence produced only a minimal effect at 45 degrees and no effect at 60 degrees from normal. Larger hailstones (1.25-in. diameter) produced indentations of about 0.56-in. diameter. In general, test results showed that penetration of the dome material will not occur at specification conditions, and that a considerable (>1.4) design margin exists in failure velocity. The results of these hailstone tests, related to the expected environment in the southwest United States, show that the loss in average dome transmittance over a 15-year period will be less than 1.6 percent. It was concluded that hailstones do not present a threat to domes from either a mechanical or optical loss standpoint.

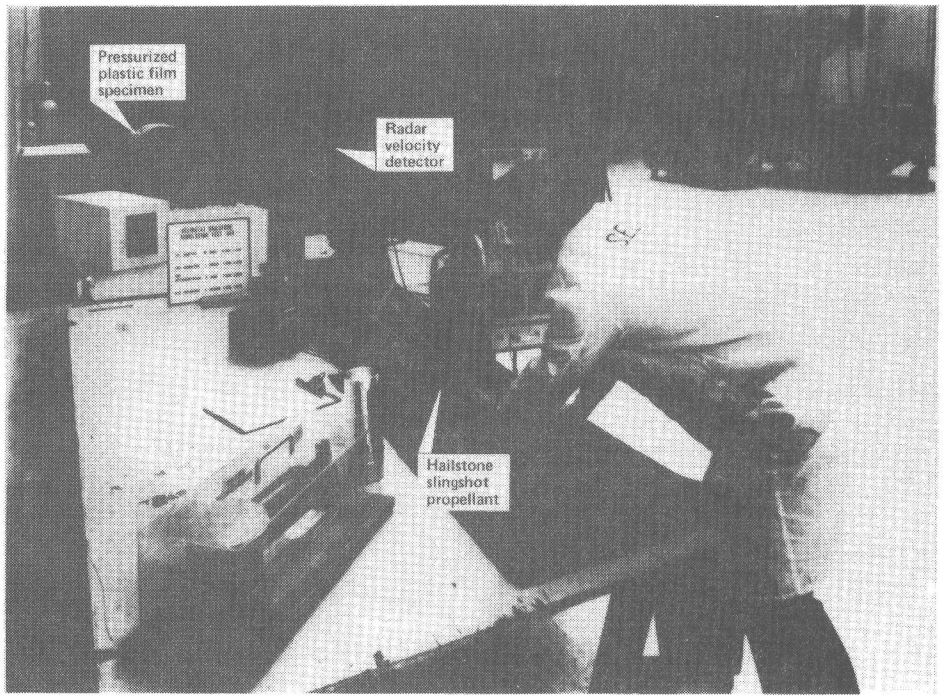

Figure 7. Hailstone Test Apparatus

¼"	• No effect
½"	• No effect
1"	• Normal incidence 75 ft/sec • Minimal effect at 45° incidence • No effect at 60° incidence
1¼"	• 0.56 inch diameter indentation at 82 ft/sec (18 month dome)

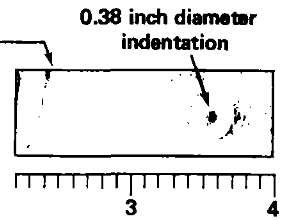

Figure 8. Hailstone Test Results on Tedlar

PROTOTYPE HELIOSTAT DEVELOPMENT

General Electric

R. H. Horton

Summary

The GE heliostat study is at the midpoint of a nine-month Phase I program. The heliostat concept being investigated is an enclosed stretched film reflector system which features semi-automatic installation, 30-minute installation time cycles, 100 percent factory manufacture with maximum cost effective automation, and cost management to assure achievement of the $\$72/m^2$-R goal.

The current configuration is shown in Figure 1. It is being designed to meet a total installed cost of \$1900 for a 40-square meter reference size and to satisfy the requirements of Specification 001. The reflector utilizes a frame consisting of eight struts which stretch the aluminized plastic film surface against the tension of the supporting guy wire system shown in Figure 2.

Using a CG-mounted design and extreme lightweight construction, the drive system operates with linear motors with 12 deg/min maximum slew rates. The control system incorporates a self-calibration system to minimize errors due to installation and manufacture as well as sun calculation errors. The system is open loop, and is shown in the schematic diagram in Figure 3.

A bag-type foundation using in-situ soil is incorporated in the enclosure design. An automatic machine digs a ring-shaped trench and inserts a plastic bag which is filled with the dirt that has been excavated. The enclosure is then manually attached to the foundation ring. Ground covers, replaceable panels, and cost effective material selection are a part of the GE enclosure design activity. A concept drawing of the installation machine is shown in Figure 4.

Highlights of the program are listed in Table I. It is anticipated that the cost performance objectives can be met or exceeded and that low-cost heliostats can be the basis for new central receiver economic attractiveness.

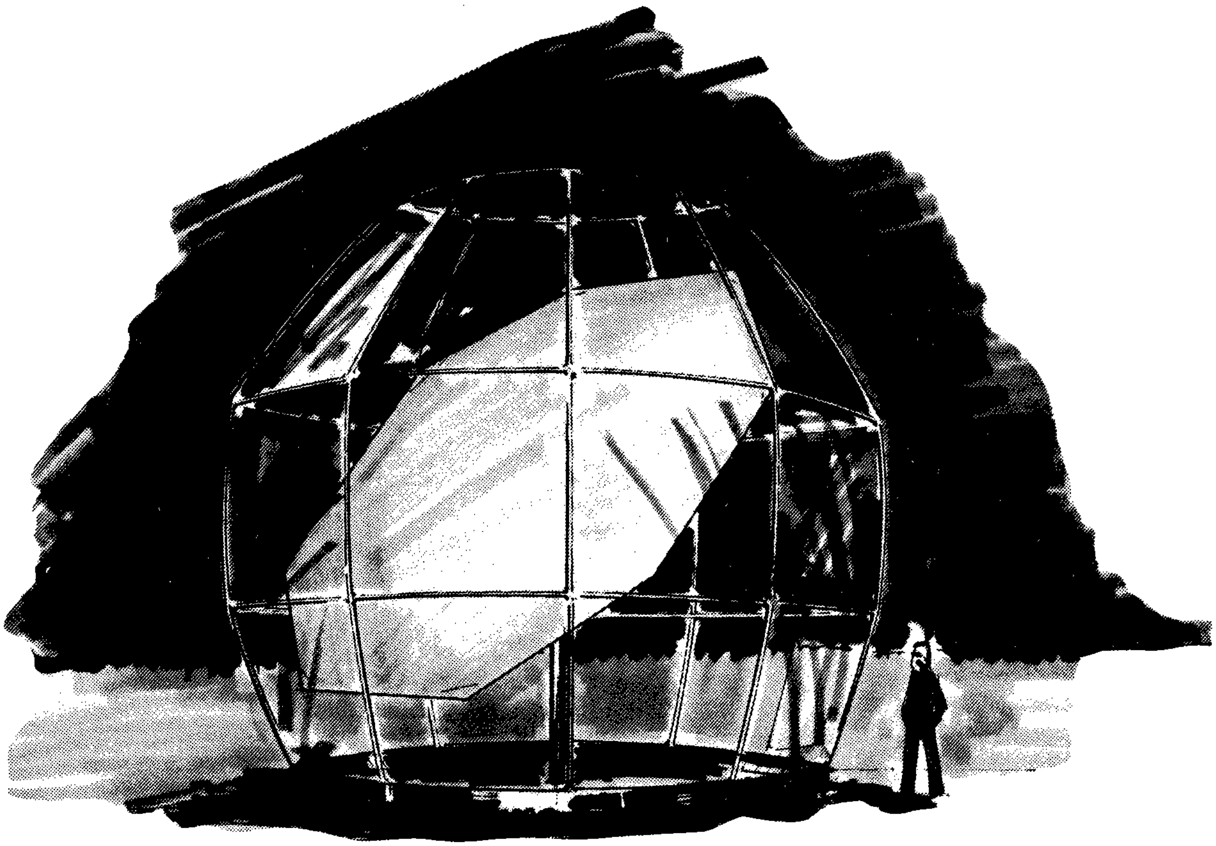

Figure 1

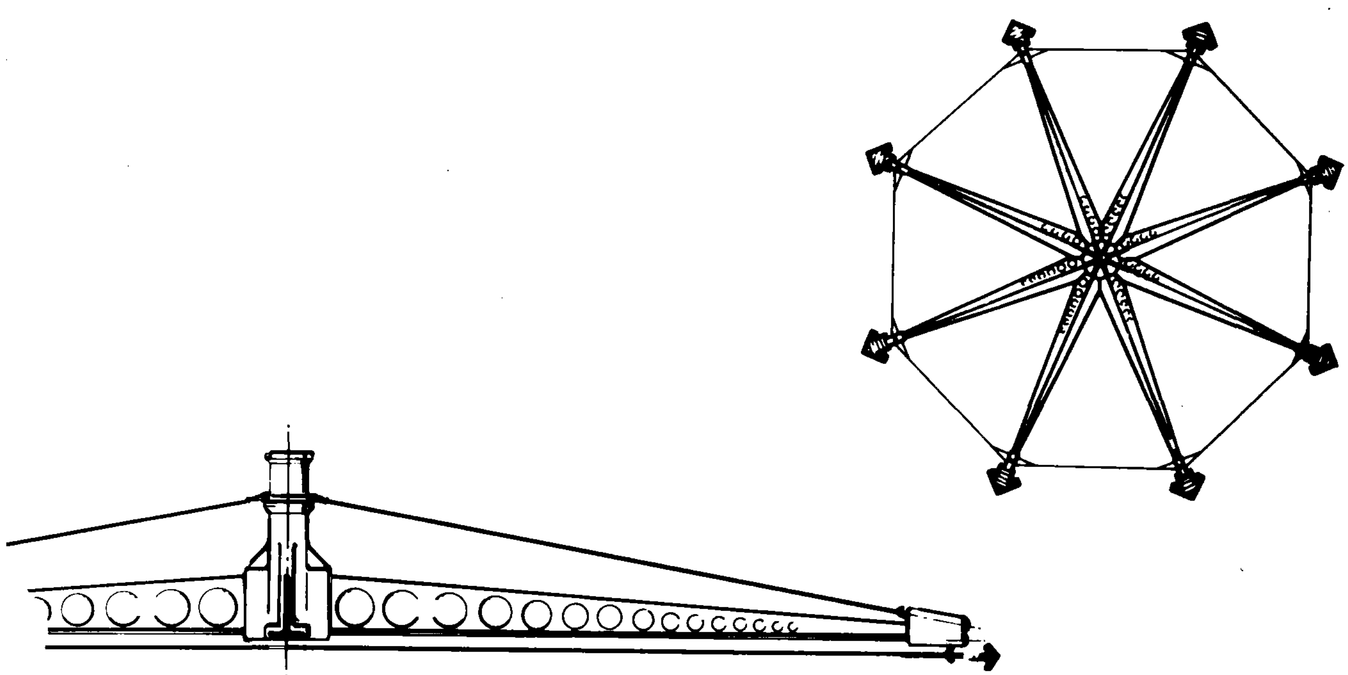

Figure 2. General Electric Stretch Frame Concept

- Open Loop
- Sun Tracking Calibration
- Linear Motor Drives
- Error Compensation

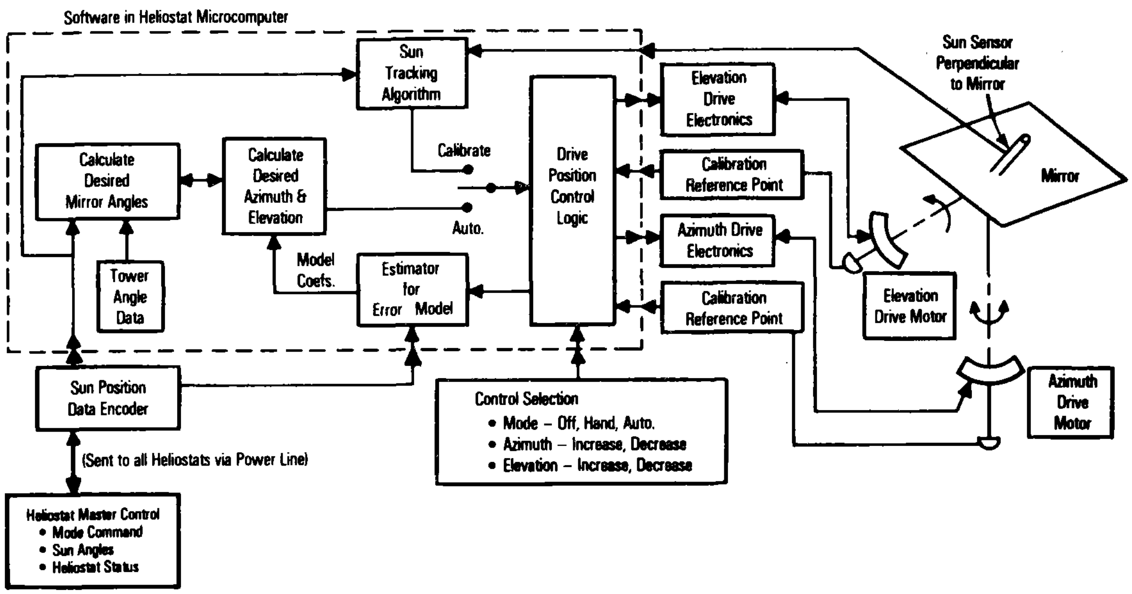

Figure 3. Controls and Drives

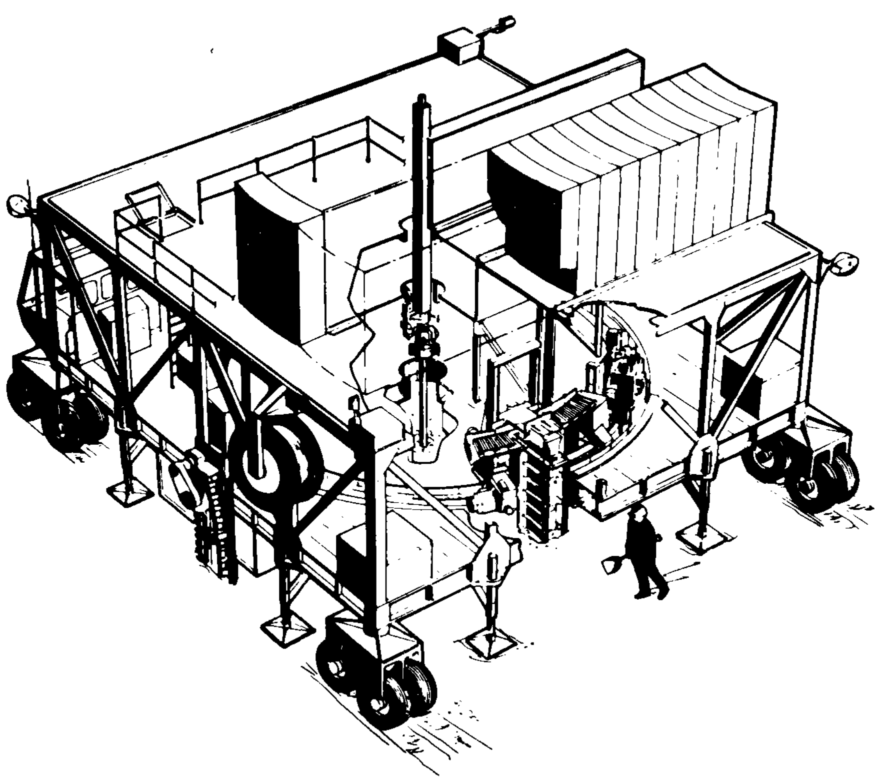

Figure 4

TABLE I

PROGRAM HIGHLIGHTS

• Materials Program Under Way
• Mylar Attachment Tests Successful
• Enclosure Model Constructed
• Strut Design Complete
• Tensioning Provision Conceived
• Design and Manufacturing Iteration
• Control System Defined
• Error Model Demonstrated
• AFM Conceptual Layouts
• Ingersoll Rand Consultation
• Cost Methodology Established
• First Cost Iteration in Process

SOLAR CENTRAL RECEIVER PROTOTYPE HELIOSTAT

McDonnell Douglas/Stearns-Roger/Arthur D. Little

C. R. Easton

Introduction

Heliostat activities during this semiannual period consisted of tradeoff studies on the design, manufacture, installation and checkout, and operations and maintenance; bench model and component tests on critical components; and preliminary designs for the heliostat, manufacturing process, installation and checkout process, and operations and maintenance process.

Design Tradeoff Studies

Design tradeoff studies were conducted on seven components of the heliostat, as illustrated in Figure 1.

Optimum Heliostat Size

The heliostat reflector area was enlarged to match the loads to the assumed drive capacity. This led to a reflector with an area of approximately 50 m^2. Further enlargement of the reflector would lead to difficulties in transportation. Hence no further optimization was conducted.

Low Cost Reflector

Four alternate low-cost reflector configurations were considered. Configurations 1 and 2 use 1/8-in., second surface, float glass mirrors. In configuration 1, the mirrors are supported on hat section stringers. For configuration 2, the mirrors are supported on a deep corrugated steel sheet. Configurations 3 and 4 employ low-cost laminated glass mirrors made with

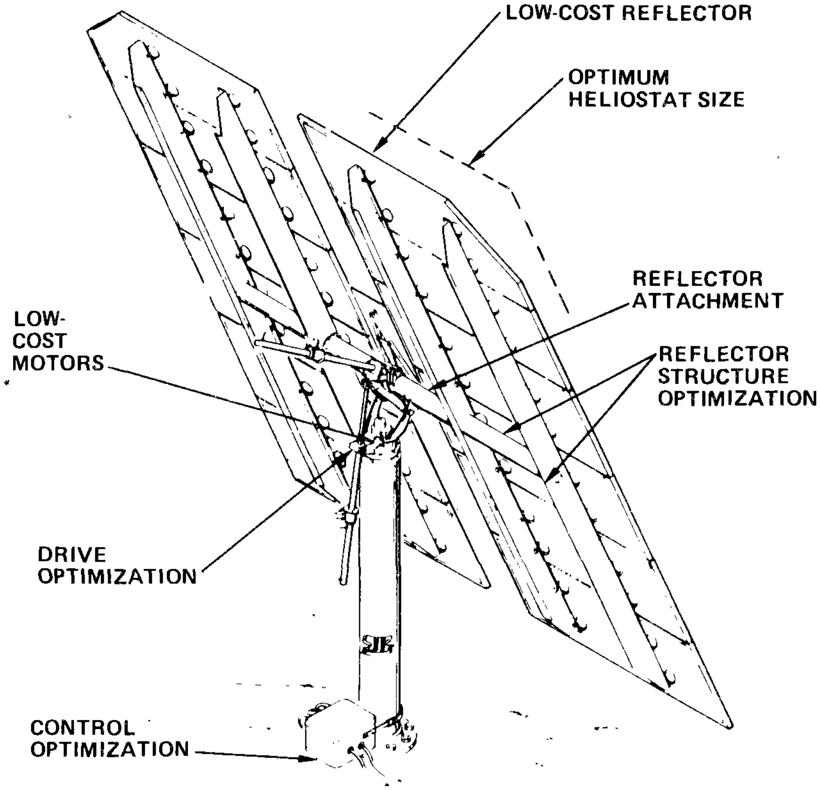

Figure 1. Baseline Azimuth Drive

a room-temperature, low-pressure curing adhesive. In configuration 3, the mirrors are supported on hat sections, and in configuration 4 they are clamped to stringers. Configurations 1 and 3 were selected based on a cost analysis and are undergoing testing.

Drive Optimization

The initial baseline design for the drive unit is shown in Figure 2. Tradeoff studies were conducted to (1) delete the Oldham coupling and the lower drive shaft bearing; (2) simplify the retainer geometry; and (3) incorporate a single input stage to replace the motor gearhead and worm gears.

Control Optimization

Design tradeoffs have been made to integrate the duties of the field controller into the heliostat controller, on the basis of improved microprocessor capability. The absolute encoders on the gimbal axes have been deleted in favor of incremental encoders on the motor shafts, together with counters and non-volatile memory chips in the heliostat controller.

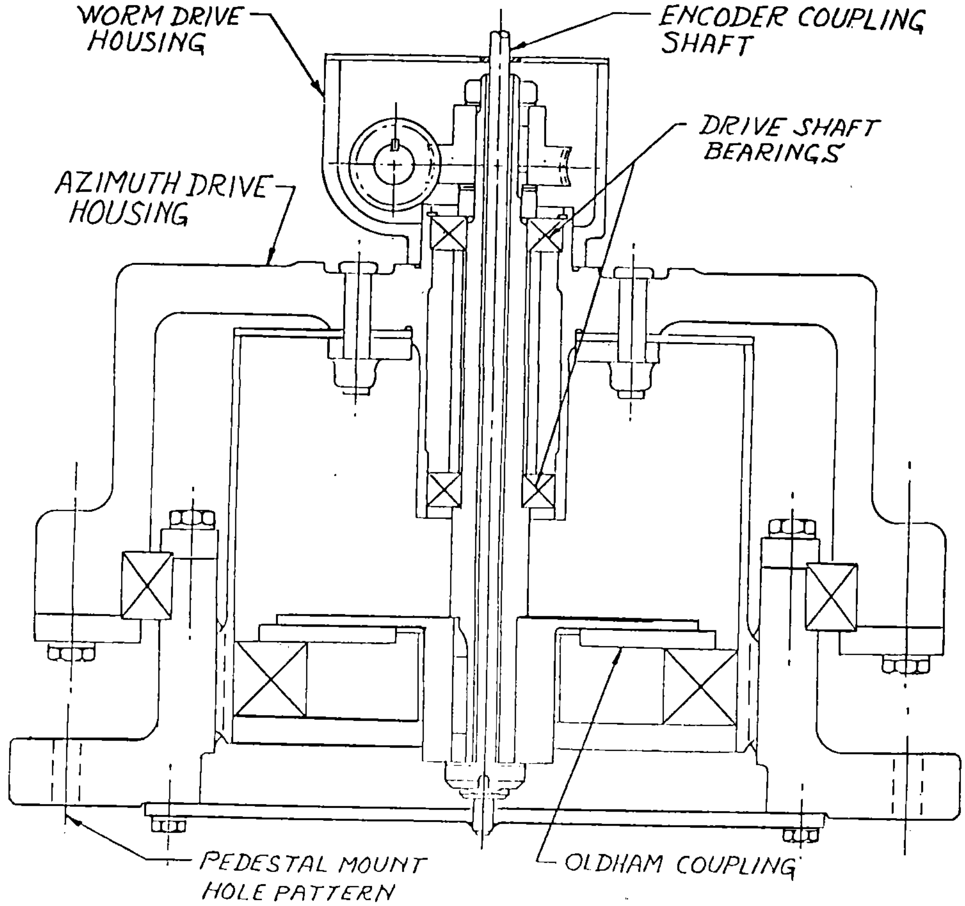

Figure 5. Initial Baseline Heliostat

Reflector Attachment

The tubular beam which supports the reflector is terminated at the inboard cross beam. Thus the reflector is divided into two separate panels (see Figure 3).

Reflector Structure Optimization

The structural elements in the reflector were resized to optimize the section characteristics to the loads of the enlarged reflector.

Low-Cost Motors

DC motors do not appear to be competitive at this time because of the cost of the switching networks and the low voltage field wiring. A 440 VAC system was selected to reduce the field wiring cost.

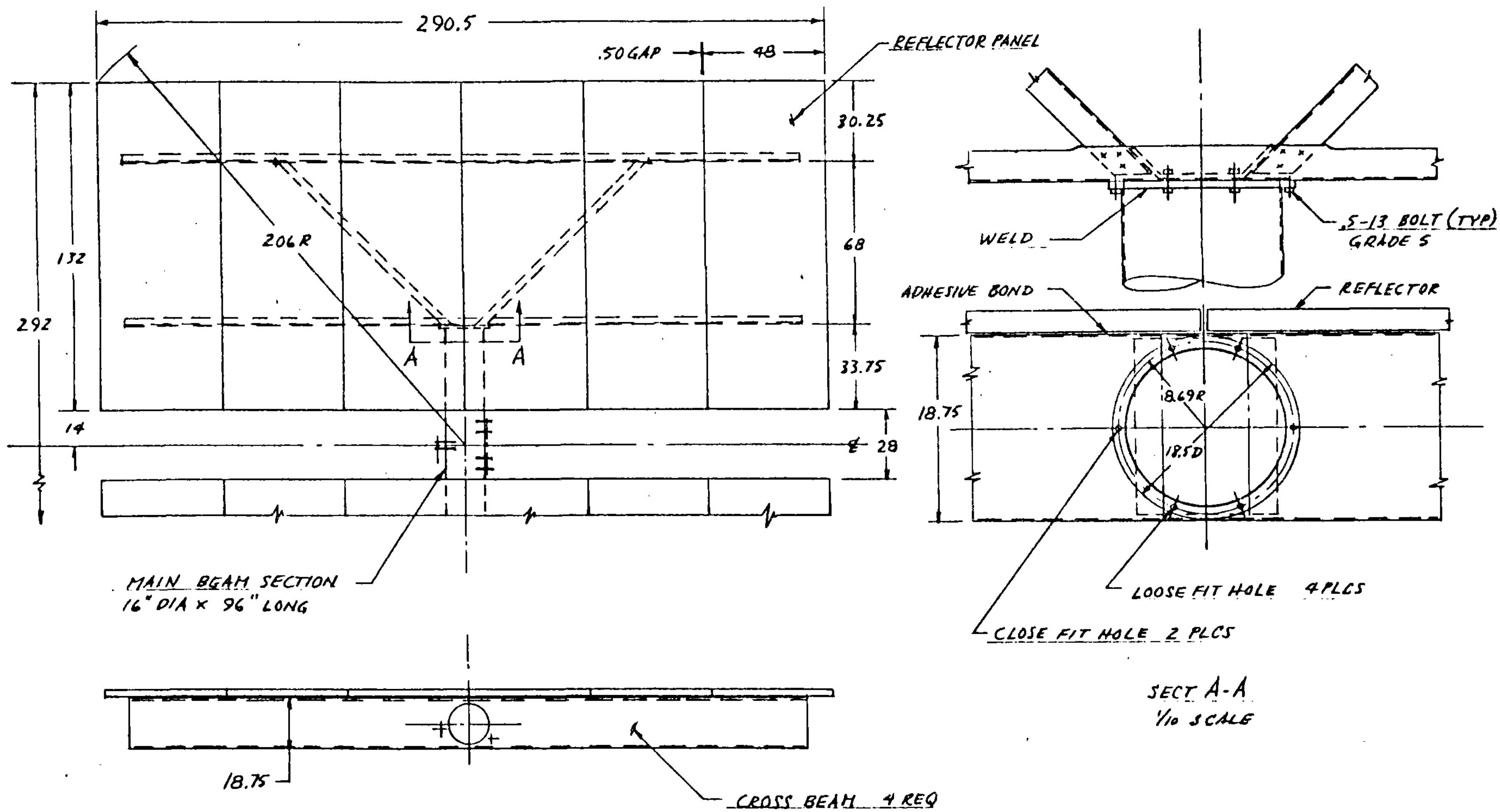

Figure 2. Two-Segment Reflector - Short Main Beam

Manufacturing Tradeoff Studies

Manufacturing tradeoff studies were performed on the eight specific areas defined below.

Integral Pedestal/Foundation

Studies were conducted to eliminate the bottom attach flange of the pedestal by setting the pedestal in the foundation. This approach has been found to be feasible and cost effective. Studies are continuing to define the best means for attaching the drive unit to the pedestal.

Drive Housing Materials Reduction

A tradeoff study has shown that a built-up housing is cost effective because of reduced weight and materials cost. Studies are continuing to define the best approach to a built-up housing.

Mirror Line Integration

At 25,000 heliostats per year, a mirror line is working to a reasonable capacity. It becomes advantageous to integrate the mirror line from the standpoint of reduced handling and transportation costs, specialized handling equipment, and line integration into the production process.

Float Glass Line Integration

The extreme production volume of a float glass line mitigates against integration because of the complexity involved in the associated handling and transportation problems.

Foam Core Finishing

This tradeoff study was resolved in favor of buying the foam extruded to the approximate size to be used and finished to specifications at the assembly plant. The decision was based primarily on the need for the foam to stand for an extended time before it stabilizes dimensionally.

Foam Core Extrusion Integration

At 250,000 heliostats per year, a foam core extrusion machine is working to a reasonable capacity. However, the foam must still be transported to the assembly and installation point. Hence the advantage of foam core extrusion capability may be marginal.

Adhesive Application

Both extrusion and spray application methods appear to be feasible. Thus the process can be selected on the basis of simplicity of integration into the production line. In particular, mirror module fabrication should use spray, and attachment to the structure should use extrusion.

Site Factory Requirement

The design provides for a heliostat which can be assembled in a site factory or on the pedestal. Selection of the most cost effective approach is in progress.

Installation and Checkout Studies

Two studies are being conducted on installation and checkout:

Optimum On-Site Transportation

This study has been completely redefined to include interfaces with the installation equipment.

Collector Checkout

This study deals with the time during the installation sequence at which the checkout is conducted. The speed with which checkout can be conducted allows a great deal of flexibility in the timing.

Operations and Maintenance Studies

Two tradeoff studies are being conducted on the operations and maintenance:

Reflector Cleaning

The cost of washing with a wash solution and deionized water rinse is being compared to the cost of a rinse and mechanical wash in deionized water. Effects of cleaning efficiency are considered, as well as the possible effect of a requirement to collect the wash solution.

Optimum Repair Levels

The location at which line replaceable units (those units replaced on the heliostat) are repaired is being optimized by computer program. The program is operational, and optimization is in progress.

Preliminary Design

The baseline design has been frozen. The results of the above tradeoff studies are incorporated in the new design, as well as many minor changes designed to facilitate manufacturing.

Manufacturing, installation, and checkout plans are in preparation. The baseline manufacturing plan employs an assembly facility located in the vicinity of the installation site (within a nominal 50 mile radius) and a dispersed raw materials and parts/components production concept using the available industrial base wherever practical. "On the pedestal" installation and final assembly is being considered as an alternate to a site assembly facility.

Bench Model and Component Tests

Tests are being conducted to aid in selecting the mirror module configuration. The tests include salt spray to help evaluate durability, thermal cycling to evaluate thermal stresses and fatigue, hail impact, and optical tests. The salt spray tests are complete and show acceptable ways of using both laminated and unlaminated mirrors. Hail impact tests are also complete and favor the laminated mirror approach. The remaining tests are in progress.

PROTOTYPE HELIOSTAT DEVELOPMENT

Solaramics, Inc.

W. D. Mitchell

The Solaramics approach to developing a low-cost heliostat is to reduce the cost through application of materials development and unique design.

The Solaramics program team consists of:

- Energy Control Systems for development of microprocessor and control software
- Applied Nucleonics for structural analysis and beam quality assessment
- Engineered Ceramic Processes for pedestal material development and production costs estimates
- Approved Engineering Test Labs for Phase II test planning and material characterization testing

General Configuration

The Solaramics heliostat consists of an array of ten panels, each four feet by ten feet for a total reflective area of 400 ft^2. Each panel is constructed of a microglass reflector bonded to a structural foam glass substrate to achieve a low-cost, high-efficiency reflector.

The design also features a low-cost ceramic pedestal foundation concept. Open-loop control is accomplished with individual microprocessors that control linear actuators which act upon bell crank drive mechanisms.

Structural Foam Glass Substrate

The foam glass is an engineered material whose strength and rigidity are optimized for this specific application. (It is not to be confused with insulation grade foam glass.) The foam glass is made from recycled soda lime window glass and is thermally compatible with the soda-lime reflector surface. The material is very low cost; long range projections indicate cost significantly below $1/square foot. (For comparison, the cost of insulation grade foam is approximately 35¢ per board foot.)

Characterization Plan

To optimize the material properties of the foam glass and establish design parameters, a characterization test is being conducted. The properties shown in Table I are being determined over a range of densities from 3 to 6 gms/cc.

TABLE I

FOAM GLASS CHARACTERIZATION PLAN

- Modulus of Rupture (tensile strength)
- Compression Strength
- Modulus of Elasticity
- Shear Strength
- Thermal Expansion
- Thermal Conductivity
- Moisture Absorption
- Freeze/Thaw Cycles
- Static Fatigue Loading

Three densities: 0.3 g/cc
0.4 g/cc
0.6 g/cc

Microglass Reflector

To maximize the reflective efficiency, a very thin (.010 in.) glass is used. By reducing the thickness of the glass cover, the effect of the iron content and the resulting IR absorption is minimized. Thus an efficiency of 93 to 94% appears achievable.

An integrated process where the glass is drawn, sensitized, and silvered as a continuous process is projected to be very economical. The reflector can then be laminated to facilitate handling and reduce breakage. The integrated process must be stressed as very important to reduce breakage and minimize handling.

Glass 0.005 to 0.010-in. thick is currently being drawn in an experimental I.R.A.D. program at Solaramics.

Low-Cost Ceramic Pedestal

A new material developed by ECP, Inc., our parent corporation, for the Electric Power Research Institute (EPRI), is planned for the pedestal foundation. The low-cost product is produced from waste glass and fly ash.

The cost projections for this material are significantly below $100 per ton which would correspond to $140 per pedestal. As a ceramic, the material is environmentally inert and is expected to achieve an exceptionally long life in this type of application.

The ground line bending moment for the heliostat design is comparable to design moment for a 40-ft Class 4 utility pole which is normally installed 5 to 6 feet into the ground. Transmission poles with ground line moments of 10 times the heliostat are installed 9 to 10 feet into the ground. To satisfy the more sensitive stability and rigidity requirement of the design, installation depths of 9 to 10 feet are anticipated. Dynamic soil analysis is currently being evaluated to verify this design and determine optimum design depth. Installation technique would include drilling the hole, positioning the pedestal with a tooling support, and grouting the space surrounding the pedestal.

Control Concepts

Though the initial proposed concept provided closed loop control, the results of an early trade study confirmed the cost/effective advantages of an open-loop control. An individual microprocessor is planned for each heliostat which employs a single commercially available chip. Control is achieved through bell cranks driven by linear actuators, powered by pulsed electric motors. Trade studies for the selection of the electric motors and solid state controllers are currently in process.

OPERATION OF THE SOLAR THERMAL TEST FACILITY

Sandia Laboratories

Billy W. Marshall

FY78 Budget Authority - $1,300,000

Introduction

The Solar Thermal Test Facility Operations Project has as its objective the operation of the 5MW$_t$ Solar Thermal Test Facility (STTF) located at Sandia Laboratories in Albuquerque, NM. The objectives for this facility, listed in Table I, include not only the primary function of providing a test facility for receivers developed in the Department of Energy Solar Central Power Systems Program, but also include heliostat evaluations and tests as well as other programs in DOE, EPRI, industry, and universities which may have a need for high-temperature, high-solar flux environments. Examples of these activities are testing of high-intensity photovoltaic cells, materials studies, and unique chemical and metallurgical process testing.

TABLE I

5 MW$_t$ SOLAR THERMAL TEST FACILITY OBJECTIVES

Perform tests on components and subsystems developed in DOE Solar Central Power Systems Program
Perform tests on other DOE solar conversion techniques-photovoltaics
Perform tests on non-DOE solar central power systems programs - EPRI
Perform tests on materials, components, subsystems developed by private industry, universities, etc - STTFUA

As a matter of review, conceptual design of the STTF was started in 1975 and construction began in the summer of 1976. Original plans called for completion in October of 1977; although the facility is not as yet complete, limited operations have been conducted, and the projected schedule calls for completion within the next few months. The STTF consists of a steel and concrete tower, computer controlled heliostats to focus and concentrate the solar energy, system control, and data collection systems, and a control/administration building to house the computer and offices.

Facility Description and Status

For descriptive purposes, the facility can be divided into three major subsystems: heliostats, master control system, and tower.

Heliostats

The facility was originally conceived to accommodate over 500 heliostats in a field surrounding the tower. During construction, foundations and control wiring for 366 heliostats were installed surrounding the tower, and 222 heliostats have been installed on the north side of the tower. Each heliostat consists of 25 1.22 m by 1.22 m facets, providing 37.16 m^2 for each heliostat and 8250 m^2 in the field. The facets are warped during fabrication for beam focus and aligned after installation.

As shown in Figure 1, the heliostat field will concentrate approximately 5 MW of thermal power onto a 3 m diameter target, and the peak output will be nearly constant throughout the year. The calculated peak intensity is approximately 2.50 MW_t/m^2.

All 222 heliostats have been installed, and heliostat alignment is nearing completion. At this time, the 78 heliostats in Zone A (nearest the tower) have been aligned to the 42.7 m location and 132 of the 144 heliostats in Zone B (north portion of the field) have been aligned to the tower top. The remaining heliostats are presently undergoing failure diagnostics and repair and will be aligned at a later date prior to test initiation. Also, the Zone A heliostats will be realigned to the tower top prior to the McDonnell Douglas receiver tests.

- 222 HELIOSTATS – 8250m^2 TOTAL REFLECTIVE AREA
- REFLECTIVITY – 70 to 80%
- MAXIMUM FLUX – 250 w/cm^2
- TOTAL POWER – 5000kw
- MAXIMUM BLACK BODY TEMPERATURE – 2570°k
- BEAM SIZE – 1m DIAMETER AT 1000kw – 3m DIAMETER AT 5000kw

a. Beam Capabilities

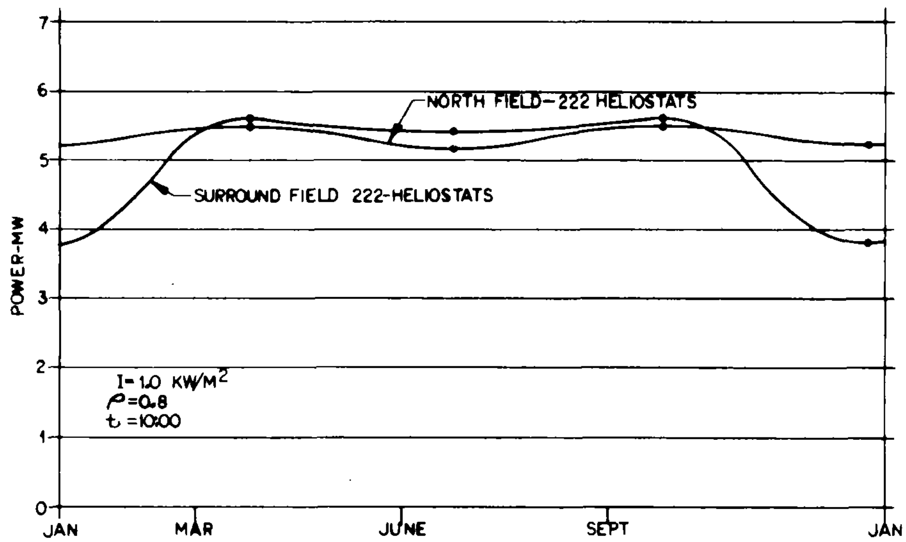

b. Output of Field to Tower

Figure 1. STTF Heliostat Characteristics

Master Control System

The facility is controlled and operated by a master control system (MCS) through the use of digital minicomputers. Nine minicomputers are used in the system which, as shown in Figure 2, is divided into three major subsystems; the MCS control sybsystem, the MCS data subsystem, and the MCS tower subsystem. Using the MCS control subsystem, the operator can display the status of any one of several key subsystems in the STTF. For example, status display of the heliostat field is shown in Figure 2. Programmed command sequences are entered into the MCS prior to the test and can be altered through the MCS during a test. The control subsystem also interfaces with the heliostat control system by analyzing pointing commands and distributing them to the heliostats through the control network shown in Figure 2.

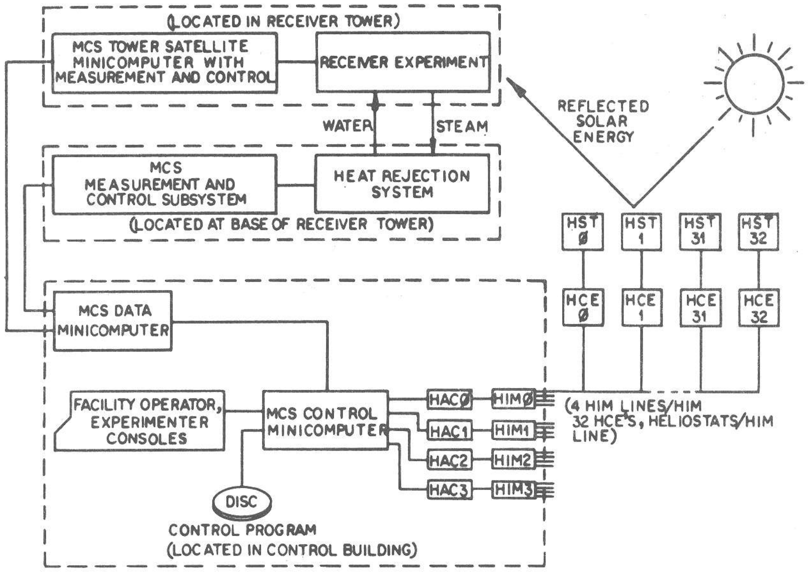

a. MCS Minicomputers

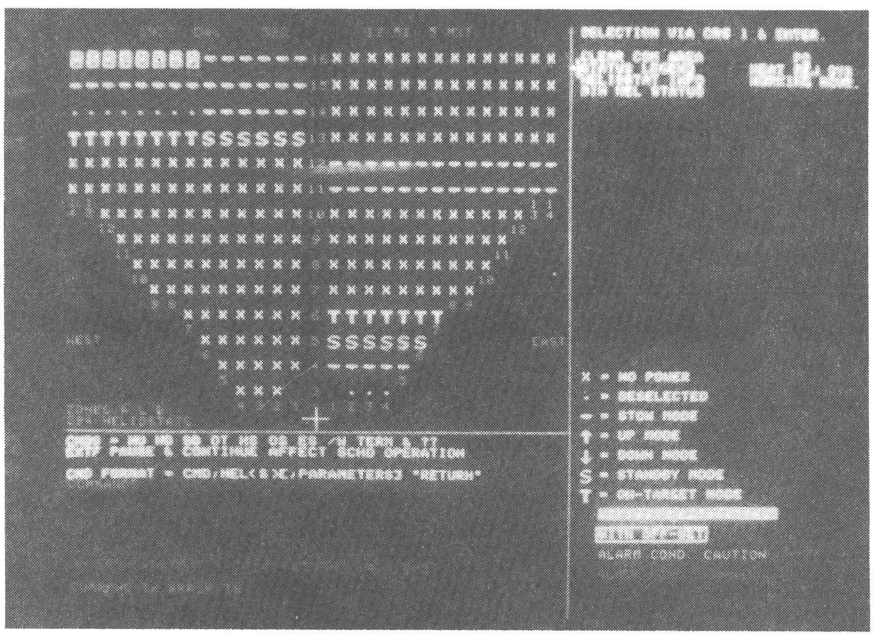

b. Status Display of Heliostats

Figure 2. STTF Master Control System

All of the computer hardware has been installed. Incorporation of the software controls and programs into the machines is in progress and completion is expected in May. The entire system was moved to its permanent location in the control building on December 15, 1977, and the computers were reconnected without difficulties on December 18. Communication was established for the first time with the Zone B heliostats, and no significant problems were incurred. The MCS is being used routinely for night operation to accumulate operation time on the heliostats.

Tower

The features of the tower are summarized in Figure 3. Items to be tested can be placed atop the tower or on any of the three platforms on the north side of the tower. Two recent photographs of the tower and heliostats are shown in Figure 4. In the tower center is an elevator with a 9.1 by 7.6 m floor area capable of lifting 90,700 kg. The elevator module also houses instrumentation panels, computer control and data hardware, and a light machine shop.

Thermal energy is dissipated through a heat rejection system (HRS) which provides boiler quality feedwater and steam at controlled conditions to test locations. A closed-loop dry cooling tower provides coolant to these loops and also provides low-temperature cooling throughout the tower. A high-pressure air cooling system is presently being installed in the tower.

Construction of the tower is at the top level, and completion is expected well before initial tests are scheduled. Structure work on the elevating module has been completed, and work is under way to complete the module interior for the computer module and machine shop. The lifting cables will be installed shortly, with checkout and lift tests anticipated for late March. The HRS is under construction but no heat rejection capability is presently available at any tower test location. The cooling towers are in place, and piping is being installed in the tower to provide low temperature cooling water to the 140-ft level by the end of March.

TEST LOCATIONS
- **TOWER TOP 61.0m**
- **NORTH TEST BAYS 48.8m, 42.7m, 36.6m**

HEAT REJECTION
- **FEEDWATER 3.0kg/s, 200°C**
- **5MW STEAM DISSIPATION 2.5kg/s, 520°C**
- **7MW DRY COOLING TOWERS 25kg/s**

DATA ACQUISITION, TRANSMISSION & CONTROL
- **A/D, D/A CONVERSION**
- **THERMOCOUPLES (K or T)**
- **STRAIN GUAGE CONDITIONERS**
- **LINEAR POSITION SIGNAL**

ELECTRICAL 115, 208, 440VAC

LIFTING DEVICES
- **ELEVATING MODULE 90,700kg**
- **BRIDGE CRANES (2) 4,500kg**
- **JIB CRANES (3) 4,500kg**

MODULAR THERMAL PROTECTION

Figure 3. STTF Tower Features

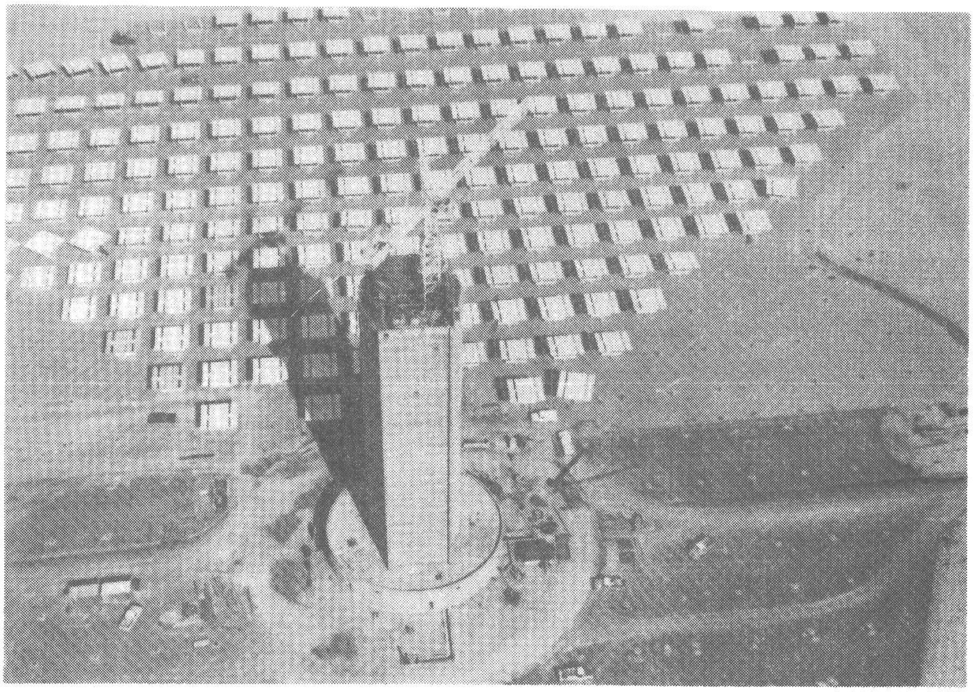

a. Heliostat Field

b. Tower

Figure 4. Solar Thermal Test Facility

In May 1977, an interim demonstration of the operation of the system was performed by focusing 71 heliostats onto a steel target mounted on the north face of the tower just below the 36.6 m test bay. During a two-minute exposure, a 0.9 by 0.6 m size hole was melted in the 6.3-mm thick plate. Calculations indicated that 1.8 MW of thermal power were incident on the target, with a concentration ratio near 1200 achieved at the center of the beam. This successfully demonstrated the system operation of the facility and preparation for the receiver tests are proceeding.

McDonnell Douglas Receiver Panel

Preparations are under way to begin tests on a single panel from the McDonnell Douglas/Rocketdyne 10 MWe pilot plant prototype receiver design. The panel is 0.89 m-wide by 12.5-m tall and will be tested at the tower top. The input thermal power is expected to range from 0.2 to 3.75 MW. The tower HRS is being modified to install the steam powered feedwater preheater required to provide 288°C (550°F) feedwater to the receiver. Because of the tall but very narrow panel geometry, a secondary concentrator attached to the panel will be required to attain the higher flux density levels. Argonne Laboratories has been contracted to provide recommendations on the concentrator shape, materials, and fabrication. Following this study, Sandia will be responsible for designing, fabricating, and installing the water-cooled concentrator.

EPRI/Boeing Receiver

This prototype, air-cooled 1-MW_t receiver is designed to investigate the performance of a closed-cycle, helium-cooled receiver for use in brayton-cycle central receiver plants. Several activities are under way at the STTF to prepare for the start of tests at the 140-ft test location in early summer. Boeing's data package and test plan requirements are being reviewed. The air supply system for both this receiver and for the EPRI/Black & Veatch receiver is being designed by Boeing. A preliminary design review on this system was held by EPRI with STTF personnel in attendance. EPRI will supply the air compressor at the tower base and the air preheater to be mounted near the receiver. The STTF is being modified to install the air supply and exhaust lines in the tower. Several high-temperature insulation materials were tested in the White Sands Solar Furnace with Boeing personnel participating. Based on these tests, materials will be selected to provide thermal protection for the exterior surfaces of the receiver. These data showed that all predicted normal and abnormal flux environments can be resisted by these materials.

Martin Marietta Receiver

Since tests on this receiver are not anticipated during FY78, support activities consist of interface meetings with Martin and Foster Wheeler. Subjects of these meetings include data requirements, test conditions, and mounting of the receiver on the elevating module.

EPRI/Black & Veatch Receiver

Preliminary discussions have been held with Black & Veatch to describe the facility and its data and control system. Tests on this receiver are tentatively scheduled for FY79, and support activities will increase in future months.

Heliostat Beam Diagnostics

Activities are under way to characterize the reflected beams from both individual heliostats and groups of heliostats in the STTF field. Data will be obtained using a number of flux measurement tools and will be compared with analytical results from the computer ray trace program, HELIOS. A summary of the diagnostic tools is presented in Figure 5. For single heliostats, a ground instrument with flux gages mounted at 7.6 cm intervals along a water-cooled 4.9 m aluminum bar is being used. The instrument, shown in Figure 5, can operate either by sweeping the bar across a fixed beam or by sweeping the beam across the stationary bar. This bar has been used previously to characterize individual mirror facets, and measurements on the complete heliostats were started recently.

The 12-ft Real Time Aperture Flux (RTAF) system and the 1-MW_t working receiver will be used to characterize the flux from a group of heliostats. The RTAF is complete except for the installation of the photon and heat flux gages. The photon gages are being calibrated at the White Sands Solar Furnace, and both types of gages will be installed in April. The working receiver is being checked out, and the flux gages installed prior to installation at the 140-ft test location. The working receiver and the RTAF will be operated together for cross reference between the two instruments. This will serve as a calibration for the RTAF, which will be used to measure the flux into the EPRI/Boeing receiver.

In support of advanced heliostat designs, including those for the 10-MWe pilot plant, the STTF will provide a number of evaluation and characterization activities. Included is beam quality evaluation, tracking and drive evaluation, and surface contour characterization. The specifics of these measurements are presently being defined but the techniques will be developed to begin evaluations of the pilot plant prototypes in the second quarter of FY79.

REAL TIME APERATURE
FLUX SYSTEM——(4000 SUNS)

DIAGNOSTIC BAR——(50 SUNS, GROUND LEVEL)

CALIBRATION SYSTEM——(50 SUNS, TOWER MOUNTED)

WORKING RECEIVER——(1MW$_t$)

ACCESSORIES

- PHOTOMETRICS
- IR PYROMETRY
- HOT WIRE ANEMOMETERS
- SPECTRAL RADIOMETRY
- DATA ACQUISITION SYSTEM (REAL TIME DATA DISPLAYS)
- HELIOS (ANALYTICAL BEAM MODEL)

a. STTF Diagnostic Tools

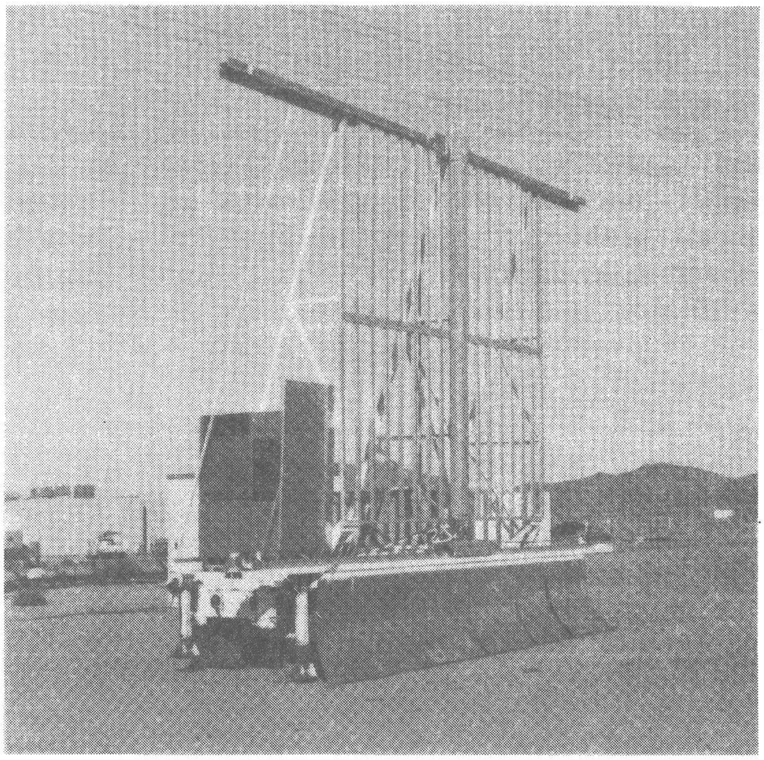

b. Beam Diagnostic Bar

Figure 5. STTF Beam Characteristics Instruments

Heliostat Reflectivity Measurements

Preliminary reflectivity measurements on the STTF mirror samples have been made. The reflectivities measured on a number of cleaned samples all are in the narrow band between 0.82 and 0.83. After five weeks exposure in the field, values as low as 0.65 were measured for samples which were visibly "dirty" and "dust covered." Measurements made on samples taken out of the field immediately after rainfall showed reflectivities near 0.75. Based on these preliminary data, a more extensive measurement program has been initiated. Fifty-four samples have been attached to fixtures on heliostats across the field. From this group, 31 samples will be selected each week for reflectivity measurements. Meteorological data will be correlated with the data, and measurements will be made following unusual weather phenomena (windstorms, heavy rainfall, or snowfall) to evaluate these effects.

Test Schedule

Figure 6 presents an FY78 milestone schedule for the facility. This schedule shows both the completion of construction and the initial tests and experiments. Figure 7 presents the projected receiver test schedules through both FY78 and FY79. Receiver tests are presently scheduled to begin in mid-July with the MDAC panel. To accomplish this test date, the receiver must be on site at the STTF by mid-May for installation and check-out. Tests on the EPRI/Boeing receiver are scheduled to begin by mid-August; however, if the MDAC receiver is delayed, greater attention will be placed on installation of the Boeing receiver. In that case, the tests could begin by August 1.

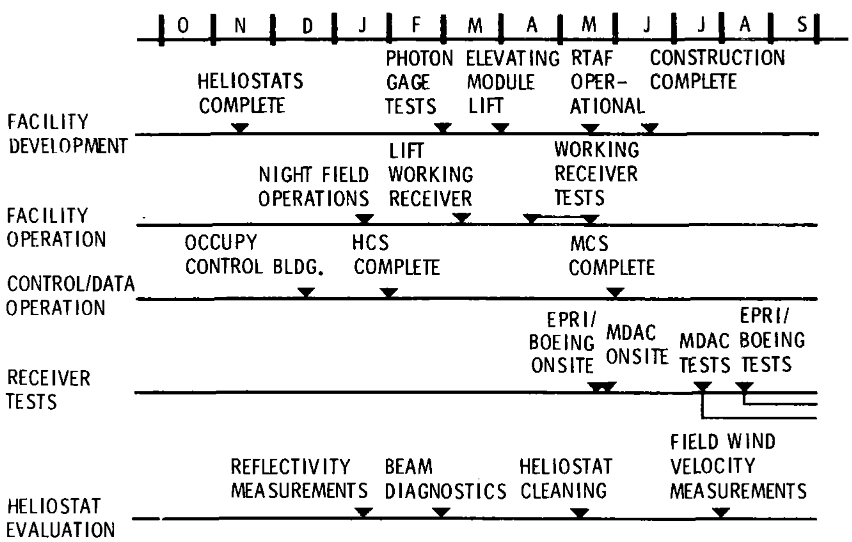

Figure 6. STTF Activities

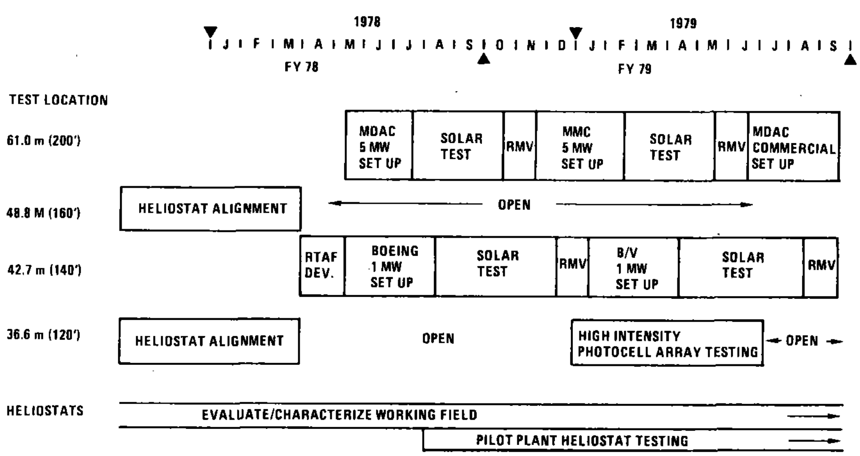

Figure 7. Tenative STTF Testing Schedule

Both of these tests are based on using the 1-MW_t working receiver at the 140-ft level as a system checkout. Figure 6 indicates that these tests will begin in mid-April and continue through May. These tests will be conducted only on weekends to avoid interference with the tower construction. As a part of these tests, the RTAF will be installed in mid-May and operated with the working receiver for the remainder of the period.

In summary, the facility is nearing completion, and no major problems have occurred. The completion date, including modifications to the HRS, is now estimated as mid-June. The projected receiver test schedule can be maintained if the installation and operation of the working receiver by mid-April can be accomplished, and there is no further delay in the total facility completion.

HELIOSTAT FIELD ANALYSIS AND DESIGN FOR SOLAR CENTRAL RECEIVER SYSTEMS

Energy Foundation of Texas
University of Houston, Texas Tech

L. Vant-Hull

Since July of 1973, the University of Houston has been involved in feasibility studies, conceptual designs, and preliminary designs of the solar central receiver. In this time we have developed a series of computer codes which allow the effective characterization and the economic optimization of the optical and thermal collection components of the system. More recently, under the auspices of the nonprofit Energy Foundation of Texas, DOE has funded six tasks proposed by the University of Houston Solar Energy Lab and one task proposed by Texas Tech University, all relevant to the central receiver concept. The specific tasks are as follows:

Investigator	Brief Title - Description
1. Wentworth	Operational Chemical Cycles: Cyclic solar decomposition of NH_3HSO_4 into 3 liquids
2. Collins	Underground Thermal Storage: Daily cycling of 500 MWt into permeable rock strata (steam) or impermeable salt caverns (oil)
3. Wendlandt	Cyclic Catalytic Solar Storage: The EVA-ADAM cycle is analyzed for cyclic operation.
4. Vant-Hull	Solar Systems Simulation: Codes are developed or improved for CR studies. A code center will be established.
5. Shamsundar	Design Procedures for Molten Salt Storage: High, medium, and low-temperature phase change systems are studied.
6. Ignatiev	Surface Morphologies of Solar Absorbers: Aimed at understanding the physics of absorption and emittance by metal blacks.

7. Minor (Texas Tech) Extreme Wind Effects on CR Systems: Wind effects predictions for the Barstow plant and design assistance for DOE contractors.

The energy storage studies are all directed toward the development of concepts suitable for large-scale cyclic systems, such as the Solar Power Tower. Work on the Sandia monitored tasks 4 and 7 will be reviewed, as well as the conclusions of the heliostat field analysis portion of our advanced central receiver feasibility study contract. The liquid sodium cooled advanced solar central receiver feasibility study portion was reported at Seattle, and the final report on that work is currently being distributed by NTIS. Under a no-cost extension of that contract, we have incorporated the June, 1977, MDAC costs and performance specifications into our computer model. Using our latest variable format optimization routine, RCELL, we have defined optimized systems at 25, 35, and 45° north latitude subject to mean monthly western U.S. weather conditions. At 35° latitude (~Barstow-Albuquerque) we also compared sloped fields, rising to the north at 0, 10, and 20°. Surprisingly, after the optimizer has readjusted the system configuration, we find only a 1.5 percent advantage at 10° slope and a 0.5 percent advantage at 20° slope (assuming no added field installation charges). Consequently, we conclude that, for external receivers, a sloped field gives no significant advantages.

The RCELL optimizer works by adjusting the heliostat spacings in each computational cell to give balanced performance throughout the field. All collector costs and loss modes are accounted for, as well as system thermal output and subsystem costs; the field boundary and F, the figure of merit, are computed. This parameter, collector cost divided by annual power production to the turbine, is iterated until it converges, and is used to compare systems such as the sloped fields mentioned previously. We have generated optimized fields in which various parameters have been varied, all at 35° latitude and zero slope. For the MDAC specified water/steam receiver, we have varied tower height, heliostat cost, land cost, and, through the input figure of merit, system size (see Figure 1). The ground coverage shading and blocking loss, number of heliostats, field boundary, etc., change from case to case. One of the more interesting results was that, for the design considered, the optimized output power varied as the 3/4 power of the tower height if the receiver and heliostat size remain unchanged. If the entire collector system is scaled uniformly with tower height, the power varies as the square of the tower height. A second finding was that the modified figure of merit only increased by 1.3 percent while the ground coverage increased by 25 percent and the energy delivered per m^2 of land increased by 28 percent when a high phantom land value was introduced for the optimization run and then subtracted. Thus central receivers can be designed for constrained quarters without serious economic penalty. A second study was a net energy analysis for the central receiver. The MDAC 100-MWe commercial baseline system was analyzed, assuming a 30-year life. All energy costs, including materials, manufacturing, transportation, and installation were considered. As is conventional in such analyses,

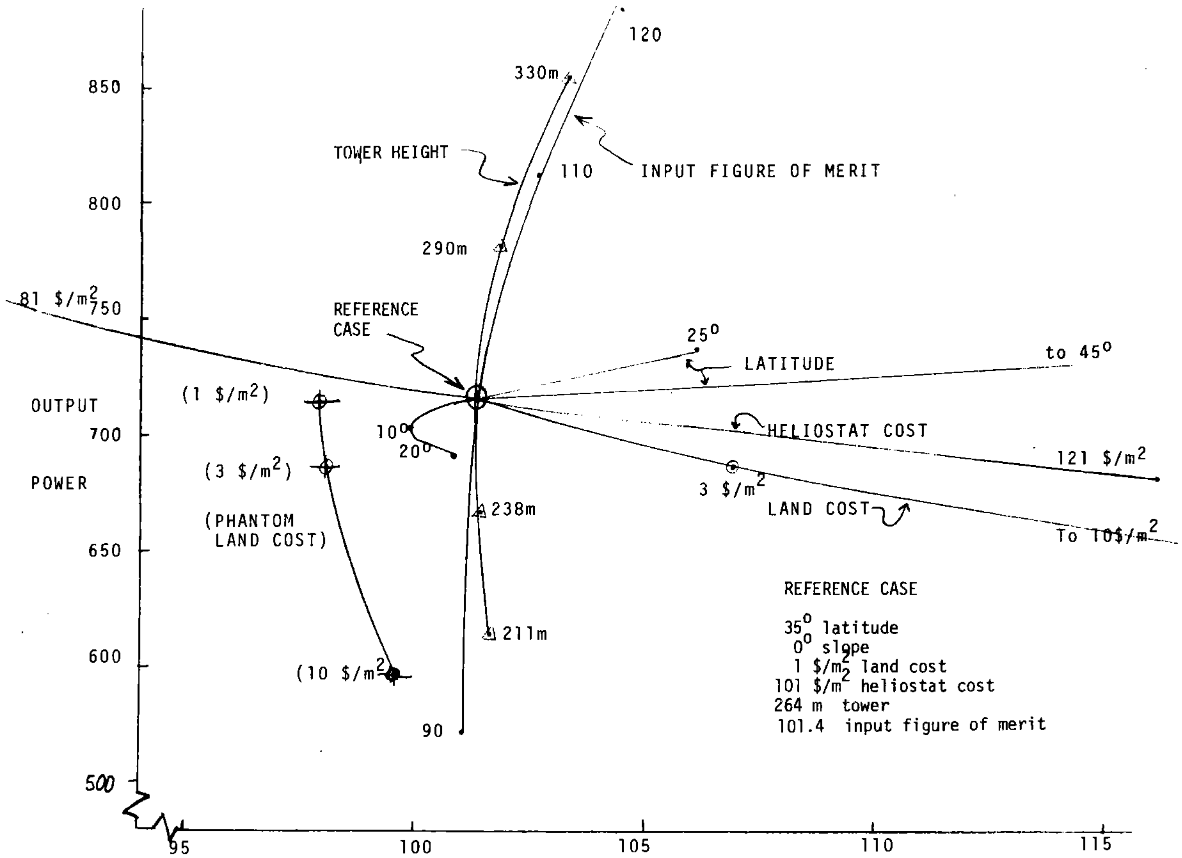

Figure 1. Figure of Merit

the energy content of the manufacturing facilities themselves was excluded, as was the energy consumed by all workmen and their families; presumably these facilities and services would be provided by society in any case. The result, shown in Table I, was that the thermal collection component energy cost was 145 days for thermal payback or 435 days for electrical payback, leading to an electrical energy amplification factor (EAF) of 25. The thermal energy cost of the thermal storage unit was equivalent to 35 days (plus 0.2 percent for oil makeup) leading to an EAF of 20.3 for the overall thermal plant. Furthermore, if the oil and the available steel are salvaged after 30 years, over 41 percent of the invested energy can be recovered. The EAF for the solar plant might be compared to ERDA 76-1 in which the EAF for a nuclear plant is evaluated as 4.0 (including the fuel charge). Thus central receiver solar plant implementation can proceed rapidly with much less drain on the nation's energy supplies than an equivalent nuclear development.

In a separate study aimed at an improved solar insolation model, it was found that an improved solar tracker was required. Our final report carries a detailed analysis of the various celestial coordinate systems, and points out

TABLE I

NET ENERGY REQUIRED FOR COMPLETE COLLECTION SYSTEM FOR 100 MWe COMMERCIAL PLANT

(Annual Electric Production = 445K MWe/yr)

Part	Energy Required MWH_t	Number of Days Needed to Provide Equivalent Energy	
		Thermal	Electric
Collection System			
Heliostat	488,622	133.6	400.8
Receiver	11,098	3.0	9.1
Riser & Downcomer	1,364	0.4	1.1
Tower	29,245	8.0	24.0
Subtotal	530,329	145.0	435.0
Thermal Storage System			
Caloria HT43	103,610	28.3	85.0
Rest of System (Materials, Manufacturing, Transportation, and Construction)	24,657	6.7	20.2
Subtotal	128,267	35.0	105.2
Number of days needed to provide energy for complete system (Total 658,596 MWH_t)	180.0	540.2	
Days after start-up system com completely paid for - Capital Energy Cost	180	540.2	
Energy Amplification Factor (30 year lifetime)			20.3

clearly the errors associated with use of mean solar time without correcting for the eccentricity of the earth's orbit, etc (see Figures 2 and 3). Errors of as much as 2 degrees are reduced to a small fraction of a degree with only minor complications of the tracker program. Under separate contract through EFT, we have been funded for further program development and code center work. With this funding we have made major improvements in our codes, recently completing a change from a very restrictive fixed 11 x 11 computational cell array to a variable format array capable of any m x m size up to 21 x 21, or even larger. This allows us to maintain or improve our resolution at some cost in computer time (11 x 11 runs typically take 1/2 to 10 minutes of HIS66/60 cpu time). Other developments have been the implementation of heliostat image code modification to handle, within our analytic framework, dished mirrors or segments and a north-facing noding aperture plane which can serve as a flat plate receiver or through which rays can be projected into the "cavity" behind it. Further development of this cavity is anticipated for continuing work on small or very high-temperature systems.

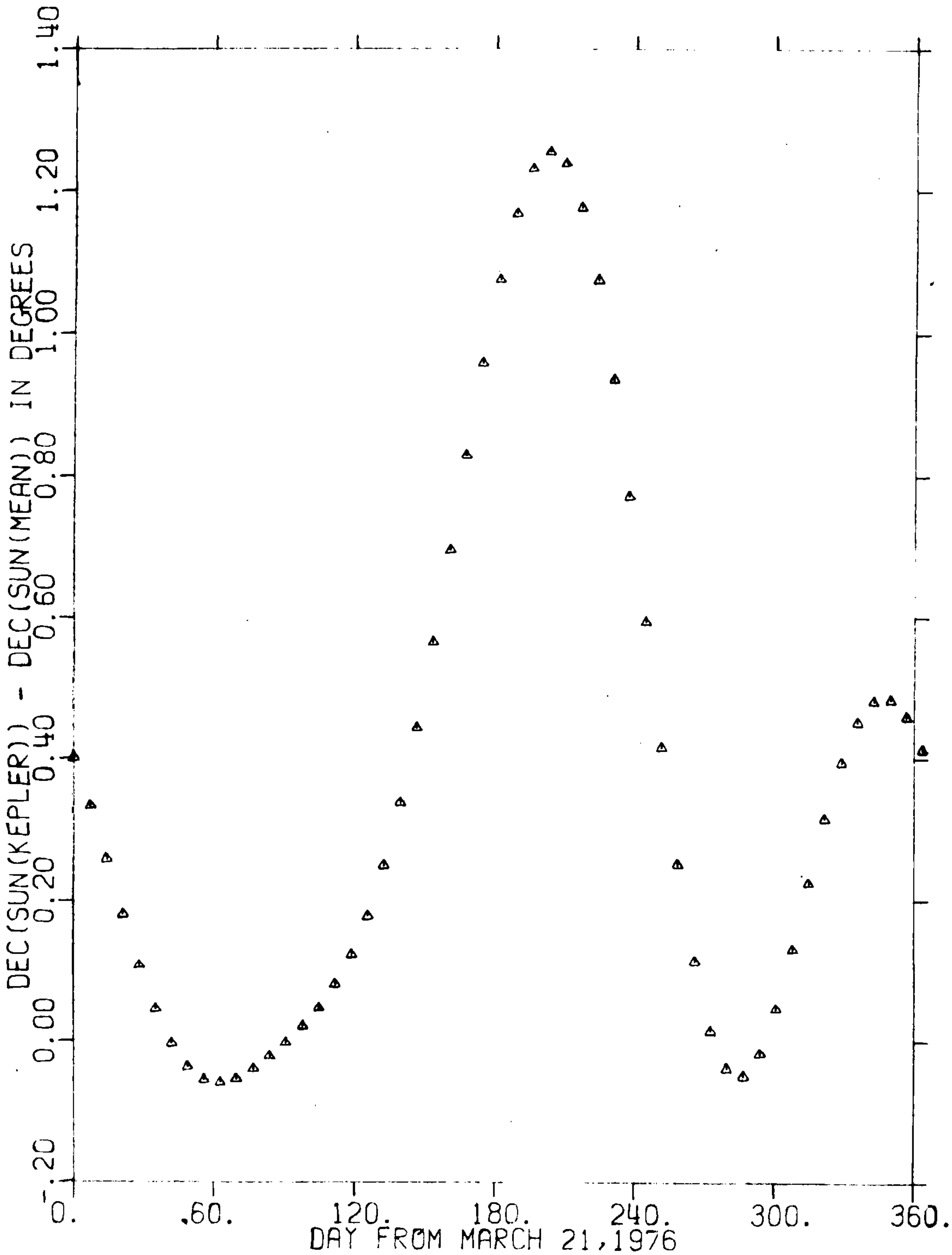

Figure 2. Difference in Solar Declination

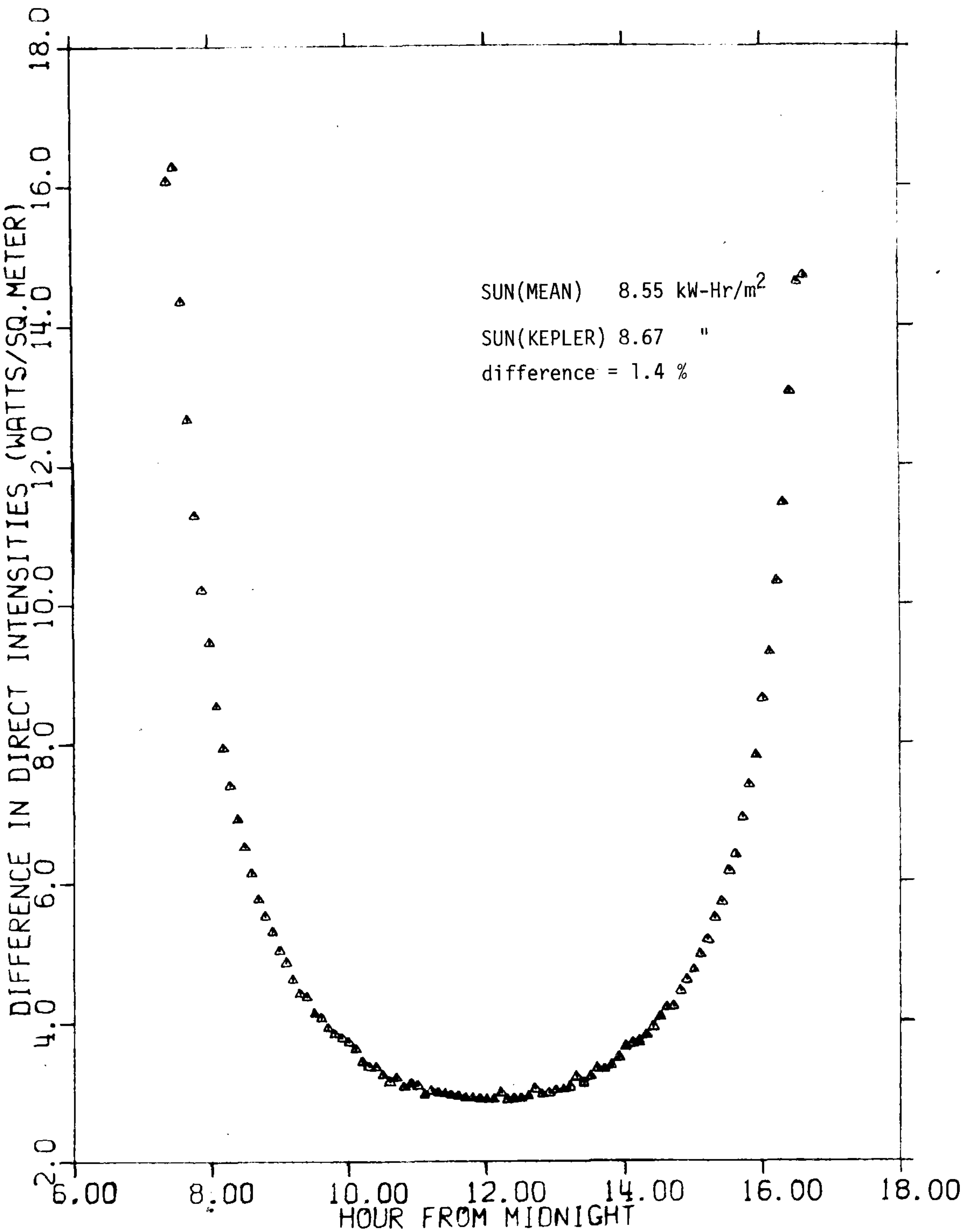

Figure 3. Direct Beam Intensity on Day 224 From March 21, 1976 (Allen's Clear Air Model)

Additional documentation of our codes has progressed, and along with the Sandia HELIOS code, a package is now available for dissemination. These codes are sophisticated, and proper implementation and interpretation probably requires a dedicated operator; however, they will be made available to those with a requirement for them. Other codes such as MIRVEL, discussed at our optical analysis workshop in July, will be integrated into the Code Center as soon as possible after our second year funding is obtained. The current contact is Fred Lipps (713) 749-4861. The proceedings of the Optical Analysis and Simulation workshop is currently being distributed through NTIS--UC 62. A second workshop, sponsored by SANDIA will be held by the University of Houston on March 26-28 and is on Central Receiver Systems Studies; central receiver subsystem contracts, utilities solar planning and dispatching, and the place of solar in national energy models will be discussed. This report should be ready in June and will also be distributed through NTIS and the UC 62 Distribution list.

Analysis of Extreme Winds on Solar Tower Generators

Summary

There are several ways in which winds may affect the design of the solar thermal power plant planned for the Barstow site. One is in the design of the tower, the receiver, the heliostats, and other components for survival in an extreme wind, such as a severe thunderstorm, frontal wind, tornado, or hurricane. A second concern has to do with wind effects on convective losses at the receiver and on heliostat control and pointing accuracy. Three specific research tasks have been identified in the general area of wind analysis.

Task (a) has consisted of formulating a risk model for extreme winds at the Daggett airport near Barstow, using historical data from this airport and other weather stations in the vicinity (see Figure 4). This task has been completed and a report is in preparation.

Task (b) has involved a review of the effects of winds striking a flat plate at a low angle of attack (edge on), and relating these effects to certain pressure coefficients in the current wind loading design code published by the American National Standards Institute, ANSI A58.1 (1972). It has been found that a variation of wind direction from the horizontal of the order of ±10 degrees is not unusual, and such variations have a strong influence in determining the force that must be resisted by a heliostat in the horizontal (stow) position. The origin of the requirement in the ANSI code that a static variation of ±10 degree be considered was also traced, and one or two alternatives to carrying out a simple static design have been suggested.

Task (c) has the objective of finding distributions of wind velocity and direction for the Barstow site, since those two parameters describing the wind both affect the efficiency of a high-temperature receiver high in the air. So far, time has only been available to acquire ten years of data concerning surface weather observations at the Daggett, China Lake, and Edwards Air Force Base weather stations, and this task is expected to carry over into the next year. The final formulation is expected to include time of day and cloud conditions, since these factors are also important for a solar thermal plant.

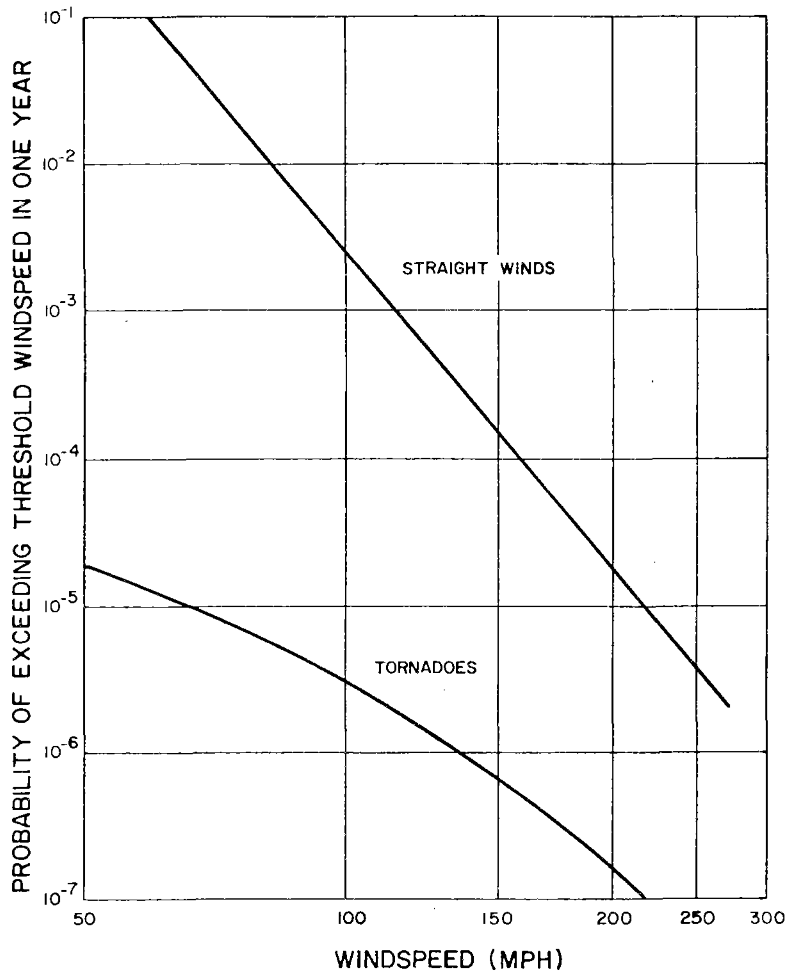

Figure 4.

INTERIM STRUCTURAL DESIGN STANDARD FOR SOLAR ENERGY APPLICATIONS

Foster Wheeler Development Corporation

T. V. Narayanan

Introduction

Foster Wheeler Development Corporation, under contract from Sandia Laboratories, is working on a program to develop an "Interim Structural Design Standard for Solar Energy Applications." The overall objectives of this program are:

1. Develop and recommend an interim structural design standard applicable to the central receiver solar thermal power system components that generally fall under the scope of the ASME Boiler and Pressure Vessel Code.

2. Identify test programs and other additonal work required to upgrade the interim standard.

The work to be performed under this contract is divided into two phases. The individual tasks in each phase and their schedule are shown in Figure 1. The original schedule submitted to Sandia is shown in solid lines, and the revised schedule is shown in dotted lines.

During the reporting period, work was concentrated in the following four areas:

- Review of CRSTPS System Components
- Review of ASME Code Design Rules and Criteria
- Reliability Considerations
- Development and Test Needs

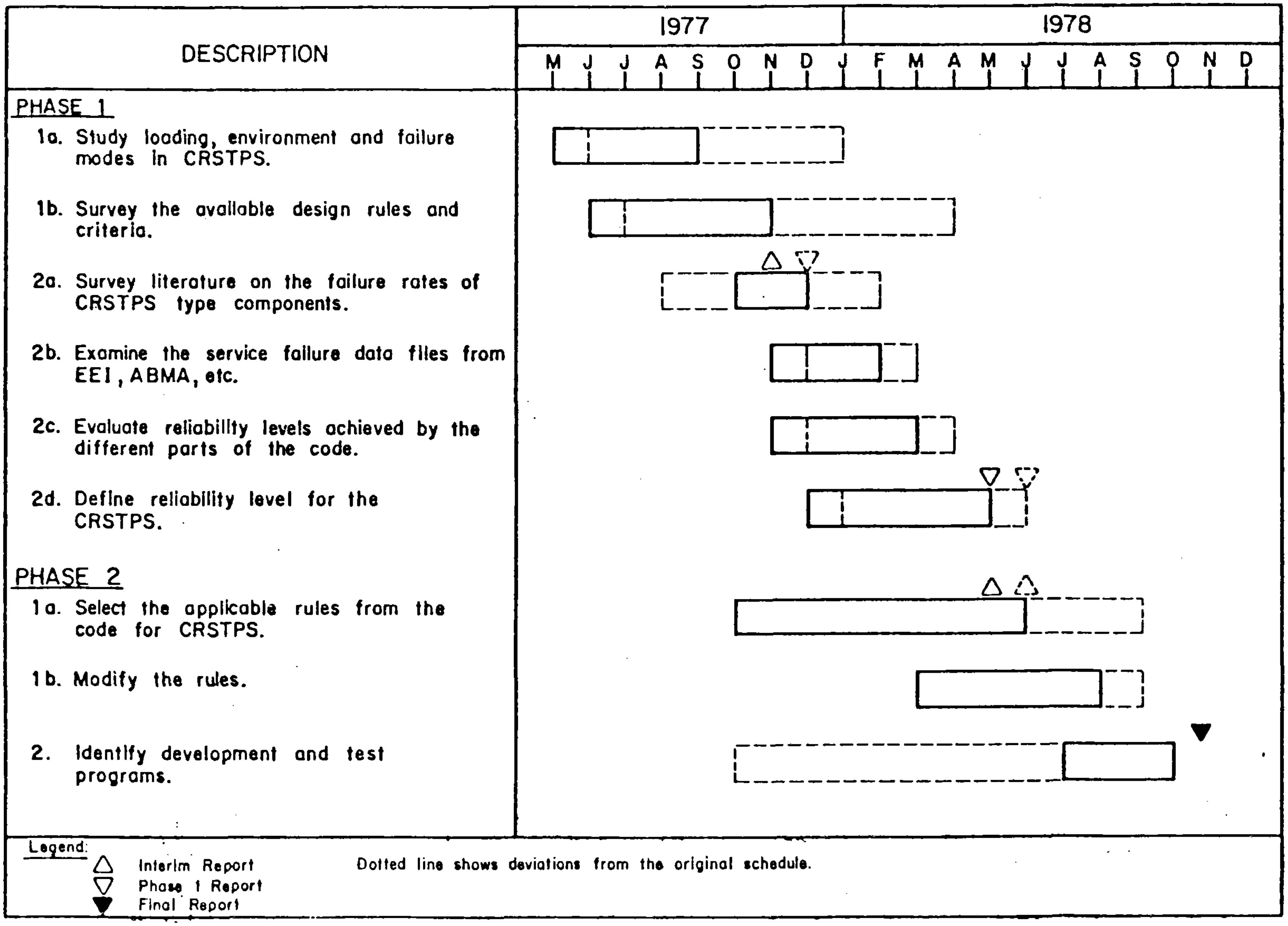

Figure 1. Program Schedule for an Interim Structural Design Standard for Solar Energy Applications

Review of CRSTPS System Components

A review of the loading, environment, and failure modes in CRSTPS receiver components that fall under the scope of the ASME Boiler and Pressure Vessel Code was completed. The basic intent of the review is to establish the design rules that must be imposed on these designs so that the users and public are safeguarded against their possible failures. The restrictions imposed on the design will depend, in large measure, on the consequences of the failure. These consequences are evaluated in this review, and the ASME Code rules that relate to these failure modes are identified (see Table I). The review of the components conducted under this program is restricted to the first-generation solar systems, namely the water-steam systems. Study of second-generation systems, such as the liquid metal, molten salt, and brayton-cycle systems, will be limited.

Matrix of Information

Table I, the Matrix of Information for the receiver subsystem, contains the following:

- List of Receiver Components: This list includes all components of the pressure boundary.
- Major Elements: These are specific items such as shell, head, nozzle, etc. for which rules are given in the Code.
- Loads: The loads associated with each component are identified. In general, the possible loads on any component are the internal or external pressure, impact loads, self weight, superimposed loads, wind, snow, shipping or seismic loads, reaction from support lugs, thermal, and vibration loads.
- Failure Modes: The possible failure modes for pressure components of a solar receiver are the following:

  - Ductile rupture
  - Creep rupture from long-term loads
  - Fatigue failure
  - Creep-fatigue failure
  - Gross distortion caused by incremental collapse and ratcheting
  - Loss of function as a result of excessive deformation
  - Buckling from short-term loadings
  - Creep buckling from long-term loadings

  Failure modes that are applicable to each element under "Loads" are listed.

- Failure Consequences: Consequences of a failure are described in terms of its impact on safety and availability. For example, a ductile rupture might cause bursting of a pressure boundary,

TABLE I

MATRIX OF INFORMATION

Receiver Component	Major Elements	Loads	Failure* Modes (FM)	Failure Consequences	Related Code Rules
Steam Drum	Shell	Internal pressure	1	FM 1 will affect safety.	Sections I and VIII-Division 1 contain tubes for all elements for internal pressure (FM 1). Section VIII-Division 2 has criteria to design all elements for internal pressure, thermal (steady state), and thermal transients. Section III has criteria for all loads including seismic.
	Heads	Thermal (steady-state)	3	FM 3 will lead to shutdown.	
	Feed-water Inlet	Thermal transients	5	FM 5 will lead to shutdown.	
		Seismic			
Header (low-temperature)	Shell	See Loads for Steam Drum	1	FM 1 will affect safety.	See Code Rules for Steam Drum (above).
	Heads		3	FM 3 will lead to shutdown.	
Header (high-temperature)	Shell	See Loads for Steam Drum.	1, 2	FMs 1 and 2 will affect safety.	Sections I and VIII-Division 1 have rules to prevent FMs 1 and 2 caused by internal pressure. Section VIII-Division 2 is not applicable for high-temperature design. Section III has criteria for all loads and failure modes.[§]
	Heads				
			4	FM 4 will lead to shutdown.	
Tubes (low-temperature)	Tubes	Internal pressure	1	FM 1 will affect safety.	See Code Rules for Steam Drum (above).
		Thermal (steady-state)	3	FM 3 will lead to shutdown.	
		Thermal transients	5	FM 5 will lead to shutdown.	
		Self-weight			
		Reactions of lugs, etc.			
		Seismic			
Tubes (high temperature)	Tubes	See Loads for Tubes (low-temperature)	1, 2	FMs 1 and 2 will affect safety.	See Code Rules for Header (high-temperature) (above)
			4	FM 4 will lead to shutdown.	
			5	FM 5 will lead to shutdown.	
Waterwalls (low-temperature)	Tubes	Internal pressure	1	FM 1 will affect safety.	See Code Rules for Steam Drum (above)
	Fins	Self-weight	3	FM 3 will lead to shutdown.	
		Attachment	5	FM 5 will lead to shutdown.	

		Seismic Thermal (steady-state) Thermal transients			
Waterwalls (high-temperature)	Tube Fins	See Loads for Waterwalls (low-temperature)	1, 2 4 5	FMs 1 and 2 will affect safety. FM 4 will lead to shutdown. FM 5 will lead to shutdown.	Sections I and VIII-Division 1 have rules to prevent FMs 1 and 2 caused by internal pressure. Section VIII-Division 2 is not applicable to high-temperature design. Section III has criteria for all loads and failure modes.
Piping (low-temperature)		Internal pressure Thermal (steady-state) Thermal transients Self-weight Seismic	1 3	FM 1 will affect safety. FM 3 will lead to shutdown.	Sections I and VIII-Division 1 have rules to prevent FM 1 as a result of internal pressure. Section III and Section VIII-Division 2 have criteria for FMs 1 and 3 and for all loads.
Piping (high-temperature)		See Loads for Piping (low-temperature)	1, 2 4	FMs 1 and 2 will affect safety. FM 4 will lead to shutdown.	See Code Rules for Header (high-temperature) (above).

*Failure Modes (FM)

1. Ductile rupture
2. Creep rupture
3. Fatigue failure
4. Creep fatigue
5. Ratcheting

§Section III also includes Code Case 1592.

which would be a safety hazard. A fatigue failure might lead to a leak, causing shutdown of the unit and affecting its availability.

- Related Rules: The applicability of the existing ASME Code rules to prevent the identified failure modes is indicated in this column. The types of loading and failure made addressed in each section of the Code are listed.

Review of the ADME Code Design Rules and Criteria

This task covers the review of the available design rules and criteria that may be applicable to solar pressure components. The review of Section I and Section VIII-Division 1 of the ASME Code has been completed. The review of Section III and Section VIII-Division 2 is in progress.

ASME Code, Section I

Section I of the Code covers rules for construction of power boilers, electric boilers, miniature boilers, and high-temperature water boilers. The approach taken by Section I is "Design by Rule." What this means is that Section I does not call for detailed stress analysis but merely sets the wall thickness necessary to keep the basic hoop stress below the tabulated allowable stress. Design rules for details have been written to hold the localized stresses at a safe level consistent with experience. Thermal stresses are not given explicit consideration.

The allowable stress for temperatures below creep range is the lowest of:

(i) one-fourth of the specified minimum tensile strength at room temperature

(ii) one-fourth of the tensile strength at temperature

(iii) five-eighths of the specified minimum yield strength at room temperature

(iv) five-eighths of the yield strength at temperature

The allowable stress for temperatures in the creep range is the lowest of the following:

- One-hundred percent of the average stress for a creep rate of 0.01 percent for each 1000 hours
- Sixty-seven percent of the average stress for rupture at the end of 100,000 hours
- Eighty percent of the minimum stress for rupture at the end of 100,000 hours

Section I gives specific design rules for the structural elements shown in Table I. These rules, in general, provide safety against ductile rupture. For components in which other failure modes such as creep and fatigue are significant, additional rules or criteria are needed.

ASME Code Section VIII, Division 1

Section VIII-Division 1 of the Code covers rules for the construction of unfired pressure vessels that are not covered in Sections I, III, and IV. The rules of this Division were formulated on the basis of design principles and construction practices applicable to vessels designed for pressures not exceeding 3,000 lb/in.^{2} (20,670 kPa). A more detailed description of the scope of this section may be found in Article U-1 of this Division.

The design philosophy of Section VIII-Division 1 was discussed in the previous section of this report. As in Section I, the rules are set to preclude ductile rupture by fixing the thickness of pressure boundaries so that hoop stress is kept within allowable limits. The allowable stresses are limited by consideration of creep rate and stress rupture. The allowable stress is based on creep and rupture data extrapolated to 100,000 hours. There are no provisions for explicit fatigue analysis in Section VIII-Division 1. However, the localized stresses are minimized as much as possible by means of design rules based on experience. For thermal stress, Section VIII-Division 1 merely mentions that it should be considered. The designer must use unspecified means to deal with these items if they are important.

The criteria used to determine the maximum allowable stress are the same as those of Section I except for nonferrous materials for temperatures below the creep range. In this case, the allowable stress is the lowest of the following:

- One-fourth the specified minimum strength at room temperature
- One-fourth of the tensile strength at temperature
- Two-thirds of the specified minimum yield strength at room temperature
- Two-thirds of the yield strength at temperature

Reliability Considerations

The ASME Code for design of pressure vessel and piping components is essentially a safety code that was established as the result of concern over a series of explosions that plagued the industry at the turn of the century. The rules that evolved have been modified and supplemented during the last six decades. They establish the minimum structural requirements for reasonably certain protection of life and property and a margin for deterioration to ensure reasonably safe useful service.

Along with safety, however, one must consider the question of the reliability achieved when using a set of design rules. Because the cost of forced outages or unavailability of a power plant system is generally high, its reduction is a major objective in power-plant design.

Tasks 2a, 2b, 2c, and 2d of Phase 1 are aimed at generating the necessary background information for developing a set of design rules for the CRSTPS that are adequate in terms of safety and reliability. The work involves review of the availability information on failure modes, failure causes, and failure rates of pressure components designed under different sections of the ADME Code; examination of the reliability requirements of CRSTPS; and arrival at a conclusion regarding the adequacy of the Code rules for meeting these requirements.

The work completed in this area during this reporting period involved a review of fifteen references relating to the reliability of power plant systems and pressure vessel components. A review of possible loads, failure modes, and failure consequences in receiver subsystem components was also conducted.

Developments and Test Needs

One of the tasks in Phase 2 of this program is the identification of the development and test programs necessary to support, verify, or upgrade the interim design standard for solar power plant components. This task was originally scheduled for the latter part of Phase 2. However, some preliminary studies in this area were performed, at Sandia's request, to evaluate the solar material testing program being conducted at ANL.

An important problem in solar receiver structures is material behavior under creep-fatigue. Information about this behavior is important to solar applications because the solar receiver tubes generally fatigue under a compressive creep condition. The available uniaxial fatigue data with tensile or compressive hold-times indicate a difference in the resulting creep-fatigue damage. However, this data may not be sufficiently indicative of the creep-fatigue effect in a multiaxial stress pattern.

ANL is performing material tests for solar power applications. In their proposal to ERDA, creep-fatigue test results for 304 and 316 stainless steel under uniaxial loading conditions showed that tensile hold-time results in substantially higher creep damage than does compressive hold time.

ANL's proposal identified a series of tests for 316H stainless-steel tubes under internal pressure and axial load to determine the effect of compressive hold-times under a biaxial stress condition. The ANL program includes fatigue tests on pressurized cylinders. The pressures considered are zero and 1100 psi (7.58 MPa) and the axial strain ranges are 0.5 percent and 0.75 percent. Hold times are 0, 1, 5, and 10 minutes.

To show what the proposed ANL tests mean and how they can be utilized in developing a solar design standard, inelastic analyses were performed on a 316H stainless-steel cylinder subjected to some of the proposed test conditions. An elastic-plastic-creep program available in-house at Foster Wheeler was used for the analysis. Kinematic hardening rule was assumed. The analyses produced the following results:

- For the zero pressure case with 0.5 percent strain range, a stress range of ±17.76 kips/in.^{2} (122.45 MPa) was obtained.
- The cylinder under 1100 lb/in.^{2} (7.58 MPa) constant pressure and 0.5 percent axial cyclic strain exhibited ratcheting initially, but shook down to a steady state.
- For the cyclic strain with a constant pressure of 1100 lb/in.^{2}, the analytical model showed a sequencing effect. For an annealed cylindrical specimen (that is, a specimen with no residual stresses and strains) subjected to a constant internal pressure, the stress and strain state during axial cycles depends on whether the axial tension or compression is applied first. The effective strain range in both cases remains the same. However, for the case in which compression was applied first, the axial stress ranged from -13.32 to 22.20 kips/in.^{2} (-91.84 to 153.10 MPa). When tension was applied first, the axial stress ranged from -17.47 to 18.06 kips/in.^{2} (-120.45 to 124.52 MPa).
- Under the constant pressure condition, the effective strain range at shakedown was 0.5 percent. Hence, one would expect the same number of cycles to result in failure in both zero and nonzero (constant) pressure conditions. This conclusion is based on the following assumptions:
    - The effective strain range governs the fatigue life.
    - Mean stress in the cycle has a relatively insignificant effect.
    - There are no hold-time effects (that is, there is insignificant creep damage).

- For a constant pressure case of 1100 $lb/in.^2$ (7.58 MPa), the maximum tensile stress of 6.79 $kips/in.^2$ (46.84 MPa) obtained circumferentially was substantially less than the axial compressive stress. It is likely that this stress situation will not exhibit much biaxial effect on fatigue life. An analysis to increase the biaxial effect with an increased pressure value of 2100 $lb/in.^2$ (14.48 MPa) led to a circumferential stress of 13.69 $kips/in.^2$ (94.39 MPa). which is comparable in magnitude to the axial compressive stress. Since analysis shows that no ratcheting should occur, this higher pressure value should result in a more meaningful biaxial load test.

Based on the above analytical results, the following recommendations regarding the ANL tests were made:

- Include tests at a constant pressure of 2100 $lb/in.^2$ (14.48 MPa).
- Run tests with tensile and compressive hold-times.
- Run 0.5 percent strain-range tests initially and review the results.
- Run one-minute hold-time tests initially and review the results.

MATERIALS TESTING FOR CENTRAL RECEIVER SOLAR THERMAL POWER SYSTEMS

Argonne National Laboratory

S. Majumdar
D. R. Diercks

Background

The present program is concerned with the determination of specific elevated-temperature mechanical properties of materials used for critical components in solar central receiver power systems. Several general features of solar central receiver operating conditions are likely to create difficult structural design problems. The first of these is the highly cyclic nature of the thermal loading of critical components. Solar plants will undergo at least one major start-up and shut-down cycle per day, with the likelihood of additional thermal cycles being imposed by intermittent cloud cover and unscheduled maintenance and repair. Thus critical elevated-temperature components may be expected to accumulate of the order of tens of thousands of thermal and associated strain cycles over a 30-year design life. In addition, repeated thermal cycling of superheater or boiler tubing while under internal pressure can lead to incremental growth or ratchetting. The analyst must therefore design against structural failure due to thermal fatigue and creep-fatigue interaction and must also avoid excessive deformation due to incremental growth.

A related feature of solar central receiver operation is the phenomenon of departure from nucleate boiling (DNB) that occurs in the boiler tubing. During daytime operation, coolant water from the condensor first experiences local, or nucleate, boiling as it travels through the boiler tubing. With further heating, general, or film, boiling occurs somewhat farther along the tubing. Since the efficiency of heat transfer from the inner wall of the boiler tubing to the coolant is greatly decreased with the onset of film boiling (i. e., the departure from nucleate boiling), a rather abrupt increase in inner wall temperature is present at the location where DNB occurs. The position of this boundary between film and nucleate boiling in the boiler tubing generally fluctuates in a cyclic manner with time, and the inner wall in this fluctuating region experiences rapid alternate heating and cooling. The frequency of the temperature and associated strain cycles is typically of the order of one cycle per second, and so 10^8 or more cycles may be accumulated over the life of the tubing. Elevated-temperature high-cycle-fatigue data on boiler tubing materials are therefore needed to design against possible failure associated with DNB.

The third aspect of solar-plant operating conditions likely to cause design difficulties is that, during steady-state operation, the boiler and superheater tubing will be loaded nonaxisymmetrically at elevated temperatures. In particular, critical passes of the superheater tubing will be loaded during daytime operation such that the outer tubing wall on the high-temperature side will experience a large compressive axial stress and a moderate compressive hoop stress. On the other hand, the inner wall on the high-temperature side will be subjected to a compressive axial stress and a small tensile hoop stress. Considerable constitutive relation information under compressive and mixed tensile-plus-compressive creep conditions will be required to permit structural analyses of the components. In addition, failure criteria for nonaxisymmetric multiaxial tensile-plus-compressive creep-fatigue conditions must be developed. Finally, the nonaxisymmetric loading further complicates the ratchetting analysis.

Elevated-temperature design rules applicable to solar-power-plant boilers and piping are set forth in Section I of the ASME Boilder and Pressure Vessel Code. However, Section I was not developed with the highly cyclic and often complex loading conditions of solar-power-plant components in mind, and no specific design rules for treating fatigue, creep fatigue, or ratchetting are provided. Applicable design rules from the nuclear portions of the Code (Section III and Case 1592) are likely to result in excessively conservative designs. For example, Case 1592 would consider the compressive loading on the hot side of the superheater tubing to be as damaging as an equal tensile loading, although available data indicate that this is not the case for many materials, at least for uniaxial loadings. The ratchetting analyses rules of Case 1592 are also likely to be overly conservative when applied to the nonaxisymmetric multiaxial loading of superheater tubing. Thus a modified set of Code rules more appropriate to the design of solar components is needed. The development of these rules, in turn, requires the creation of a supportive base of mechanical-properties data.

In some of the more advanced designs for future solar central receiver systems, the use of liquid sodium is proposed as the coolant in the central receiver tower. The heated sodium would flow from the tower to a steam generator at ground level, where the steam to drive the turbines would be produced. Such an arrangement offers several advantages over the direct generation of steam in the receiver tower, including (1) the benefits of the superior heat-transfer characteristics of the sodium coolant, (2) the elimination of the high internal pressure in the receiver tubing, and (3) the elimination of problems associated with stress-corrosion cracking and departure from nucleate boiling in the receiver tubing. Considerable information has been obtained on sodium effects on structural materials in the Liquid-Metal Fast-Breeder Reactor (LMFBR) program. However, this information, particularly with respect to material sodium compatibility and sodium effects on elevated-temperature mechanical properties, needs to be reviewed and extended to the materials and anticipated operating conditions associated with solar central receiver systems.

Program Description

The present program has been developed in response to the needs outlined above and is divided into three subtasks. The first subtask is being performed in support of solar central receiver designs developed by Martin Marietta Corp. and by Honeywell Inc., and is concerned with the biaxial creep-fatigue testing of Type 316H stainless steel superheater tubing. Current design procedure for the superheater tubing is to perform a creep-fatigue analysis using elevated-temperature nuclear rules (Code Case 1592) but to ignore creep damage due to compressive stresses. Thus hold times under compressive stresses are assumed to be nondamaging. As stated above, this assumption appears to be reasonable for austenitic stainless steels under uniaxial loading conditions, but it has never been verified for biaxial loading situations, particularly where the stress is tensile in one direction and compressive in the other. Furthermore, virtually no creep-fatigue data exist for Type 316H even under uniaxial loading conditions. Under this subtask, biaxial creep-fatigue tests (constant tensile hoop stress and cyclic axial strain with hold times in compression) will be performed on Type 316H superheater tubing material. Times-to-failure will be accelerated by increasing the magnitude of the axial strain range over that expected in service and by using considerably shorter compressive hold times.

Under the second subtask, a comprehensive survey of available information on sodium effects on candidate materials for solar thermal electric piping and steam generators is being conducted. The survey includes information on sodium effects on mechanical properties, sodium compatibility, mass-transfer effects and friction adhesion, and self-welding behaviors in a sodium environment. Recommendations for future testing are also included.

The third subtask is concerned with mechanical-properties data generation in support of the ASME Code development. This work interfaces directly with a program being conducted by Foster Wheeler Energy Corporation entitled "An Interim Structural Design Standard for Solar Energy Applications." A critical phase in this development is the formulation and execution of an extensive mechanical-testing program to generate the required design-limits data. This mechanical-testing program is to be conducted by Argonne National Laboratory. As an initial effort under this subtask, a test matrix is being developed for the high-cycle fatigue testing of Incoloy 800H boiler tubing under biaxial (constant internal pressure plus cyclic axial loading) conditions. Available fatigue data for Incoloy 800 and 800H, totaling some 480 data points, have been collected and are being analyzed.

Projected schedules and levels of effort for the three subtasks are as follows:

Subtask	Begin	End	Total Man Years
1	7/77	8/78	1.5
2	10/77	8/78	0.5
3	2/78	2/80	4.0

Status of Subtask 1

Approximately 30 ft of Type 316H stainless steel tubing (1" OD and 0.12" nominal wall thickness) have been procured from Pacific Tube Co., Los Angeles. Initially four biaxial fatigue specimens as depicted in Figure 1 were machined. One of these specimens was used for measuring the temperature profile in the specimen. Forty-four thermocouples were spot welded to the specimen along four azimuthal planes. The specimen was then mounted on the biaxial fatigue machine with the mandrels and the extensometers in position (Figure 2). Several temperature profiles were measured after displacing the induction coil either axially or transversely and then recentering

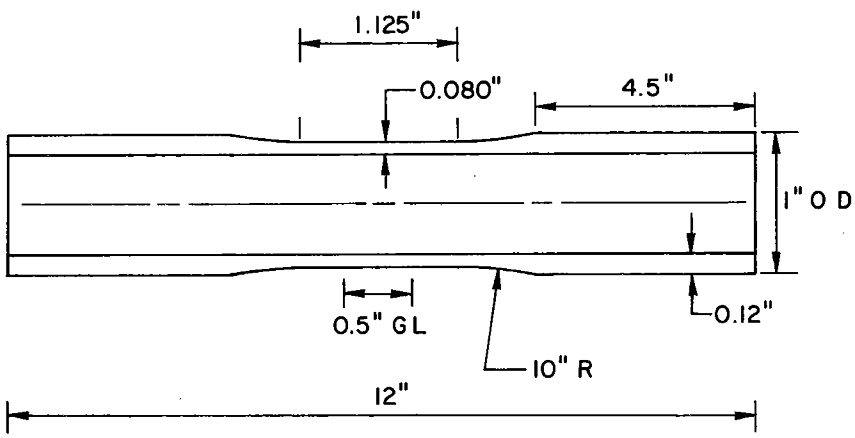

Figure 1. Biaxial Fatigue Specimen

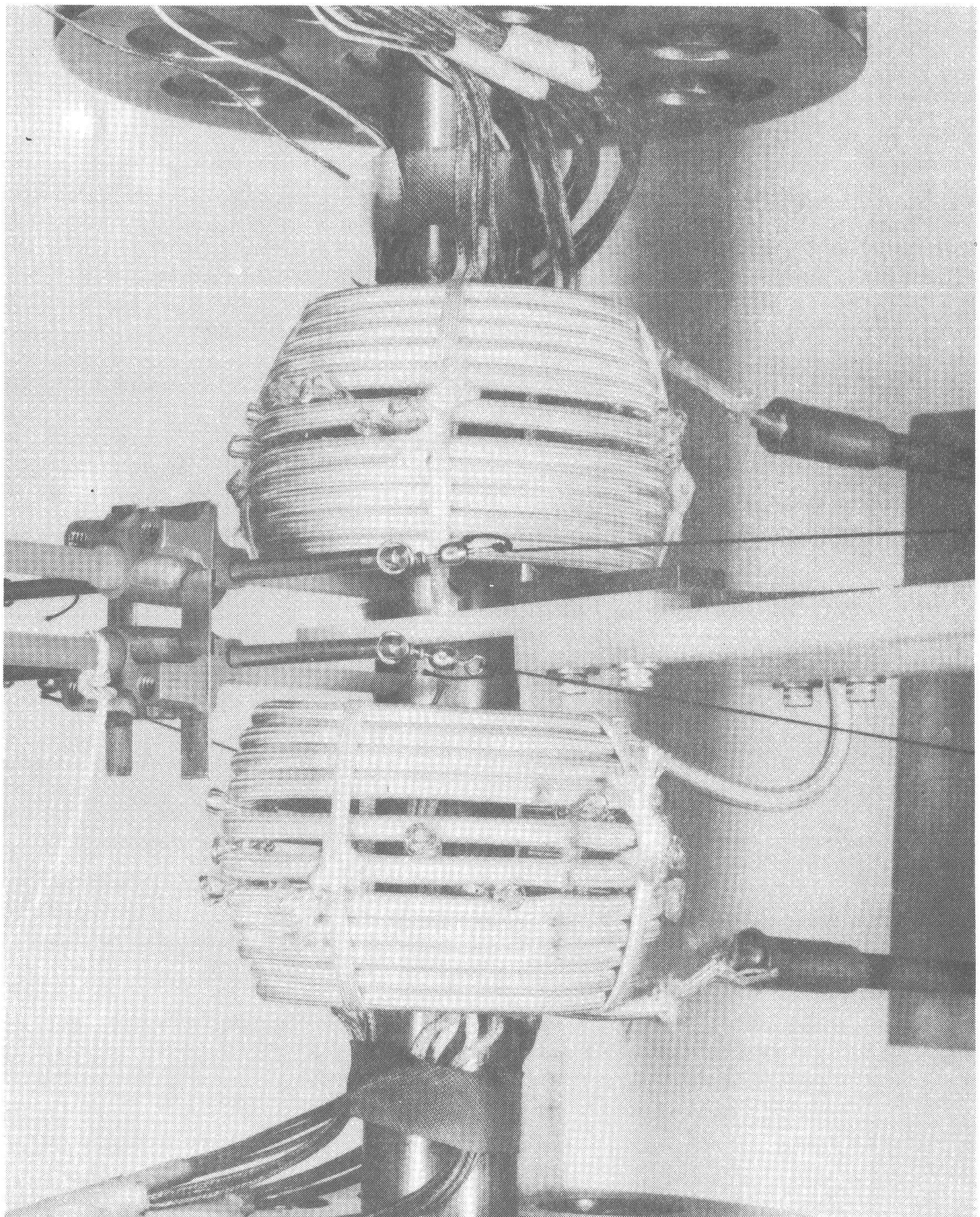

Figure 2. Test Setup For Biaxial Fatigue

the coil as would be done in an actual test. Two such temperature profiles are shown in Figure 3, which shows that the temperature profile is reproducible to within 10°F. The maximum temperature gradient within the central 1/2" of the specimen, where both the axial and diametral extensometers will be attached, is of the order of 15°F. In an actual test, the temperature in the specimen is controlled by means of control thermocouple located away from the center and at a location where the wall thickness of the specimen is larger. It is estimated that the uncertainty in the temperature at the central 1/2 inch of the specimen is ±15°F. Such an indirect means of controlling the temperature of the specimen is unavoidable because, if the control thermocouple were spot welded at the center of the specimen, it would produce a starter crack which would result in a premature failure of the specimen.

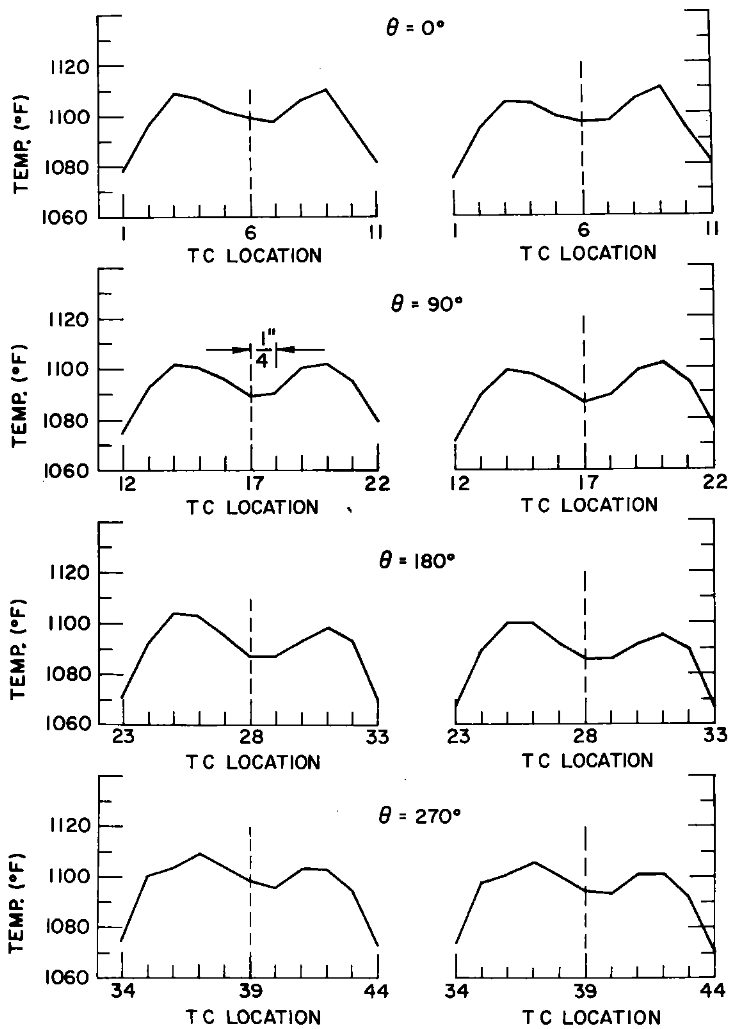

Figure 3. Typical Temperature Profiles in the Biaxial Fatigue Specimen

Three fatigue tests from the test matrix (Table I) have been completed to date. Two of these tests were conducted at a test temperature of 1100°F at 0.5 percent axial strain range with zero internal pressure. The third test involved the same axial strain range but with an internal pressure of 1100 psi. The results are summarized in Table II. As a comparison, test results reported in the literature for uniaxial hourglass shaped specimen of Type 316 stainless steel at the same temperature and strain range vary from 10780 to as high as 106622. It appears that a constant internal pressure of 1100 psi has very little effect on the fatigue life of the specimen. In fact, the effect of the internal pressure is to decrease the axial plastic strain range slightly. Although the total diametral ratchetting strain is small (about 1 percent), it is interesting to note that the specimen continued to ratchet throughout the test, albeit at a smaller and smaller rate.

At a meeting among representatives of Argonne National Laboratory, Sandia, Livermore, and Foster Wheeler on November 10, 1977, it was decided to review the test matrix in Table I after completing the 0.5 percent strain range tests. Depending upon the extent of ratchetting, the test matrix will be repeated for internal pressure of 2100 psi and the 0.75 percent strain range tests will be given the least priority.

Status of Subtask 2

In support of the design of a proposed sodium cooled solar-thermal central receiver system, a survey of available information, entitled "Sodium Effects on Candidate Materials for Solar-Thermal Electric Superheaters and Steam Generators," is being conducted at Argonne.

Information on the mechanical properties, sodium corrosion, nonmetallic elements transfer characteristics, stress-corrosion cracking, and wastage resistance associated with sodium-water reactions was obtained from various LMFBR programs.

As a result of this literature review, we will identify the most promising materials for solar applications and key areas that require further technological development.

Status of Subtask 3

Available fatigue data for Incoloy 800 and 800H have been collected and a report will be published tabulating all the data. A test matrix for high cycle fatigue testing of Incoloy 800H tube under a biaxial state of stress will be proposed in the near future.

TABLE I

PROPOSED TEST MATRIX FOR SUBTASK 1

Temperature ≈ 1100°F
Cyclic axial strain rate = 0.004 s^{-1}

Axial Δ_t (%)	P_i (psi)	Hold Time (min)	Expected Life N_f	Expected Life t_f (h)
0.5	0	0	30,000	20
	1100	0	20,000	14
	1100	1C	20,000	350
	1100	5C	20,000	1680
	0	1C	30,000	520
0.75	0	0	7,000	7
	1100	0	5,000	5
	1100	1C	5,000	90
	1100	10C	5,000	840
	0	1C	7,000	124

Total time ≈ 3650

Add 50% for Duplicate Tests ≈ 1825

Total testing time ≈ 5475

TABLE II

SUMMARY OF BIAXIAL FATIGUE DATA OF
TYPE 316 STAINLESS STEEL AT 1100°F

Test No.	Internal Pressure (psi)	Axial Strain Range[1] Total (%)	Axial Strain Range[1] Plastic (%)	Diametral Strain Range Total (%)	Diametral Strain Range Plastic[2] (%)	Axial Stress Range (ksi)	Hoop Stress (ksi)	N_f Cycles	Diametral Strain @ Failure (%)
997	0	0.513	0.188	0.201	0.094	71.49	0	14156	-0.02
999	0	0.503	0.188	0.192	0.094	69.26	0	8110	-0.02
1001	1100	0.502	0.167	0.187	0.080	73.77	6.08	16661	+1.14

[1]Axial strain rate = 0.004 s^{-1} in all tests.

[2]Poisson's ratio value of 0.32 was determined from test nos. 997 and 999, and was used to calculate the diametral plastic strain range for test no. 1001.

AN EXPERIMENTAL INVESTIGATION OF CONVECTIVE LOSSES FROM SOLAR RECEIVERS

University of Illinois at Urbana-Champaign

A. M. Clausing
G. L. Clark
M. H. Mueller

The magnitude of the convective loss from a central receiver, especially an external receiver, is expected to exert a significant influence on the thermal efficiency of solar thermal-electric power generation systems. Unfortunately, the magnitude of this loss component is hard to estimate since the high temperature and large size of a central receiver combine to place its operating conditions well outside the envelope of known experimental data. In addition, the interaction between free and forced convection mechanisms, for this geometry, is not well understood. Thus the possibility of obtaining useful results from the extrapolation of existing data is considered remote.

The intent of this study is to experimentally investigate the interaction of free and forced convection mechanisms under conditions which approach the extremes expected during receiver operation. To accomplish this task, a low-speed cryogenic wind tunnel is being constructed at the University of Illinois at Urbana-Champaign (UIUC). When completed, the UIUC facility will drastically extend the range of available combined convection data, improve understanding of combined convection mechanisms, and thus improve receiver convective loss predictions.

Figure 1 shows some characteristics of a typical 10-MWe external receiver. Using these dimensions and operating conditions, the significant dimensionless parameters for free and forced convection, the Reynolds number (Re) and Grashof number (Gr) respectively, can be calculated. The formulation of these parameters and typical values for a 10-MWe receiver are given in Figure 2. The ratio, $Gr/(Re)^2$, a measure of the relative contributions of free and forced convection, is of the order of one. This indicates that both free and forced convection are of significance. The large Reynolds and Grashof magnitudes indicate that the flow field surrounding the receiver is turbulent.

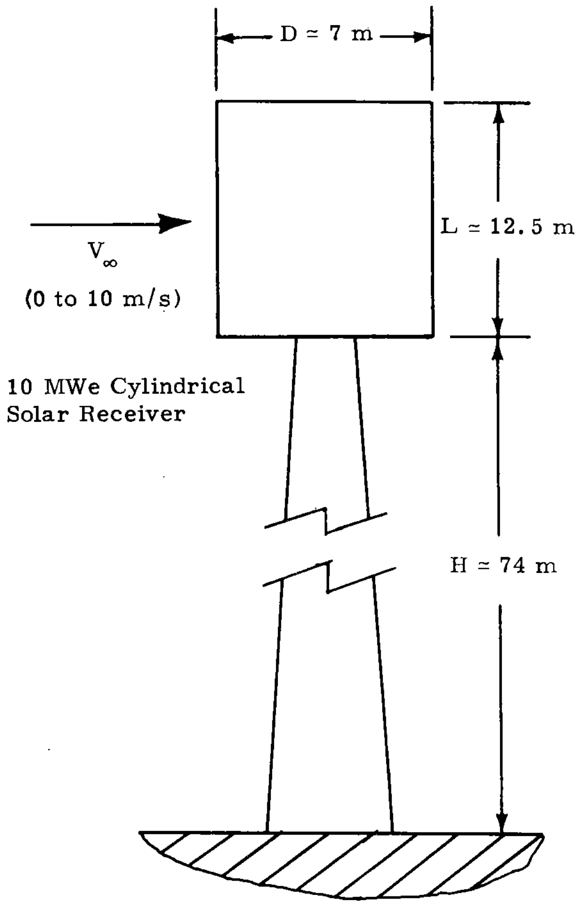

Figure 1. Dimensional Schematic of a Typical 10-MWe External Receiver

$Re \equiv \dfrac{\rho V D}{\mu}$	$0 < Re < 3 \times 10^{13}$
$Gr \equiv \dfrac{\rho^2 g \beta \Delta T L^3}{\mu^2}$	$5 \times 10^{12} < Gr < 1 \times 10^{13}$
$\dfrac{Re}{Gr^{1/2}} = \dfrac{V_\infty D}{(g \beta \Delta T L^3)^{1/2}}$	$0 < \dfrac{Re}{Gr^{1/2}} < 1$
$P_r = \dfrac{\mu C_P}{K}$	0.7

Figure 2. Significant Dimensionless Parameters and Typical Values For a 10-MWe External Receiver

Modeling Method--A Cryogenic Environment

The use of a conventional wind tunnel for convective modeling, at the large Reynolds and Grashof numbers encountered in receiver work, is prohibitively expensive due to the large test section required. Indeed the literature reveals no reported data in the range of interest. What is needed is an economical method of generating receiver conditions. Increasing the gas density through tunnel pressurization is one possibility, but this technique is very expensive. The use of other fluids has also been considered, but the changes in $\rho^2\beta/\mu^2$ and ρ/μ, for normal fluids, are completely inadequate to balance the reduction in $(\Delta T)L^3$ and vD that are possible with reasonable size models at realistic temperatures. In addition, the Prandtl number of candidate fluids is typically much different than that of air, introducing an uncontrolled variable into the study.

A novel technique, the use of cryogenic temperatures for convective modeling, is used in this study to obtain significant increases in both $\rho^2\beta/\mu^2$ and ρ/μ, in order to simultaneously obtain large Grashof and Reynolds numbers. During the last several years, some of the advantages of cryogenic modeling have been recognized and used by aerodynamicists. Low-temperature modeling is an excellent tool in this application, but the cryogenic wind tunnel is even more effective for low-speed heat transfer research at high Reynolds and/or Grashof numbers since the Mach number can be allowed to approach zero and since the increase in the Grashof number is even more spectacular than that of the Reynolds number. The respective gains with decreasing temperature are shown in Figures 3 and 4.

The UIUC cryogenic wind tunnel is shown schematically in Figures 5 and 6. It is designed to simultaneously obtain large Reynolds and Grashof numbers and to investigate the regime where $Gr/(Re)^2$ is of the order of one. The 2:1 aspect ratio of the test section was chosen to approximate that of the external receivers under consideration and to yield the largest practical vertical length L, a necessity for the generation of large Grashof numbers. The critical parameter L^3 is a factor of 37 greater in the UIUC facility than in any presently operational cryogenic wind tunnel.

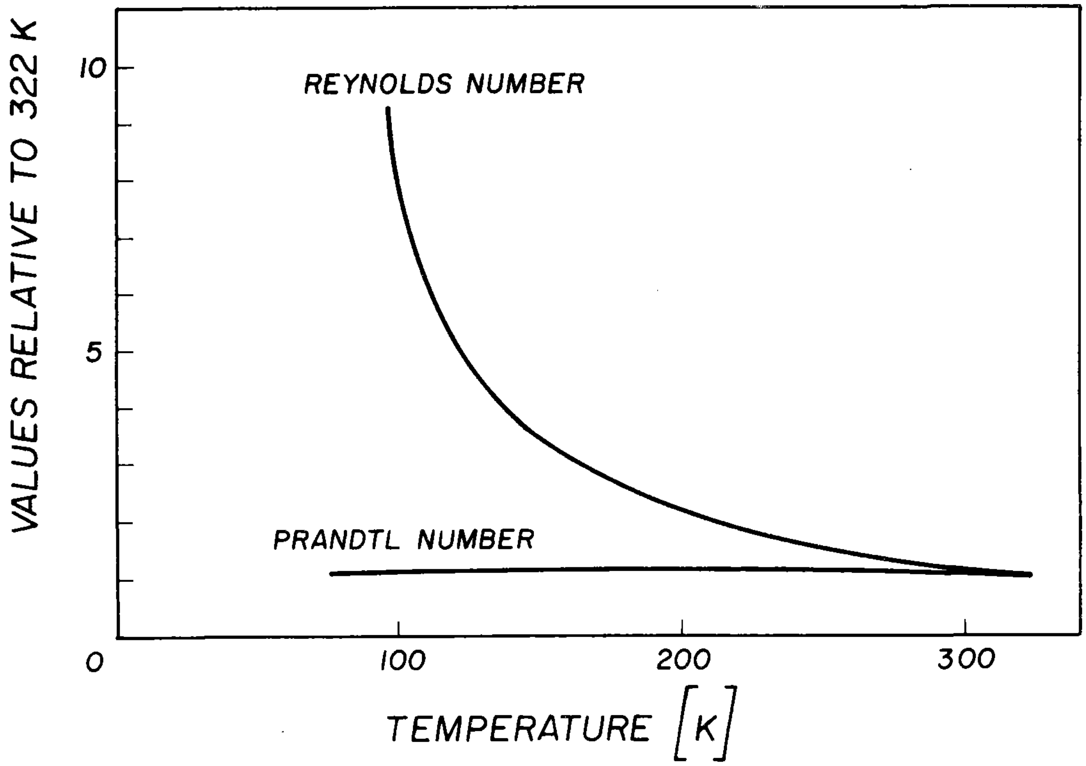

Figure 3. The Effect of Cryogenic Temperature on Reynolds Number

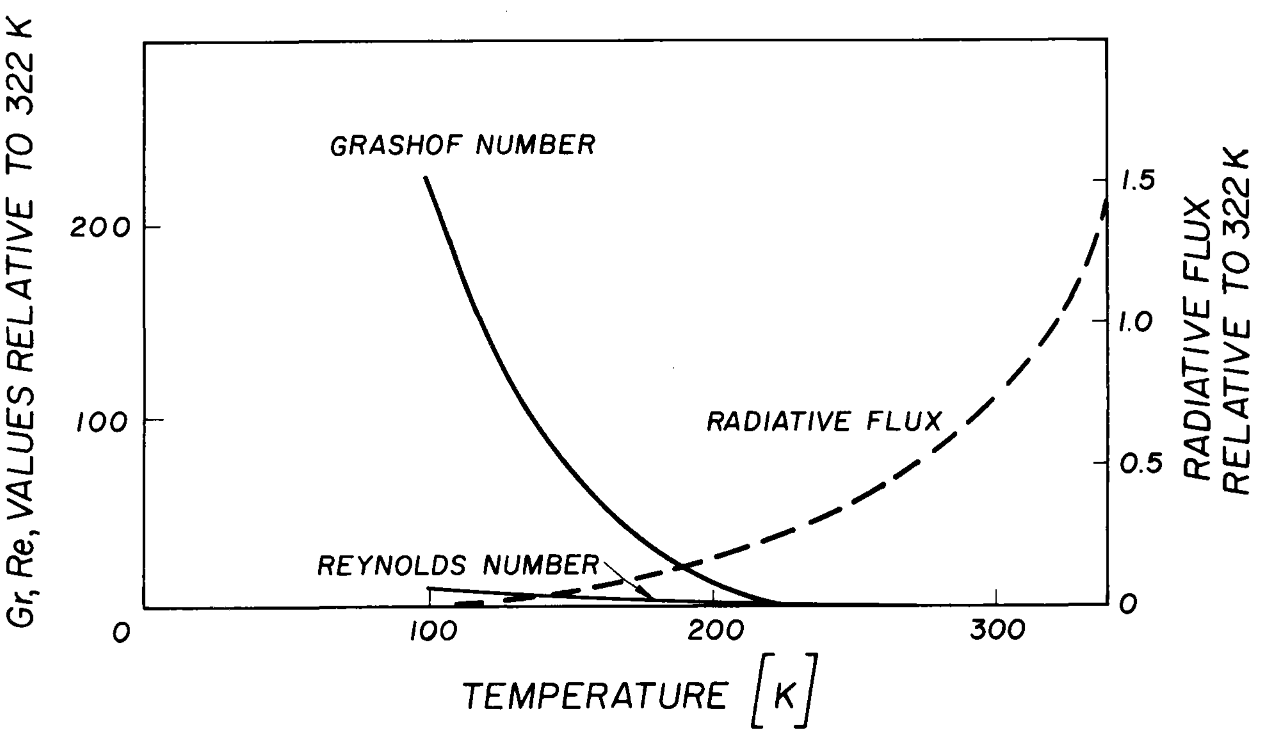

Figure 4. The Effect of Cryogenic Temperature on Grashof Number

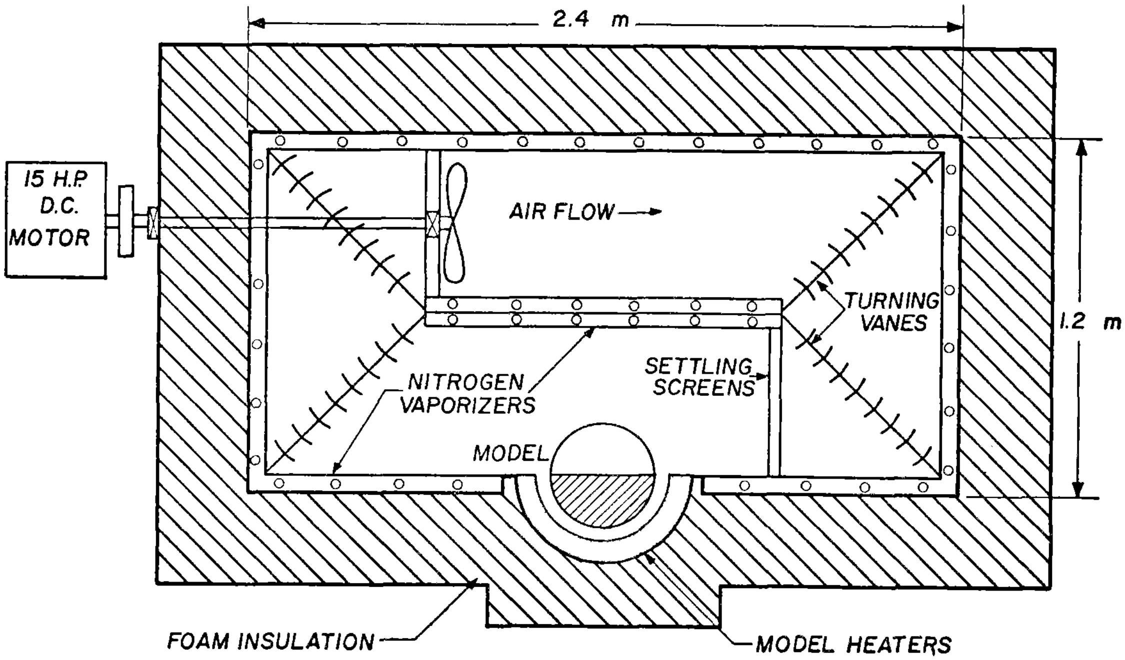

Figure 5. Top View Schematic of the UIUC Cryogenic Wind Tunnel

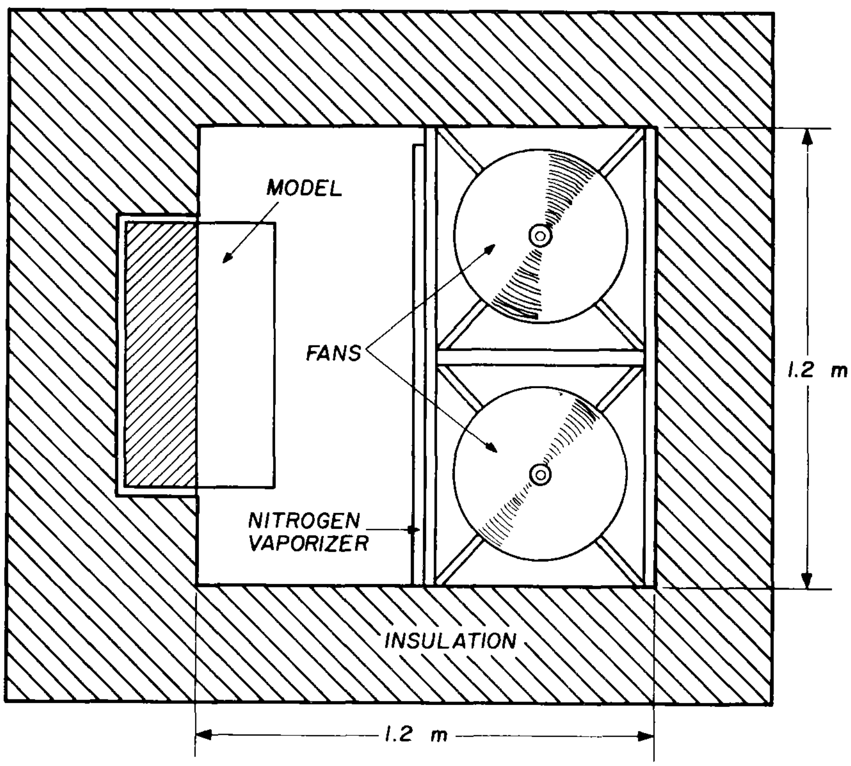

Figure 6. Cross Sectional Schematic, Through the Middle of the Test Section, of the UIUC Cryogenic Wind Tunnel

Data Acquisition and Analysis

After consideration of several measurement schemes, a transient technique for gathering the necessary heat-loss data was selected. In this method, the model is heated to a specified temperature distribution in a separate pre-chamber. When the desired level and distribution have been established, the model is injected into the test section.

This transient injection technique is especially desirable in a cryogenic wind tunnel, since it minimizes run-time and hence required cooling at high velocities. In addition, it allows short runs at power levels which exceed the cooling capacity of the tunnel, through utilization of the thermal capacitance of internal tunnel structures.

Current Status

Following the design and subsystem-testing phases of the program, completed in the fall of 1977, tunnel construction was initiated. It is currently 75 percent completed and shakedown testing is scheduled to begin in April.

HYDRAULIC STABILITY OF SOLAR BOILERS

University of Minnesota

Herbert S. Isbin

Funding: Sept. 1, 1977 to June 30, 1979 - $47,000

Objective

The objective is to develop a numerical calculational program for analyzing transient steam-water flows in heated parallel channels. The mode is to be applied to geometries typical for solar boilers and is to have the capabilities for investigating parameters which might influence the dynamic stability of the flow in the individual channels. Model verification is to be achieved through comparison of predicted results with experimental results already available in the open literature and from experimental results obtained by DOE contractors. The specific type of dynamic instability to be investigated is known as the density wave instability. The flow oscillations are of low frequency and are related to the time required for the fluid to pass through the channel. Feedbacks between flow, pressure drop, and vapor generation interact to affect the stability of the system.

Schedule

The schedule calls for an early version of a model that is capable of performing the transient analyses by June 30, 1978. Incorporation of additional features into the model and additional comparisons of predicted with experimental results are to be made by December 30, 1978. Completion of the project is set for June 30, 1979.

Present Status

The early version of the model has been developed to study the hydraulic stability in heated, parallel channels. For the two-phase regions, conservation equations are written for the mixture flow, for the vapor flow employing drift velocity formulations, and for the energy of the mixture flow. Pressure variations are small compared to the system pressure and thus the effects on the density and enthalpy of each phase are neglected. This simplification permits the decoupling of the momentum balance. A computer program has been developed to calculate the axial variations for the void fraction, enthalpy, fluid temperature, and quality for a channel with a prescribed axial heat flux. The first application of the program has been for steady-state initializations. The model includes evaluation of net vapor generation for subcooled liquid flows for nonuniform axial heat fluxes.

We are in the process of trying to improve our schemes for the numerical evaluations of the transient flows, recognizing that there are questions of consistency, convergence, and stability of the numerical schemes.

In our review of the literature on flow oscillations, we note that numerical instabilities in the calculational schemes might have been overlooked in past studies. On the other hand, stability boundaries obtained analytically from the set of equations using small perturbations linearized around a steady state, though very informative, may overstate the conditions for unstable operating ranges. Factors which affect flow stability which have been reported include the following:

<u>With respect to mathematical modelling</u>

a. Inclusion of the thermal nonequilibrium effects, such as the void generation in the subcooled liquid region, predicts enhanced stability at low subcoolings and decreased stability at high subcoolings.

b. Increases in the drift flux enhance stability.

c. Above a given characteristic subcooling, stability is enhanced with increases in subcooling. At subcoolings less than the characteristic value, the stability is enhanced by decreasing subcooling.

d. Increases in inlet liquid velocity enhance stability.

e. For a given inlet liquid velocity, increases in heat flux decrease stability.

f. Inlet orificing is a strong stabilizing factor, while exit orificing strongly decreases stability.

With respect to empirical results

a. Reduction of the heated length increases stability.

b. Inlet restrictions enhance stability and exit restrictions decrease stability.

c. Increased system pressure enhances stability.

d. The effect of inlet subcooling on flow stability exhibits a minimum. Above the minimum value, increases in subcooling enhance stability, and below the minimum, decreases in subcooling enhance stability.

e. Increased inlet velocity enhances stability and increased power increases the frequency of the flow oscillations.

f. The effect of nonuniform heat fluxes may or may not decrease the flow stability.

g. Generally the wall effects have been insignificant because of relatively small thermal capacitance used in the experiments.

Model developments reported in the literature present dimensionless groups for mapping regions of stable and unstable flows, and reasonable agreement with experimental results have been achieved. To our knowledge, the models have not treated a case similar to the geometry and conditions for operation of the solar boiler tubes. Most tests and models have been limited to exit qualities significantly less than one and thus one should not attempt to extrapolate the trends. Our intention is to use these results for initial tests of our model studies.

References

J. A. Boure, A. E. Bergles, and L. S. Tone, "Review of Two-Phase Flow Instability," 71-HT-42, ASME-AIChE Heat Transfer Conference, Tulsa, Oklahoma, August 15-18, 1971.

M. Ishii, "Thermally Induced Flow Instabilities in Two-Phase Mixtures in Thermal Equilibrium," Ph.D. Thesis, Georgia Institute of Technology, June 1971.

P. Saha, "Thermally Induced Two-Phase Flow Instabilities, Including the Effect of Thermal Nonequilibrium Between Phases," Ph.D. Thesis, Georgia Institute of Technology, June 1974.

S. Kakas and F. Mayinger, Two-Phase Flows and Heat Transfer, Vol. 1, Hemisphere Publishing Corporation, Washington, D.C., 1977.

W. T. Hancox, "Prediction of Oscillating, Diabatic Steam-Water Flows," Ph.D. Thesis, University of Waterloo, March 1971.

R. T. Lahey, Jr., and F. J. Moody, The Thermal-Hydraulics of a Boiling Water Nuclear Reactor, American Nuclear Society, Hinsdale, Illinois, 1977.

CENTRAL RECEIVER PLANT CONTROL SIMULATION MODEL

McDonnell Douglas

E. Riel

The solar central receiver system consists of five basic subsystems which are coupled together physically and also both directly and indirectly through master control. The overall system is dynamic in nature due to both the variability of the basic energy sources as well as its various operational modes and conditions. Because of this, simulation is a highly desirable tool to aid in the design and integration of a solar power plant. The following presentation defines this simulation, its objectives, the simulated subsystem models, and presents typical simulation results in addition to the role of the simulation in basic design and system integration.

Simulation Objectives

The purpose of the plant control simulation effort was to provide an analytical tool for evaluating the stability and dynamic performance characteristics of a coupled solar power plant. The requirements for the simulation model were that it be efficient to operate in order to perform parametric analysis and establish subsystem performance and stability sensitivities. The simulation model must also be of sufficient fidelity and accuracy in order to design and evaluate the control system and evaluate subsystem transit performance. In order to provide the capability for man-in-the-loop interaction and also support system integration and testing, the simulation model must be capable of operating in real time and interfacing with real hardware. For these reasons, a hybrid approach was selected for the simulation models.

Power Plant System Simulation Functional Schematic

The total power plant system is composed of five major subsystems: the collector, receiver, thermal storage, electrical power generation, and master control subsystems. The power plant system simulation (Figure 1) incorporates mathematical models of the dynamics of the physical processes and controls for each of the major subsystems. The collector subsystem is essentially uncoupled from the rest of the system, and therefore the models of the insolation and collector subsystem have been simplified into a lumped insolation history--all other subsystems are modeled in detail in order to describe and evaluate their dynamic behavior. The receiver model is described as a three-phase system featuring nonsteady fluid flow throughout the receiver panels. The model includes multiple solar panels as well as a complete model of the receiver temperature and pressure control systems. The thermal storage subsystem is highlighted also by three-phase fluid flow, featuring both thermal storage charging and extraction flow loops with their representative control systems. Included in the thermal storage subsystem are individual models of the desuperheater, thermal storage heaters, the thermal storage unit, and the thermal storage steam generators. The electrical power generation subsystem model consists of a matehmatical model of the turbine, generator, and equivalent electrical load. The turbine is modeled as a dual input multi-stage turbine with bleed ports. The turbine model includes a representation of the shaft angular acceleration with the

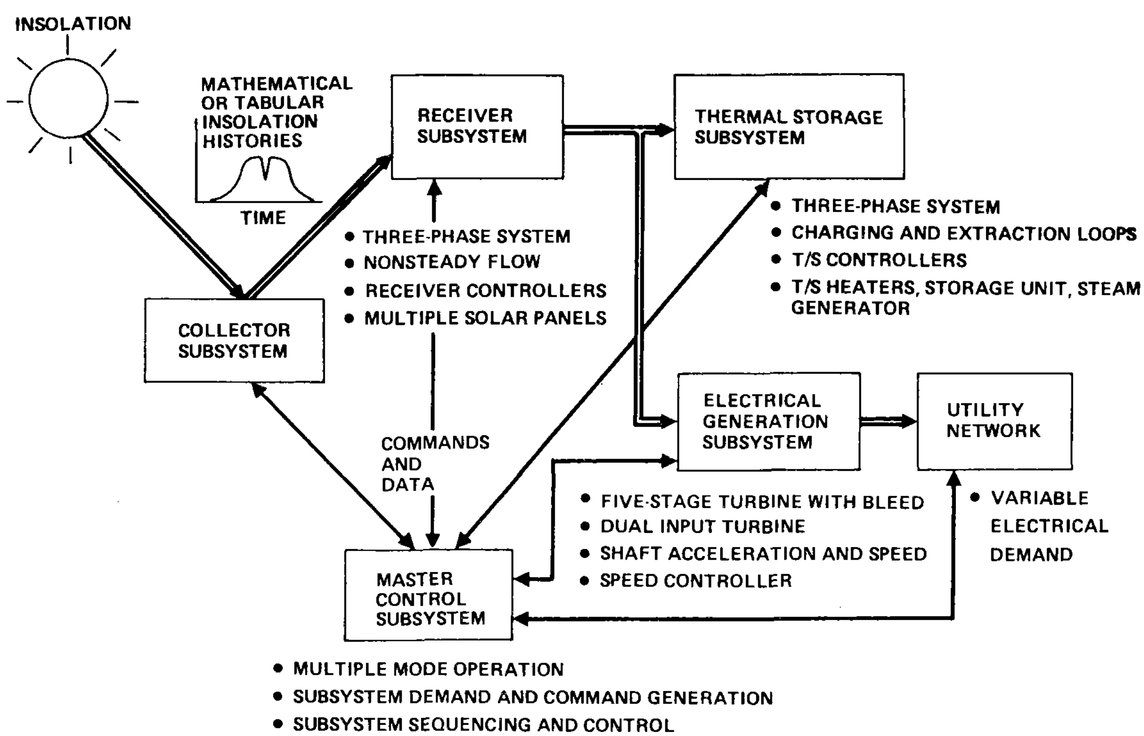

Figure 1. Power Plant System Simulation Functional Schematic

appropriate speed and variable load control systems. The model of the master control subsystem coordinates the independent subsystems providing the appropriate subsystem commands and set points as well as performs the scheduling and sequencing necessary for multiple modes of operation.

System Simulation Flow Diagram

The plant control simulation can be expanded to describe in more detail each subsystem model as well as the manner in which they are coupled together (Figure 2). The receiver model consists of a preheater and boiler sections. Input to the receiver consists of feedwater and an equivalent solar flux on the walls of the receiver panels. Inlet water flow is controlled primarily by means of a temperature control system which senses outlet temperature and regulates the inlet flow by means of a proportional control valve. The boiler section is divided into multiple panels each of which is subdivided into three sections of subcooled water, saturated steam, and superheater steam. The outlet flow from each panel is manifolded and directed either to the thermal storage subsystem or to the turbine. The steam flow to thermal storage is directed through a control valve to a desuperheater which reduces

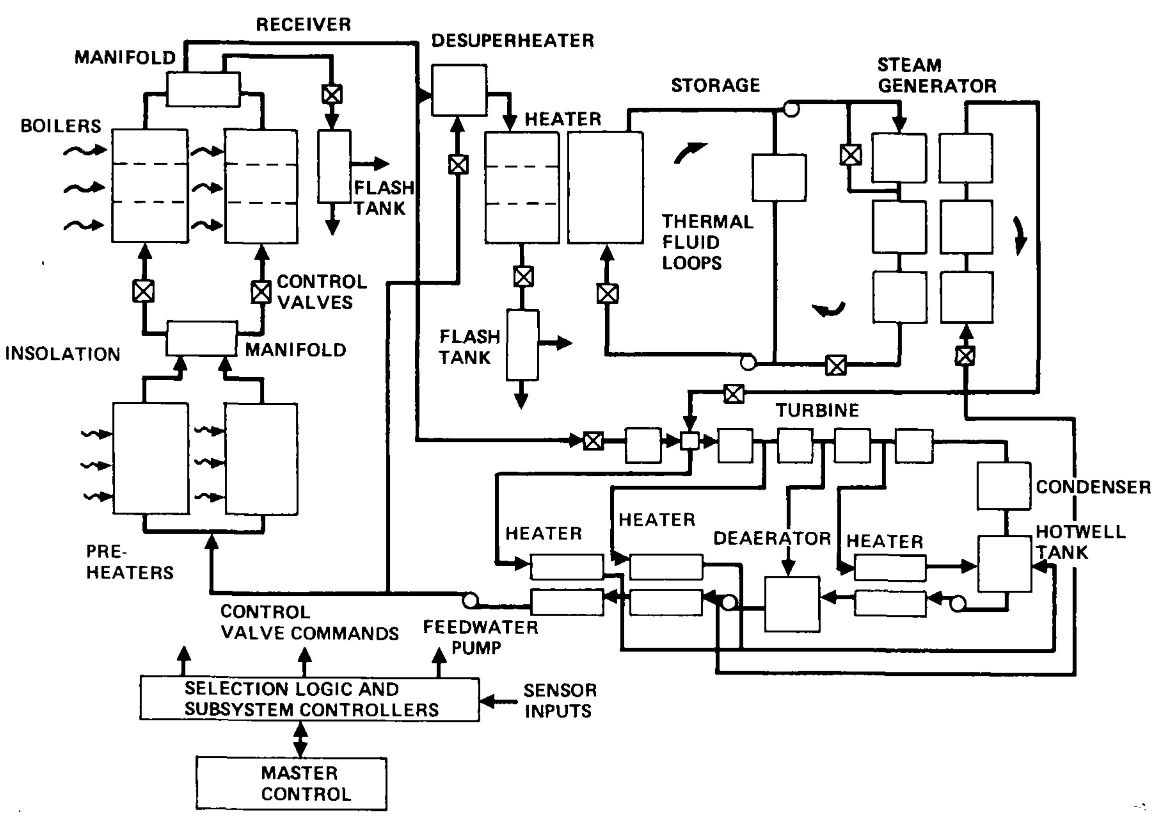

Figure 2. System Simulation Flow Diagram

and regulates the steam temperature to the thermal storage heater. The heater panel is described as a parallel counterflow heat exchanger with circulating oil and driving steam. As in the receiver, the heater is subdivided into superheat, saturated steam, and subcooled liquid sections. The charging loop is completed with models of the controllers, sensors, control valves, pumps, and the thermal storage unit. The extraction loops model consists similarly of the pumps, control valves, controllers and a three-stage generator. The outlet steam is then directed through a control valve which regulates the outlet steam into the secondary admission port on the turbine. The turbine is modeled by a multiple-stage impulse turbine with appropriate bleed ports to the feedwater system. The turbine torque and shaft acceleration are described as a function of the inlet flows and steam conditions at each stage. The feedwater system is modeled as a series of pumps, condenser, deaerator, and feedwater heaters which essentially establish inlet pressure and temperature conditions at the preheater. The master control system model consists of the scheduling and sequencing logic, issues set point commands to controllers, and closes and configures control loops where required. The plant control simulation includes models of all of the major subsystems, hardware components, and control systems which effect system stability and dynamic performance.

Receiver Simulation Model

The receiver simulation model (Figure 3) consists of a preheat panel and a boiler panel which is divided in three variable length sections. Inputs to the receiver are inlet feedwater pressure and temperature, a solar flux history impingent on the panel walls, and the outlet is receiver steam flow at superheated pressure and temperature conditions. The receiver mathematical model is a lumped parameter system which consists of a set of 10 coupled nonlinear differential equation which describes the process. These equations of state describe the dynamics of the process and are derived based on conservation of energy on the wall and fluid, mass balance for non-steady flow and the ideal gas law. The fluid flow equations are based on theoretical flow through nozzles and orifices and include flow losses within the pipes and valves. The insolation is modeled as an equivalent solar flux which is distributed across each of the variable section lengths. The heat balance equations include losses due to both radiation and convection and also incorporate variable convection heat transfer coefficients as a function of flow rate and fluid state. The variable properties of the fluid in terms of enthalpy, specific volume, and saturation temperature and pressure are incorporated into steam tables which are resident within the simulation. The receiver simulation model describes the dynamics of the process in terms of the instantaneous temperature, pressure, flow and fluid masses in each section. Also included are realistic models of the sensors, control valves, and controllers which regulate the process.

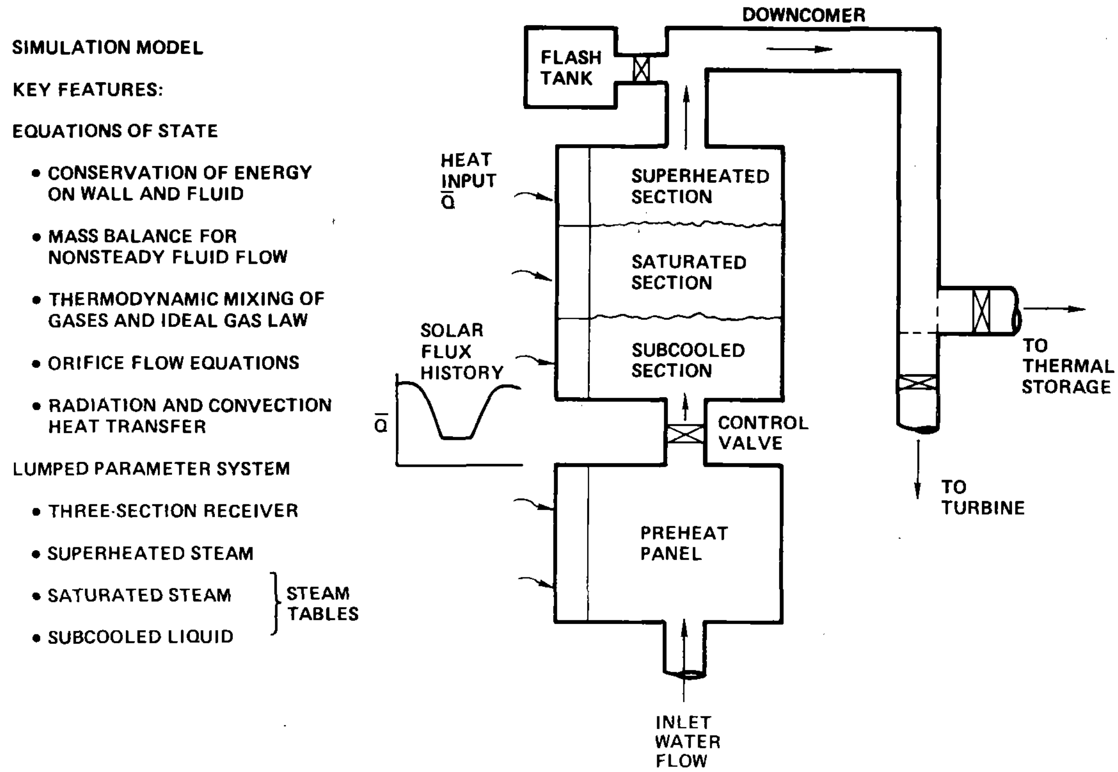

Figure 3. Receiver Simulation Model

Thermal Storage Simulation Model

The thermal storage simulation model (Figure 4) consists of individual mathematical models which describe the physical process in the desuperheater, thermal storage heater, thermal storage unit, and thermal storage steam generator. The level of detail for the simulation is analogous to the receiver in that the model describes the dynamics of the water-steam phase change process. The dynamics of the lumped system temperatures, pressure, flows, and energy states throughout the system are described by a coupled set of nonlinear differential equations. Besides the physical process themselves, mathematical models of the physical hardware such as control valves, sensors, pumps, and controllers are incorporated into the simulation. For example, a control valve is simulated as a second order response system with static flow coefficients which are nonlinear and a function of the valve stroke. Temperature sensors are modeled as first-order time constants and controllers as either analog or digital PID type controllers. Pumps are modeled as differential pressure as a function of flow and speed with appropriate response times.

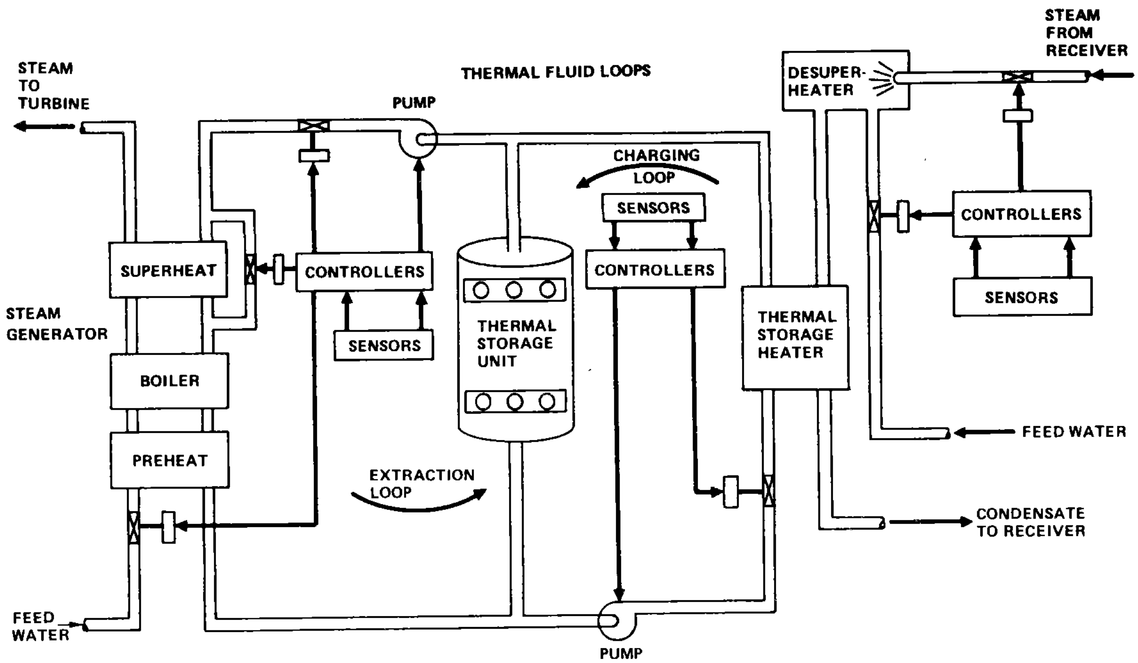

Figure 4. Thermal Storage Simulation Model

The thermal storage simulation model describes the dynamics of both the thermal fluid and steam flow loops as well as the storage device while operating in either the charging or extraction mode or in a combined cycle mode of operation.

Turbine Generator Simulation Model

The turbine generator simulation models a multi-stage impulse stage steam turbine with dual inputs and an electrical power generator. The simulation model (Figure 5) transforms the available energy from a form of steam through an impulse-momentum exchange in the turbine blades into mechanical energy and then into electrical energy in the generator. The model consists primarily of a dynamic torque balance on the turbine generator shaft between the applied torque (impulse-momentum exchange in the turbine blades), the electrical load torque due to the generator, various damping and loss torques due to mechanical, electrical, friction, and flow losses, and the associated time constants within the turbine due to the flow of gas within a constrained volume. The applied torque is modeled as a function of the type of stage, turbine blade geometry, blade efficiencies and the relative velocity between the fluid and turbine blades. The steam expansion through the turbine is modeled as a non-ideal, nearly isentropic expansion through each turbine stage finally exhausting into a constant pressure condenser. The load torque on the turbine shaft when a synchronous load is applied is modeled as proportional to the load output current and the generator phase angle.

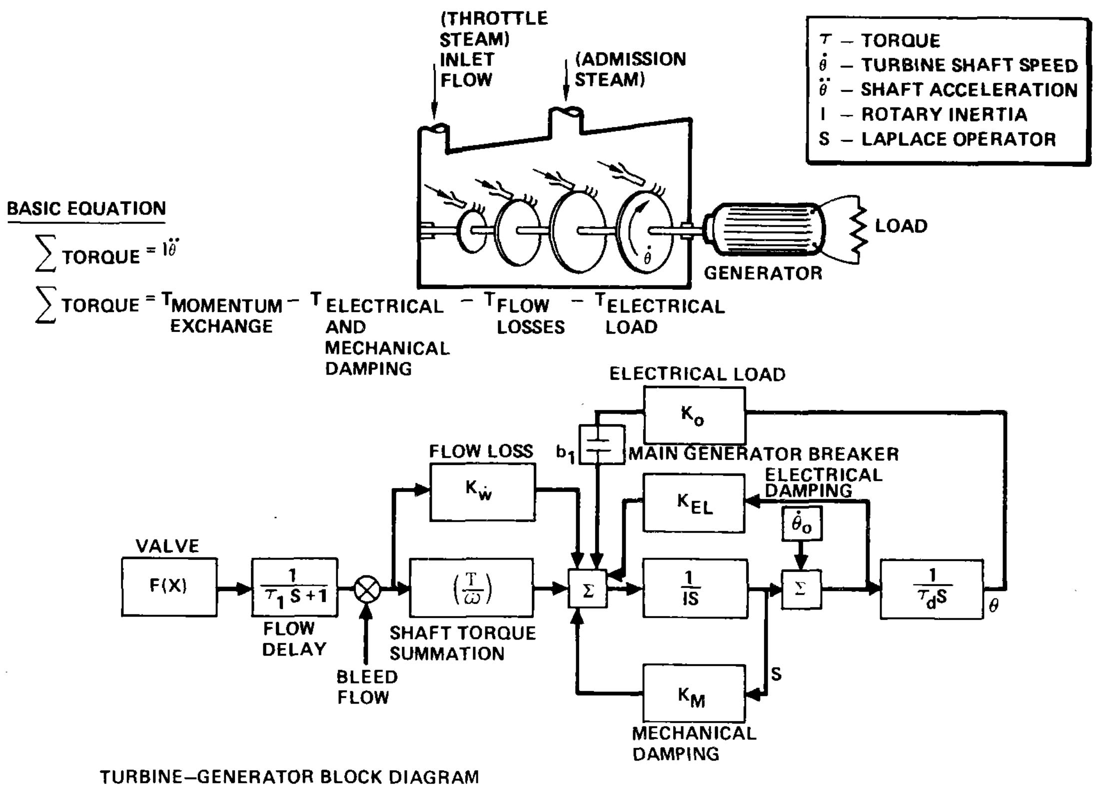

Figure 5. Turbine Generator Simulation Model

Insolation Model

In order to investigate the dynamics of the solar power plant it is necessary to describe the primary insolation driving function. Of particular importance is the short term dynamic response of the system due to cloud passage over the heliostat field (Figure 6). For purposes of the simulation, the insolation is described as an attenuation in solar flux as a function of the relative position between the cloud and the field. For a typical configuration of a north to south passing cloud, the solar attenuation on a typical north, west, and south receiver panel is shown as well as an average of all panels. For example, for a cloud of the approximate size of the field, the north panel flux decreases as the cloud passes over the field, then the west panel sometime later, and finally, the south panel and then a similar sequence, only with increasing flux as the cloud passes by.

The solar attenuation data is derived off line using computer simulations of the total heliostat field for a particular cloud engagement scenario. The data is then reduced to this form, resulting in a realistic model of the insolation on selected segments or individual panels on the receiver.

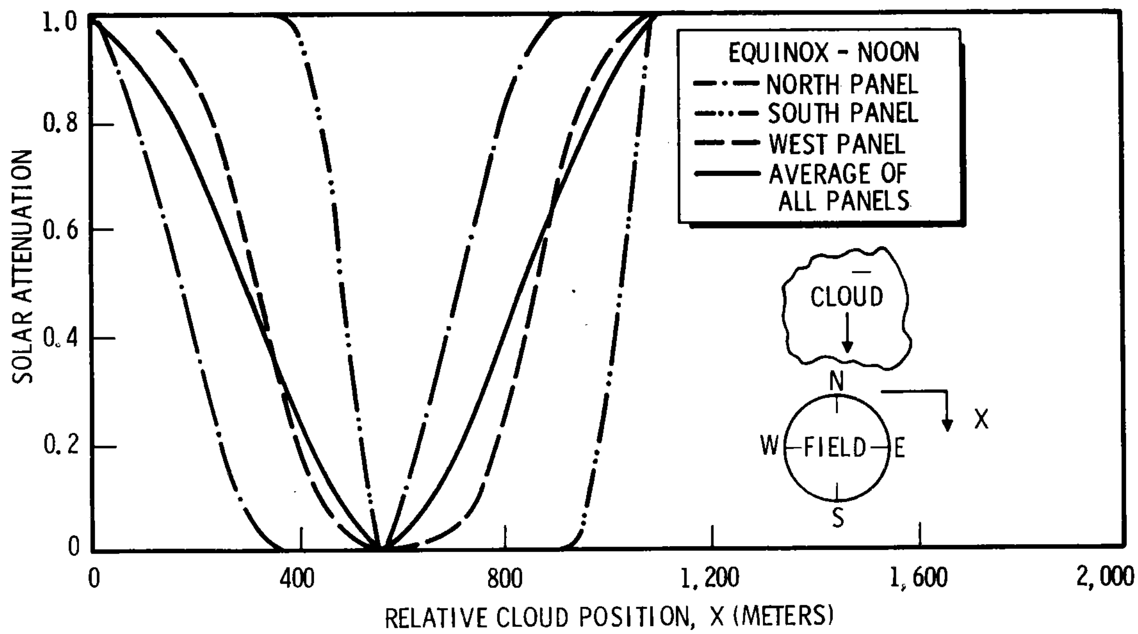

Figure 6. Insolation Simulation Model

Plant Control Simulation Statistics

The plant control simulation is a relatively large simulation (Figure 7). It consists of high fidelity individual models of the receiver, thermal storage, electrical power generation system, and the master control subsystems. The total simulation consists of the nonlinear differential equations with approximately 40 system nodes or states described. The physical hardware simulated consists of 9 valves, 13 sensors, 3 pumps, and 9 controllers. Nonlinear functions in terms of fluid properties and insolation histories consist of 16 functions of one variable and 9 functions of 2 variables.

In order to implement this total simulation model into a hybrid simulation requires the following hardware:

- 2 Applied Dynamics (AD-4) analog computers
- 1 Sigma 5 digital computer
- Peripheral elements such as teletype, line printer cord reader, disc drive, 2 mag-tape units, and 4 8-channel brush recorders

At present, the hardware utilization is at about 50 percent of the hybrid analog capability and 25 percent of the digital capability. The hybrid simulation utilizes 46 integrators, 40 summers, 25 function table hook-ups, a digital program with approximately 2000 Fortran statement, and 24K of storage.

The simulation operates in real time and had taken approximately one year to develop.

SYSTEM EQUATION CHARACTERISTICS

- SUBSYSTEMS SIMULATED – RECEIVER, THERMAL STORAGE, EPGS, MASTER CONTROL
- SIMULTANEOUS SOLUTION OF ≈46 NONLINEAR DIFFERENTIAL EQUATIONS, 40 NODES
- PHYSICAL HARDWARE COMPONENTS SIMULATED – 9 VALVES, 13 SENSORS
- NONLINEAR FUNCTIONS – 16 FUNCTIONS OF ONE VARIABLE, 9 FUNCTIONS OF 2 VARIABLES

HYBRID SIMULATION HARDWARE

- SIMULATION HARDWARE
  - TWO APPLIED DYNAMICS (AD-4) ANALOG COMPUTER, ONE SIGMA 5 DIGITAL COMPUTER
  - TELETYPE, LINE PRINTER, CARD READER, DISC DRIVE, TWO MAG-TAPE UNITS, 4-8 CHANNEL BRUSH RECORDERS
- PRESENT HARDWARE UTILIZATION
  - 46 INTEGRATORS, 40 SUMMERS, 25 FUNCTION TABLE LOOK-UPS
  - DIGITAL COMPUTER PROGRAM, 2,000 FORTRAN STATEMENTS, 23K STORAGE
  - REAL TIME OPERATION, 10 TO 20 ms UPDATE RATE
- TIME TO DEVELOP EXISTING SIMULATION ≈ 1 YEAR

Figure 7. Plant Control Simulation

Typical System Response to a Solar Disturbance

The simulation can be used to generate transient responses in order to evaluate dynamic behavior. Figure 8 demonstrates the capability of the simulation to evaluate the performance of total coupled power plant system. For the purpose of demonstrating this capability, the system is placed in a normal mode of operation with intermittent clouds. The receiver is supplying both primary steam to both the turbine and thermal storage. The steam generator is in a low idle mode and also supplying the turbine. The desired condition is to remain at constant output power independent of the insolation disturbance. For the first case, there is no crossfeed commands from the receiver to the steam generator. The steam generator remains in an idle

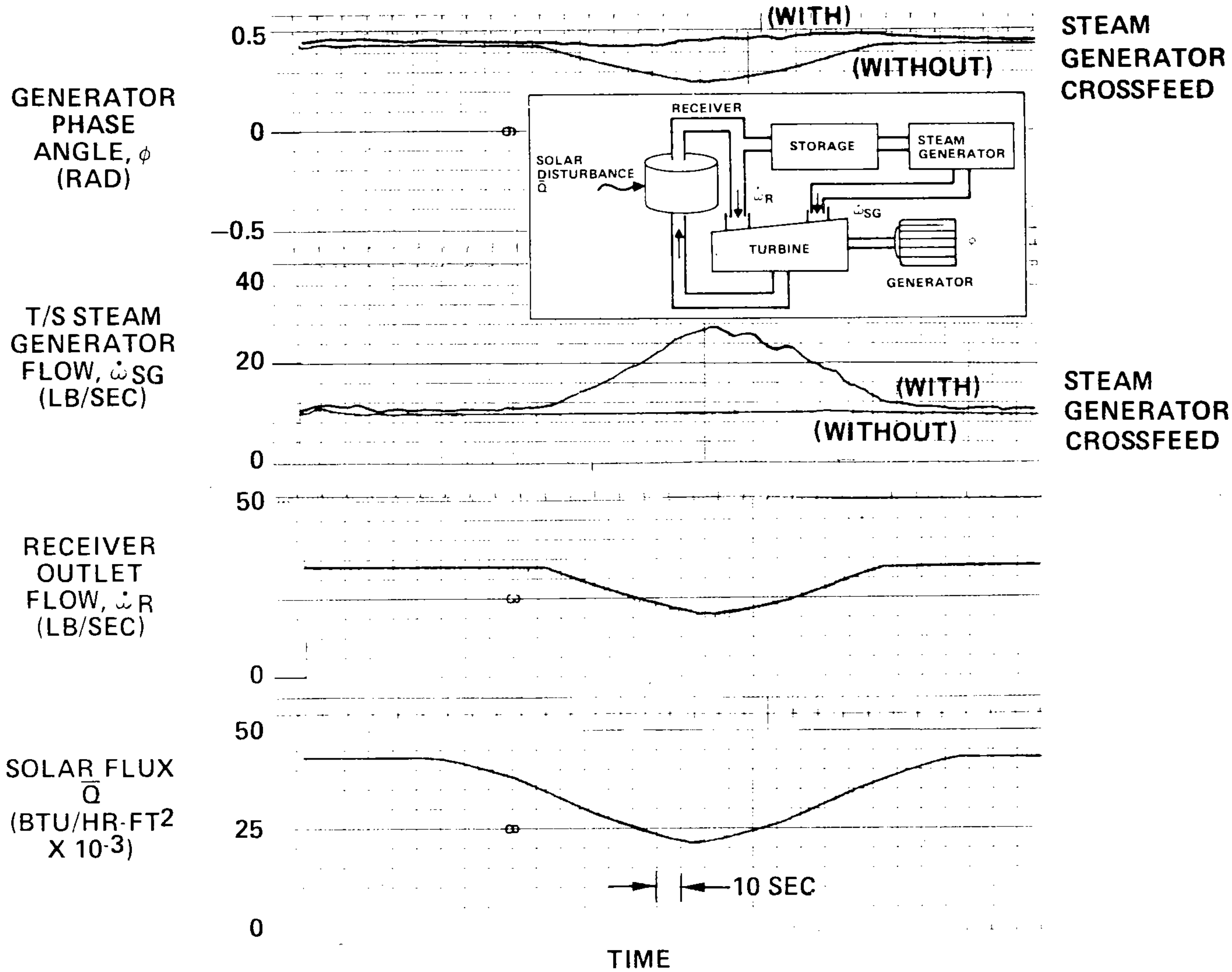

Figure 8. Typical System Response to a Solar Disturbance

mode and the generated output power degrades as the cloud passes over the field. For the second case, the steam generator responds to a crossfeed command and compensates for this loss of power as shown in the figure. These results are presented not to be final design results but are preliminary simulation results designed to demonstrate the capability of the simulation to support the design of plant control. For this selected condition, the response of the steam generator and receiver control systems can be evaluated with respect to some established requirement on output power given a specific insolation disturbance.

Typical Parametric Results Using System Simulation

The system simulation can also be used to define subsystem performance sensitivities and to support parametric analyses. For this configuration, the controllability of the receiver outlet steam temperature is established as a function of cloud velocity for a nominal simulated receiver control system. A cloud with a reference velocity ($\dot{X}$) passes over the heliostat field resulting in a transient degradation in the solar flux impinging on the receiver panels. The receiver control system senses a loss in superheat temperature and reacts to compensate for this loss of power by regulating the inlet feedwater to the receiver to maintain a constant outlet steam condition (Figure 9). Because of the limited response time capability of the receiver control system, the steam outlet temperature varies from the command temperature. This

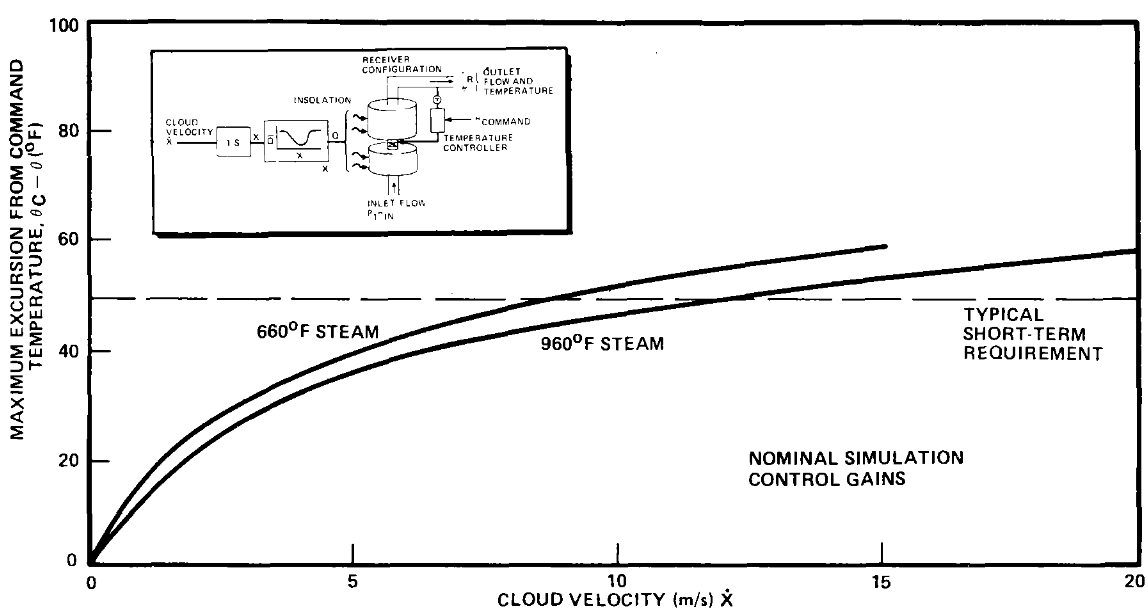

Figure 9. Typical Parametric Results Using System Simulation

maximum variation in outlet steam temperature is then determined by a series of simulation runs each time varying the reference cloud velocity. These results are shown for both rated steam (960°F) and derated steam (660°F) operating conditions. Typical design cloud velocities range up to 20 meters/second. For rated steam input to a turbine, a typical short term requirement on temperature variation is 50°F. For derated steam at 660°F, an acceptable variation in steam temperature is 60°F, which would result in saturated steam in the downcomer. The simulation results are not to be presented as final system design results but only representative of a nominal simulated control system response. Given the requirements, it is through simulation that a need can be established for either a faster response time requirement on the receiver, an alternate approach to receiver control, or a higher temperature operating point in the case of rated steam conditions to meet the requirements.

Simulation Configuration For System Integration Testing

The hybrid simulation (Figure 10) is a valuable tool for use in the design of the plant control system. In essence, the simulation provides the capability to design and verify the performance of subsystem controllers and master control in a realistic simulated environment. Once the system design is completed and transformed into real hardware in terms of the subsystem controllers and real time software algorithms for master control, the real hardware components can be interfaced with the hybrid simulation. This provides a realistic simulated environment for the checkout and verification of the hardware prior to integration into the actual plant. The actual master control computer, software and control hardware can be dynamically exercised in both normal operating modes, mode transitions, and non-nominal operating conditions, including simulated failure modes. This hybrid capability also provides for operator interaction with a simulated plant through the master control system hardware.

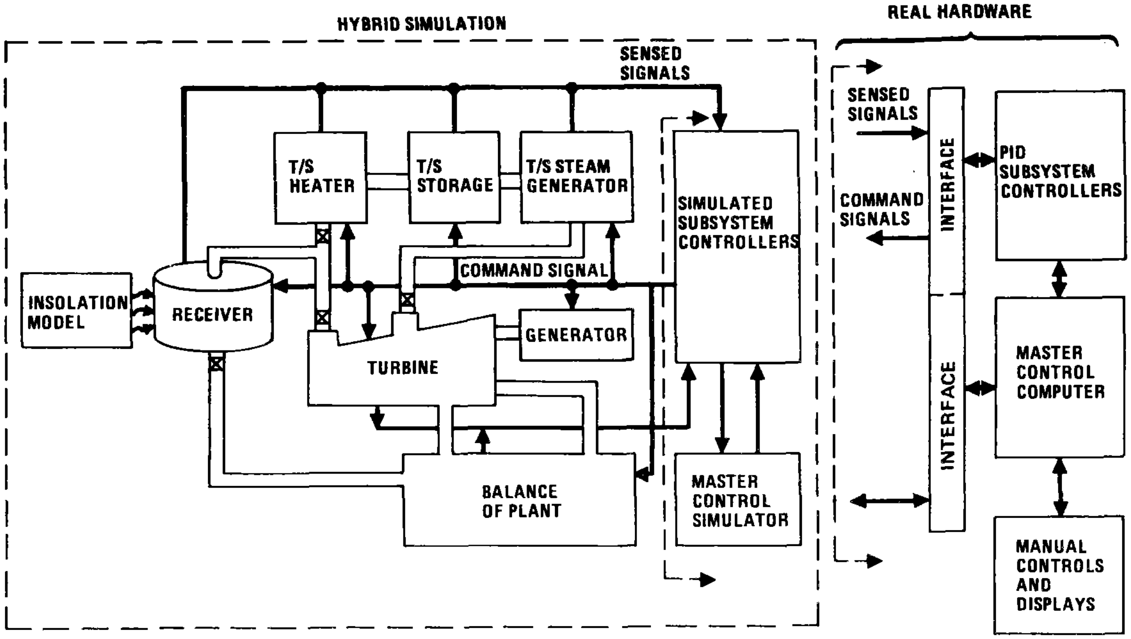

Figure 10. Simulation Configuration For System Integration Testing

Summary

The central receiver plant control simulation is presently operational. The receiver, thermal storage, electrical power generation, and master control subsystems are operational as either independent subsystems themselves or as a total operational coupled power plant system. The results presented in the earlier sections are evidence of that capability.

The simulation is a power tool for the design and performance evaluation of the central receiver power plant. The simulation can be used to support the definition of both top level system performance requirements as well as individual subsystem dynamic performance requirements. It is an effective tool for the design of both subsystems and the overall system, for the design of plant control software, and also for the checkout and verification of plant control hardware and software using the hybrid simulation as a test bed for system integration.

HELIOSTAT MANUFACTURING COST ANALYSIS

Battelle-Pacific Northwest Laboratory

Kirk Drumheller

Introduction

Objectives

The purposes of this study are to:

1. Provide a complete reference list of manufacturing requirements for heliostats.
2. Identify most significant areas for quality and cost improvement (including product design and manufacturing process and equipment development).
3. Provide a base for uniform cost analyses.
4. Identify potential product or manufacturing problems.

This is done by completing a detailed manufacturing analysis which provides materials, labor, equipment, and facility costs for each step in the manufacturing process. In the present analysis, estimates are very preliminary and are intended to provide a format rather than specific numbers.

Manufacturing Requirements--Even though heliostats have been around for centuries, many people not familiar with them feel a degree of uneasiness when heliostat manufacturing is mentioned. The identification of all of the steps involved in making one illustrates the extreme simplicity and lack of unknowns in the process. Hopefully, this will reduce concern on the part of firms considering entry into the field.

Best Areas for Quality and Cost Improvement--The major cost center approach used in the May, 1977, Preliminary Design Reviews[1, 2, 3, 4] identified areas such as the drive and the reflector unit as early possibilities for significant cost improvement. However, identification of sound approaches to such improvements requires a more detailed knowledge of the area.

Uniform Cost Analysis Base--Many estimates of heliostat costs have been made in the past on the basis of rough comparisons in dollars per pound or comparisons with some related structure. While such estimates may indicate a ballpark range, they are not adequate for decision making based on economics. They are also of minimum value in identifying areas for improvement. One primary purpose of the more detailed, but preliminary, analysis provided herein is to establish a framework for future comparisons on the basis of uniform technical economics rather than "feel."

Heliostat designers and suppliers often provided cost summaries with cost centers, as shown in Figure 1. Without detailed backup, it is difficult for an independent observer to evaluate the validity of estimates on the basis of such broad cost centers. However, a skilled production estimator can quickly evaluate an estimate in terms of machine time, operator requirements, and equipment requirements. This is particularly true in the case of heliostats, which are--except for a mirror sandwich--conventional fabrication. Utilizing a uniform format for future cost analyses will simplify comparison.

With a realistic estimate of direct manufacturing costs, individuals or companies can add their normal indirect costs to arrive at a reasonable selling price. Given a specific design, estimates can be made with nearly the same degree of confidence that an estimator would have in preparing a bid to build a building or fabricate a part on a fixed-price competitive basis.

Identification of Potential Problems--The addition of detail to cost center estimates and the development of detailed manufacturing plans will provide a more orderly system for problem identification and resolution.

Approach

The approach to this study has been to develop a program format which, hopefully, includes all of the significant cost elements to be considered in heliostat costing. Reference heliostat designs are then prepared, and the production costs for each reference design are estimated and summarized. For comparison purposes, it is assumed that a single company or operation performs the complete job, from materials procurement through installation and startup of the heliostat field.

4190.1 Collector Equipment

- 4190.11 Reflective Unit
  - 4190.111 Reflective Surface
  - 4190.112 Mirror Backing Structure
  - 4190.113 Heliostat Support Structure
  - 4190.114 Protective Enclosure
- 4190.12 Drive Unit
  - 4190.121 Azimuth or Mirror Module Drive
  - 4190.122 Elevation or Outer Frame Drive
  - 4190.123 Mirrors
  - 4190.124 Positions and/or Limit Controls
  - 4190.125 Emergency Power Supply System
  - 4190.126 Power Distribution Equipment and Wiring (including lightning protection)
- 4190.13 Sensor/Calibration Equipment
  - 4190.131 Sensor Unit
  - 4190.132 Sensor Tower
  - 4190.133 Calibration Equipment
  - 4190.134 Wiring Between Heliostat and Sensor
- 4190.14 Control Equipment
  - 4190.141 Field Control and Electronics
  - 4190.142 Computer Hardware for Heliostat Control (including lightning protection)
  - 4190.143 Signal Distribution Equipment and Wiring
- 4190.15 Foundation and Site Preparation
  - 4190.151 Foundation, Excavation, and Installation
  - 4190.152 Site Preparation
- 4190.16 Design and Engineering Costs
  - 4190.161 Design Costs
    - 4190.1611 Reflective Unit
    - 4190.1612 Drive Unit
    - 4190.1613 Sensor/Calibration Equipment
    - 4190.1614 Control Equipment (including software development)
    - 4190.1615 Foundation and Site Preparation
  - 4190.162 Engineering Support During Manufacturing, Installation, and Checkout
- 4190.17 Packing and Shipping to Plant Site
- 4190.18 Field Assembly, Installation, and Checkout
  - 4190.181 Heliostat and Control Equipment
    - 4190.1811 Field Assembly
    - 4190.1812 Installation and Checkout
  - 4190.182 Sensor/Calibration Equipment
    - 4190.1821 Field Assembly
    - 4190.1822 Installation and Checkout
    - 4190.1823 Calibration
- 4190.19 Lightning Protection

Figure 1. Cost Centers For Heliostat Cost Estimates

Cost Summary

Costs are summarized in the format of Figure 2. This includes all cost items in a business, as summarized on an IRS corporate income tax form. The costs shown in this figure total $100 per square meter for a 40-square meter heliostat, a total of $4,000. They illustrate the cost goals which must be met and can serve as cost element first-cut budget numbers in the program to meet and exceed overall cost goals. In this figure, the

	Per Heliostat, Dollars	Total For 200,000 Heliostats Per Year, $1,000
Gross Profit	1,200	240,000
Other Income	--	--
Total Income		
Gross Receipts, Less Returns		
Gross Receipts, Less Returns and Allowances	$ 4,000	$ 800,000
Less Cost of Goods Sold	2,800	560,000
Gross Profit	1,200	240,000
Other Income	--	--
Total Income	1,200	240,000
Compensation of Officers	50	10,000
Salaries and Wages (not deducted elsewhere)	90	18,000
Repairs	50	10,000
Bad Debts	10	2,000
Rents, Light, and Heat	50	10,000
Taxes		
Interest		
Amortization	225	45,000
Depreciation		
Contributions	20	8,000
Advertizing	10	2,000
Pension, Profit-Sharing, Etc.	80	14,000
Employee Benefit Programs	30	6,000
Other Deductions	30	6,000
Legal and Accounting Fees	30	6,000
Consultants	10	2,000
Travel	40	8,000
Product Development	85	17,000
Total Deductions	800	160,000
Taxable Income	400	80,000
Net After Taxes	200	40,000

Figure 2. Cost Element Summary

direct materials costs, direct labor costs, and fixed charge costs are based on limited analyses. The other numbers are simply to fill blanks at this point. The development of realistic cost element numbers is in progress.

The direct material cost is the biggest single item. This number is based on informal quotations on about half of the materials. It does not provide for process losses, but neither does it provide for improvements. Hence it is within a reasonable range.

Reference Design

The manufacturing analysis will use a specific reference design. Where the same components or subassemblies will be a part of two or more designs, duplication of the analysis for the component or subassembly is not required.

The very preliminary analysis used here as an example is based on a McDonnell Douglas design.[4] It is emphasized that the analysis is not complete enough for the numbers to be used for anything other than illustration of a format.

Electrical design, power distribution, controls, and lightning protection are not included in this preliminary analysis example. The items covered account for approximately 85 percent of the cost of the installed heliostat field.

This preliminary analysis does not go back to basic materials production. Future studies should consider analyses of the processes for specialized materials such as very thin, low iron glass.

Assumptions

Typical assumptions for the operating conditions to be used in the manufacturing analysis are shown in Figure 3. The "Man-Hours Per Heliostat: of Figure 3 is used to determine the paid man-hours. The detailed manpower estimates are based on the number of men required to operate a step, using the 1512 man-hours per shift from Figure 3 and assuming that a second man is required if the piece rate exceeds 1512. If one man is required, he is paid for 2080 hours. This is generally conservative because, in practice, parts of men at a step may be used for other operations.

Parts List

Parts lists are prepared for each subassembly. These refer to the drawing number for details and summarize material requirements. All basic materials requirements can be obtained from the parts lists.

Production Rate 200,000 Heliostats/Yr (approximately 1,000 MWe/Yr)

Operating Efficiency	90%
MH Per Work Day	7
Work Days Per Year	240

Hrs/Yr = 240 Days/Yr x 7 MH/Day x .90 Operating Efficiency - 1512 mhr/Yr Shifts

Operation Shifts Per Day	2
Hr/Yr, Two Shifts	3024

Operating Yields and Quantity Requirements

	Loss	Required Per Year	Required Per Hour
Mirror Assembly	1%	203,000	67.13
Reflector Assembly	.5%	201,000	66.47
Finished Heliostat		200,000	66.14

Man Hours Per Heliostat

Use 52 x 40 mh/yr = 2080 mh/yr paid

For 200,000 Heliostats, 1 man = $\frac{2080}{200,000}$

= 0.014 mh/heliostat

One man on each of 2 shifts is 0.0208 mh/heliostat

Figure 3. Operating Assumptions

Parts lists will ultimately be prepared on each of the components in Figure 1. However, the initial analysis is done only on the more significant items. A typical parts list is shown in Figure 4. The basic materials costs in this estimate are based on telephone quotations, except where noted as an allowance, and are considered reasonable.

A significant point apparent in examining parts lists is that the most significant materials costs are readily visible. Since materials costs are the most significant item in the heliostat cost, the parts lists alone provide identification of potential targets for cost reduction.

Process and Equipment Description

A reference process is described for the production of the reference design. An example flow sheet for fabrication of the mirror sandwich is shown in Figure 5.

PART NO.	ASSEMBLY	PART DESCRIPTION	BASIC MATERIALS UNIT COST	ASSEMBLY COST
R-1	1	TORQUE TUBE, 10.75 OD x .250 WALL x 206.25 lg 10" STANDARD LOW CARBON STEEL PIPE	$ 623/C FT	107.21
R-2	2	DRIVE ATTACHMENT FITTINGS, 1" x 2" x 36" MILD STEEL	4.57	9.14
R-3	2	RING FLANGES, INBOARD, 0.188" THICK, 10.5" D APPROX	2.43	9.72
R-4	2	RING FLANGES, OUTBOARD, 0.188" THICK, 14" D APPROX.		
R-5	2	CROSS BEAMS, INBOARD 11 g (0.120") GALV. LOW CARBON STEEL SHEET, 14" DEEP x 215.50" lg (APPROX. 20" x 215.50" FLAT PATTERN)	31.27	62.54
R-6	2	CROSS BEAMS, OUTBOARD, SAME AS ABOVE	31.27	62.54
		BOLTS, 0.75 D x ALLOW		2.00
		MISC. - WELDING ROD, GAS, ELECTRICITY, ALLOW		5.00
		TOTAL		258.15

Figure 4. Typical Parts List

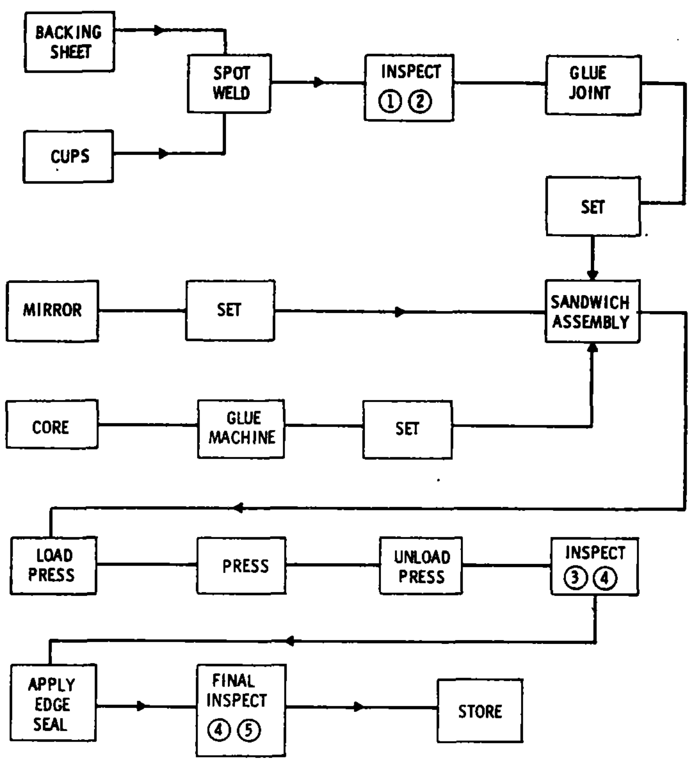

INSPECTION TYPES

1. STATISTICAL ULTRASONIC
2. STATISTICAL DESTRUCTIVE STRENGTH
3. ULTRASONIC
4. VISUAL
5. STATISTICAL DESTRUCTIVE TEST

Figure 5. Example Process Flow Sheet - Mirror Assembly

Process Description--For example purposes, the process for core blanks, parts M-1 and M-2, is described below.

Receive

Forklift - bundles 5 ft high, 2 deep - 60", 30 x 2 = 60 per pallet; move 30 pallets per hr - 30 x 60 = 1800 per man, 1 man-hours per shift.

Inspect

Flatness and dimensional, primarily optical with roller feed, machine rate, 20 per minute, 20 x 60 = 1200 per hr.

Integrity, ultrasonic and radiograph--combine with flatness and dimensional. Spares provided in components only.

Chemical analysis and dimensional stability, statistical checks. Destructive tests, microwave heating, outgas sampling, bending, and heating.

Store

20 working days storage, 30 heliostats per pallet

$$\frac{200{,}000 \text{ H/yr}}{240 \text{ work days/yr}} = 833 \text{ H stored} = \frac{833}{30} = 28 \text{ pallets stored,}$$

$$200 \text{ ft}^2 \text{ per pallet, 3 deep} = \frac{28}{3} \times 200 = 1866 \text{ ft}^2\text{--use 2000}$$

Clean

Vacuum cleaner to suck off loose plastic particles with roller feed.

Equipment Description--A preliminary description of equipment for the mirror assembly follows:

Weld Cups

Spot welder, mechanized to automatically feed backing strips and cups, place them, and weld 6-8 spots simultaneously.

Set Mirror

Automatic transfer of mirror to flat surface for setup, positioning, and vacuuming surface to be glued.

Glue Core

Plywood core type gluer to automatically feed core pieces to set of rollers which apply glue to both sides of core.

Set Core

Catcher to collect, assemble, and locate glued cores on mirror.

Glue Backing

Machine to apply glue to backing strip to be glued.

Manpower, Equipment, and Space Requirements

Manpower--Manpower requirements for manufacturing operations are estimated in the Manufacturing Cost Worksheets as illustrated in Figure 6. These forms are also used for the tabulation of equipment requirements and floor space requirements. For this preliminary analysis, estimates are mostly simply judgments of one individual. As work progresses, it is expected that the numbers will be converted to actual requirements based on more specific process and equipment descriptions.

In Figure 7 the direct labor man-hours from these worksheets are summarized, along with the direct materials costs from the parts lists.

Equipment--Equipment cost estimates from the Manufacturing Cost Worksheets are summarized in Figure 8. For the initial analyses, the estimates of tooling and equipment costs are also very preliminary. These costs can vary greatly with conceptual design, refined process requirements, the ingenuity of the designers, and with time. Hence they should be used only with the thought that individual equipment item costs may vary by a factor of five or more, and the overall may vary by a factor of three or more. However, it should also be noted that large variations in the cost of equipment will not overly affect the cost of the product.

Space Requirements--Space requirements are established using the Manufacturing Cost Worksheet equipment space estimate and the in-process storage space estimate (see Figure 9 for example). These are incorporated into a plant layout as shown in Figure 10. The layout of Figure 10 is for the mirror assembly plant only. The estimated space requirements for each piece of equipment in the Manufacturing Cost Worksheets and estimated in-process storage requirements are incorporated into the layout along with provision for aisle space and a reasonable work flow.

PART NO. M
NO. PER ASSEMBLY 1
NO. PER HELIOSTAT 6
HELIOSTATS PER YEAR 200,000
OUTPUT FROM STEP. HEL. 200,500

PART NAME MIRROR ASSEMBLY
OUTPUT FROM STEP, PCS/HR 398 - 1,203,000
NET YIELD .99
STARTING NO. PER YR. 1,218,000
STARTING NO. PER HR. 404

PAGE NO.
PREPARED BY
DATE

OPERATION	REQUIRED THRUPUT PCS/HR.	PIECES PER HR. PER MACH.	REJ. RATE %	MACH. REQ. MIN.	SPARE	TOTAL	MACH. COST PER MACH.	TOTAL	NO. OPER. PER SHIFT	MAN HRS./ HELIO	FLOOR SPACE PER MACH.	TOTAL	OTHER (MATERIALS, TOOLING, ENERGY)
WELD CUPS	1616	300		6	1	7	200	1400	6	1248	200	1400	
FEED PARTS	-	-		1					2	.0416	-	-	
SET MIRROR	404	240		2	1	3	200	600	2	.0416	500	1500	
GLUE CORE	1616	920		2	1	3	300	900	2	.0416	500	1500	
SET CORE	1616	920		2	1	3	300	900	2	.0416	500	1500	
GLUE BACK'G	808	480		2	1	3	100	300	2	.0416	300	900	
SET BACKING	808	480		2	1	3	100	300	2	.0416	200	600	
LOAD PRESS	404	240		2	1	3	250	750	2	.0416	500	1500	
PRESS	404	240		2	1	3	1000	3000	2	.0416	300	900	
UNLOAD PRESS	404	240	-	2	1	3	250	750	2	.0416	500	1500	
INSPECT	404	800	1	1	1	2	2000	4000	2	.0416	500	1000	
									SUBTOTAL			12,300	

Figure 6. Manufacturing Cost Work Sheet (Manpower, Equipment, Space Requirements)

	DIRECT MATERIAL $	DIRECT LABOR MH	DIRECT LABOR $ AT $10/MH	TOTAL DIRECT $
MIRROR ASSEMBLY	440.46	3.0	30.00	470.46
REFLECTOR SUPPORT STRUCTURE	258.15	3.0	30.00	288.15
DRIVE, ALLOW	500.00	-	-	700.00
PEDESTAL	94.79	1.0	10.00	104.79
FOUNDATION	74.25	0.5	5.00	79.25
CONTROLS, ALLOW	500.00	-	-	400.00
POWER SUPPLY, ALLOW	300.00	-	-	200.00
INSTALLATION, ALLOW	100.00	2.0	20.00	120.00
	2,267.75		95.00	2,362.65
INDIRECT MANUFACTURING EXPENSE, ALLOW				500.00
				2,862.65

Figure 7. Summary - Direct Materials and Labor Costs Per Heliostat

	EQUIPMENT FIRST COST, $1,000
MIRROR PANEL ASSEMBLY	
ASSEMBLY	11,950
CORE BLANKS	3,750
MIRROR	7,250
BACKING SHEET	1,700
BACKING SHEET	1,500
CUPS	2,800
SUBTOTAL	28,950
REFLECTOR SUPPORT STRUCTURE	
ASSEMBLY	11,750
TORQUE TUBE	1,350
DRIVE ATTACHMENT FITTINGS	2,200
RING FLANGES	1,750
CROSS BEAMS	2,900
SUBTOTAL	18,375
PEDESTAL	
ASSEMBLY	4,600
TUBE	1,000
RING	650
SUBTOTAL	6,250
FOUNDATION	3,300
FIELD INSTALLATION	9,000
DRIVE, CONTROLS, POWER SUPPLY, ALLOW FOR LOCAL	8,000
ASSEMBLY	5,000
TOTAL, DIRECT MANUFACTURING EQUIPMENT	$ 73,875

Figure 8. Manufacturing Equipment Cost Summary

PART NO.	PART DESCRIPTION AND CALCULATION	FLOOR SPACE PER 1,000 (ft^2)	QUANTITY PER HOUR	HOURS OF IN PROCESS STORAGE	IN PROCESS STORAGE QUANTITY	IN PROCESS STORAGE SPACE, Ft^2
M-1 AND M-2	CORE BLANK, USE 2x85 x 114, STACK 10' HIGH, 6 PER FT., 60 HIGH, 60 ÷ 1000 - 17 STACKS x 7 x 10 - 1190 ft^2/1000	1190	404	4	1616	1923
M-3	MIRROR, .125 x 85 x 114, ON EDGE, WITH SPACER, USE .250, 4/", 48/ft, 85 HIGH, 10 ft LONG, 48÷100 - 20 ft x 10 ft	200	404	4	1616	323
M-4 AND M-5	BACKING SHEET, .022 x 38 x 48 x 114, USE .022 x 86 x 114, 12/.022 - 545/ ft, 545 ÷ 1000 x 2 ft, SAY 4 ft x 10 ft	40	404	4	1616	65
M-6	CUPS .064 x 10" D	5	1616	4	6464	33

Figure 9. In Process Storage Mirror Assembly and Components

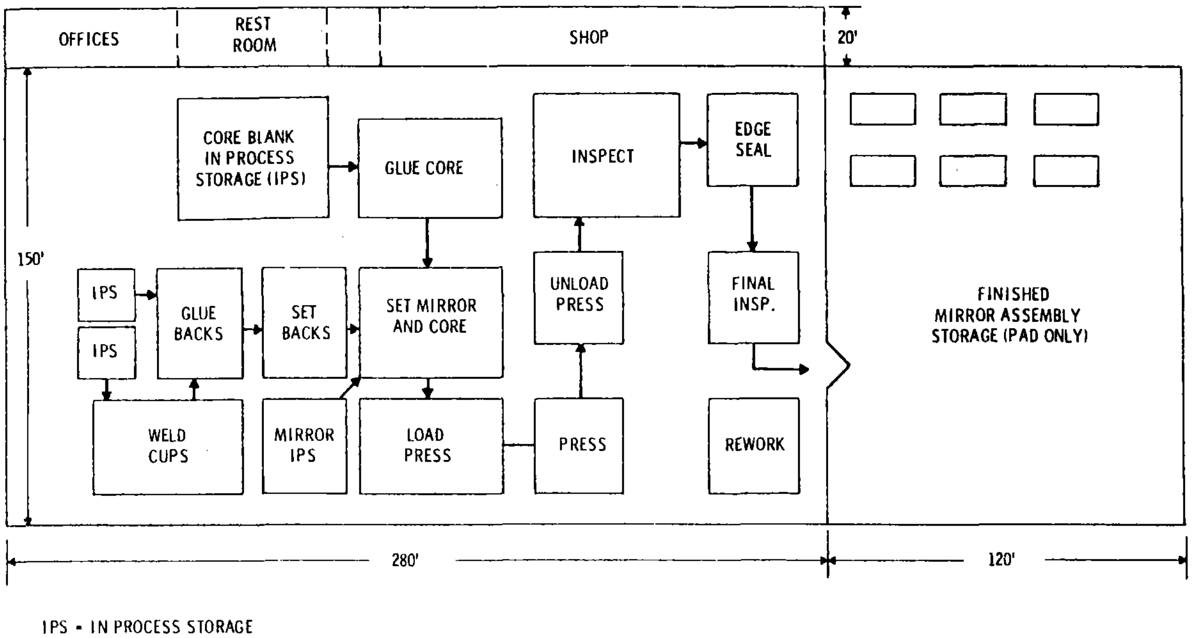

Figure 10. Mirror Assembly Plant Layout

People Summary

A typical manufacturing organization is shown in Figure 11. A reference total organization is shown in Figure 12. These are used with the estimates from the manufacturing cost worksheets to estimate the number of manufacturing people and the number of total organization people. These are summarized in Figure 13. Typical salaries are applied and used in the total cost summary, Figure 2.

Supporting Facilities

Based on the manufacturing requirements and the total organization, requirements are made for supporting facilities such as offices, office equipment, parking lots, and compressed air, steam, water, and electrical supply, and chemical storage and distribution. These estimates are included in Figure 14, Building Requirements. The supporting equipment shown in Figure 15 for this preliminary analysis is a judgment estimate.

Capital Cost Summary

Capital cost estimates are summarized in Figure 16. Based on fixed charges of 15 percent, the cost of capital per heliostat in this rough estimate is $225. This value is used in Figure 2 to cover amortization, depreciation, and taxes other than income taxes.

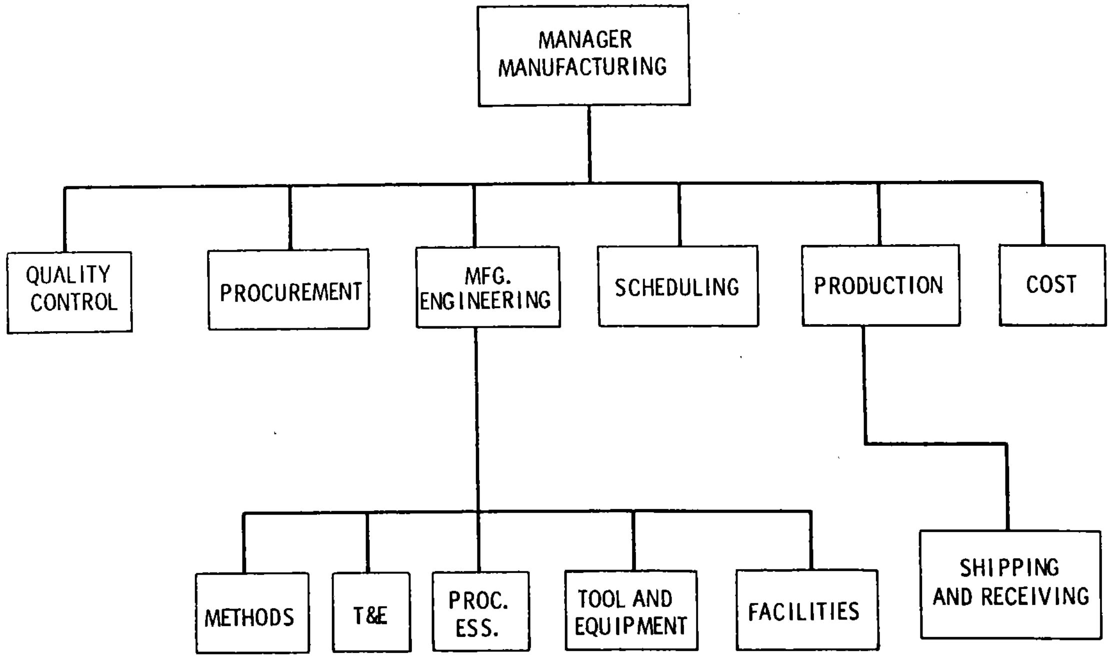

Figure 11. Manufacturing Organization

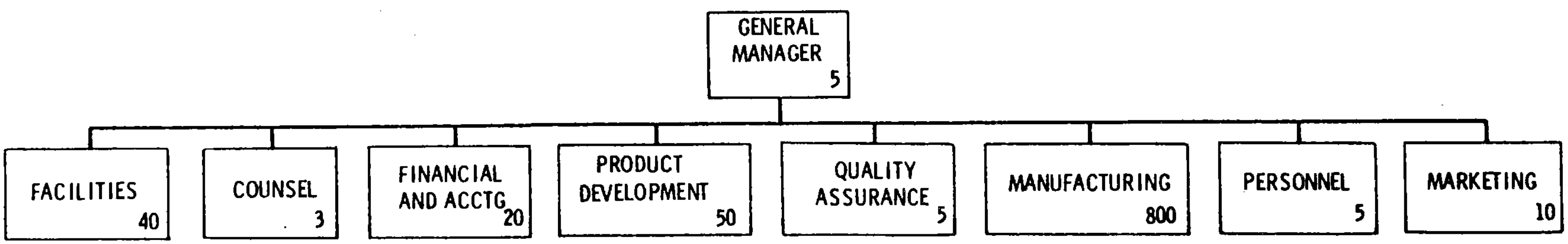

Figure 12. Total Organization

DIRECT MANUFACTURING		
MIRROR ASSEMBLY		
ASSEMBLY		33
CORE BLANKS		7
MIRROR		7
BACKING SHEET		8
BACKING SHEET		9
CUPS		6
	SUBTOTAL	70
REFLECTOR SUPPORT STRUCTURE		
ASSEMBLY		28
TORQUE TUBE		10
DRIVE ATT.		10
RING FLANGES		6
CROSS BEAMS		9
	SUBTOTAL	63
PEDESTAL		
ASSEMBLY		10
TUBE		12
RING		6
	SUBTOTAL	28
FOUNDATION		7
FIELD INSTALLATION		30
OTHER		200
	TOTAL DIRECT	398
INDIRECT MANUFACTURING		
MANUFACTURING SUPERVISION		20
MANUFACTURING MANAGEMENT AND ADMINISTRATION		10
MAINTENANCE		30
QUALITY CONTROL		30
PROCUREMENT		15
MANUFACTURING ENGINEERING		15
SCHEDULING		5
COST		5
	TOTAL INDIRECT MANUFACTURING	130
SUPPORTING PERSONNEL		
GENERAL MANAGER		5
COUNSEL		3
FINANCE		20
PERSONNEL		5
MARKETING		10
FACILITIES		40
	TOTAL SUPPORTING	83

Figure 13. Number of People Summary

	FLOOR SPACE (ft^2)	WAREHOUSE	PAD (ft^2)	OFFICE
MANUFACTURING (INCLUDES PROD, OFFICES, MAINTENANCE, AND SHOP)				
MIRROR ASSEMBLY, 170 x 280				
REFLECTOR SUPPORT STRUCTURE				
DRIVE				
PEDESTAL				
FOUNDATION				
CONTROLS				
POWER SUPPLY				
COMPONENT ASSEMBLY				
INSTALLATION				
ENGINEERING				
ADMINISTRATION				
SERVICES (STEAM, AIR, WATER, ELEC.)				
	500,000	150,000	150,000	80,000
UNIT COST, $/FT^2				
TOTAL COST				
TOTAL				

Figure 14. Building Requirements

	COST
QUALITY CONTROL	10,000,000
MAINTENANCE	10,000,000
PRODUCT AND PROCESS DEVELOPMENT	3,000,000
ADVANCED ENGINEERING	5,000,000
TOTAL	28,000,000

Figure 15. Support Equipment

	COST (Thousand $)
LAND AND BUILDINGS	80,000
EQUIPMENT	180,000
SUPPORT FACILITIES	40,000
TOTAL	300,000
AT 15% FIXED CHARGES, COST PER YEAR IS	45,000,000
COST PER HELIOSTAT IS $\frac{45,000,000}{200,000}$ \$225	

NOTE THAT SUMMARY DOLLARS MAY EXCEED INDIVIDUALS BECAUSE OF DIFFERENT ASSUMPTIONS, CONTINGENCIES, ETC.

Figure 16. Capital Cost Summary

References

1. Central Receiver Solar Thermal Power System Preliminary Design Report, SAN/1111-8, Boeing Engineering and Construction Company, April 29, 1977.

2. J. C. Powell, Solar Pilot Plant, Phase 1, Preliminary Design Report, SAN/1109-8, Honeywell Incorporated, May 1, 1977.

3. Central Receiver Solar Thermal Power System, Phase 1, Preliminary Design Report, SAN/1110-77-2, Martin Marietta Corporation, April 1977.

4. Central Receiver Solar Thermal Power System, Phase 1, Pilot Plant Preliminary Design Report, SAN/1108-8, McDonnell Douglas Astronautics Company, November 1977.

HELIOSTAT DEVELOPMENT FACILITY

Sandia Laboratories, Livermore

W. G. Wilson

An area has been designated at Sandia Livermore for a Heliostat Development Facility (HDF) to be used for evaluating components, control systems, and complete heliostats. In addition, testing techniques, measurement systems, and materials data will be developed.

Objective

In general, the intent is to provide a dedicated facility for the systematic improvement of heliostat cost/performance. As such, the facility will be used to check the feasibility of new concepts, test design improvements, develop evaluation instrumentation, and establish the minimum requirements necessary for adequate heliostat performance.

This facility is intended for heliostat features in the early stages of evolution, as opposed to the comparative type of testing conducted at the STTF on prototype heliostats. Substantial interaction between the conceptualization of ideas and the trying out of hardware is intended at the HDF. It is expected that frequent modification will be made to the hardware being tested, the evaluation instrumentation being used, and indeed, the test objectives themselves. These multi-degrees of freedom are intended to speed the development of all aspects of heliostat technology. As feasibility is established at the HDF, the information will be provided to contractors, other test facilities, and utility users.

Status

Heliostats of four different designs have been installed at the facility. These heliostats were fabricated and tested by their developers (Boeing, Honeywell, Martin Marietta, and McDonnell Douglas - Figures 1 through 4 respectively) under Pilot Plant Phase I subsystem research experiment contracts. The Martin Marietta heliostat shown in Figure 3 has subsequently had nine new facets installed, and the MDAC design has had the laminated mirror facets replaced by foam-backed designs. These heliostats will be used to gather extended field operational test data and to identify potential degradation mechanisms unique to each design. We intend to operate these heliostats simultaneously for approximately 1000 hours of automatic tracking. They will be exposed to identical environmental conditions which will be recorded and correlated to beam flux distribution and pointing accuracy. Although this activity does not correspond exactly with the stated intent of the facility, these designs represent the state-of-the-art, and hence a logical point of departure.

Two large screens have been installed to serve as targets for the heliostats. Each target measures 24 by 28 feet and is elevated 6 feet above the ground. The slant ranges to the targets are approximately 600 and 1200 feet. The 600-foot range is for the Boeing and the McDonnell Douglas designs; the 1200-foot range is for the Honeywell and Martin Marietta heliostats. Figure 5 shows a view of the targets from the heliostats. Figure 6 gives a better perspective to the heliostat arrangement and shows the position of the control equipment trailer in the rear.

A digital radiometric measurement system has been designed for the performance evaluation of heliostats at the HDF. Figure 7 shows a schematic of the concept. In operation, sunlight incident on the heliostat under test is reflected onto one of two large targets, where the image is recorded by a video camera. The output of the camera is fed to a digitizer which breaks the video frame into a 100 x 100 point array and assigns one of 256 gray levels to each point. This data is temporarily stored within the digitizer for input into a computer at compatible rates. Digitization of the complete video frame is accomplished in 67 ms. A pyrheliometer and photodiode mounted on the target provide continuous calibration of the system while additional inputs furnish data on wind speed, wind direction, temperature, relative humidity, and solar radiation.

Continuous video taping of the camera output and subsequent transfer to video disc will allow frame-by-frame analysis of the heliostat image in the case of high-frequency phenomena (e.g., high wind gust conditions). Further flexibility will be provided by an image analyzer system which will present a real time pseudo-color representation of iso-intensity contours and an isometric projection of beam intensity for immediate analysis. Other techniques

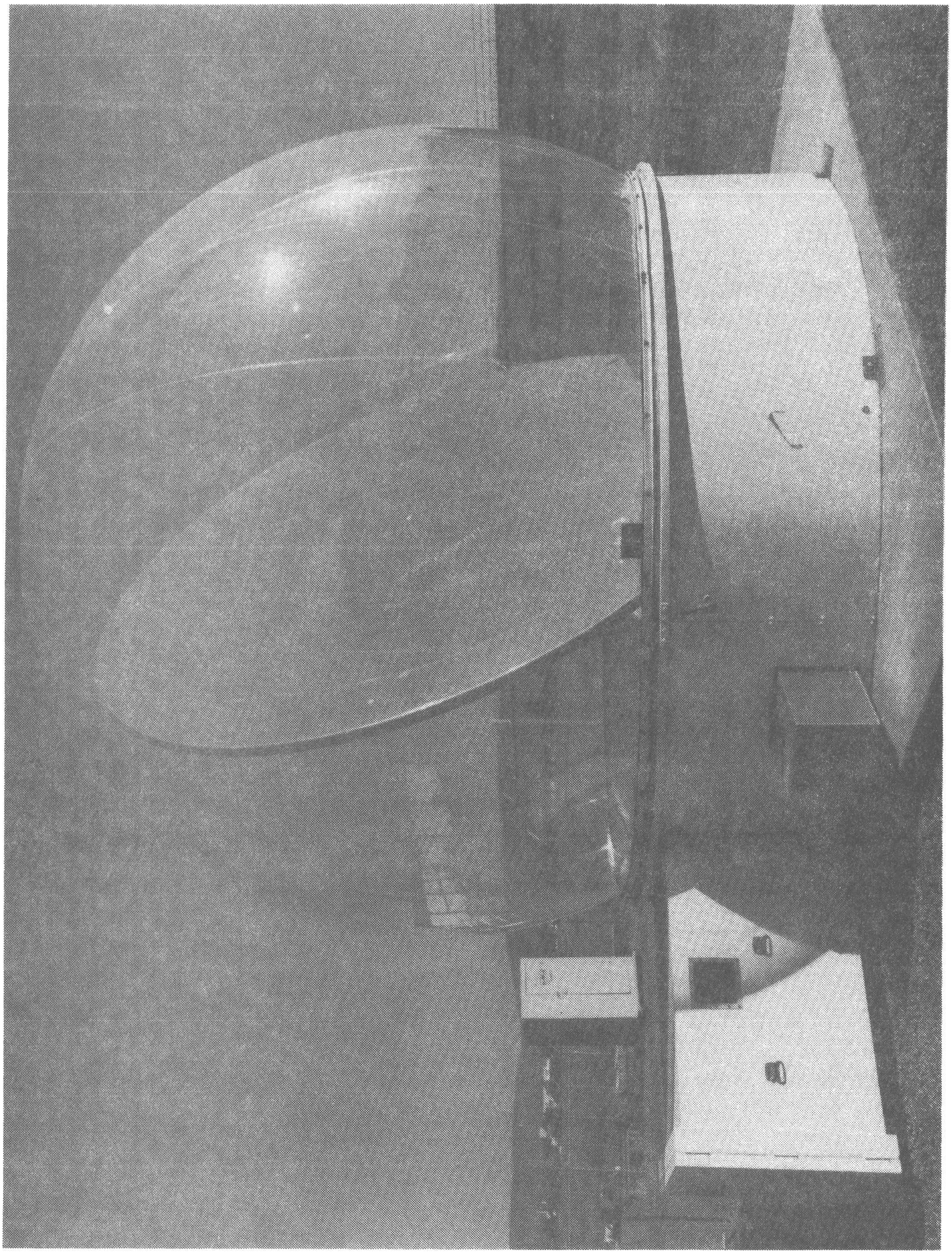

Figure 1

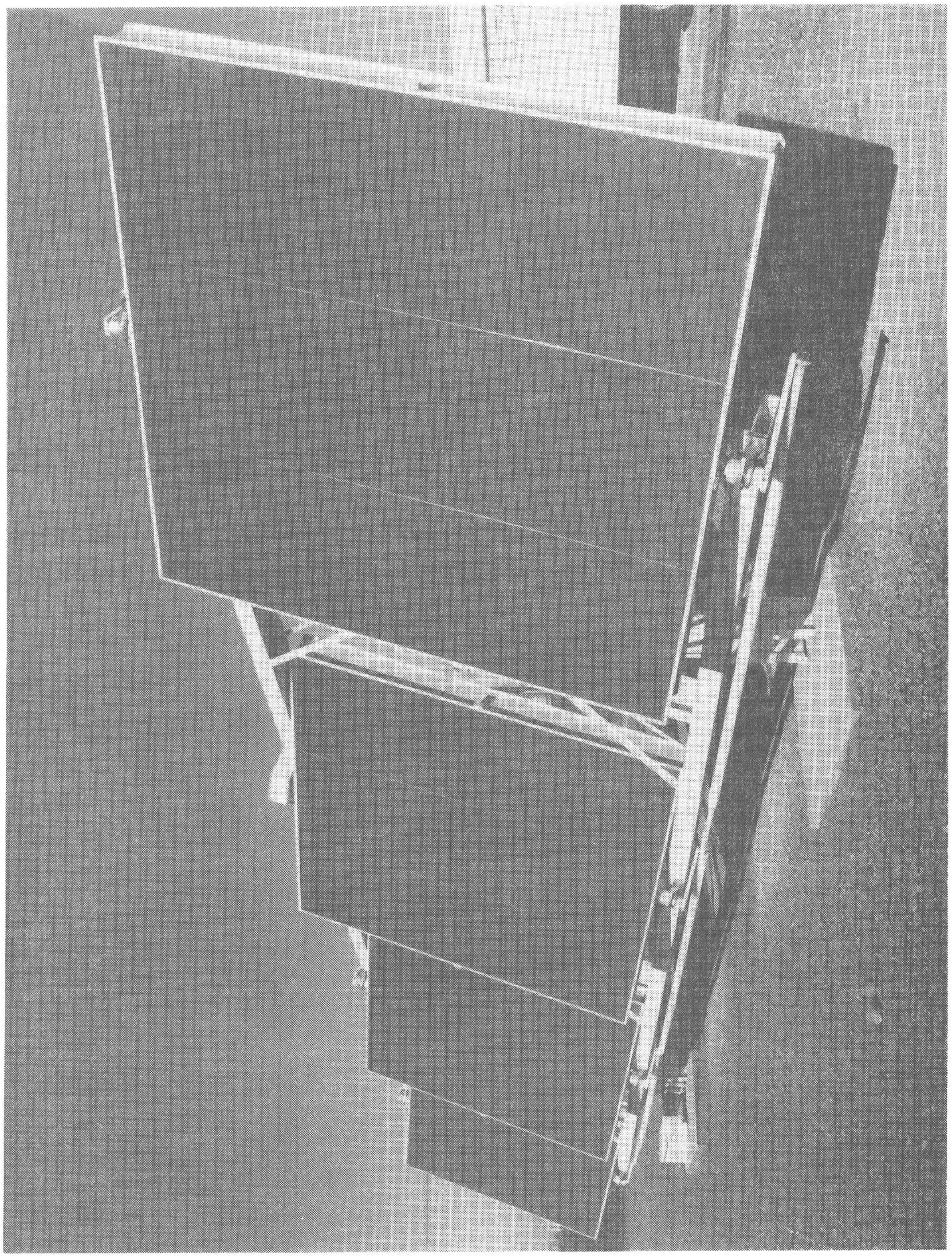

Figure 2

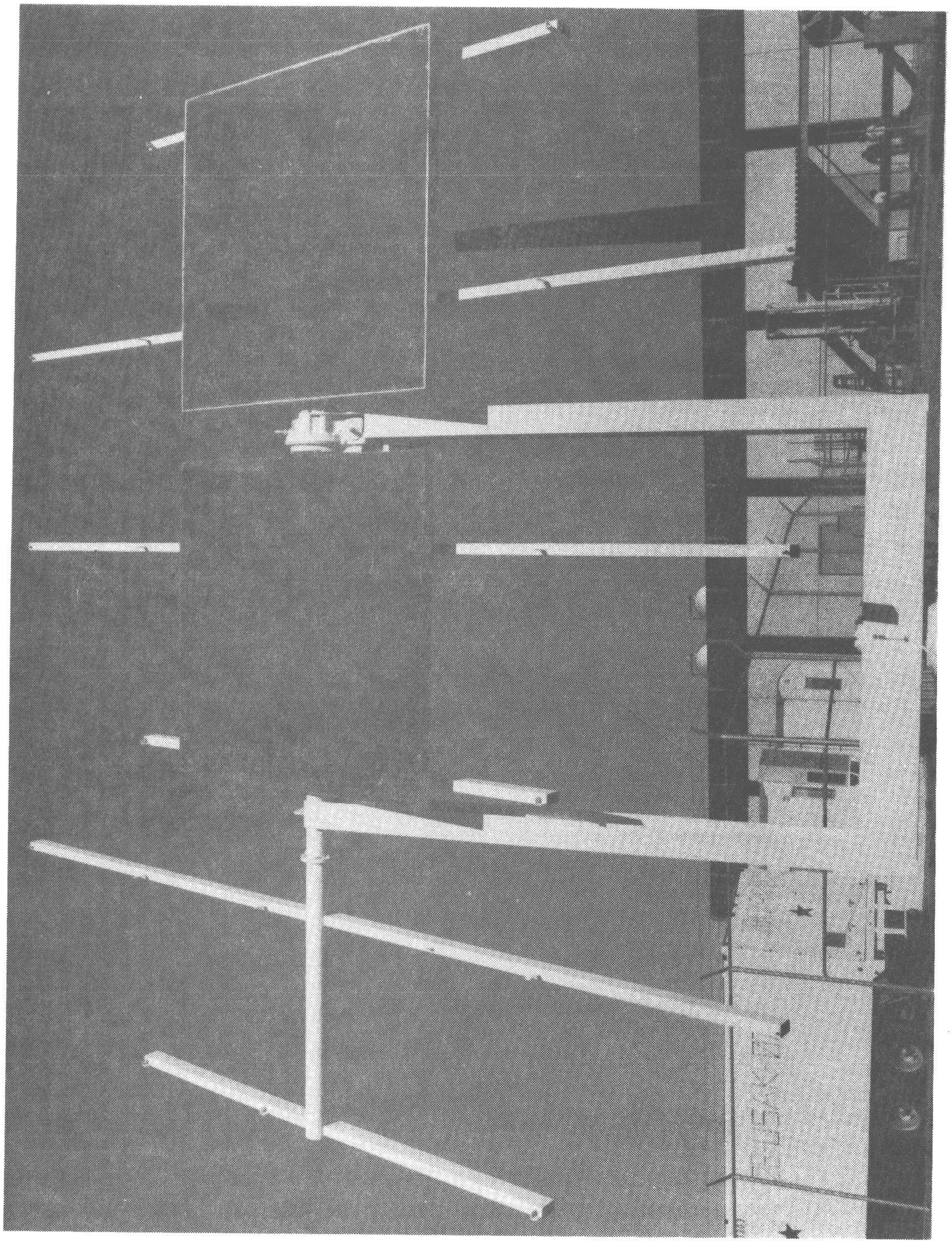

Figure 3

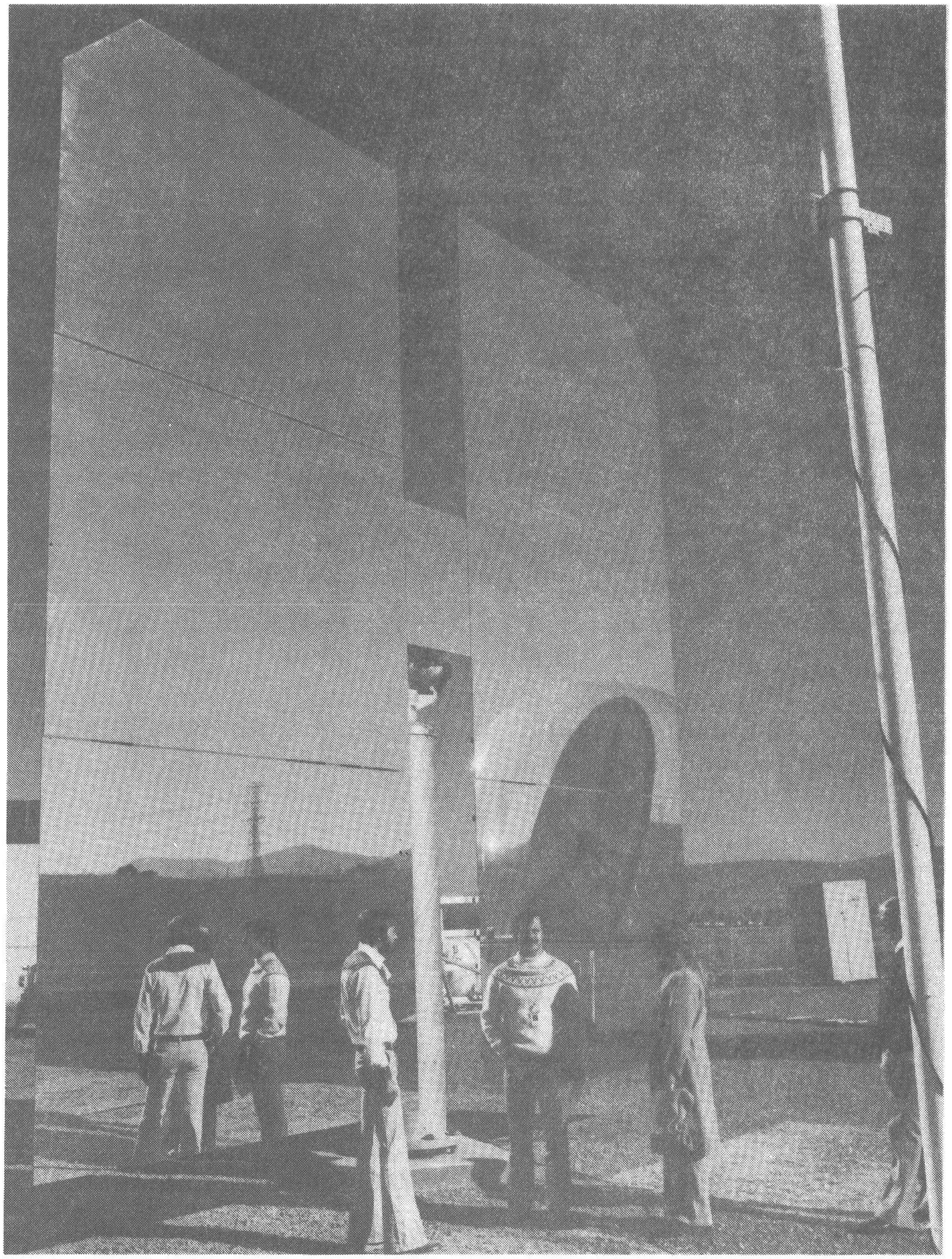

Figure 4

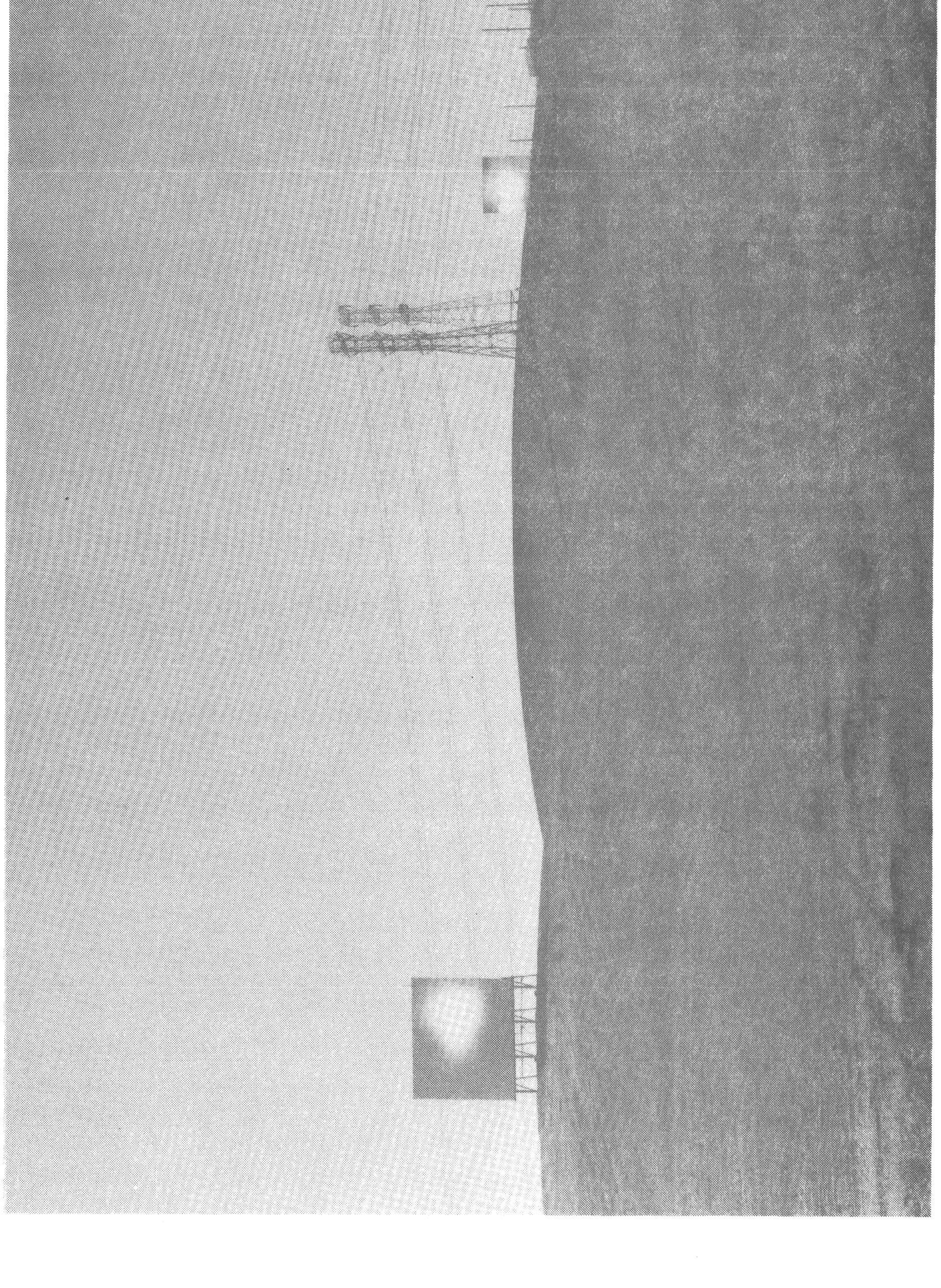

Figure 5

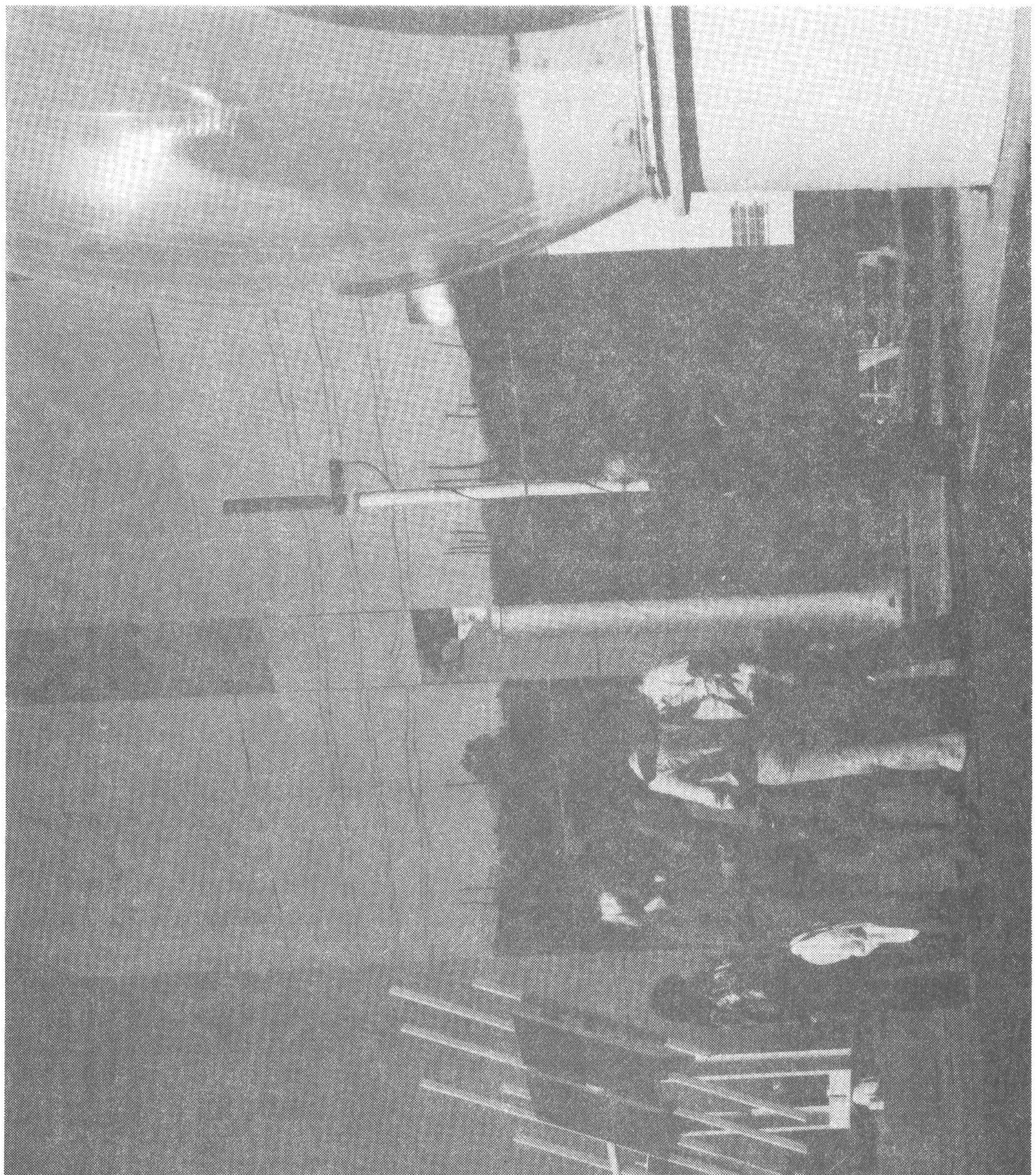

Figure 6

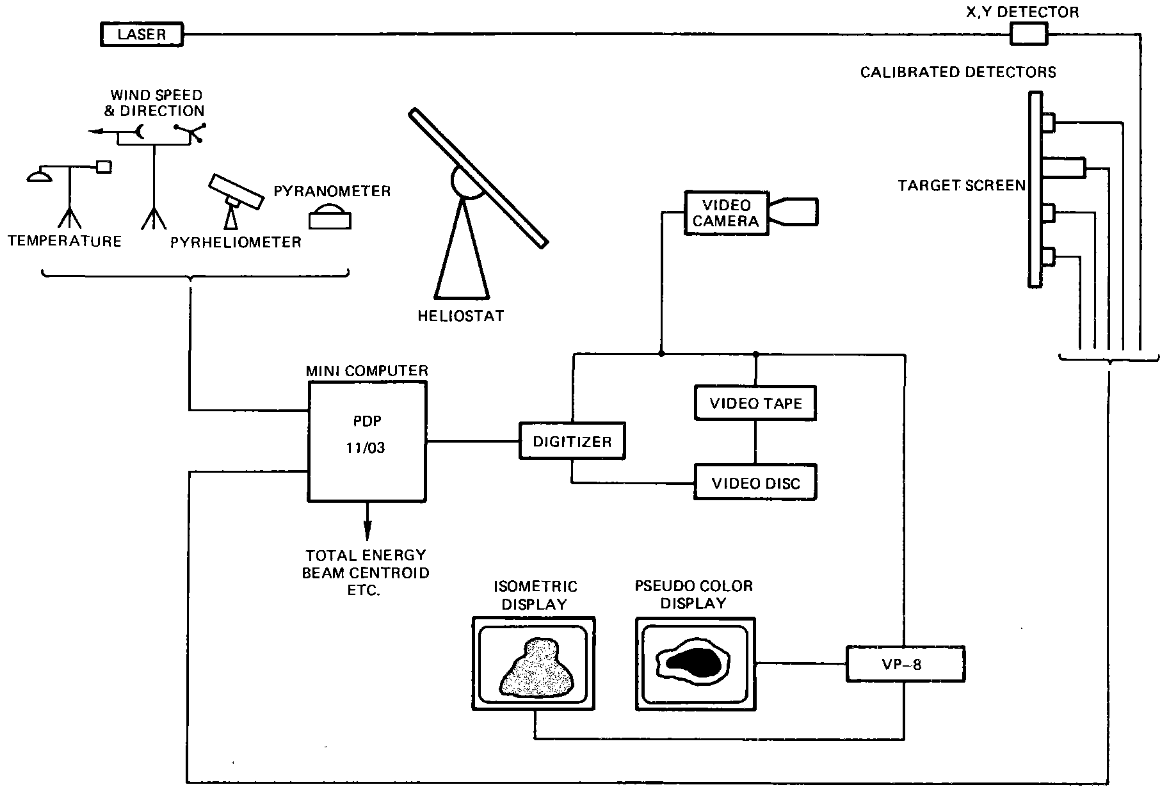

Figure 7

will also be implemented (i.e., a two-dimensional diode array, photodetectors, etc.) to compare the accuracy and calibrate the system.

The digital radiometric system will be capable of measuring total beam power; beam flux density distribution; and pointing and tracking accuracy as a function of time, environmental conditions, and sun angle. The equipment necessary to assemble the system is on order.

Milestones

The milestones currently established for the facility are shown below. It is anticipated that the measurement system will be installed by April and the scheduled long-term testing of the four heliostats completed by October.

- Complete Installation of Heliostats - January 1978
- Measurement System Calibrated - April 1978
- Heliostat Evaluations Started - April 1978
- Preliminary Evaluation Complete - October 1978

HELIOSTAT DUST BUILDUP AND CLEANING STUDIES

Sandia Laboratories

R. S. Berg

Introduction

Cleaning of accumulated dirt is beginning to be recognized as a major factor in the overall cost performance of most solar energy systems. Dirt accumulation can result in losses of over 25 percent after relatively short outdoor exposure. Long-term effects are not understood and need further study.

This paper describes the range of techniques that can be used to reduce dirt accumulation and to discuss some of the corresponding experiments being performed at Sandia. The methodology used was to first study the mechanisms of dirt impingement and adhesion and the time development of adhesion forces. The behavior of adhesion forces leads to restrictions on the periods when dirt is most susceptible to removal and on the potential removal techniques that can be successfully used. Several experiments using a variety of these techniques are being pursued.

Deposition Mechanics

The actual dirt deposition rates and bond strengths are functions not only of the type of dirt particles and surface materials, but of numerous factors such as environmental conditions, geographical and site effects, design features, and time effects. Airborne particles must have a sufficiently low Stokes (terminal) velocity to remain suspended. Stokes velocities of particles as a function of their sizes are shown in Figure 1.

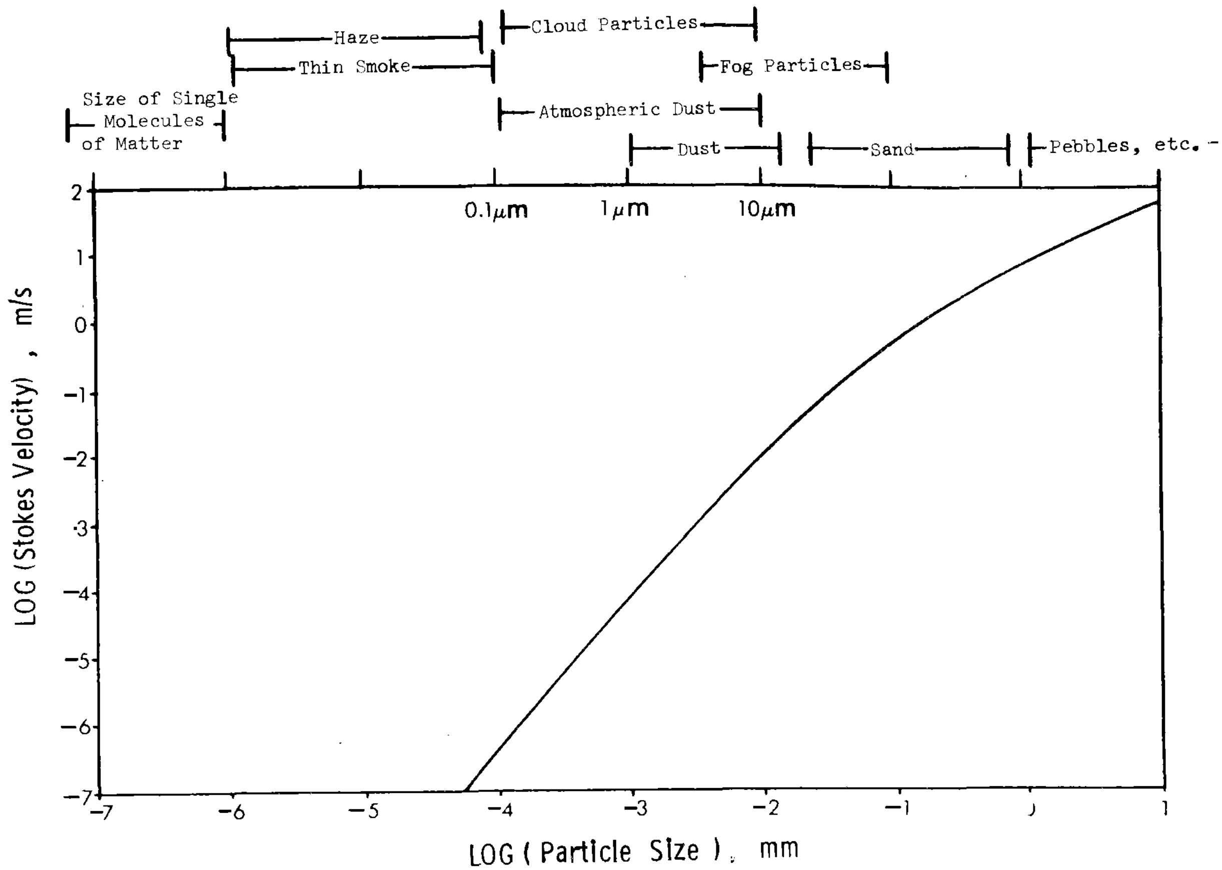

Figure 1. Particle Sizes and the Corresponding Stokes Velocities For Particles Found in the Atmospheric Aerosol

Particles impinge on a surface because of the complex fluid mechanical interaction of the dirt-laden airstream with the entire heliostat structure. The mechanisms of interaction of an airstream with a structure are listed in Table I. Very small particles ($d \lesssim 0.1$ μm) are transported by convective diffusion to the surface where they readily adhere because of their high surface energy/volume ratio. Larger particles, which are engulfed by the growing boundary layer, fall by sedimentation onto the surface. When the airstream moves over an edge at an angle to the overall direction (such as with a parabola or heliostat facet), turbulent eddies and dead spaces in the airstream are created. In such a case, particles which are not able to follow the eddies impact into the surface. Particles can also be thrown into dead spaces and fall out of the airstream by sedimentation.

TABLE I

MECHANISMS OF IMPINGEMENT FOR
WIND-CARRIED PARTICLES

Mechanism	Affected Particles (Size, Stokes Velocity)	Affecting Property
Convective diffusion	$d \lesssim 0.1\ \mu m$	Boundary layer
Impact	$d \gtrsim 1\ \mu m$, $v_S <$ air velocity	Air turbulence
Sedimentation	$d \gtrsim 1\ \mu m$, $v_S >$ air velocity	Air turbulence, dead spaces

The adhesion mechanisms holding particules that have fallen onto a surface are shown in Table II. These are affected not just by the materials comprising the surface and dirt, but also by the environmental conditions, particularly the humidity. Under normal dry conditions, the adhesion is dominated by surface energetics. When high humidities are present, intense physical and chemical bonds can develop. The high energy densities near the particle/surface contact region result in the condensation of water from the atmosphere even when the relative humidity is less than 100 percent. In geographical regions most suited to solar energy applications (such as Albuquerque, NM, and Barstow, CA) sufficient water is available almost nightly to condense at the dirt/surface contact zone. With the presence of water, the bonding mechanism changes because water can leach soluble materials from the dirt, air, and reflector surface.

/c/

TABLE II

DUST ADHESION MECHANISMS FOR 10-20 μm PARTICLES
ON A SURFACE

Mechanism	Relative Force Size	Affecting Material Property	Applications
Gravity	1 g	Mass	
Electrostatic	$\gtrsim$ 1 g	Surface (coating) conductivity	Conducting polymers, precipitations
Charge double layer	$\approx$100 g	Contact potential or difference in electron affinities	
Surface energy	$\approx$100 g	Solid surface relaxation	Surfactants, teflon coating
Capillary force	$\gtrsim$10,000 g	Fluid surface relaxation	Detergents
Chemical/physical	?	Chemical activity	

Cleaning

In looking at the mechanics of dust deposition and the time development of the adhesion, it becomes apparent that only certain cleaning strategies will be effective. The strategies can be arranged according to the time scale over which they act. They are:

1. Keep dirt from settling and adhering to the surfaces.
2. Wash off the dirt with low surface energy detergent-type solutions before strong chemical or mechanical bonding can develop.
3. Use chemically or mechanically active cleaning techniques capable of breaking the chemical and mechanical bonds.
4. Modify the surface so that strong bonding cannot develop.

Strategies 2 and 3 are primarily maintenance oriented, while strategies 1 and 4 are materials and design oriented. The problem of reducing dirt accumulation is not strictly a maintenance one, and we feel that the best solution may require some materials and design modifications.

Strategy 1 involves primarily noncontact, continuous techniques which require additional materials and design features. However, they do not generally require labor. Table III lists several techniques which should affect dirt accumulation and are being investigated at Sandia.

TABLE III

TECHNIQUES WHICH CAN AFFECT DUST ACCUMULATION

Action	Comment
Inverting while inactive	Relative importance of sedimentation in particle settling
Aerodynamic streamlining	Prevention of turbulent eddies and dead spots
Electrostatic biasing	Several hundred volts with normal electric field rejects particles
Vibrating the surface	
Thermally induced air currents	Boundary type of phenomenon used on astronomical telescopes
Flowing air	Boundary type of phenomenon used on astronomical telescopes

Strategy 2 involves frequent washing with detergent-type (low surface energy) water solutions. Used by itself, ordinary washing has the disadvantage that to be most effective, it must be done after only a few humidity cycles (perhaps every 1 to 3 days), since strong particulate bonding can develop very rapidly. Such washing is usually thought to be very labor-intensive. In addition, there are environmental questions concerning the water requirements both for the quality of wash water and quality of dumped waste water.

Strategy 3 involves a number of chemical and mechanical techniques for supplementing the washing. Many of the chemical techniques suffer from both environmental and health problems. Sandia is investigating several automated, high-pressure techniques that can conserve water and which mechanically attack particles bonded to the surface by using high-pressure spray. This strategy may also involve controlled exposure to frost and snow, which can mechanically wipe a surface.

Strategy 4 involves either surface modifications or the use of a substitute surface. Substitute surfaces may be either permanent coatings to make the surface inert or temporary coatings, such as surfactants, that can be periodically restored as part of a wash cycle. Sandia is studying some coating possibilities.

Experimental Investigations

Reducing Dust Deposition

The techniques described in Table III are of interest only in regard to their ability to reduce the accumulation of particulates. In order to test these techniques in a controlled laboratory environment, a dust exposure system has been assembled for exposing surfaces to calibrated amounts of a relatively well-defined Arizona desert dust. The system consists of a low velocity (0-25 m/s) atmospheric pressure wind tunnel fitted with a dust injector/disburser unit. It is capable of producing particle number densities 10^4 times greater than the number of particles (larger than about 1 μm diameter) present in the normal aerosol. Outdoor dust accumulation levels from 5-6 weeks' exposure in Albuquerque have been simulated in about 10 minutes in the wind tunnel.

Preliminary tests have been performed on an electrostatic repulsion technique. The resulting dust accumulation was significantly less than on a control glass slide exposed at the same time. A more detailed characterization of this technique and small scale field tests are being planned.

Some preliminary testing also has been performed on the use of spoilers which modify the airstream boundary layer by making it turbulent. Wind tunnel tests have indicated that less dust is deposited on regions behind the spoilers. Much more extensive work in this area is needed. The other techniques listed in Table III are under study and will be instrumented and tested in wind tunnel experiments.

Cleaning Solution Investigations

The usefulness of cleaning detergents is being investigated on reflector materials in parabolic troughs. The initial work was on a second-surface FEP Teflon mirror, which ordinarily should be much easier to clean than most materials because of its low surface energy. Samples left facing up, which accumulated dirt like a gutter. were completely uncleanable without mechanical wiping, which damaged the surface. Figure 2 shows the effect of cleaning the FEP, as measured on a bidirectional reflectometer.

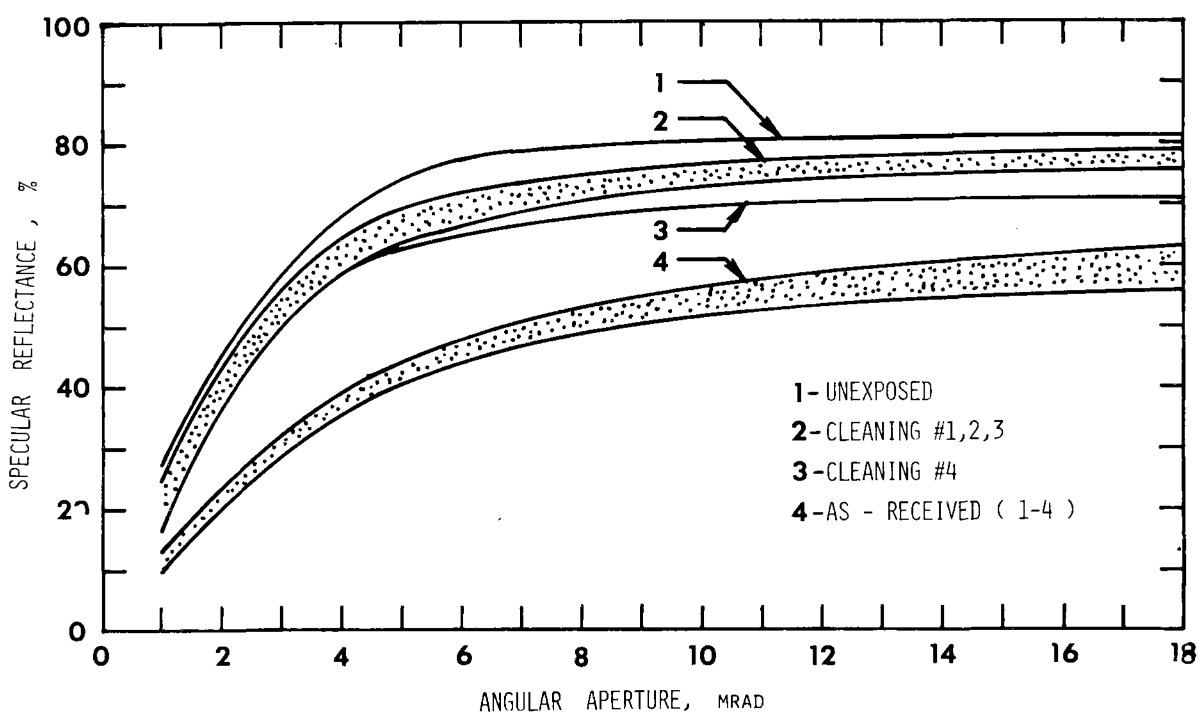

Figure 2. Dirt Accumulation and Cleaning of Aluminized FEP Teflon

Weathered (as-received) materials were obtained from the Sandia Solar Thermal Test Facility (STTF) and were subjected to one of the following four cleaning procedures: (1) high-pressure water, (2) Jet-X with detergent, (3) a mist spray of a commercial cleaner (C-120) from the McGean Chemical Co., and (4) hot soapy water with a cloth wipe. All were followed with a deionized water rinse. The clean surface had the same hemispherical reflectance as before exposure, implying that the loss was due to scattering from both residual dirt particles and scratches in the FEP. The effect of mechanical damage can be seen dramatically by comparing the cleaning of FEP, Figure 2, with a similar cleaning on a glass mirror, Figure 3. Vertical displacements of the curves are due to the very broad light scattering by dust particles.

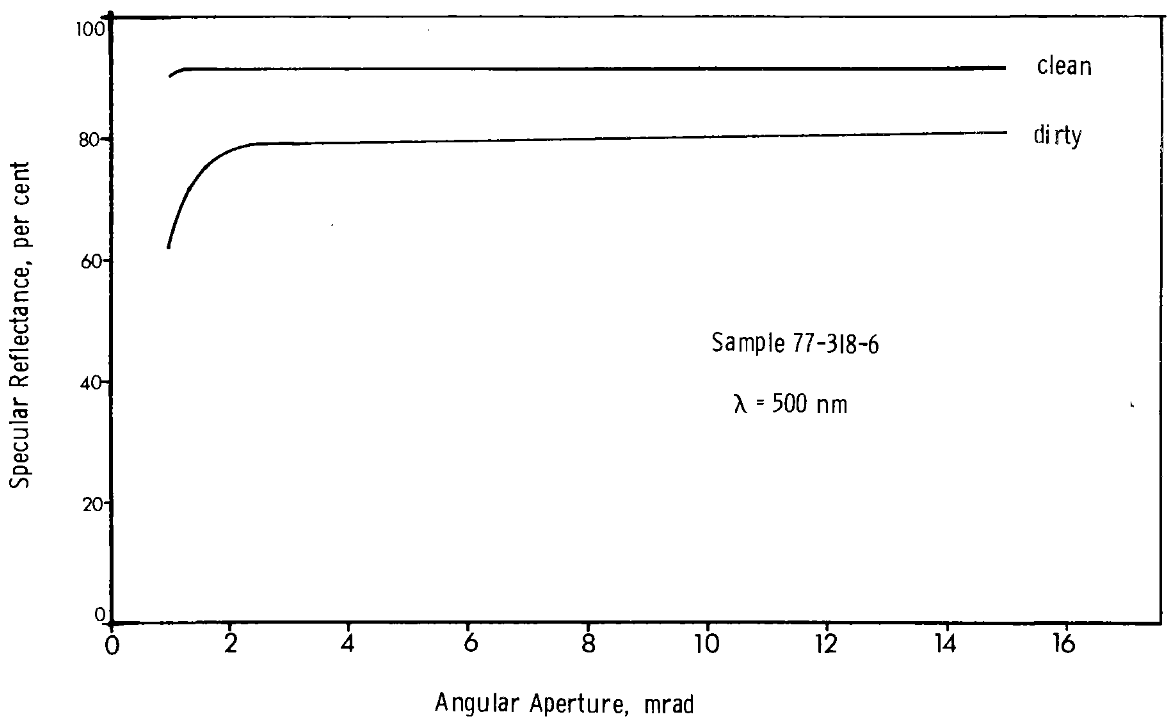

Figure 3. Dirt Accumulation on Silvered Glass

Rinsing with tap water was unacceptable because it left water spots. A series of mirrors was rinsed every 3 to 4 days with a deionized water rinse, which removed most of the accumulated dirt. However, there was a steady buildup of residual dirt that had to be removed with a detergent solution every 2 weeks. Criteria for the types of detergents required have been developed. They must be (1) effective in reducing the surface tension, (2) low cost in the mixing ratios used, (3) capable of being handled and mixed in automated equipment, and (4) biodegradable and able to meet EPA standards. In addition, the cleaning agent may have some chemical activity (such as nonneutral pH) which must not result in any long-term degradation of the mirror surface.

High-Pressure Spray Washing

In order to begin establishing a base for cleaning with semiautomated techniques, several tests were performed at the STTF using a high-pressure spray of 3 GPM water at 300 psi with several different detergents and solvents. These tests indicated that it was possible to recover 80-90 percent of the reflectance loss from short-term environmental influences. Another test was performed at the Triton Corporation of Houston, TX, consisting of high-pressure sprays of 500, 1500, and 10,000-psi tap water streams on dirty mirror samples. Reflectivity tests were performed on samples sprayed at each of the three pressures. All recovered about 95 percent of the original 0.83 average solar reflectance. Triton has been contracted to supply the STTF with a mirror washing vehicle outfitted with high-pressure spray and mixing equipment.

Dirt Characterization

Work has also been done on development of statistical methods for evaluating the variations of the reflectivity losses over the solar spectrum and for different positions on the mirror. This technique allows investigation of both wavelength dependence and specularity of the surface. Dust results in optical loss in the form of scattered light, which shows up in the diffuse component of the reflected beam. The diffuse reflectance as a function of wavelength for four different loss levels is shown in Figure 4 for silvered glass mirrors exposed in Albuquerque. Losses ranged from 6.6 percent to 24.1 percent at 500 nm (0.5 μm). Each curve can be normalized by the diffuse reflectance at 500 nm wavelength to yield a "universal" curve. This means that a measurement of the reflectance loss at 500 nm can be used to characterize the loss for the entire solar spectrum for the mirror. The solar-averaged loss has been calculated to be 0.78 ± 0.04 times the loss at 500 nm. Work is also progressing to determine the statistical number of measurements necessary to characterize an entire mirror surface based on measured reflectivity variances and source beam diameters.

The time dependence of the dust deposition and mirror orientation effects are also being studied in roof-top experiments. Samples mounted at 0° (horizontal), 30°, 45°, and 60° accumulated losses that were the same to within experimental errors. Long periods without rain in Albuquerque afford the opportunity to study short-term steady-state dirt levels. Figure 5 shows the effect of dirt accumulation on a mirror sample over a several week period. The large improvement after several weeks is due to a rain and snow storm that cleaned the surface.

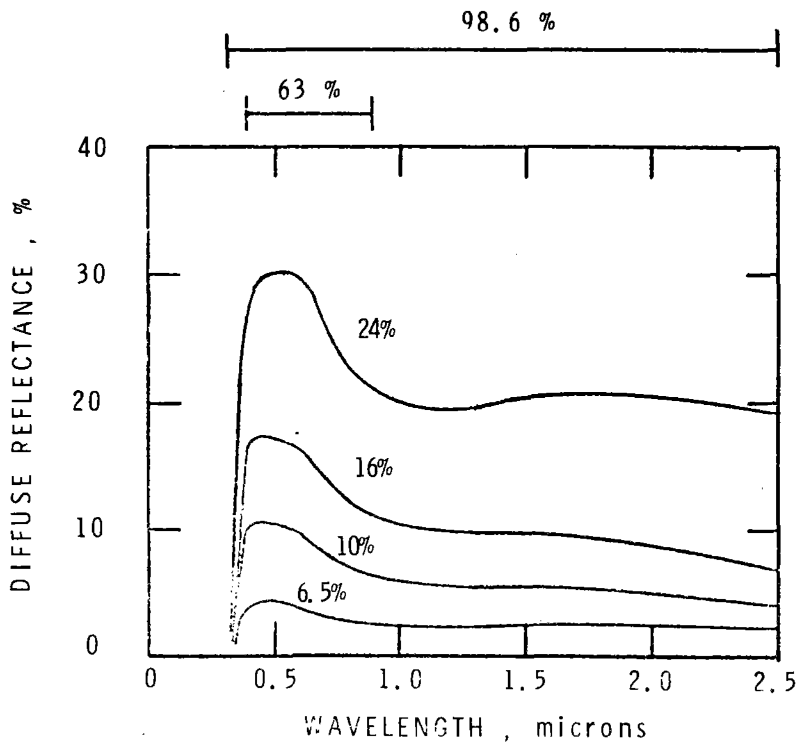

Figure 4. Diffuse Reflectance of Various Amounts of Dirt Accumulated on Silvered Glass Mirrors

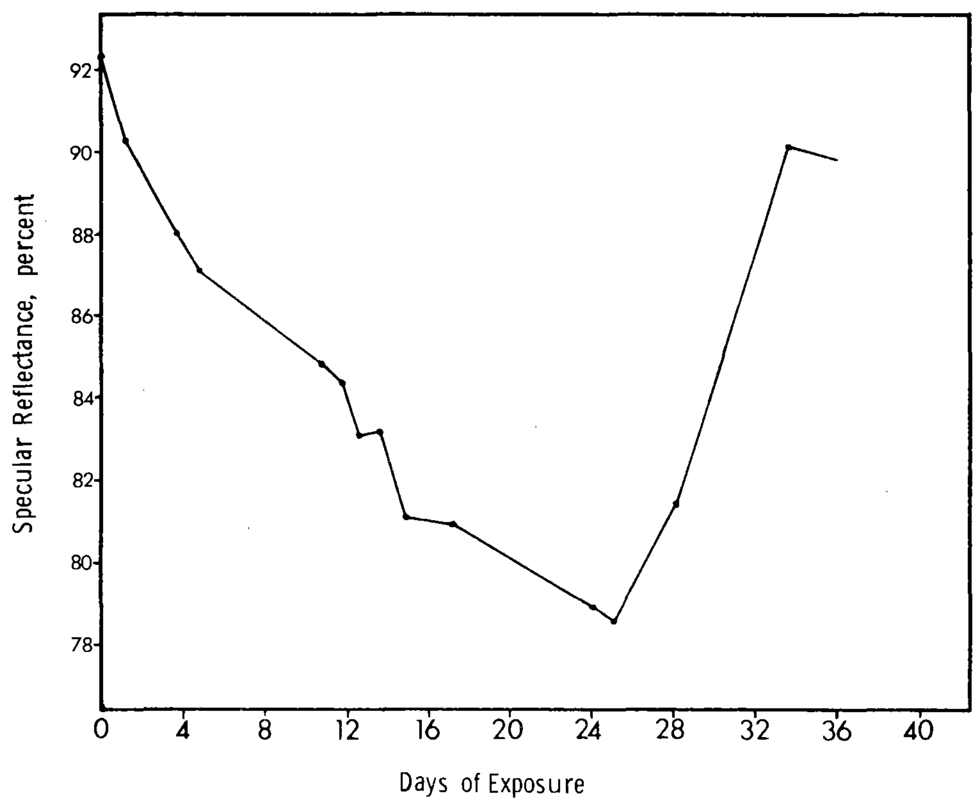

Figure 5. Specular Reflectance Loss and Natural Cleaning of a Silvered Glass Mirror Over An 8-Week Period in Winter of 1977-78

Conclusions

The behavior of dirt and several cleaning strategies has been studies. It was found that

1. Dirt deposits onto mirrors due to the fluid mechanical interactions of the dirt-laden airstream with heliostat structures and adheres due to the forces from surface energetics.

2. Intense chemical and physical bonds develop due to the interaction of condensed water vapor with the dirt and mirror surfaces.

3. The optical loss is caused by absorption and scattering of light by dirt. The loss can be characterized by a small number of measurements due to the scattering behavior of the dirt. Total solar loss for a second-surface glass mirror exposed in Albuquerque is 0.78 ± 0.04 times the spectral loss at 500 nm.

4. Continuous dust repulsion techniques can be used to reduce the rate at which dust accumulates. Electrostatic repulsion and boundary layer modification techniques have been successfully tested in laboratory wind tunnel experiments.

5. Water and detergent solution rinsing can be effective when used at relatively frequent intervals.

6. High-pressure sprays above 500 psi can recover up to 95 percent of the reflectance loss from dirt accumulation.

Much more work is needed in all areas of dirt characterization and cleaning technology to establish limits on the requirements for and capabilities of cleaning.

EVALUATION OF SPECIFICATION OF REFLECTOR PANEL MATERIALS FOR HELIOSTATS

Battelle Pacific Northwest Laboratories

M. A. Lind

Funding = $130K

Introduction

This program will provide DOE with background information and procurement specifications for materials which have potential applications in heliostat construction. The program will include comprehensive surveys, technical analysis, and laboratory investigations. Two areas of major emphasis will be glass for second-surface mirror applications and core materials for sandwich-type reflective surface support structures. Also to be investigated are methods of edge sealing and adhesive bonding.

The tasks included in this program are summarized below.

Task 1 - Glass Characterization and Specification

1. Survey sources, both domestic and foreign.
   - which companies will produce low distortion, 1/8-in., low-iron, float glass, or a suitable alternative.

2. Determine availability of production lines.
   - define possible schedule, deadlines, and windows for production of special runs in existing float lines.
   - investigate alternate existing processes such as gravity drawn fusion, etc.
   - investigate feasibility of setting up special lines for pilot plant production run.

3. Estimate costs and lead times and industry interest for both pilot plant runs and future commercial runs.

4. Define specification for pilot plant glass

   - interact with sources to provide a realistic specification that will both meet the needs of the pilot plant and be within the capabilities of the glass producers without prohibitive cost increases.

   - factors to be considered include: flatness; parallism; stress; transmission; edge, bulk, and surface flaws; and ream or cord durability.

5. Evaluate alternatives

   - provide background for recommendation on desirability of government-furnished equipment (GFE).

   - define follow-on and recommend additional work.

Task 2 - Reflective Surfaces/Substrates Characterization and Specification

1. Evaluate and specify polystyrene, extruded as per McDonnell Douglas module.

   - define characteristics important to heliostat applications.

   - define which polystyrenes should be considered; first emphasis to be placed on Styrofoam 1B.

   - make measurements of important characteristics where needed to supplement manufacturers' data.

   - define specifications for pilot plant foam core material keeping in mind future commercial development.

2. Survey alternative core materials

   - survey other types of polystyrene and foam materials.

   - survey aluminum and other honeycomb materials.

   - recommend future development areas.

3. Survey methods of edge sealing and adhesive bonding used in sandwiches.

   - survey present methods and materials for providing foam/core glass seal

   - survey alternate methods of protecting glass/silver interface

   - recommend future development areas.

MILESTONES

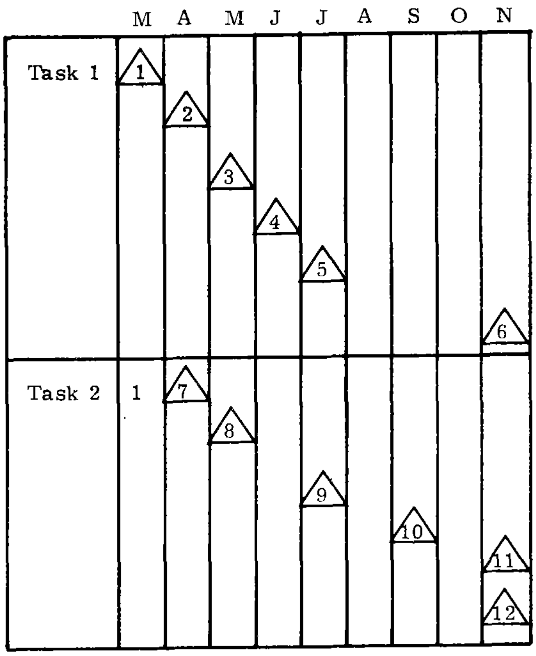

1. Funding authorization received.
2. Initial survey of glass companies completed - report of preliminary survey.
3. Report on production availability lead times, and schedule to establish whether glass should be government-furnished.
4. Glass specification formalized.
5. Preliminary evaluation of alternative process.
6. Final report and recommendations on glass.
7. Define characteristics of foam core material important in heliostat applications.
8. Complete evaluation of Styrofoam 1B.
9. Polystyrene specifications drafted.
10. Preliminary survey of alternate core materials completed.
11. Preliminary survey of edge sealants completed.
12. Final report and recommendations on reflective surface/substrate.

THERMAL ENERGY STORAGE FLUID TESTING AND ANALYSIS

Sandia Laboratories

V. P. Burolla

Introduction

The choice of a working fluid for the thermal energy storage subsystem began several years ago with a literature search of manufacturers' data. It then progressed to some limited testing of candidate fluids and eventually evolved into several detailed studies to determine the fluid degradation mechanism. The end objective of all these programs is to enable the design of a thermal energy storage system using the most economical fluid available. To this end, Martin Marietta, McDonnell Douglas/Rocketdyne, and Sandia Laboratories, Livermore, are involved in a coordinated effort.

Program Review

Although the intent of this presentation is to outline and describe the research effort presently under way at Sandia Livermore, a brief description of past efforts and goals may perhaps lead to a better understanding of why the existing test programs have been selected and what we intend to accomplish.

In Phase I of the program, McDonnell Douglas/Rocketdyne assessed the overall suitability of several candidate heat transfer fluids based on available manufacturers' data, industry experience, initial fluid costs, and basic safety requirements. Essentially, Phase I could be considered as a selection process for future testing.

Phase II was started originally to identify the most economical fluid available for sensible heat storage. To do this, the fluid had to be tested in an environment similar to the one it would see in actual use. Again, the McDonnell Douglas/Rocketdyne team was responsible for the testing, which consisted of heating glass flasks filled with various oils in various environments and measuring weight loss and viscosity changes as a function of time. The thrust here was to pin down a reasonably accurate replacement rate for the fluid since this recurring cost would effect the economics of the system. The environments chosen represented exposure to normal materials of construction and granite rock. The results of the testing, however, were somewhat perplexing which prompted a limited but extensive analysis of all fluid samples from the McDonnell Douglas/Rocketdyne tests. The analysis consisted of molecular weight distributions, infrared spectrophotometry and specific heat determinations all done at Sandia Livermore. Even after the analysis was completed, there remained a sufficient number of unanswered questions to instigate further research into the problem of fluid degradation.

The objective of the third and final phase was to understand the behavior of Caloria HT43 sufficiently well in order to predict accurately what the degradation rate would be in actual use and to understand the behavior well enough to enable design of a fluid maintenance unit to economically minimize the degradation rate. This objective is being met with a four-point program under a combined effort by Martin Marietta, McDonnell Douglas/Rocketdyne, and Sandia Livermore.

Martin Marietta personnel are presently involved in a test to first validate the degradation rates of Caloria HT43 as reported in the literature for closed systems and to compare their data with the McDonnell Douglas/Rocketdyne data obtained in open systems. Next, Martin Marietta will test the operation and feasibility of a vacuum distillation unit for prolonging the usable life of the fluid.

Rocketdyne personnel are examining the behavior of Caloria HT43 under a fluid flow condition in a fluid flow loop test.

Sandia Livermore personnel have designed static fluid degradation tests that more closely simulate storage conditions and also provide samples of gaseous and condensable degradation products for analysis.

The fourth aspect of the program involves a detailed analysis scheme involving all the contractors and some commercial labs.

The benefit of this four-point program becomes apparent when combining the data from the contracts. Ultimately, there will be enough data to provide reliable and accurate degradation rates for a variety of operating conditions, to provide verification of scale up/down parameters, to provide a data base for the compatibility of Caloria HT43 and various types of rock, and to gain invaluable experience in handling fluids of this nature to minimize start-up problems.

Sandia Livermore Tests and Analyses

Sandia first became involved in this research when detailed analysis of the samples from the McDonnell Douglas/Rocketdyne tests became necessary. The original analysis looked at the change in the molecular weight distribution, the changes, if any, in the chemical structure, and changes in specific heat. The techniques proved very complimentary and very informative but all the data obtained could not answer some very puzzling questions about irregularities in the weight loss rates and viscosity changes as reported by Rocketdyne.

The perplexities introduced by this first series of tests made it apparent that in order to truly finalize a value for the degradation rates a new series of tests should be initiated which would eliminate some of the variables in the previous tests. To be specific, it was decided not to have a continuous nitrogen purge through the test vessels but rather an initial purge which would be maintained by appropriate check valves. To further guarantee an airtight seal, all components that would see high temperatures were either welded or secured with high-temperature, gas-tight fittings. Glass vessels were necessary for two reasons: to allow simple monitoring of fluid level for fluid replenishment determinations and to eliminate the catalytic effect of any metal that could otherwise be present. The above requirements led to the vessel design shown in Figure 1. Note that the fill/sample tube and even the thermocouple well are made of glass. The vessels are approximately 5.0 cm OD and can hold about 200 grams of fluid at 302°C. Those vessels with rocks in them had stainless steel fill/sample tubes and stainless-steel thermocouple wells. The ratio of the surface area of the metal tubes to the volume of the liquid is roughly equivalent to the ratio of the surface area of a thermal storage tank that would see the oil and the volume of oil in the tank.

The vessels are placed in molten salt baths in groups of four. Each vessel sits in a stainless-steel tube well, slightly larger than the OD of the vessel. This is done primarily for safety considerations to isolate the molten salt from the hot oil should one of the vessels crack. The salt bath is maintained at temperature with a temperature controller which governs the power to a hot plate directly underneath the bath. Temperature measurements are taken on every vessel every hour by a data logger. Liquid level is checked every 500 hours and fresh oil added when necessary. Whenever oil is added, the fill lines are evacuated and back-filled with nitrogen three times to eliminate entrained oxygen. The amount of fluid added is obtained by weighing the charging vessel before and after filling.

The vessels are never allowed to exceed 1/3 psi pressure, and the bleed lines are vented to room temperature cold traps and a molecular sieve loaded vapor trap. Sampling of the fluid is done directly from the center of the vessel under conditions that again do not allow oxygen to enter the vessel or dissolve in the oil.

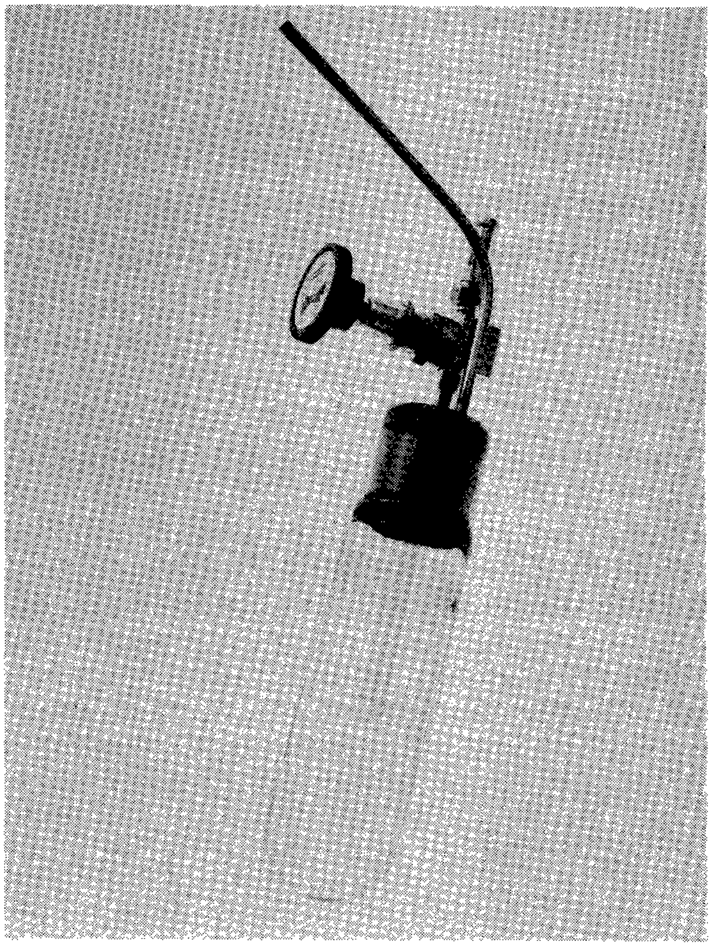

Figure 1

The analyses that are being done include: gel permeation chromatography (GPC) for molecular weight distribution, gas chromotographic distillation curve for true boiling point determinations, viscosity changes, density changes, and an infrared spectrum to detect changes in the chemical structure of the fluid. To date, some interesting observations have been made. The most obvious was the quantities of steam produced from the rocks as the vessels were heated. Evidently, the rocks contained sufficient quantities of water to cause catastropic fracturing of the rocks even as late as 600 hours into the test. These miniature explosions do not seem to be energetic enough to cause any damage but they can be frightening. Another interesting point is the lack of condensable liquids in the room temperature traps, which seems to indicate that all of the decomposition products must be gases at ambient conditions. Finally, the degradation rates in general are much higher for the first 500 hours than in subsequent 500 hour periods, but this preliminary data (see Table I) must be treated very cautiously as it has not been adjusted for temperature excursions that were experienced during some start-up problems.

TABLE I

PRELIMINARY DATA*

Fluid Replenishment Rates:		
Fluid Alone		
302°C (575°F)	0-500 hours	8.0% (46%/yr)
	500-1000 hours	1.4% (8.2%/yr)
316°C (600°F)	0-500 hours	9.7% (57%/yr)
Fluid + Rock and Metal		
302°C (575°F)	0-500 hours	20% (117%/yr)
	500-1000 hours	3.2% (19%/yr)
316°C	0-500 hours	8.0% (46%/yr)

*NOTE: This is very preliminary data which has not been adjusted for temperature excursions during testing.

The figures in brackets are yearly replenishment rates based on the oil being at the high temperature for an average of 33 percent of the time. However, it may also be indicative of the effects to be expected from rocks that contain significant amounts of absorbed oxygen or dissolved oxygen in the oil. Further testing and data reduction should answer these questions. Perhaps too, this effect is indicative of the problems that can occur if the thermal storage system experiences significant overtemperatures due to faulty controls or poorly maintained equipment.

Schedule

Testing of the fluid is expected to continue through part of August (see Figure 2) unless the degradation rate is excessive. Hopefully, a total of 6000 hours of testing will be sufficient to notice any peculiar trends or to establish a normal steady-state degradation rate. Data points are taken every 500 hours or sooner if appropriate. Analyses are conducted throughout the test program and a report will be published near the end of August.

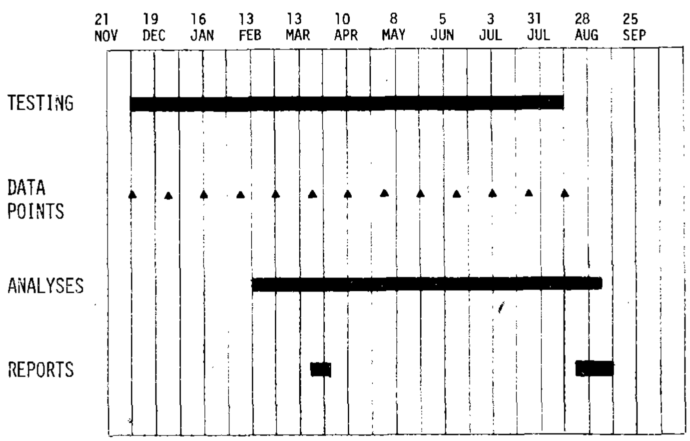

Figure 2. Sandia Degradation Studies Schedule

STORAGE FLUID MAINTENANCE UNIT STUDY

Martin Marietta

J. Myers

Background

Exxon's heat transfer oil Caloria HT43 was chosen as a heat storage fluid for the Martin Marietta Phase I, central receiver solar thermal power plant. This fluid is recommended for use in commercial heat transfer systems that operate with bulk fluid temperatures up to 600°F and film temperatures up to 650°F. The reported pyrolitic decomposition rate for this oil is small. However, even a small decomposition rate can have a significant economic impact due to the large quantities of oil required for thermal storage systems. A literature search revealed some data (Figure 1) to quantify the decomposition rate as a function of oil storage temperature. This data was obtained by placing a small quantity of oil in a sealed container and subjecting the oil and container to elevated temperatures for various lengths of time. The fraction of the liquid that boils away at a temperature lower than the minimum boiling temperature of the fresh fluid is labeled low boilers; the fraction that boils at temperatures higher than fresh fluids is called high boilers. The sum of the high and low boilers represented the total decomposition for these tests. Low boilers will decrease the viscosity of the oil. Also, a portion of the low boiler will go over as volatiles with a resulting oil weight loss. High boilers have the effect of increasing the oil viscosity and freezing point. If the concentration of high boilers is allowed to increase uncontrolled, the oil viscosity will eventually be increased to the point that the oil can no longer be used in a pumping system.

The decomposition data (Figure 1) indicates that at 600°F, a total decomposition of 2.5 percent by weight per week can be expected. Industrial operating experience does not support this laboratory data. There are cases where Caloria HT43 has been used for years in a trouble-free system. Records of the make-up fluid required are generally not available. Other operating systems have experienced decomposition rates much larger than that shown in Figure 1. In some of these commercial systems, the data must be qualified with the comment that the heat transfer fluid had been

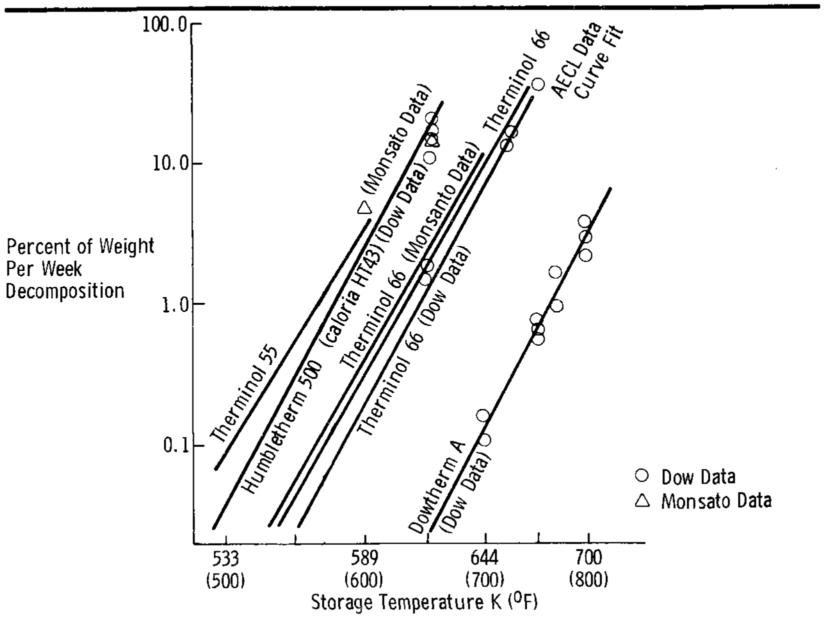

Figure 1. Total Oil Decomposition Rate As a Function of Temperature

contaminated at one time or another with another process fluid. Thus the data from industrial operating experience does not appear to be helpful in determining decomposition rates.

Test Objective

To better understand the decomposition rates and how this decomposition might be controlled in a thermal storage application, a two-phase program has been initiated. The first phase will generate decomposition data in a closed system, at 600°F, similar to that reported in the literature with the exception that the testing will be conducted on a large oil sample (316 lbs). This decomposition data will then be compared with the literature data. During the second phase testing, a large oil sample (approximately 300 lbs) will be tested in an environment that simulates the thermal storage. The sample temperature will be maintained at 600°F, and the sample pressure will be maintained at or below 5 psig. During this test phase, a side stream will be drawn off the oil tank and processed through a vacuum distillation system to remove the high and low boilers. The reprocessed oil, with high and low boilers removed, will be returned to the tank. The weight loss due to high and low boiler removal will be made up with fresh oil to keep the sample volume constant. The decomposition data determined in this way can then be compared with the Phase I decomposition rate data to determine: (1) if the side stream vacuum distillation system can control the concentration of high and low boilers in the bulk storage fluid, and (2) if the addition of the vacuum distillation system will affect the overall decomposition rate.

Phase I Testing

The sample tank has a 100-gallon volume and consists of a 24-inch diameter cylinder 3/8-inch thick and 42 inches high. The tank heads are ASME dished heads. This tank is constructed from mild steel and is ASME certified for operation at 100 psig at 800°F. The tank heating system consists of six 500-watt band heaters mounted to the external surface of the tank plus two 500-watt heaters, one each on the tank nozzles (one nozzle on each head). The nozzle heaters extend through the six inches of mineral wool insulation, and the nozzle heaters compensate for the heat loss through the nozzles so that a cold spot is not generated at the interface of the nozzle and the tank. The power to all heaters is controlled from variable voltage power supplies. The tank is instrumented with eight thermocouples (T/C). The three on the cylindrical section of the tank feed into an over temperature control system that removes all power from the system if actuated. Three thermocouples are located in thermowells in the oil at different levels to measure oil temperature. The last two thermocouples are located on the tank wall at the nozzle penetration and are used to control the heat input to the two nozzle insulation penetration heaters. An air-motor driven stirrer (see Figure 2) mounted to the nozzle on the top of the tank helps keep the oil sample isothermal and homogenous in its composition.

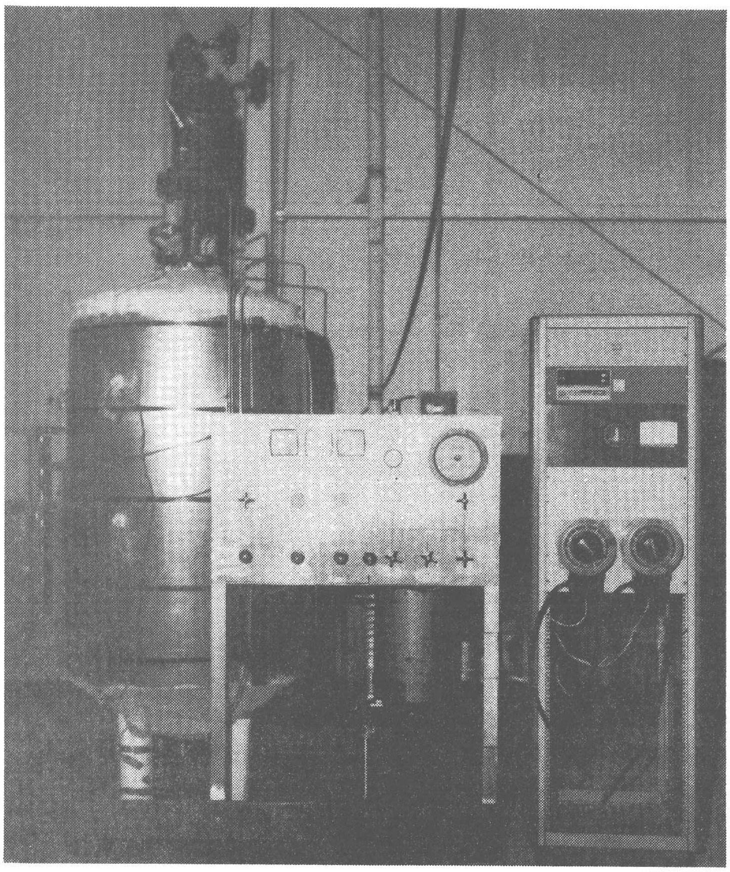

Figure 2. Phase 1 Test Setup

During Phase 1, the tank was loaded with 316 lbs of oil. The tank and oil were then evacuated to degasify the oil. The tank ullage was backfilled to atmospheric pressure with GN_2, and the tank and oil temperature were elevated to 600°F. The excess pressure created during heat-up was vented to atmospheric pressure. The tank and oil were sealed, and the temperature was maintained at 600°F. Weekly oil samples are being extracted from the tank using an evacuated oil sampling device that allows a hot oil sample to be taken without exposing the oil to the air. A series of tests is being run on these samples. These tests are to: (1) determine decomposition products (high boilers and low boilers) using gas chromograph distillation, (2) determine the engineering properties including viscosity and density, and (3) determine the chemical composition changes in the oil including molecular weight distribution, IR and NMR spectra, iron concentration, and colride concentration.

The sample testing is a joint Martin Marietta/Sandia Laboratories effort. The viscosity, gas chromograph distillation and molecular weight distribution tests are being done by Sandia Laboratories, with the remainder being done by Martin Marietta.

At the end of the six-week Phase 1 test period, the oil will be allowed to cool. Any residual pressure will be vented through a meter to determine the volume of gas vented. A gas sample of the vented gas will be taken for composition analysis, and the total weight of the vented gas will be estimated. The remaining oil will be drained into a clean drum and weighed.

Phase 2 Testing

After the Phase 1 testing, the tank will be cleaned with petroleum ether, purged with dry GN_2, and the vacuum distillation system will be installed. The vacuum distillation system is designed to operate at 10 tor. All compounds that do not boil above 575°F and 10 tor (high boilers) or do not condense below 290°F and 10 tor (low boilers) will be extracted from the system. The remaining fluid will be returned to the tank. Figure 3 shows the vacuum distillation system during its assembly.

After the distillation system is connected, fresh oil will be loaded into the tank, and the tank will be evacuated and heated using the same procedure that was described in Phase 1. The vacuum distillation system will be brought on line. Weekly samples will be taken of the bulk oil in the tank, the high boilers, the low boilers, and the return oil from the vacuum distillation system. The same sample test described under Phase 1 will be made on each of the samples.

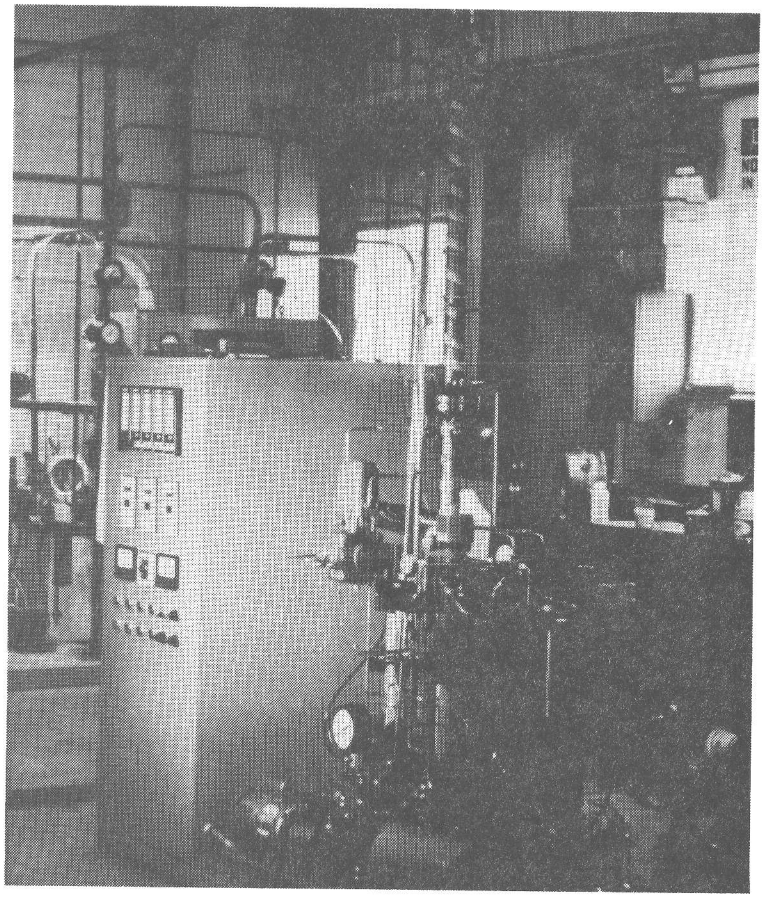

Figure 3. Vacuum Distillation System

Results to Date

At this time, the Phase 1 testing has completed its second week of exposure to a 600°F environment. The temperature versus time for the oil is shown in Figure 4, and the ullage pressure versus time is shown in Figure 5. From the pressure increase we can say that clearly some low boilers are being generated and are coming off the liquid as a gas. At this time, we do not have the results of the sample GC distillation so an evaluation of the early decomposition rates cannot be made. The IR and NMR data show no change over the first two weeks of test. The viscosity data is not yet available. The density data indicate no change.

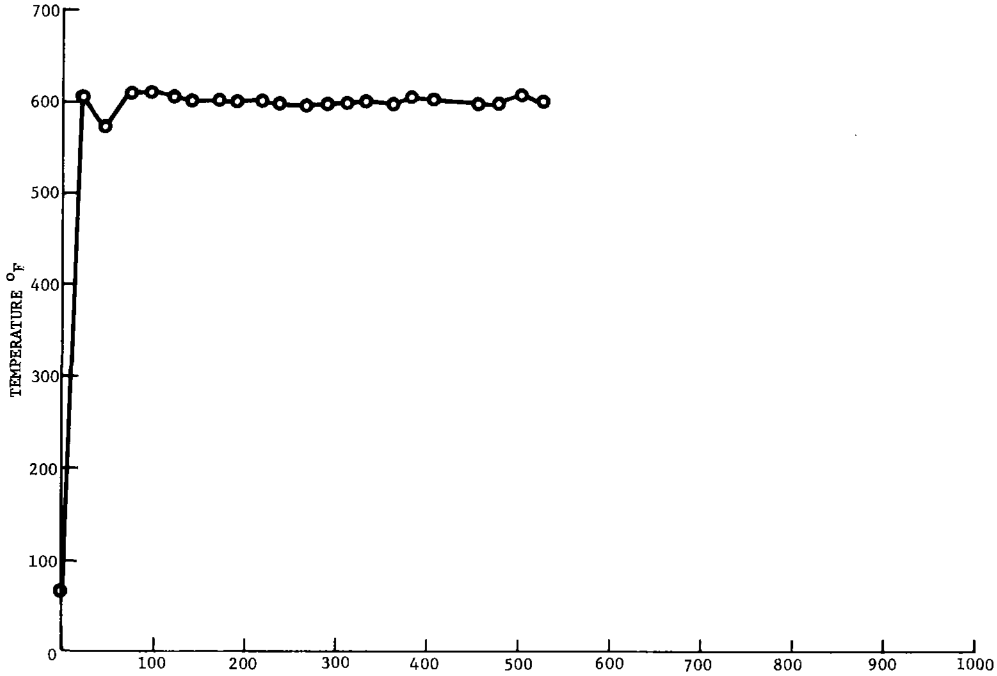

Figure 4. Bulk Oil Temperature Versus Time

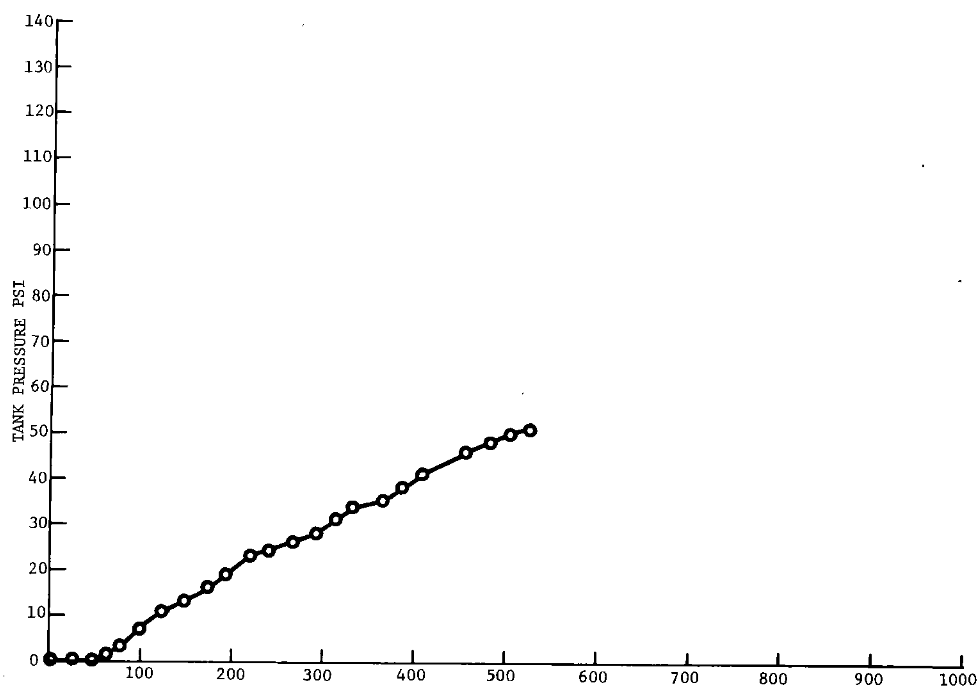

Figure 5. Tank Pressure Versus Time

EXTENDED TESTING OF STORAGE FLUIDS AND FLOW LOOP EXPERIMENT

McDonnel Douglas/Rocketdyne/Sheldahl/
Stearns-Roger/University of Houston/West Associates

J. M. Friefeld

During this semiannual period, the basic thermal storage fluid prequalification tests were continued and extended. These activities were intended to expand the data base developed during the thermal storage subsystem research experiment (SRE) tests.

The preliminary design of the pilot plant thermal storage subsystem culminated in the configuration shown in Figure 1. Steam from the receiver (not used by the turbine) is cooled and condensed in the thermal storage heater, which causes a temperature increase in an organic heat transfer oil. The hot oil, as shown in Figure 1, is introducted into the top of a thermal storage vessel containing two sizes of crushed rock. A thermocline moves from the top of the tank to the bottom of the tank during the charging process. When energy is to be extracted, the hot fluid at the top is withdrawn and passed through a steam generator to generate working fluid for the turbine at the conditions shown in Figure 1.

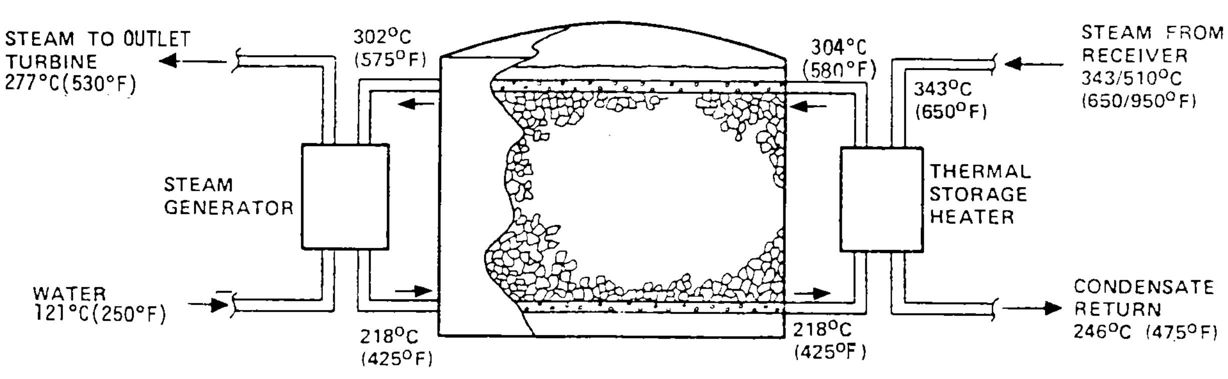

Figure 1. Pilot Plant Thermal Storage Subsystem Design

Based on this design, a number of technological issues were raised for resolution during the SRE tests. The demonstration of large-scale thermocline efficiency was accomplished using a 4-MWh tank (27,000 gallons). Issues involving long-term fluid-rock compatibility and long-term thermal cycling were partially resolved during the SRE tests; hence the continuation of the fluid test program. Table I shows the status of all the test programs conducted in support of the thermal storage preliminary design. All activities are continuing with the exception of the testing of Therminol 55, which was found to be inappropriate for operation at the pilot plant conditions. These studies are being conducted at the Rocketdyne Canoga Park facility with the exception of the fluid decomposition analysis, which is being performed at Sandia Laboratories in Livermore, California.

TABLE I

THERMAL STORAGE SUBSYSTEM TECHNOLOGICAL STATUS

	Completed	Continuing
• Large Scale Thermocline Demonstration	X	
• Long-Term Fluid/Rock Compatibility		
Caloria HT43		X
Therminol 66		X
Therminol 55	X	
Mobiltherm 123		X
Sun Oil 21		X
• Model Subsystem Flow Loop		X
• Analysis of Fluid Decomposition*		X
• Operational Fluid Test Procedures		X

* At SLL

Fluid evaluation studies are being conducted in two parts. First, different fluid combinations are being held at elevated temperatures for long periods of time to determine basic stability and material compatibility. The long-life compatibility test has accumulated durations in excess of 8,000 hours, which corresponds to 3-1/2 years of pilot plant operation. Details of the accumulated durations for all the candidate fluids are shown in Table II.

TABLE II

THERMAL STORAGE FLUID TEST STATUS

Thermal Stability and Material Compatibility	Temperature °C (°F)				
	287(550)	302(575)	316(600)	329(625)	343(650)
Caloria HT43, hrs	6136	8029	6373	-	-
Therminol 55, hrs	1983	2153	2083	-	-
Therminol 66, hrs	4121	6932	2573	7116	6942
Mobiltherm 123, hrs	2604	3955	3884	-	-
		Surface Temperature °C (°F)			
Surface Fouling		316(600)	329(625)	343(650)	
Caloria HT43, hrs		7808	9556	6404	
Therminol 66, hrs		3745	15027	15195	
Mobiltherm 123, hrs		3452	2252	932	

The second test concerns surface fouling, particularly deposition on the heat exchange surfaces in the thermal storage heater (Figure 1). This test is performed by immersing an electrical heater in the stagnant fluid and recording the current necessary to maintain surface temperature at a particular level in excess of the fluid bulk temperature. Some of the fluids have been tested at times corresponding to six years of pilot plant operation. Details of the accumulated durations for the various fluids is shown in Table II.

The results of the tests are as follows. Caloria HT43, which is the current fluid baseline, has shown excellent stability and compatibility with the rocks and materials of construction. A new fluid which promises to be on the market shortly has been found which appears to be quite competitive with Caloria HT43. This new fluid, Mobiltherm 123, is quite similar to Mobiltherm 600, which was considered for use three years ago but was removed from production by the Mobil Corporation. A preproduction sample of Mobiltherm 123 was procured and tested, along with Caloria and the Therminol in the test setup. The results are compared in Figure 2, which indicates the annual cost of makeup fluid for the pilot plant as a percentage of pilot plant capital costs. As shown, the Therminols have excessive make-up costs due, in the case of Therminol 66, to high fluid costs, and in the case of Therminol 55 to excessive boiloff rates.

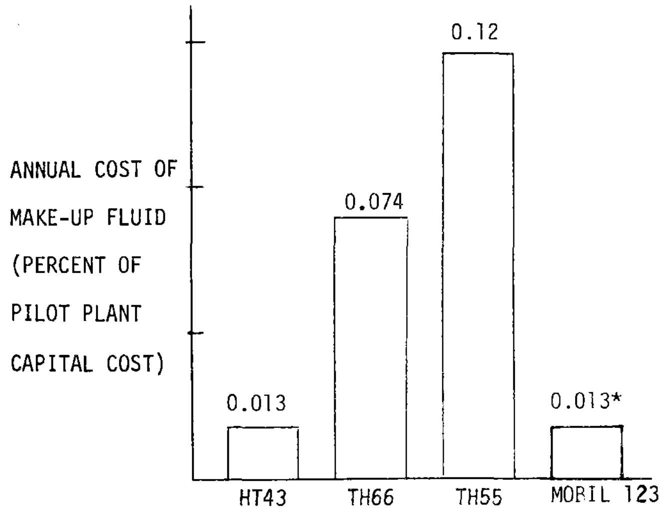

*Preproduction sample

Figure 2. Results From Fluid Prequalification Tests

The surface fouling tests are summarized in Table III. Listed are the wall temperatures and accumulated test times, together with visual observations relative to the condition of the surface. Therminol 66 has shown no visible fouling in any case, and no current reductions are necessary to maintain proper temperature differentiation. In the case of Caloria HT43, there has been some visual observation of very slight deposits on the heater surfaces; however, current changes which would indicate a reduction in heat flux due to a significant fouling factor were totally absent.

TABLE III.

HEATED SURFACE FOULING TEST SUMMARY

Test No.	Fluid	Wall Temp. °C (°F)	Test Time (hr)	Visual Observations
1	Caloria HT43	316(600)	7808	Deposits near bottom of heater
2	Caloria HT43	329(625)	9556	Slight deposit near bottom of heater
3	Caloria HT43	343(650)	6404	Slight, patchy deposit near bottom of heater
7	Caloria HT43	316(600)	360	
4	Therminol 66	316(600)	3745	No visible fouling
5	Therminol 66	329(625)	15027	No visible fouling
6	Therminol 66	343(650)	15195	No visible fouling

The last test currently being conducted is a model subsystems flow loop. This is a laboratory-scale setup (Figure 3) which contains, on a miniaturized basis, all elements that would be present in the pilot plant thermal storage subsystem. The test setup includes a pump, a hot surface for determining if fouling will occur, an electrical heater to heat the fluid, a miniature thermal storage unit, and a fluid cooler. The objective of the test is to extend the previously described tests by having the fluid and rock undergo cyclic heating and cooling as they would in an actual pilot plant operation. The flow loop is currently operating in a satisfactory manner. More than 1500 hours have been accumulated to date, and continuous operation (24 hours, 7 days) is being conducted. The TSU bed is being held at 575°F while the fluid heater outlet temperature is 610°F. To date, there have been no indications of fluid degradation and on inspection of the heated surfaces, no indication of surface fouling.

The last task to be conducted concerns the derivation of standard tests for fluid monitoring. These tests would be conducted on site during pilot plant operation to aid the operator in the determination of thermal storage fluid condition. The derivation of these tests is due to start in May, 1978, after an extended amount of test duration is obtained on the model subsystem flow loop.

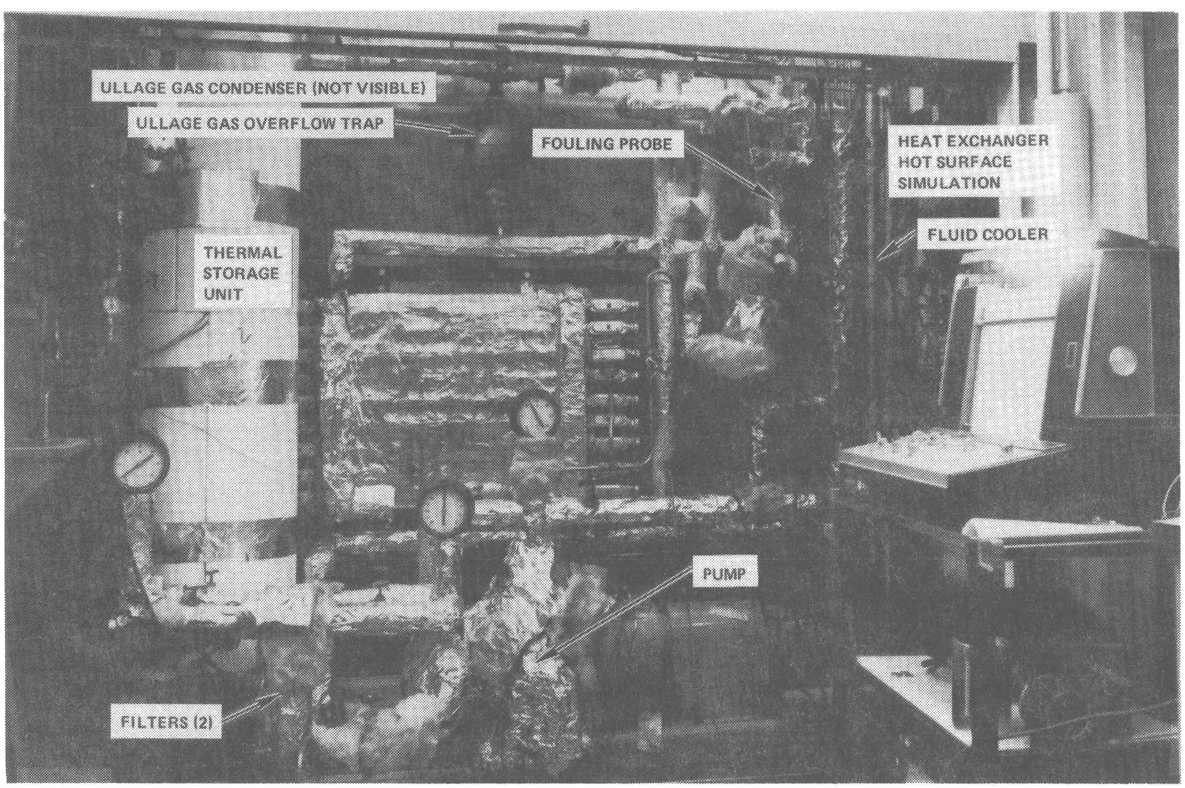

Figure 3. Model Subsystem Flow Loop

UNLIMITED RELEASE

INITIAL DISTRIBUTION:

TIC/UC-62 (298)
T. B. Cook, Jr., 8000; Attn: W. J. Spencer, 8100
C. H. DeSelm, 8200
B. F. Murphey, 8300
L. Gutierrez, 8400
A. N. Blackwell, 8010
R. C. Wayne, 8450
A. C. Skinrood, 8452 (245)
F. J. Cupps, 8265/Technical Library Processes Division, 3141
Technical Library Processes Division, 3141 (2)
Reports & Central Technical File, 8266-1 (3)